

An Approach of Clustering Features for Ranked Nations of E-government 2012

Yu-Chien Ko, Hamido Fujita*

Department of Information Management, Chung Hua University, 30012, ShinChu, Taiwan, e-mail: eugene@chu.edu.tw

*Software and Information Science, Iwate Prefectural University, 020-0173, Takizawa, Japan, e-mail: issam@iwate-pu.ac.jp

Abstract: E-government is important for national development. However, the significant features for E-government stages have not been analyzed intelligently. This research proposes a method, clustering features for rankings (CFR), to find stages and features for E-government. The results show that the adult literacy is significant for the beginning stage and the gross enrollment in education for the mature stage. Technically, dominance-based rough set approach is used to generate criteria's evidential weights of nations' rankings and rough set is then used to identify the clustering features composed of dependency rules. The rules comprise the most relevant and important criteria and the ranking intervals as the intelligent knowledge.

Keywords: E-government; clustering features; rankings; dominance-based rough set approach (DRSA); rough set (RS)

1 Introduction

Clustering [1, 2, 3] and Classification [1, 2, 3, 4, 5, 6, 7, 8, 9, 10] of the roughness theory have successfully presented features knowledge (in terms of indiscernibility relations) as intelligent knowledge since 1982. Technically, the roughness classification can partition a given set of objects and the roughness clustering can identify natural grouping of objects. The features can be obtained by choosing either classification or clustering technique. However, neither of them alone, can provide information needed for decision making. For instance, classification only provides the local information restricted by the given set of objects and the natural grouping is short of expert's opinions. A complementary view between classification and clustering evolves an integration to give intelligent features [11, 12]. This research aims to propose an integration method for E-government Development Database of United Nations (UN-EGDD) 2012 [13] in analyzing stages (clustering features composed of continuously ranking intervals). Under the

consideration of rankings these stages signify the development of E-government in terms of dependency rules which are presented in Section 2.3, 3.2 and 4.

E-government seems natural due to the arrival of the information age [14]. It can improve government performance, enhance business efficiency, provide online service to people, and so forth [15, 16]. So far, there is no mathematical model which can quantitatively and naturally identify stages for E-government. According to the characteristics of UN-EGDD, the natural stages could guide the development of E-government [16]. The difficulties of solving the natural stages are summarized below.

- UN-EGDD assumes fixed weights for criteria. This assumption negates the existence of stages. The reason is that stages, at different levels, have different focuses, i.e., weights vary with stages.
- The stages based on rankings are hard to identify. The interval rankings from nation to nation are not easy to define.

1.1 The Objectives

Under considerations of the research background and the problems above, this research aims to identify clustering features with criteria relevance and importance to rankings. The natural clusters will be explained with continuous stages in terms of the dependency rules. The ranking intervals depending on the criteria will imply the features of E-government stages.

1.2 The Conceptual Methodology

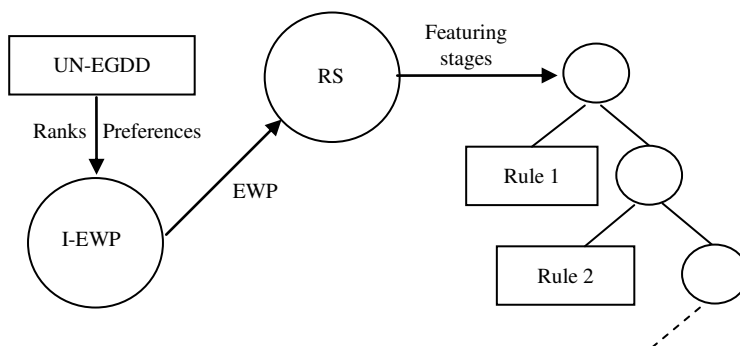


Figure 1
The conceptual CFR

To achieve the objective and solve the research concerns above, our methodology named clustering features for rankings (CFR) is designed and implemented in two phases. First the classification posteriori by I-EWP (induction of preferences based on preferences) for nations' ranks [17]. These posteriori are evidential weights based on preferences (EWP). In the second phase, EWP replace the preferences in the information systems to discover clustering features by Rough Sets (RS). The resulted clusters are presented as a hierarchical tree shown in Fig. 1.

1.3 The Organization of This Paper

This paper has two parts. The first is about the implementation of CFR. The second is about applying CFR on UN-EGDD. The remainder of this paper is organized as follows: Section 2 reviews UN-EGDD, I-EWP, and RS. Section 3 presents the propositions for CFR, Section 4 addresses the application results, Section 5 presents discussion on CFR and finally Conclusions provides the concluding remarks to close the paper.

2 Literature Review

This section contains three parts, first is about UN-EGDD, second is about I-EWP to provide criteria's relevance and importance information to rankings, and third is about clustering of RS.

2.1 UN-EGDD

E-government originates in 1993 when US President, William Clinton, announced a six-month review of the federal government, named as National Partnership for Reinventing Government (NPR), and asked Vice President, Al Gore to identify problems and find out solutions for reorganizing the federal bureaucracy, analyzing job performance of federal employees, reviewing each administrative agency and report recommendations to Congress on government reforms [18]. In the autumn of 1993, Vice President Gore presented a report to Clinton and the public about "Reengineering Through Information Technology" [19]. In early 1997 various initiatives of E-government started to enable anyone who wants to transact business with the government electronically [20].

UN-EGDD publication was undertaken by a group of senior E-government researchers and advisors at the United Nations Department of Economic and Social Affairs. The Division for Public Administration and Development Management plays the core to manage the data collection [13]. The criteria of E-government are described in the Table 1 which has preference dataset.

Table 1
Criteria of UN-EGDD

Criteria	ONLINE SERVICES
q_1	Emerging stage with limited and basic information
q_2	Enhanced stage with greater public policy and governance sources of current and archived information, such as policies, laws and regulation, reports, newsletters, and downloadable databases
q_3	Transactional stage allowing two-way interaction between the citizen and his/her government
q_4	Connected stage with integration of G2G, G2C and C2G
	TELECOMMUNICATION INFRASTRUCTURE
q_5	Estimated internet users per 100 inhabitants
q_6	Number of main fixed telephone lines per 100 inhabitants
q_7	Number of mobile subscribers per 100 inhabitants
q_8	Number of fixed internet subscriptions per 100 inhabitants
q_9	Number of fixed broadband facilities per 100 inhabitants
	HUMAN CAPITAL
q_{10}	Adult literacy rate
q_{11}	The combined primary secondary, and tertiary gross enrolment ratio

2.2 I-EWP

The evidential weight proposed by Keynes in 1921 is based on the probability relations to express the rational belief about the importance and relevance between a primary proposition (premise) and a secondary proposition (conclusion) [21, 22]. The main idea claims that the doubtful arguments relevant to decision should be considered quantitatively, instead of by logic only. Its application requires considering not only the knowledge of decision makers but also circumstances for induction [23], thus can estimate the evidential relevance like goodness and risk [3, 24]. Recently, the evidential weight is further extended to EWP [17] which is summarized below.

EWP is implemented from the induction rule, $q_{j,i}^{\geq} \rightarrow Cl_i^{\geq}$, as presented in Property 2. Four properties of [17] are used in this research. Property 1 presents the information system of I-EWP. Property 2 explains the induction rules of I-EWP. Property 3 talks about the induction evidence. Property 4 is about the reliability measures for EWP.

Property 1: The information system of I-EWP

$I-EWP = (U, Q, f, R, Cl_i^{\geq})$, where each object y has a rank assigned by decision makers, $U = \{y \mid y = 1, \dots, n\}$, $Q = \{q_1, q_2, \dots, q_m\}$, $f : U \times Q \rightarrow R$, R is a

ranking set calculated from preferences, $R \in \{1^{th}, 2^{th}, \dots, n^{th}\}$, Cl_t^{\geq} is a ranking union having nations at least t , t is a rank place like 10^{th} , and Cl_t^{\geq} is a dominance class defined by decision makers.

Property 2: An induction rule of I-EWP

$q_{j,t'}^{\geq} \rightarrow Cl_t^{\geq}$ represents how a criterion q_j supports nations to achieve the top t positions where $q_{j,t'}^{\geq}$, ($q_{j,t'}^{\geq} = \bigcup_{s \geq t'} q_{j,s}$), is also a ranking union containing the top t' positions with respect to q_j . This rule associates the ranking evidence within criterion q_j to the ranking union Cl_t^{\geq} . The association is independent to addition or removal of other criteria thus the rules are independent each other. Our design can be conceptualized as in Fig. 2.

Property 3: The induction evidence

Under the induction rule $q_{j,t'}^{\geq} \rightarrow Cl_t^{\geq}$, there are two approximations defined with boundaries \underline{x} and \bar{x} where $\underline{x} \in Cl_t^{\geq}$, $\bar{x} \in Cl_t^{\geq}$, and the rank of \underline{x} is always higher than or equal to that of \bar{x} . \underline{x} is assumed as the boundary of the important evidence and \bar{x} as the boundary of the relevant evidence. These two types of evidence are defined as:

Important evidence: $D_p^+(\underline{x})$ located in the area above \underline{x} in Fig. 2

Relevant evidence: $D_p^+(\bar{x})$ located in the area above \bar{x} in Fig. 2

The important evidence belong to the upper part of the relevant evidence in Fig. 2. The approximations based on the induction evidence are defined as:

Important approximation: $\underline{P}'(Cl_t^{\geq}) = D_p^+(\underline{x}) \cap Cl_t^{\geq}$;

Relevant approximation: $\bar{P}'(Cl_t^{\geq}) = D_p^+(\bar{x})$;

Doubtful region: $D_p^+(\bar{x}) - D_p^+(\underline{x})$.

Important approximation contains the important evidence belonging to the ranking interval above, i.e., Cl_t^{\geq} . It is same as the lower approximation of DRSA. Relevant approximation contains the evidence above the boundary \bar{x} and requires that \bar{x} belongs to the ranking interval of Cl_t^{\geq} . Doubtful region contains the evidence that are relevant but not important. The noise in this area is dissimilar to the important evidence, and is called distinguished noise. Therefore, the noise within approximations is defined as: Undistinguished noise: $D_p^+(\underline{x}) - \underline{P}'(Cl_t^{\geq})$ and Distinguished noises: $D_p^+(\bar{x}) - D_p^+(\underline{x}) - \bar{P}'(Cl_t^{\geq})$.

The distinguished noises are objects away from the important evidence, and normally located in the doubtful region. The undistinguished noises mixing with the important evidence within the Important approximation and cannot be separated each other by objective methods. Obviously, the more evidence in $\underline{P}'(Cl_i^z)$ the more important P is; the more noise in $\overline{P}'(Cl_i^z)$ the less relevant P is. Due to the impact of noises, \underline{x} and \overline{x} are non-deterministic priori. Therefore, \underline{x} and \overline{x} are presented as slash lines in Fig. 2. They can be obtained by approximating the optimal classification with the minimum distinguished noises.

Property 4: Measures of EWP

Three measures related to EWP of Fig. 4 are defined below.

- Evidence-accuracy rate (α') [3, 24]

An accuracy rate presents the ratio of ‘Important approximation’ to ‘Relevant approximation,’ i.e., the degree of the properly classified evidence relative to the possibly relevant evidence, and is defined as:

$$\alpha' = \frac{|\underline{P}'(Cl_i^z)|}{|\overline{P}'(Cl_i^z)|} \text{ where } \alpha' \text{ for a logical implication represents the degree of}$$

necessary condition of ‘Important approximation’ in the relevant evidence.

- Evidence-coverage rates (CR') [8, 24]

A coverage rate expresses the ratio of ‘Important approximation’ relatively belonging to the ranking union, and is defined as:

$$CR' = \frac{|\underline{P}'(Cl_i^z)|}{|Cl_i^z|} \text{ where } CR' \text{ for a logical implication represents the degree of}$$

sufficient condition that ‘Important approximation’ influences the ranking union.

- Evidence-certainty rate (Cer') [8]

A certainty rate expresses the ratio of objects in ‘Important approximation’ relatively belonging to Important evidence:

$$Cer' = \frac{|\underline{P}'(Cl_i^z)|}{|D_p^+(x)|} \text{ where } |\cdot| \text{ means the number of evidence in a set. } Cer'$$

represents the degree of reliability of $\underline{P}'(Cl_i^z)$.

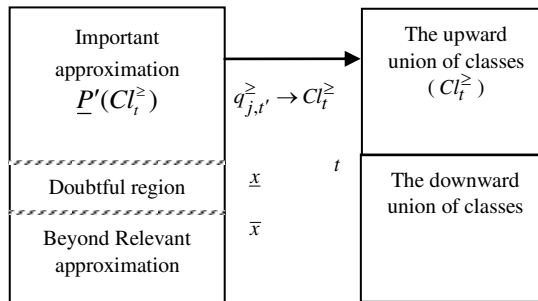


Figure 2

Approximations based on the induction evidences

- The values of EWP

The classification rate for $q_{j,t'}^{\geq} \rightarrow Cl_t^{\geq}$ needs to consider both, the sufficient and necessary conditions. The product of CR' and α' will be a unique value on an indifference curve, which originates from the product of sufficient and necessary ratios for the indifferent induction rules. The induction measures are independent to addition or removal of other criteria. The product values thus can be used for preference orders. Further, the quality of classification needs address the reliability concern. According to the logical implication, a quality classification can be formulated as:

Quality classification \Leftrightarrow Minimum uncertainty

‘Quality classification if and only if minimum uncertainty’ can be processed by mathematics to get a unique value on an indifference curve. Therefore, the value of EWP, g_j'' , for criterion q_j is the quality classification rate considering the minimum uncertainty, i.e., $g_j'' = \text{Max} \{ \alpha' \times CR' \times Cer' \}$.

2.3 Rough Sets (RS)

Rough sets proposes an approximation space based on equivalence relations. The objects within an equivalence classes have the same characteristics. The criteria dependency represents a measure about the association degree between the partitions based on criteria. The complicate dependency has the association between two set of criteria. The basic dependency [5] related to the clustering features, is described next.

An approximation space presented by a mathematical model is formulated as:

$A = (U, R)$ where U is a set of objects not necessary with preference data and $R \subseteq U \times U$ represents an equivalence relation on U .

The equivalence classes of R are denoted as: $R^* = \{X_1, X_2, \dots, X_i, \dots\}$ where i is an index for a relation. For any subset $X \subseteq U$ the lower and upper approximation of X is defined as:

$\underline{A}(X) = \bigcup_{X_i \subseteq X} X_i$ and $\overline{A}(X) = \bigcup_{X_i \cap X \neq \emptyset} X_i$ where $\underline{A}(X)$ is the union of all those elementary sets in A , which are individually contained by X , whereas $\overline{A}(X)$ is the union of all those X_i of which has a non-empty intersection with X .

A knowledge presentation for the dependence relationship between criteria is built as:

$KRS = (U, C, D, V', \rho)$ where C is the set of attributes, D is the set of action attributes, V' represents the value set which does not require preferences within the same attribute, $\rho: U \times (C \cup D) \rightarrow V'$ is an information function, $V' = \bigcup_{C \cup D} V_a$, V_a is a domain of a attribute (attribute is same as a criterion in this research due to numerical values only), and $a \in C \cup D$. The dependency measure between two sets of attributes, A and B , based on KRS is presented as:

$$\gamma_A(B) \text{ where } \gamma_A(B) = \frac{POS_A(B)}{|U|}, 0 \leq \gamma_A(B) \leq 1, A \subseteq C, B \subseteq D,$$

$POS_A(B) = \bigcup_{Y_i \in B^*} \underline{A}(Y_i)$ where $POS_A(B)$ is the positive region of B^* in A , and $B^* = U / B = \{Y_1, Y_2, \dots, Y_i, \dots\}$ represent a set of U partitions constructed from equivalence relations based on B .

3 CFR

This section presents definitions of CFR with two phases. First is about replacing preferences with EWP, presented in Definition 1. Second is the clustering features generated by RS, presented in Definition 2 to 6.

3.1 Replacing preferences with EWP

The quality classification rates generated from I-EWP are expressed as $\{g_{ij}''\}$ where i is an index for a nation, $i \in [1, \dots, n]$, j is an index for a criterion, $j \in [1, \dots, m]$. $\{g_{ij}''\}$ is abbreviated as EWP in this paper. g_{ij}'' only performs locally and the natural clusters of EWP cannot be clear at a glance of g_{ij}'' only. The reason for the local performance of g_{ij}'' is that its effectiveness exists only on a part of

nations. To give a natural clusters on all collections of g_{ij}'' , g_{ij}'' are used to replace the values corresponding to nations and criteria in Property 1.

Definition 1: Replacement

$$\forall_{i \in \{1, \dots, n\} \text{ and } j \in \{1, \dots, m\}} (r_{ij} = g_{ij}'')$$

where $r_{ij} \in R$ and $f : U \times Q \rightarrow R$ in Property 1

3.2 Generation of Clustering Features

The analysis of clustering features needs to globally consider the topology of dataset. There are three definitions to present the design and implementation. Definition 2 for the information system CFR. The domain values corresponding to nations and criteria are formed by transforming EWP into orders row by row. Users can see which criterion is the most relevant and important to some rank assigned by decision makers. Definition 3 presents how the roughness relations are formed. Definition 4 presents the dependency rules.

Definition 2: The information system of CFR

The information system of CFR, containing n tuples of $(r_{i1}, r_{i2}, \dots, r_{im})$, is defined as $CFR = (U, Q, Cl, R', \rho)$ where

$$R' = \left\{ \begin{array}{l} 1 \quad r_{ij} = \max\{r_{i1}, r_{i2}, \dots, r_{im}\} \\ 0 \quad \text{otherwise} \end{array} \right\} \text{ and } \rho : U \times Q \rightarrow R'.$$

Definition 3: Approximation space of CFR

The approximation of CFR is defined as $A = (U, \Gamma)$ where $\Gamma = (x_i, x_{i'})$ means x_i and $x_{i'}$ have a relation on a criterion which is of the most significant; $(x_i, x_{i'}) \in \Gamma$ iff $(x_i, r_{ik}) = (x_{i'}, 1)$ and $(x_{i'}, r_{i'k}) = (x_i, 1)$, i and i' are indexes of nations. Therefore, the equivalence class, having the same relevant and important criterion, is formulated as: $A^* = \{X_1, \dots, X_k, \dots\}$ where k is an index of clusters, $k \leq m$, and $A = Q$. The number of clusters equal to or less than the number of criteria in Q makes operation simple and easy.

Definition 4: Ranking intervals

The ranking intervals are defined as $Cl^* = \{Cl_{>L_k}^{\leq H_k}, \dots, Cl_{>L_k}^{\leq H_k}, \dots\}$ where $Cl_{>L_k}^{\leq H_k} = \{Cl_i \mid L_k < t \leq H_k\}$. For the class $Cl_{>L_k}^{\leq H_k}$, H_k is the high boundary and L_k is the low boundary. These intervals will map to the equivalence classes of Definition 2. Through the mapping, nations in an interval have the same features

as the corresponding approximation. In our design, CI^* is an assumption in the beginning. The size of CI^* counts on the dependency measure and approximation operation next.

Definition 5: Dependency measure for *CFR*

A ranking interval ($CI_{>L_k}^{\leq H_k}$) depending on an equivalence class (X_k) is presented as a rule $X_k \rightarrow CI_{>L_k}^{\leq H_k}$. The dependency measure is defined as:

$$\gamma_{\{q_k\}}(CI_{>L_k}^{\leq H_k}) = \max \left\{ \frac{POS_{\{q_k\}}(CI_{>L_k}^{\leq H_k})}{|U_k|} \right\} \text{ where } \{q_k\} \text{ is a set criteria for the}$$

equivalence class X_k , $X_k = (U_k, \Gamma_k)$, and $\Gamma_k = (x_i, x_{i'})$ means x_i and $x_{i'}$ have a relation on the same criterion q_k . Therefore, nations having the most relevant and important on criterion q_k are grouped together to support the rule, $X_k \rightarrow CI_{>L_k}^{\leq H_k}$.

Under this definition, at most m stages can be available.

Definition 6: Approximation operations

Considering to have a bigger cluster provides a disjunctive operation on approximations, X_k and $X_{k'}$, an is defined to expand the ranking interval. The larger approximation will have more criteria in the relational condition, i.e., A has more criteria in P and fewer partitions in U/P .

$$\underline{A}(X_k \cup X_{k'}) = \underline{A}(X_k) \cup \underline{A}(X_{k'}) \text{ if } k \text{ and } k' \text{ belong to the same stages}$$

$$\underline{A}(X_k) \cap \underline{A}(X_{k'}) = \emptyset \text{ if } k \text{ and } k' \text{ belong to different stages}$$

4 The Application Results

The application results of CFR have three parts in Table 2. The first, shows two clusters. The second, presents the maximum evidential weight of $r_{i1}, r_{i2}, \dots, r_{im}$ in EWP column. The third, presents EWP orders of Definition 2 in R' column. The cells having values lower than the maximum weight are presented as empty.

Table 2
EWP orders for E-government stages

Ranks	Nations	Stage	EWP		R'	
			$g_5^{\#}$	$g_{11}^{\#}$	$r_{i,3}$	$r_{i,11}$
1	Liechtenstein	1		1.00		1
2	Monaco	1		1.00		1
3	Switzerland	1		1.00		1
4	Iceland	1		0.75		1
5	Luxembourg	1		0.80		1
6	Denmark	1		0.67		1
7	Republic of Korea	1		0.77		1
8	Netherlands	1		0.67		1
9	Sweden	1		0.67		1
10	United Kingdom	1		0.69		1
11	France	1		0.84		1
12	Norway	1		0.85		1
13	Germany	1		1.00		1
14	Belgium	1		1.00		1
15	New Zealand	1		0.93		1
16	Andorra	1		0.88		1
17	Finland	1		0.82		1
18	Malta	1		0.78		1
19	Antigua and Barbuda	1		0.77		1
20	Canada	1		0.73		1
21	Austria	1		0.79		1
22	Croatia	1		0.84		1
23	Singapore	2	0.87		1	
24	States	2	0.83		1	
25	Israel	2	0.80		1	
26	San Marino	2	0.85		1	
27	Barbados	2	0.82		1	
28	Italy	2	0.80		1	
29	Estonia	2	0.77		1	
30	Russian Federation	2	0.84		1	
31	Ireland	2	0.83		1	
32	Australia	2	0.81		1	

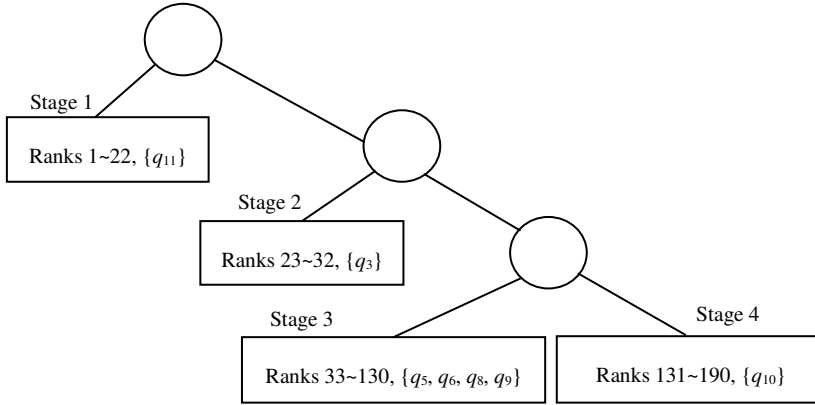


Figure 3
The stages of UN-EGDD

The clustering features are named as stages for illustration in Fig. 3. Their dependency rules are presented below.

Rule 1: If a nation's q_{11} is the most relevant and important then the nation belongs to Sage 1 where the dependency rule as $X_{11} \rightarrow CI_{>23}^{\leq 1}$,

$$\gamma_{\{q_{11}\}}(CI_{>L_{23}}^{\leq H_{11}}) = 1,$$

$$X_{11} = \{\underline{A}(x_i, x_{i'}) \mid (x_i, x_{i'}) \in \Gamma \text{ iff } (x_i, r_{i,11}) = (x_{i'}, r_{i',11}), r_{i,11} = 1, \text{ and } r_{i',11} = 1\}$$

Rule 2: If a nation's q_3 is the most relevant and important then the nation belongs to Stage 2 where the dependency rule as $X_3 \rightarrow CI_{>33}^{\leq 23}$,

$$\gamma_{\{q_3\}}(CI_{>L_{33}}^{\leq H_{23}}) = 1,$$

$$X_3 = \{\underline{A}(x_i, x_{i'}) \mid (x_i, x_{i'}) \in \Gamma \text{ iff } (x_i, r_{i,3}) = (x_{i'}, r_{i',3}), r_{i,3} = 1, \text{ and } r_{i',3} = 1\}$$

Rule 3: If a nation's $q_5, q_6, q_7, q_8,$ or q_9 is the most relevant and important then the nation belongs to Stage 3, where the dependency rule as

$$X_{5689} \rightarrow CI_{>130}^{\leq 33}, X_{5689} = X_5 \cup X_6 \cup X_8 \cup X_9, \gamma_{\{q_5, q_6, q_8, q_9\}}(CI_{>L_{130}}^{\leq 33}) = 0.88,$$

$$X_{5689} = \{\underline{A}(x_i, x_{i'}) \mid (x_i, x_{i'}) \in \Gamma \text{ iff } (x_i, r_{i,5}) = (x_{i'}, r_{i',5}), r_{i,5} = 1 \text{ and } r_{i',5} = 1,$$

$$(x_i, r_{i,6}) = (x_{i'}, r_{i',6}), r_{i,6} = 1 \text{ and } r_{i',6} = 1, (x_i, r_{i,8}) = (x_{i'}, r_{i',8}), r_{i,8} = 1 \text{ and } r_{i',8} = 1,$$

$$(x_i, r_{i,9}) = (x_{i'}, r_{i',9}), r_{i,9} = 1 \text{ and } r_{i',9} = 1\}$$

Rule 4: If a nation's q_{10} is the most relevant and important then the nation belongs to Stage 4 where the dependency rule as $X_{10} \rightarrow CI_{>L_{491}}^{\leq H_{130}}$,

$$\gamma_{\{q_{10}\}}(CI_{>L_{491}}^{\leq H_{130}}) = 0.94, \text{ and}$$

$$X_{10} = \{\underline{A}(x_i, x_{i'}) \mid x_i, x_{i'} \in \Gamma \text{ iff } (x_i, r_{i,10}) = (x_{i'}, r_{i',10}), r_{i,10} = 1, \text{ and } r_{i',10} = 1\}$$

CFR has two merits. The first, is to integrate classification and clustering together through the characteristics of the information system. One is the characteristic of preferences and the other is EWP. Even DRSA and RS function differently, they can complement each other to discover unknown information. The second, is to simply and easily find the number of clusters. The resulting clusters are featured with the equivalence relations, composed of the most relevant and important characteristic.

5 Discussions

This section has two parts. One is about the technique discussion. The other is a case study for the clustering stages of E-government.

5.1 Technique Discussion

The technique discussion section has four parts. They are goals, methodology, applications and comparison. This research aims to transform the local information from classification to discover a global topology for E-government. The topological clusters map to the ranking intervals thus providing users a global view for E-government stages.

The methodology of CFR takes top relevance and importance as the requirement for the “indiscernability” relationship. EWP contain the characteristics related to a nation’s rank. The dependency rules based on EWP thus can present the clustering stages and features, leading to a view for the ranking levels of E-government. The application of CFR on UN-EGDD successfully discovers the topology of E-government has four stages, such as, Adult literacy, Infrastructure development, Online transaction, and expanding e-service through enrollment.

The functions comparison of CFR with DRSA and RS is processed with fair benchmarking, i.e., information system of preferences. The comparison in clustering features and ranks classification are listed in Table 3. The ranks classification is able to separate nations according to the ranking intervals and the clustering features can give natural groups with the dependency rules. The result shows that CFR has both functions of DRSA and RS, and provides an extension beyond DRSA or RS individually.

Table 3
The functions comparison of DRSA, RS, and CFR

	DRSA	RS	CFR
Clustering features	0	1	1
Ranks classification	1	0	1
Total functions	1	1	2

5.2 The Case Study

These dependency rules show that the rankings of UN-EGDD depend on four stages. These stages can be explained by the clustering features such as:

- Stage 1, the educational enrollment plays a critical role to sustain e-government at the top. United Nations E-government Survey 2012 reports a big challenge in development, i.e., low e-service usage. Generally, citizens still use government website much more for information than for transactions. Enrollment, grant application, and so on in education can achieve two merits [25].
 - Closing existing gap of e-service availability and usage;
 - Significantly moving usage beyond the realm of information to more complex transactions and services such as e-consultation.

This stage reveals that the expanding usage of e-service can advance the full benefit of E-governments.

- Stage 2, the transactional interactions between government and citizens is the key to fulfilling online service. United Nations E-government Survey 2012 specifies that the sustainable development of the use of Information and Communication Technology (ICT) requires e-participation to contribute the socio-economic uplift of the people. E-government will play a role of proactive facilitator to treat people as active partners, by promoting user uptake, addressing the needs and concerns of the citizenry, especially the vulnerable. Furthermore, greater efficacy and effectiveness in the sustainable development can achieve solving the digital divide [26].
- Stage 3, the telecommunication infrastructure plays the most significant role in developing the fundamentals of E-government. The infrastructure relates to investment, maintenance, needs of cooperative and shared resources, telephone density, Internet penetration, existing speeding of technology change, allowance for convergence, etc [27]. As the evolution of increasingly powerful and user-friendly technologies, E-government can take the advantages, to provide more effective and integral participation thus generate more opportunities of interaction with citizens [28].
- Stage 4, the adult literacy, is the more significant in influencing the least developed nations. United Nations E-government Survey 2012 points out that lack of infrastructure and functional literacy are two difficulties of the least developed nations, such as, some of the African nations. These two factors illustrate low service provision and user uptake for the majority of the populations such as India, Bangladesh, Bhutan, Pakistan and Nepal [29].

Conclusions

This research proposes the CFR method to integrate DRSA and RS. The result shows four clustering features of the E-government stages. Technically, CFR generates evidential weights of criteria for nations' ranks by DRSA then, partitions nations into the equivalence classes by RS. The tree structure of clustering stages shows how UN-EGDD rankings depend on criteria. In the case study, enhancing adult literacy, building telecommunication infrastructures, providing online transactional interactions and expanding usage of e-service through education enrollments are critical points from the birth of E-government to the later mature stages.

References

- [1] Pawlak, Z., Skowron, A. (2007) Rough Sets: Some Extensions, *Information Sciences* 177(1): 28-40
- [2] Pawlak, Z., Skowron, A. (2007) Rough Sets and Boolean Reasoning, *Information Sciences* 177(1): 41-73
- [3] Pawlak, Z. (1997) Rough Set Approach to Knowledge-based Decision Support, *European Journal of Operational Research* 99(1): 48-57
- [4] Pawlak, Z. (1982) Rough Sets, *International Journal of Information and Computer Sciences* 11: 341- 356
- [5] Pawlak, Z., Wong, S. K. M., Ziarko, W. (1988) Rough Sets: Probabilistic versus Deterministic Approach, *International Journal of Man-Machine Studies* 29(1): 81-95
- [6] Słowiński, R., Stefanowski, J. (1989) Rough Classification in Incomplete Information Systems, *Mathematical and Computer Modelling* 12(10–11): 1347-1357
- [7] Pawlak, Z., Grzymala-Busse, J., Slowinski, R., Ziarko, W. (1995) Rough Sets, *Commun. ACM* 38(11): 88-95
- [8] Pawlak, Z. (2002) Rough Sets and Intelligent Data Analysis, *Information Sciences* 147(1–4): 1-12
- [9] Pawlak, Z. (2004) Flow Graphs and Intelligent Data Analysis. *Fundamenta Informaticae* 64(1-4): 369-377
- [10] Pattaraintakorn, P., Cercone, N., Naruedomkul, K. (2006) Rule Learning: Ordinal Prediction based on Rough Sets and Soft-Computing, *Applied Mathematics Letters* 19(12): 1300-1307
- [11] Liu, H., Yu, L. (2005) Toward Integrating Feature Selection Algorithms for Classification and Clustering, *IEEE Transactions on Knowledge and Data Engineering* 17(4): 491-502

- [12] Dy, J. G., Brodley, C. E. (2000) Feature Subset Selection and Order Identification for Unsupervised Learning, In Proc. 17th International Conf. on Machine Learning, Morgan Kaufmann, 247-254
- [13] United Nations E-Government Development Database, <http://unpan3.un.org/egovkb/>
- [14] Howard, M. (2001) e-Government across the Globe: How Will “e” Change Government? *Government Financial Review* 17(4): 6-9
- [15] Yildiz, M. (2007) E-government Research: Reviewing the Literature, Limitations, and Ways, *Government Information Quarterly* 24(3): 646-665
- [16] United Nations, United nations E-government survey 2012: E-government for the people, United Nations Department of Economic and Social Affairs, United Nations, New York, 2012. [http://unpan3.un.org/egovkb/global_reports/index.htm /](http://unpan3.un.org/egovkb/global_reports/index.htm/)
- [17] Ko, Y.-C., Fujita, H., Tzeng, G.-H.: A Simple Utility Function with the Rules-verified Weights for Analyzing the Top Competitiveness of WCY 2012, *Knowledge-Based Systems*, 58: 58-65 (2014)
- [18] <http://govinfo.library.unt.edu/npr/whoweare/historyofnpr.html>
- [19] <http://govinfo.library.unt.edu/npr/library/papers/bkgrd/brief.html>
- [20] <http://govinfo.library.unt.edu/npr/whoweare/historypart4.html>
- [21] Keynes, J. M. (1921) *The Weight of Argumens, A Treatise on Probability*, Macmillan, London
- [22] Keynes, J. M. (1921) *The Meaning of Probability, A Treatise on Probability*, Macmillan, London
- [23] Keynes, J. M. (1921) *The Foundations of Statistical Inference, A Treatise on Probability*, Macmillan, London
- [24] Greco, S., Matarazzo, B., Slowinski, R. (2001) Rough Set Theory for Multicriteria Decision Analysis, *European Journal of Operational Research* 129(1): 1-47
- [25] United Nations (2012) Chapter 6 - Expanding Usage to Realize the Full Benefits of E-government, United Nations E-government Survey 2012: E-government for the People, United Nations Department of Economic and Social Affairs, United Nations, New York
- [26] United Nations (2012) Chapter 2 - Progress in Online Service Delivery, United Nations E-government Survey 2012: E-government for the People, United Nations Department of Economic and Social Affairs, United Nations, New York
- [27] United Nations (2012) Chapter 3 - Taking a Whole-of-government Approach, United Nations E-government Survey 2012: E-government for

the People, United Nations Department of Economic and Social Affairs, United Nations, New York

- [28] United Nations (2012) Chapter 4 - Supporting Multichannel Service Delivery, United Nations E-government Survey 2012: E-government for the People, United Nations Department of Economic and Social Affairs, United Nations, New York
- [29] United Nations (2012) Chapter 1 - World e-government Rankings, United Nations E-government Survey 2012: E-government for the People, United Nations Department of Economic and Social Affairs, United Nations, New York

Model Predictive Controller-based, Single Phase Pulse Width Modulation (PWM) Inverter for UPS Systems

Syed Faiz Ahmed, Ch. Fahad Azim, Hazry Desa, Abadal-Salam T. Hussain

Universiti Malaysia Perlis, Centre of Excellence for Unmanned Aerial System,
01000, Kangar, Perlis, Malaysia

E-mail: syedfaiz@unimap.edu.my, fahad.azim@hamdard.edu,
hazry@unimap.edu.my, abadal@unimap.edu.my

Abstract: This research article discusses a Model Predictive Control(MPC) based, digital control strategy for single-phase Pulse Width Modulated (PWM) voltage source inverters, used in Uninterrupted Power Supplies (UPS) for single-unit systems. In this research work, the development of inverter system based on state-space model is first studied and then MPC technique is implemented as control strategy for single inverter. The experimental setup includes a single inverter using a switch and a de-bouncing circuit and a DSP Kit. Experimental results for open-loop and closed-loop single inverter system using a linear and a dynamic load is presented. The effectiveness of the proposed algorithm for controlling the system has been examined and the dynamic performance and the robustness property are demonstrated. The system has been implemented and tested with different loads. The results show that the inverter performs reasonably well.

Keywords: Model Predictive Controller; Pulse Width Modulated; Single Phase Inverter; UPS

1 Introduction

The PWM inverter is used in a wide variety of industrial applications, such as power supply; adjustable speed AC servo drives [1] and uninterruptible power supply (UPS) [2]. In such applications, the basic function of the PWM inverter is to convert the DC power to AC power. The quality of the output AC power is highly dependent on the performance of the PWM inverter.

A good AC power supply should have low harmonic output, under disturbances and uncertainties, good dynamic response to disturbance, and remain stable under all operating conditions. In recent years, many attempts have been made to

develop various control schemes for PWM inverters, to meet the above mentioned requirements. Some of the schemes are Fuzzy adaptive proportional-integral-derivative (PID) control [3], dead beat control, one sampling ahead preview control, and sliding mode control [4-5].

Many feedback control techniques may exhibit good dynamic performance but in this paper a Model Predictive Control (MPC) technique is proposed to control a single inverter. MPC employs a strategy known as the receding-horizon approach [6]. Based on the dynamic model of the system, MPC starts predicting the future control action in such a way that it minimizes a specific objective function over a prediction horizon. Once MPC completed its prediction process, it implements optimal control action and at the next sampling interval, the control estimation is repeated again with the new available information.

2 Low Total Harmonic Distortion Output Voltage Control & Inverter Current Control

Techniques for producing low Total Harmonic Distortion (THD) in PWM inverters (single-phase) have discussed in several prior works. In the early days, the carrier-modulated PWM techniques such as the triangular wave comparison PWM were very popular [7]. Microcomputer-based techniques using preprogrammed PWM patterns have also been utilized. In these techniques, the PWM patterns are generated by computing switching edges that satisfy certain performance criteria such as controlling the fundamental component and eliminating specified harmonics [8]. These techniques have drawbacks of slow voltage regulation response and phase displacement with load varies. More recent PWM techniques also include time optimal response switching PWM [9].

With the advances in Digital Signal Processing (DSP) Technology, digital instantaneous real time control of voltage and current for PWM inverters has been the focus of many research works. Among these are the real-time deadbeat-controlled PWM and other techniques based on instantaneous feedback controls [10]. These techniques may achieve very fast response times for load disturbances when properly designed, but it is also known that these systems have a high THD for non-linear loads. Techniques based on sliding mode control theory and intelligent control using fuzzy logic or neural networks have also been attempted. Like the previously mentioned techniques, these techniques also lack the ability to completely reject the harmonic disturbances in the output voltage waveforms due to non-linear loads. Recently, the use of the internal model principle to achieve very low THD output voltage in single phase PWM inverters has been reported [11]. The theory is based on the internal model principle proposed by which states that the asymptotic tracking of controlled variables toward the corresponding references in the presence of disturbances (zero steady state tracking error) can be

achieved if the models that generate these references and disturbances are included in the stable closed-loop systems. In other words, if we include the frequency modes of the references and the disturbances to be eliminated in the control loop, then the steady state error will not contain these frequency modes. Applying the internal model principle into the output voltages control in a three-phase PWM inverter means that the fundamental frequency mode (50 Hz or 60 Hz) has to be included in the controller since the references vary at this frequency. Elimination of the voltages errors due to the load currents at other harmonics frequencies can then be achieved by including the frequency modes of these harmonics into the controller. The repetitive control guarantees zero steady state error at all the harmonic frequencies less than half of the sampling period [12]. However, the repetitive control is not easy to stabilize for all unknown load disturbances and cannot deliver very fast response for fluctuating load [13]. The latter problem is solved by including a ‘one sampling ahead preview controller’ and the stability result are enhanced by providing adaptive mechanisms for unknown load disturbances.

3 Model Predictive Control

MPC (Model Predictive Control), as the name suggests it is a controller that predicts the future value and implements the control action accordingly. The main task of the MPC is to solve the problem of generating future input values for a process model. Hence, it is necessary to have a dynamic model of process system i.e process model [14]. Different parameters (control variables and disturbance with constraints) from the process model are taken into accounts that are compulsory requirement for MPC to solve the problem based on the process model and process measurements as shown in Figure 1. The process through which MPC predicts the future values is shown in Figure 2. At time k (current time), MPC takes measurement data from the process model’s output. First objectives and constraints of desired output, set point and manipulated variable are defined, than MPC starts predicting the future control action by choosing the suitable values of control horizon M and prediction horizon P . Once MPC completes its prediction process, it implements best control action and then move to next time step i.e $k + 1$, this process repeated up to some define time instants T .

At previous time point t_{k-1} , the optimal objective function is calculated and generates control action, u_k which depends on the previous state vector $x(k-1)$ which will be input vector for the next interval $[t_{k-1}, t_k]$. At the next time point t_k a new input u_{k+1} for the process model will be calculated from objective

function that depends upon present state vector $x(k)$, similarly at the next time point t_{k+1} again a new control action u_{k+2} will be calculated from updated objective function and this process repeated over the interval $[t_{k-1}, T]$ to determine the optimal solution for the process model.

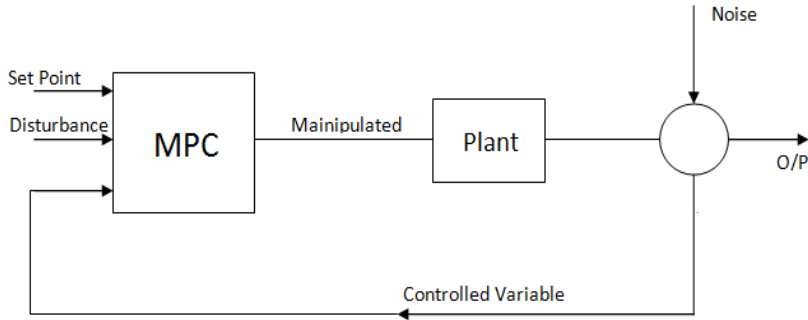


Figure 1
MPC based process model system

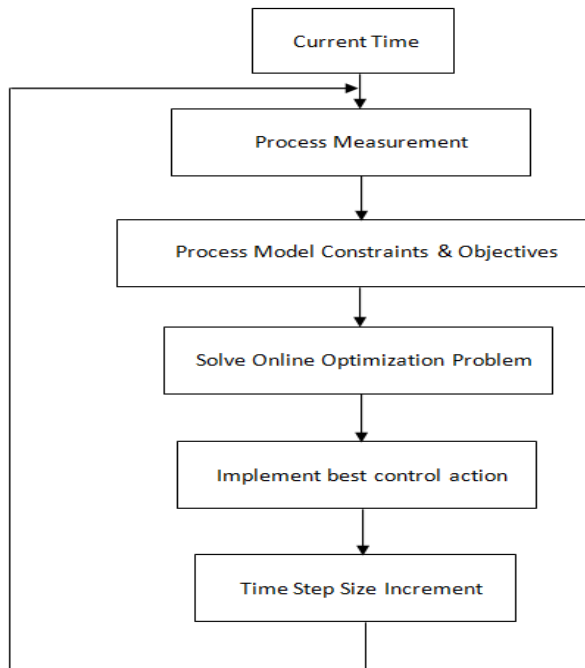


Figure 2
Model predictive control scheme

4 Modeling and Controller Design of the System

In this section, first, discrete state space model of single phase inverter is developed and then on the bases of that model, a Model Predictive Controller is designed to achieve better closed-loop control of the single phase inverter system.

4.1 Modeling of a Single-phased Inverter

The inverter circuit basically comprises of AC to DC converter and controlled DC to AC converter systems with an output LC filter as shown in Fig. 3. The controlled switching sequence of this inverter is changeable up on the requirement of the user i.e inverter output waveform must be same as desired waveform. The state variables of Figure 3 single phased PWM controlled inverter are the output voltage V_o and its derivative, i.e

$$x(t) = \begin{bmatrix} V_o \\ \dot{V}_o \end{bmatrix} \quad (4.1)$$

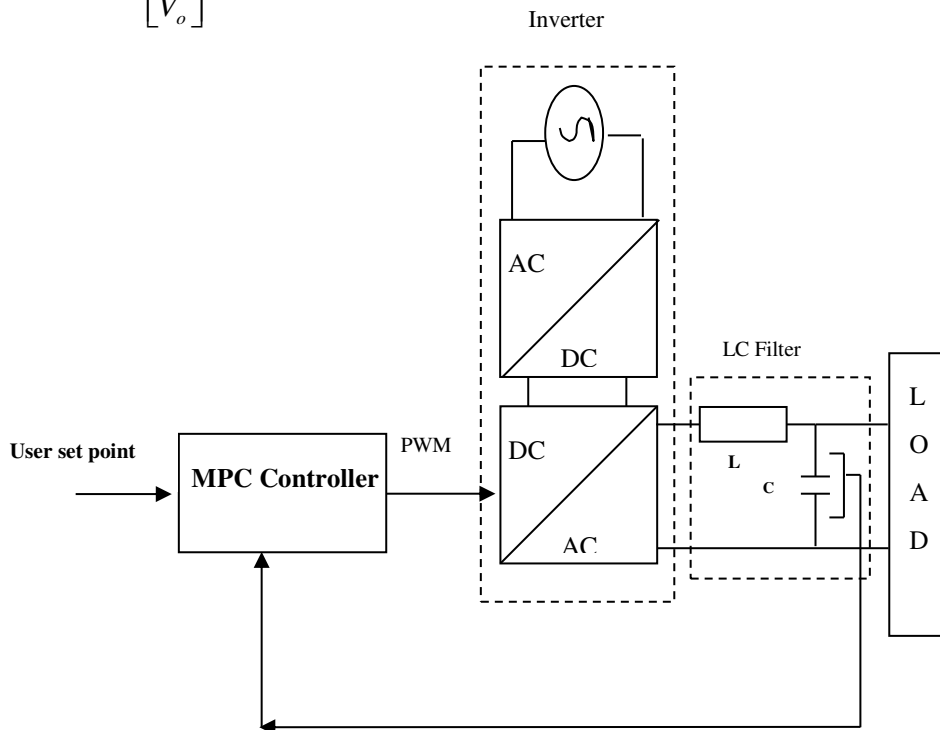


Figure 3
Single phased MPC based inverter

And the system can be modeled using following state-space model:

$$\dot{\mathbf{x}}(t) = \mathbf{A}\mathbf{x}(t) + \mathbf{B}u(t) \quad (4.2)$$

$$\mathbf{y}(t) = \mathbf{C}\mathbf{x}(t) \quad (4.3)$$

Where:

$$\mathbf{A} = \begin{bmatrix} 0 & 1 \\ -\frac{1}{LC} & -\frac{r}{L} \end{bmatrix}$$

$$\mathbf{B} = \begin{bmatrix} 0 \\ \frac{1}{LC} \end{bmatrix}$$

And

$$\mathbf{C} = [1 \quad 0]$$

Where u is the input voltage, r is the inductor equivalent series resistor, $L= 20 \mu\text{H}$ and $C= 1500 \mu\text{F}$ are the value of Inductance and Capacitance respectively. By choosing T as sampling time state space model of equation (4.2) and (4.3) will become discretized state space model as:

$$\mathbf{X}(kT + T) = \mathbf{R}\mathbf{X}(kT) + \mathbf{S}\Delta u(kT) \quad (4.4)$$

$$\mathbf{y}(kT) = \mathbf{C}\mathbf{X}(kT) = V_o(kT) \quad (4.5)$$

Where

$$\mathbf{R} = \begin{bmatrix} \bar{R}_1 & \bar{S}_1 & 0 \\ 0 & 0 & 0 \\ c & 0 & 1 \end{bmatrix}$$

With

$$\bar{R}_1 = e^{AT}$$

$$\bar{S}_1 = \left[\int e^{AT} dt \right] \mathbf{B}$$

$$S = \begin{bmatrix} S_0 \\ 1 \\ 0 \end{bmatrix}$$

And

$$C = [1 \quad 0 \quad 0 \quad 1]$$

4.2 Controller Design

Model predictive controller is selected for better controlling of the inverter, it predicts control signal in such a way, that it minimizes define cost function that is error signal between the output voltage and desire voltages of the inverter over specified prediction horizon. MPC starts predicting the future control action by choosing the suitable values of control horizon M , prediction horizon P and control-weighting factor r use for unwarranted control activity compensator. Once MPC completes its prediction process, it implements best control action and then at the next sampling interval, the control estimation is repeated again with the new information. As a result, the performance of the system increases.

Thus the objective function for single phase inverter can be formulated as:

$$E_c = \sum_{j=1}^p \left\| V_o^*(kT + jT) - \hat{V}_o(kT + jT|kT) \right\|^2 + r \sum_{j=1}^M \left\| \Delta u(kT + jT - T) \right\|^2 \quad (4.6)$$

Subject to the constraint:

$$\Delta u(kT + jT - T) = 0 \forall j > M \quad (4.7)$$

And the optimal solution to the optimization problem of the inverter:

$$U_{opt}(kT) = K_1 V_0^*(kT) + K_2 \mathbf{X}_{opt}(kT) \quad (4.8)$$

Therefore the control law will be:

$$\Delta u(kT) = K_1 V_0^*(kT) + K_2 \hat{\mathbf{X}}(kT) \quad (4.9)$$

Where X_{opt} and \hat{X} are the optimal and estimated state vectors respectively and K_1 & K_2 are the controller gains.

5 Generation of PWM Signals

The main outputs from the controller are the PWM generation signal and the direction signal, which are fed into the inverter. Fig. 3 shows the PWM signal obtained from the PWM inverter. The digital controller used in this experiment supports a wide operating voltage range of ± 10 V. The maximum supply voltage to the controller must not be greater than 10 V. The PWM signals with various duty cycles according to the different supply voltages between operating range are described below.

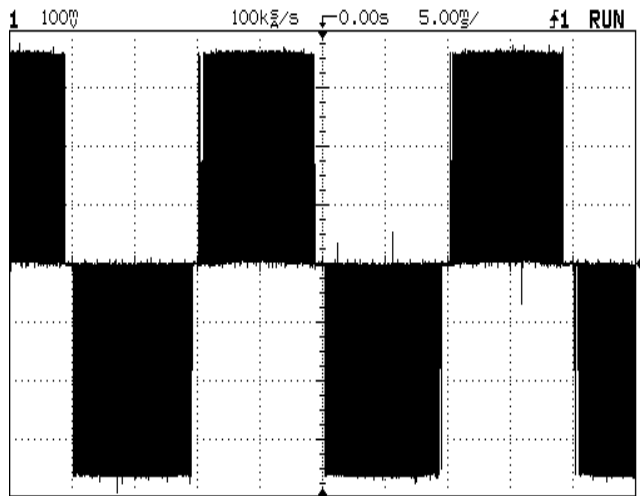


Figure 3
PWM signal from the amplifier

5.1 PWM Signals with Various Duty Cycles

The PWM signal is used to encode a specific analog signal level digitally. The PWM signal is still a digital signal because, at any given instant, the full DC supply is either fully “ON” or “OFF”. The voltage and current supply to the analog loads, by means of ON and OFF pulses train. The on-time is the time during which the DC supply is applied to the load, and the off-time is the period during which DC supply is switched off. Given a sufficient bandwidth, any analog value can be encoded with PWM.

Figs. 4, 5 and 6 shows the PWM output when the duty cycle is 25%, 50% and 75% respectively. The command input voltages are as follows: 1.25 V, 2.5 V, and 3.75 V respectively.

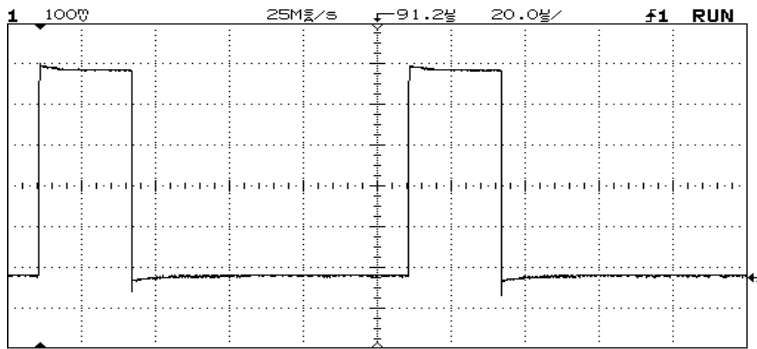


Figure 4
PWM signal at 25% duty cycle

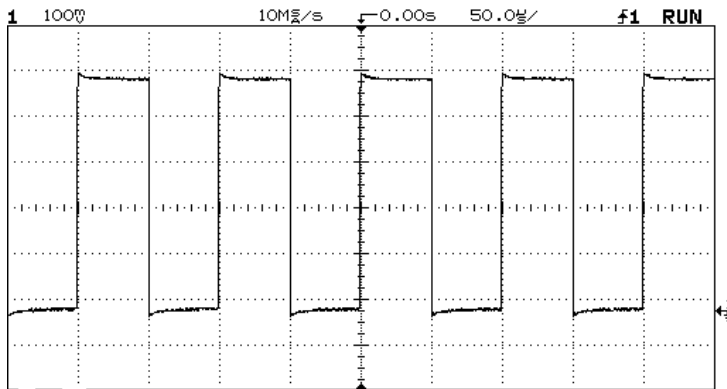


Figure 5
PWM signal at 50% duty cycle

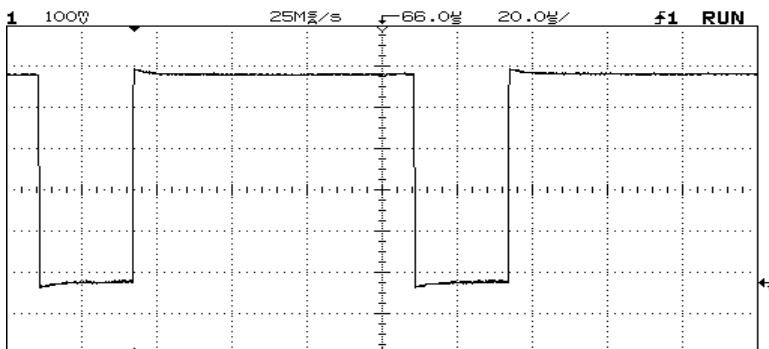


Figure 6
PWM signal at 75% duty cycle

6 Experimental Results for Single Inverter System

The experimental setup has been set as shown in Figure 7. The PWM input to the inverter is based on a sinusoidal reference voltage of amplitude 0.95 V from the digital processor. With a DC voltage of 40 V to the inverter, the desired output voltage of the system should be a sinusoidal waveform of 70 V peak to peak. The output voltage has been measured after the LC filter under no load and load conditions. Resistive loads of 100 Ω and 200 Ω were used in the closed-loop test.

In the closed-loop system, the output voltage is measured using the voltage sensor and feedback to the controller for control actions to be taken.

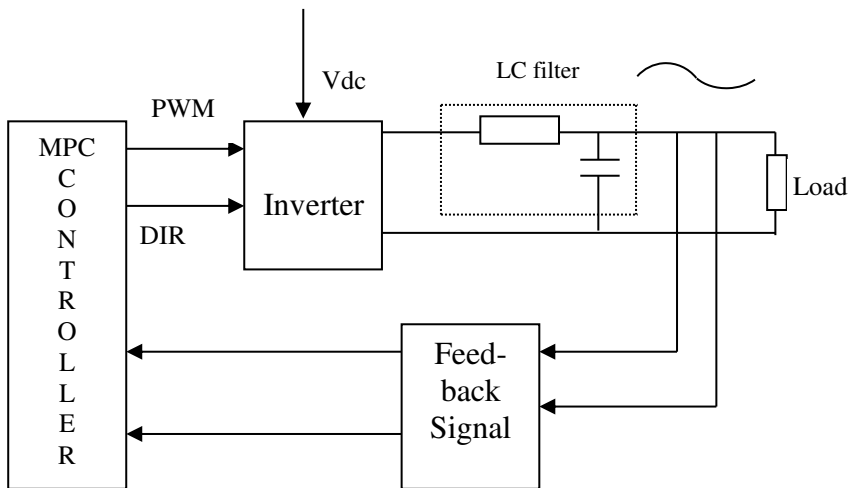
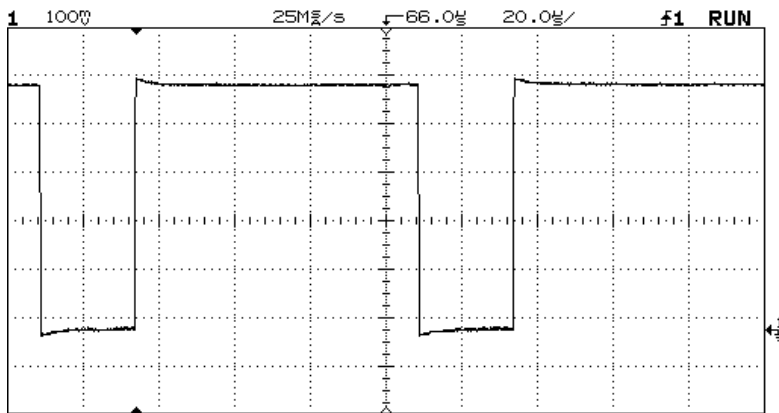


Figure 7

Block diagram of the experimental setup

6.1 Experimental Results of Open-Loop System

Figure 8 shows the experimental result for the open-loop system under no load condition when the DC voltage supply to the inverter is 40 V. The reference input voltage is 70 V_{pp}.

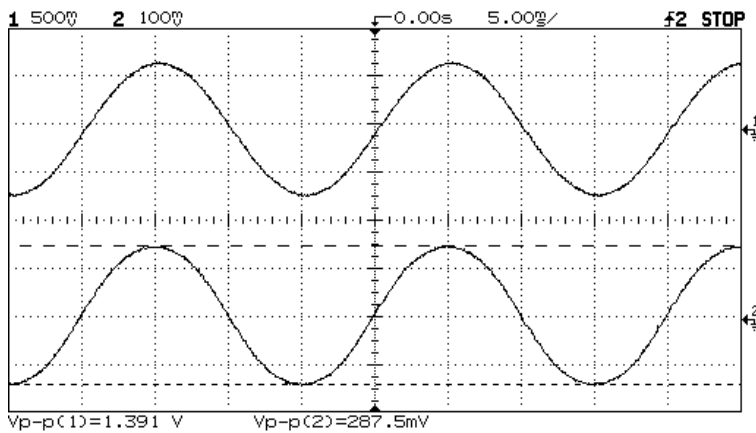


Channel 1: Output Voltage = 73.45 Vpp, 25V/div & Channel 2: Output Current = 0, .25A/div

Figure 8

Experimental result: Open-loop system under no load condition

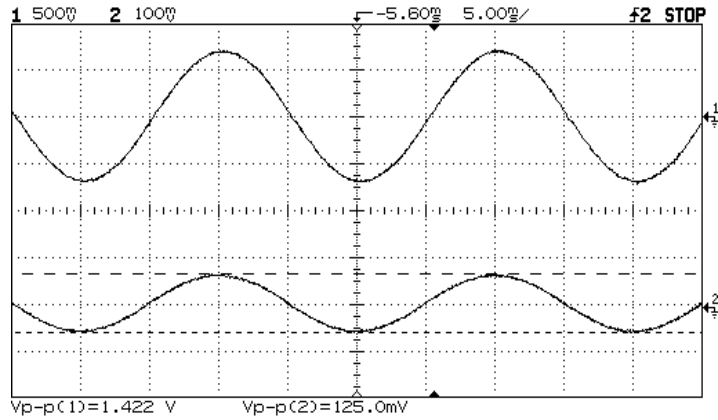
Figure 9 illustrates the output response of the open-loop system under a load of 100Ω and Figure 10 represents the output response of the open-loop system under a load of 200Ω .



Channel 1: Output Voltage = 69.55Vpp, 25V/div, Channel 2: Output Current = 0.34775A, .25A/div

Figure 9

Experimental result: open-loop response under 100Ω resistive load



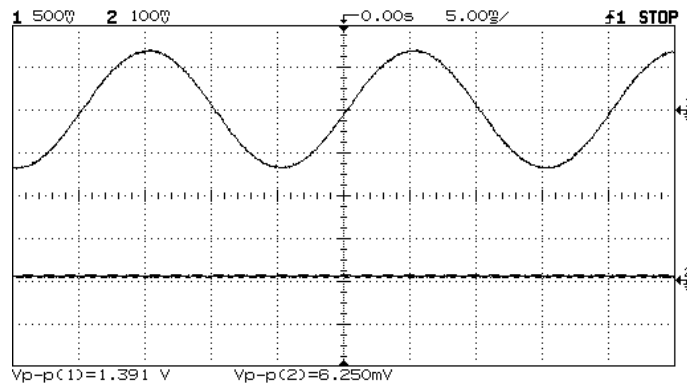
Channel 1: Output Voltage = 71.1Vpp, 25V/div, Channel 2: Output Current = 0.17775A, .25A/div

Figure 10

Experimental result: open-loop response under 200Ω resistive load

6.2 Experimental Results of Close-Loop System

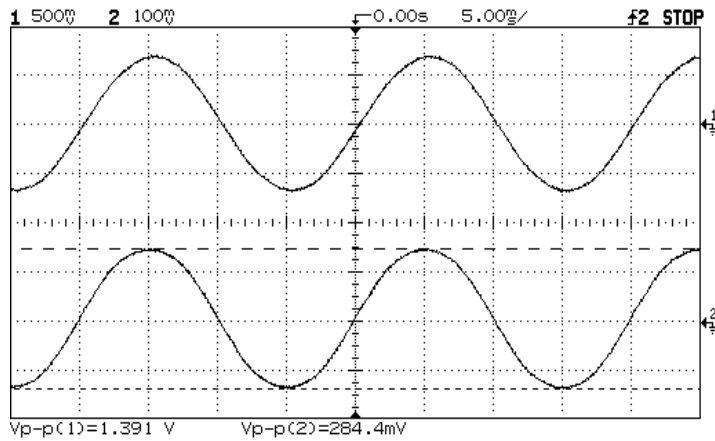
Figures 11, 12 and 13 describe the closed-loop results of the system under no load, 100Ω and 200Ω load conditions, respectively.



Channel 1: Output Voltage = 69.55 Vpp, 25 V/div, Channel 2: Output Current = 0 (no load)

Figure 11

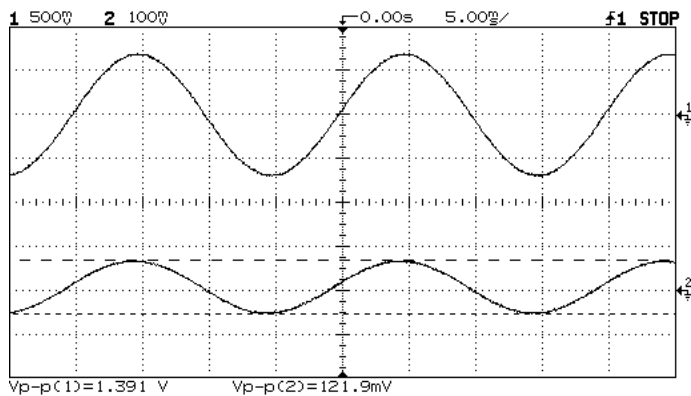
Experimental result: Closed-loop system response under no load condition



Channel 1: Voltage Output = 69.55 Vpp, 25 V/div, Channel 2: Current Output = .34775 A, .25 A/div

Figure 12

Experimental result: Closed-loop system response for **100Ω** load



Channel 1: Voltage Output = 69.55 Vpp, 25 V/div, Channel 2: Current Output = .173875 A, .25 A/div

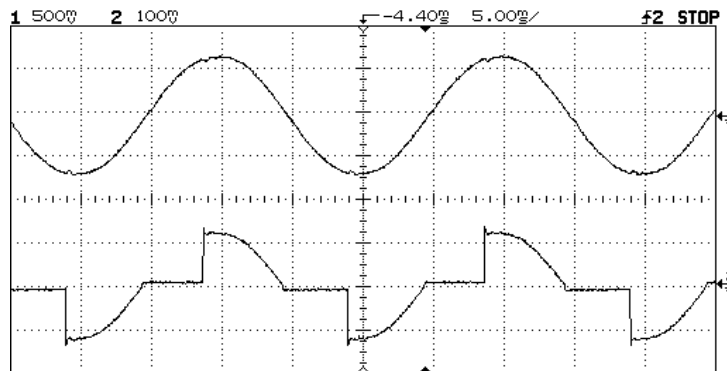
Figure 13

Experimental result: Closed-loop system response for **200Ω** load

In the closed-loop system with the MPC controller, the output was able to maintain at the value of 69.55 V peak to peak, even when the load was varied from zero to 100Ω and to 200Ω. Moreover, the MPC scheme is effective in improving the robustness of the PWM inverter, suffering from load variations to generate sinusoidal output voltage.

6.3 Experimental Results for Traic Load

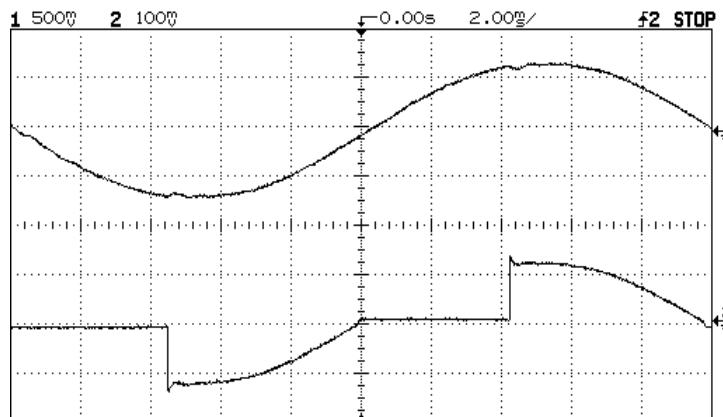
Figure 14 and 15 shows the results for the closed-loop system with Triac load. In Figure 15 the transient response is magnified, so that the effectiveness of the controller can be appreciated more profoundly. This figure illustrates that the distortions during switching are minor, and the harmonics introduced to the system are negligible. Good power quality is maintained during the transient. The MPC controller gives a satisfactory result for the Triac load.



Channel 1: Voltage Output = 70 Vpp, 25 V/div, Channel 2: Current Output, .25 A/div

Figure 14

Experimental result: Closed-loop system response with dynamic load



Channel 1: Voltage Output = 70 Vpp, 25 V/div, Channel 2: Current Output, .25 A/div

Figure 15

Experimental result: Closed-loop system response with dynamic load (magnified)

Conclusion

The DSP was successfully programmed to perform real time control of a PWM inverter to convert DC voltage to AC voltage. It has been demonstrated that the system performs well with the output voltage, remaining sinusoidal, even with load variations. The PWM inverter control routine block has been implemented. A state-space model was developed and a MPC technique has been implemented to perform closed-loop control of a single inverter to obtain the desired response and attain a good level of robustness, with respect to load disturbances. Open-loop and closed-loop control of the system has been implemented and tested with different loads. The results of the open-loop and closed-loop system, with MPC control were presented. The results have shown that the inverter performs reasonably well.

References

- [1] Pedersen, J. K.; Thogersen, P Fully Digital-controlled PWM Inverter with Software-based Modulation for AC Machine Control, Industrial Electronics Society, IEEE Conference, Vol. 2, 1990, pp. 996-1001
- [2] A. Tuladhar, H. Jin, T. Unger, and K. Mauch, "Control of Parallel Inverters in Distributed AC Power Systems with Consideration of Line Impedance Effect," IEEE Trans. Ind. Appl., Vol. 36, No. 1, 2000, pp. 131-138
- [3] Jia De Li; Wu Qiong; A Switching-Inverter Power Controller Based on Fuzzy Adaptive PID Strategic Technology, (IFOST), 6th International Forum on, Vol. 2, 2011, pp. 695-699
- [4] Oettmeier, M.; Heising, C.; Staudt, V.; Steimel, A. Dead-Beat Control for a Single-Phase 50-kW, 16.7-Hz Railway-Grid Representation Inverter Featuring Variable Grid Parameters, Power Engineering, Energy and Electrical Drives International Conference, 2009, pp. 279-284
- [5] Huseinbegovic, Senad; Perunicic-Drazenovic, Branislava A Sliding Mode-based Direct Power Control of Three-Phase Grid-connected Multilevel Inverter, Optimization of Electrical and Electronic Equipmen, 13th International Conference, 2012, pp. 790-797
- [6] Di Cairano, S.; Yanakiev, D.; Bemporad, A.; Kolmanovsky, I. V.; Hrovat, D. Model Predictive Idle Speed Control: Design, Analysis, and Experimental Evaluation, Control Systems Technology, IEEE Transactions. Vol. 20, Issue: 1, 2012, pp. 84-97
- [7] Chivite-Zabalza, F. J.; Izurza, P.; Calvo, G. Voltage Balancing Control in 3-Level Neutral-Point-clamped Inverters Using Triangular Carrier PWM Modulation for FACTS Applications, Power Electronics and Applications, 14th European Conference Proceedings, 2011, pp. 1-10

- [8] Bowes, S. R.; Bullough, R. I. Optimal PWM Microprocessor-controlled Current-Source Inverter Drives, *Electric Power Applications*, IEE Proceedings B, Vol. 135, Issue 2, 1988, pp. 59-75
- [9] Božiček, A.; Blažič, B.; Papič, I. Performance Evaluation of a Time-Optimal Current Controller for a Voltage-Source Converter and Comparison with a Hysteresis Controller, *Power Delivery*, IEEE Transactions, Vol. 26, Issue 2, 2011, pp. 859-868
- [10] Fukuda, S.; Yoda, T. A Novel Current-Tracking Method for Active Filters Based on a Sinusoidal Internal Model for PWM Invertors, *Industry Applications*, IEEE Transactions on, Vol. 37, Issue 3, 2001, pp. 888-895
- [11] Lu, Wenzhou; Zhou, Keliang; Yang, Yunhu A General Internal Model Principle-based Control Scheme for CVCF PWM Converters Power Electronics for Distributed Generation Systems, 2nd IEEE International Symposium, 2010, pp. 485-489
- [12] Keliang Zhou; Kay-Soon Low; Wang, D.; Fang-Lin Luo; Bin Zhang; Yigang Wang Zero-Phase Odd-Harmonic Repetitive Controller for a Single-Phase PWM Inverter, *Power Electronics*, IEEE Transactions, Vol. 21, Issue 1, 2006, pp. 193-201
- [13] Ahmed, S. F. "A New Approach in Industrial Automation Application" Embedded System Design for Injection Molding Machine." Multitopic Conference, 2007. INMIC 2007. IEEE International. IEEE, 2007
- [14] MH Tanveer; D Hazry; SF Ahmed, NMPC-PID-based Control Structure Design for Avoiding Uncertainties in Attitude and Altitude Tracking Control of Quad-Rotor (UAV), *IEEE International Colloquium on Signal Processing & its Applications (CSPA)*, 2014, pp. 117-122

From Exploring to Optimal Path Planning: Considering Error of Navigation in Multi-Agent Mobile Robot Domain

István Nagy

Óbuda University, Bánki Donát Faculty of Mechanical and Safety Engineering
Institute of Mechatronics and Vehicle Engineering
Népszínház u. 8, H-1081 Budapest, Hungary
nagy.istvan@bgk.uni-obuda.hu

Abstract: In this paper a complex path planning model is presented. The model building starts by mapping the totally unknown environment, then the geometrical map of the “work space” is built-up. Afterwards, based on the determined error of navigation, the reduced free space of the environment is created. The path planning process is begins with this reduced environment. At first it determines some cruises (corridors) for the multi-agent traffic, and then comes the builds up the graph-map of the cruises. Based on the weighting of the graphs, the algorithm selects the time-optimal, dynamically optimal, and collision-free path, from among the possible ones, connecting the starting and docking positions. The final path is created with fitting some B-Spline curves to the selected graph-like one in consideration of movements of the other agents.

Keywords: mobile robot; multi-agent; path planning; map building

1 Introduction

Multi-agent mobile robot systems play a significant role in robotic systems. Collaborative robots started their career with the beginning of Artificial Intelligence (AI). Among the first collaborative robots' projects the different competitions in robotic soccer can be mentioned [1], [2] possibly having a peak in an international joint project called “RoboCup Coach Competition” [3], [4].

While the robot soccer leagues gives an exciting task to the researchers working in AI, there exist several other fields of research where the multi-agent systems can be useful. The “teamwork” plays a larger role, not only in human work, but in the robotics world, too.

Nowadays, “swarmbots” is a very often-used expression (see e.g [5], [15]). These are collaborative robots, which can autonomously execute some predefined task or

series of tasks. The control of the agents can be centralized or decentralized. In case of decentralized control, the communication between the agents is more frequent, because the agents have to know about the activities of other agents and have to plan their own actions based on the behaviour of other ones. In the case of centralized control, the agents are communicating with a central control unit that has more or less accurate information about the positions and activities of the agents. The swarm of “*mini-robots*” could be perfectly used for exploring unknown environments where human beings are unable to get in. Each agent should be equipped with sensors and an antenna and would be able to map the environment. But here is the question of with regards to hardware vs. software. What we need is a small and “smart” agent with high mobility. In contrast with this, here are the physical dimensions of sensors, accumulators, motors, and locomotion. Based on these parameters, the minimal physical dimension of the agent can be estimated, which, in our opinion, has not been typical for the “*swarm-technology*” as of yet. On the other hand, nowadays, a lot of control strategies exist in swarm-bot theories. Can we tell that the theory preceded technology in this case? For this reason, we decided to use the expressions *multi-agent system* (MAS) and *self-organization* instead of swarm-bot or swarm-technology in this paper.

In this paper, the so-called ‘centralized control theory’ is improved. A multi-agent mobile robot system is used for exploring an unknown environment by using a new approach. The agents are equipped with 16 ultrasonic (US) sensors equally placed around the body. The process takes the difference between the short and long range activation of the sensors. The equipment of the agents, the ultrasonic measuring system used in this paper is similar to that of the system introduced in [6]. The main difference between the two approaches is in the map building process. The number of agents and the work space (WS) are also different. While in the previously mentioned paper the motion strategy was implemented with the help of some genetic algorithm (GA) based module, in this project the motion strategy of the agents is calculated using a *remote host* computer. Moreover, in this paper the process is not finished with the creation of the map, but continues with path planning based on the navigation’s error defined in the multi-agent domain.

2 The Multi-Agent System Used for Potential Field-based Map Building

As it can be seen in Figure 1 the multi-agent system (MAS) used for potential field (PF) based map building is not a pure distributed or centralized system. The independent agents can communicate with each other, but the sensed data is sent to the *remote host* computer, i.e., the sensed data is shared with all of the agents.

As result, a global potential map of the environment can be created on the remote host computer, and since the agents send their current position to the remote host, the motion strategy is computed by the remote host, as well. The theory of this map building process was initiated by Liu and Wu in [7]. In this paper, based on their theoretical results, this approach is improved, extended, and implemented in *MATLAB* environment. The novelties presented in this paper include the extension of the map building with the path planning process, as well. The movement strategy is derived from the distance measurement results taking into consideration the current locations of the agent vs. obstacles and non-visited locations. We assume that that the agents, based on the distance and orientation details of their movements, are capable to determine their actual position. The behaviour of the agent (the direction of the next step) is selected after the processing of these (measured distance) parameters.

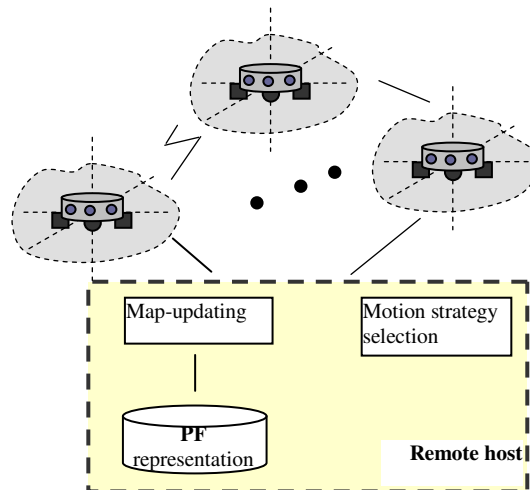


Figure 1.
The structure of the multi-agent system

The process of map building in pseudo codes can be written as follows:

```

Until non-visited location  $\neq 0$ 
  Begin
    move to new location  $\{P_0(x_0, y_0)\}$ 
    take 16 measurements  $\{L_0 = [D_1^0, \dots, D_{16}^0]\}$ 
    send location and measured data to the remote host
    associate neighbours,  $\{P_j(x_j, y_j)\}$ 
    calculations
    update map
    next motion planning
  End

```

2.1 The Coordinate System of the Agents and the Distance Calculations

Generally, the kinematics of a single agent, in vectorial form, can be expressed with the following equation, in the x,y coordinate plane:

$$\mathbf{P}(j) = \mathbf{F}(\mathbf{P}(0), \mathbf{u}(0)) + \mathbf{v}(0); \quad (1)$$

where $\mathbf{F}(\mathbf{P}(0))$, $\mathbf{u}(0)$ denotes the (non-linear) state transition function and $\mathbf{v}(0)$ is the noise source assumed during the measuring of the actual position. The model applied here ignores the measurement noises, i.e., $\mathbf{v}(0)=0$. The control input is $\mathbf{u}(0)=[T(0), \Delta\theta(0)]^T$, where $T(0)$ stands for the distance between points $\mathbf{P}(0)$ and $\mathbf{P}(j)$ and $\Delta\theta(0)$ marks the change of the orientation of the agent. Considering these conditions the new location of the agent, in scalar form, can be expressed by

$$\begin{bmatrix} x_j \\ y_j \end{bmatrix} = \begin{bmatrix} x_0 \\ y_0 \end{bmatrix} + T(0) \begin{bmatrix} \cos(\Delta\theta_0) \\ \sin(\Delta\theta_0) \end{bmatrix} \quad (2)$$

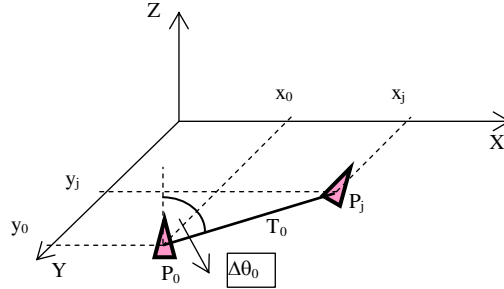


Figure 2.

The coordinate system of the agent and the distance calculation

2.1.1 Proximity Measurements and Distance Association in a Neighbouring Region

The agents measure the distances of their initial position (P_0) and the surrounding obstacles with their 16 US sensors and the data is stored in a vector $\mathcal{L}^0 \equiv [D_1^0, \dots, D_{16}^0]$. Based on these distance measurements the locations of the obstacle-free areas can be evaluated too. It is known that the measuring gives an accurate result if the direction of sensing is parallel with the plane of the movement (usually this is set) and also perpendicular to the plain of the sensed obstacle. Unfortunately, in many of the cases this latter cannot be ensured. For that reason, the distance measured in the next step (distance measured from $\mathbf{P}(j)$ position) will be evaluated based on:

$$\hat{D}_i^j = D_i^0 - T_0 \cos \beta; \quad i = [1, \dots, 16] \quad (3)$$

where β is the angle between the sensing directions of positions $\mathbf{P}(0)$ and $\mathbf{P}(j)$. Set out from this, the estimated proximity values in location $\mathbf{P}(j)$ are stored in vector $\hat{L}_j \equiv [\hat{D}_1^j, \dots, \hat{D}_{16}^j]$. Let D_i^j denote the true distance of the obstacle from $\mathbf{P}(j)$. In this case, the difference between the measured and true distances equals the error in direction i : $\varepsilon_i \equiv |D_i^j - \hat{D}_i^j|$. For a better approximation of estimated distance, a weighting function has been introduced for the elements of vector \hat{L}_j . This weighting function is a function from the agent's position to the location $\mathbf{P}(j)$. The weighting must be equal to 1, when the robot is exactly in $\mathbf{P}(j)$ position.

$$w_j = \exp(-\eta T_0^2) \quad (4)$$

where η is some positive gain factor and T_0 is the distance, see Figure 2.

2.2 Self-Organizing and Potential Field Calculation

The potential field is calculated based on well-known repulsive forces, which are derived from the measured distances. It means that the base for the PF calculation depends on vector \hat{L}_j and its components, with the following condition:

$$[\hat{D}_1^j, \dots, \hat{D}_{16}^j] \geq 0 \quad (5)$$

The potential field, in location $\mathbf{P}(j)$, is calculated from the data of each sensors (i) of each robot (r) in each step (k). The estimation of the amplitude of the potential is:

$$\hat{u}_j^k \equiv \sum_{i=1}^{16} \exp(-\lambda \hat{D}_i^j) \quad (6)$$

where λ is a positive gain. If at some locations condition (5) is not satisfied, the process discards them or assumes an obstacle. At step k the set of calculated potential amplitudes, $\Omega_j^k \equiv [\hat{u}_j^{k1}, \dots, \hat{u}_j^{kr}]$, is calculated based on:

$$\Omega_j^k = \Omega_j^{k-1} \cup Q \quad (7)$$

where:

$$Q = \begin{cases} \hat{u}_j^{kr}; & \text{if } \hat{L}_j \text{ satisfies (5)} \\ 0; & \text{otherwise} \end{cases} \quad (8)$$

Because of confidence of the estimated results, a weighting vector $W_j^k \equiv [w_j^{k1}, \dots, w_j^{kr}]$ is associated to Ω_j^k and the acceptable PF value is calculated as:

$$u_j^k = \begin{cases} \hat{u}_j^{kr}; & \text{if } \forall i \in [1, r], w_j^{ki} = 1; \\ \sum_{i=1}^r \hat{u}_j^{kr} \cdot \bar{w}_j^{ki}; & \text{otherwise} \end{cases} \quad (9)$$

where \bar{w}_j^{ki} is a normalized weight component of W_j^k and calculated as follows:

$$\bar{w}_j^{ki} = \frac{w_j^{ki}}{\sum_{n=1}^r w_j^{kn}}; \quad (10)$$

2.3 The Motion Selection Process

The agents can apply one of the three variants of the motion defined in [7]. In each of the three variants the next movement is calculated based on:

1. motion direction (ϕ)
2. motion step (d_s)

The location of the agent in step ($k+1$) can be written:

$$P_0^{k+1} = P_0^k + d_s \cdot e^{j\phi}; \quad (11)$$

2.3.1 Motion: Directional-1

This motion is derived from the standard deviation (*std*) of the PF map for all sensing sectors (16 sectors) within a given maximum step length (d_m) at steps $k-1$, and k . Let Vector Δ store the standard deviation of the differences between the PF values at step k and $k-1$ in each of the (16) sensing sectors. For component i it takes

$$\Delta_i = std(\{l_{ij} \mid l_{ij} = u_{ij}^k - u_{ij}^{k-1}, \forall j \in \varepsilon_i, i = 1, 2, \dots, 16\}); \quad (12)$$

Let vector Λ store the standard deviation of the PF values at step k for *all locations* in the same sensing sector:

$$\Lambda_i = std(\{v_{ij} \mid v_{ij} = u_{ij}^k, \forall j \in \varepsilon_i, |j-i| \leq 1\}); \quad (13)$$

In equations (12), (13) ε_i , ε_v denote sensing sectors i and v , respectively. Finally, the robot selects its movement direction (ϕ_i) in sensing sector i so that it satisfies:

$$\begin{aligned} \phi_i \mid_{\Delta_i} &= \max(\Delta_1, \dots, \Delta_{16}) \\ \forall j, P_j &\notin \tau_i, \end{aligned} \quad (14)$$

where τ_i denotes sensing sector i and P_j stands for location j . After determining the movement sector, the agent will choose the exact location within the selected sector $P_0^{k+1}(x_0, y_0)$ and the PF value around this location: $(x_0, y_0) \mid_{(x_0, y_0)} = \max(1, \dots, 16)$. (15)

2.3.2 Motion: Directional-2

This strategy is almost the same as the strategy detailed in sub-subsection 2.3.1, except that the exact location of agent $k+1$, $P_0^{k+1}(x_0, y_0)$, within the selected sector, is chosen based on the minimum criteria of vector \mathbf{A} , that is:

$$(x_0, y_0) \Big|_{\Lambda_i(x_0, y_0)} = \min(\Lambda_1, \dots, \Lambda_{16}); \quad (16)$$

2.3.3 Random Motion Strategy

According to this strategy the agent selects its motion randomly. The direction of movement is selected randomly among the sensing sectors ($[1, \dots, 16]$). The movement's step length is also randomly selected in the range of ($l, \max. \text{movement step}$) ($[1, \dots, d_m]$).

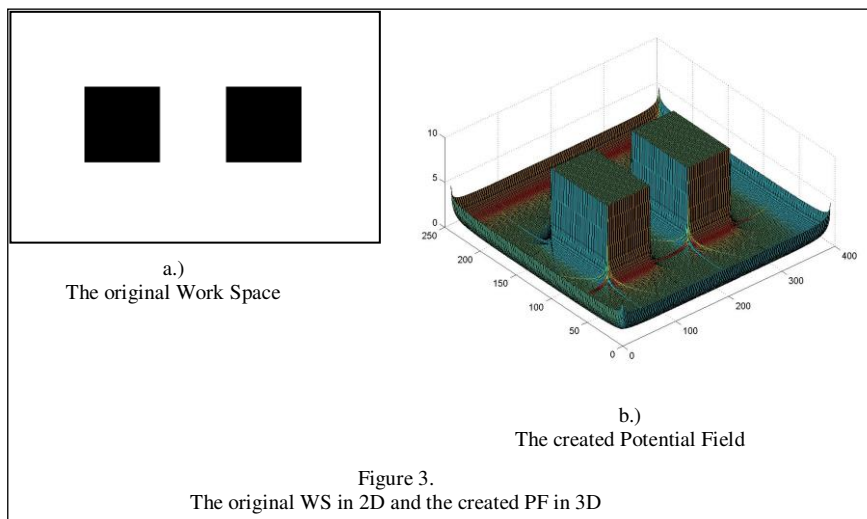
$$\phi_i = \text{rand}([1..16]); \quad (17)$$

$$ds = \text{rand}([1..d_m]);$$

2.4 Case Study 1 - PF created with 6 Robots

In the following, the effectiveness of the PF creation is illustrated by an example. In this simulation, six robots explore an unknown environment. The environment is represented by a *bmp* image, which is used only for validation of the results.

The potential field is created in MATLAB SW environment.

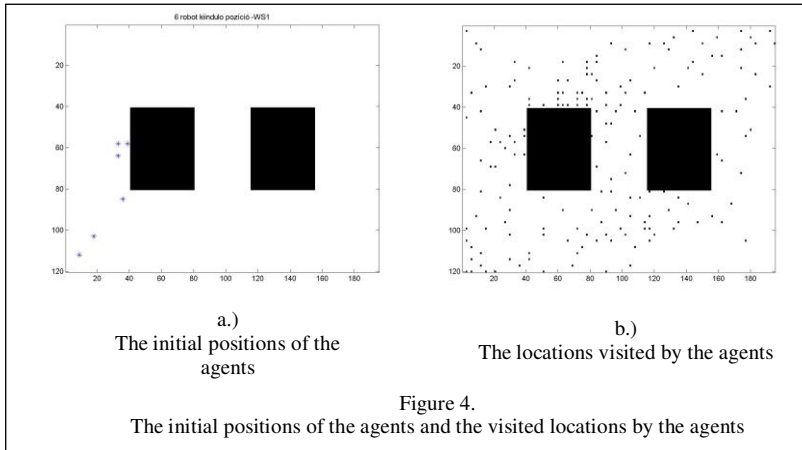


The program executed 40 cycles (steps, maximal running step=40), with 6 robots. Each robot was equipped with 16 ultrasonic sensors, meaning 16 sensing sectors/agent. During the simulation, the program used motion strategy *Directional-1*. The coefficients η and λ were chosen in interest of displaying

appropriately. The program parameters are summarized in Table 1. Figure 4 contains the starting positions of the agents (see Figure 4a) and all the visited locations of the agents during the 40 cycles (see Figure 4b).

Table 1
The parameters used in process

Specification	Value
Number of Agents	6
Number of sensors/agent	16
Maximum running step	40
Maximum movement step (d_m)	8
Coefficient (η)	1/600
Coefficient (λ)	1



3 The Path Planning Process

The path planning process is initialized with the created 3D PF of the environment. Firstly, this entire 3D potential field has to be projected down to two dimensions. In ideal case, the 2D PF and the original workspace (WS) (see Figure 3b) should be identical, but unfortunately it is a very rare case because of the unavoidable error of the potential field creation. There are several sources causing error, but the most significant of them can be derived from the ultrasonic proximity measurement (see section 2.1.1: $\varepsilon_i = |D_i^j - \hat{D}_i^j|$). The second error factor also depends on the distance measurement. The difference is that in this case the

estimated local potential field value (u_j^k) is calculated vs. the true potential field value (\bar{u}_j). Here K stands for the total number of visited locations on the WS and k corresponds to the actual step.

$$\varepsilon^k \equiv \sqrt{\frac{1}{K} \sum_{j=1}^K (u_j^k - \bar{u}_j)^2} ; \quad (18)$$

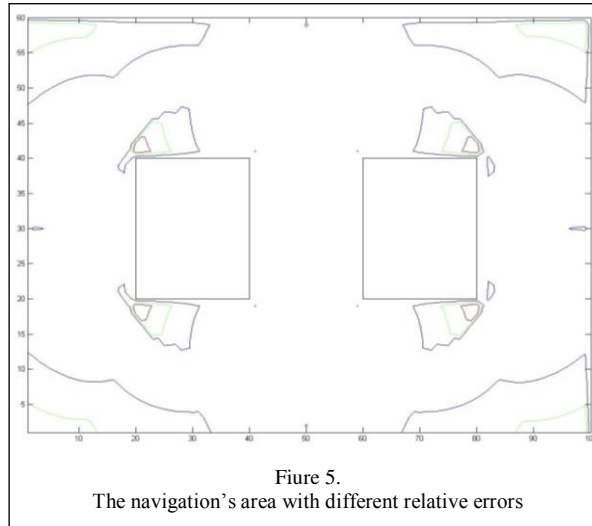
In view of these errors, the *free space* [8] of the WS can be created. (Just for interest: these errors can be seen in Figure 3b, where the local PF value is increasing in direction of axis z . It occurs near to the bounds of the WS and at the obstacles.)

3.1 The Creation of the Area of Navigation

The area of navigation (AN) is a part of the work space, where the mobile robot (agent) can freely move within the given conditions. Usually the given conditions are related to the accuracy of the positioning of the agent, because this gives the basic parameter for the navigation [8]. If the relative/absolute error of the device responsible for the positioning is known, the error of the position can be determined on the entire WS. In the present case, this device is the ultrasonic sensor, with the previously mentioned proximity-error. A more detailed analysis of the error would be exceeding the objectives of the paper, especially because it is neglected. Although, the major part of the errors, in case of similar measuring systems (SONAR), are caused by (1) the false echoes from the corners, (2) the non-perpendicular measuring angles, and (3) the outer noises. Certainly, other types of measuring systems, like the LIDAR, LADAR or RADAR systems have different absolute/relative distance errors. In accordance with this, the created area of navigation of the WS will look like the original WS reduced by the “error zones” at the corners. The created AN with different relative errors can be seen in Figure 5.

An interesting question is whether the area of navigation can or cannot be created on a multi-agent domain? We find that:

- If in the MAS the agents are homogeneous, with the same construction and measuring system, it can be created, at least theoretically,
- If in the MAS the agents are inhomogeneous (with different construction and measuring system) then each type of agents should have their own navigation area.



3.2 The Path Planning

The path planning process starts on the created area of navigation, but it is not sure that the whole area of navigation is accessible for each agent.

Definition: Area of navigation (AN) is accessible for mobile robot (agent) R , if: for $(\forall x, y \in AN)$ holds that any “ x ” can be connected with any other “ y ” (where $x \neq y$) in such a way that each point of the connecting line (or curve) is an element of the AN. Moreover, if we are working with a non point-represented robot, the following condition has to be fulfilled: $d(\overline{\mathcal{NA}}^{(i)}, \overline{\mathcal{NA}}^{(i+1)}) > 2r$, where “ r ” is the radius of the circle around the mobile robot and d is the distance between two neighbouring *non*-area of navigations $(\overline{\mathcal{NA}}^{(i)}, \overline{\mathcal{NA}}^{(i+1)})$ (usually obstacles).

3.2.1 Path Planning in Single Agent Model

In the case of a single agent, the situation seems to be clear. A single AN is given with accessible territories. The path planning process begins with determining the starting (S) and docking (G) positions. The only question is how to optimize the path. In this case the optimization process has two phases:

- 1 Searching for the path with the lowest weight on the weighted and oriented graph-like path. This corresponds to the optimization of the dynamics (smoothness) of the path.
- 2 Generating a B-spline curve to the selected graph-like path. This corresponds to some kind of time-optimization of the path.

Besides of these, it is possible to generate the so-called “fast” and/or the “safe” path between positions S and G . The difference between them is that the *safe* path lies on the *centreline* (Voronoi diagram) of the AN, and the *fast* path is generated based on the *visibility graph method* between C and G .

3.2.1.a Graph-like Path Generation

In the case of a single agent, firstly the Voronoi diagram of the AN is created, and then by the “linearization” of this curve the topology of the AN is obtained [9]. Then the weighting of the graph can be divided into 2 parts:

1. Weighting of the edges: here, the weighting can be multi-parameterized. Namely, the edges are not weighted based on length only ($w_l S_{(i)} L$), but, mainly in multi-agent domain, can also be weighted based on the traffic density ($w_{(n)} S_{(i)} TrD$). In this case the weighting of an edge is:

$$W_{S_{(i)}} = w_l S_{(i)} L + \dots + w_{(n)} S_{(i)} TrD; \quad (19)$$

2. Weighting of the nodes: with the decomposing of the graph-nodes, each cross-point of the graph can obtain multiple weightings. With this procedure, we can consider the complexity of the planned path, that is, the relative incidence and sharpness of the turns. The weighting of the “ n ” signed sub-segment of node J , in knowledge of angle α is (see also Fig. 6.)

$$Wn_{(J)} = w_n |180 - \alpha_{(i,j)}^0|; \quad (20)$$

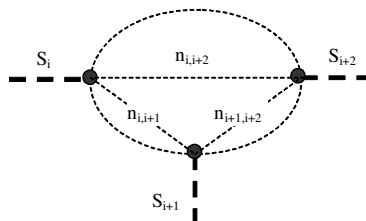


Figure 6.
Weighting of the graph nodes

Generally, the final cost function (Cf) is calculated as the sum of the weightings of the edges and nodes:

$$Cf = \sum_i W_{S_{(i)}} + \sum_j Wn_{(J)}; \quad (21)$$

3.2.1.b Spline Generation

Several methods exist to generate a spline over a polygon (graph-like path). In this particular case, the conditions for the curve generation are the following:

- $S, G \in b(t) \in AN$; - the curve has to contain the starting and docking position and has to be on AN.

- The curve must pass the graph-nodes of the selected route
- The curve must satisfy C^2 continuity
- For each point of the curve, $\forall(x,y \in b(t)) \in AN$ has to be held

Suppose that the *configuration points* of the curve $[p_0, \dots, p_n]$ are given with their respective time values at the graph-nodes of the selected route. The task is to find the function $p_i(t)$ in such a way that it satisfies C^2 continuity, i.e., in the form of a 3-degree polynomial. This can be achieved through the equation system written in (22), from which the derivatives $[p'_0, \dots, p'_n]$ can be determined and substituted to define the segments and consequently the composite function $p(t)$ (see (23)). For mathematical proof, see [9].

$$\begin{bmatrix} 1 & 0 & \dots & & & & \\ T_1 & 2(T_0+T_1) & T_0 & 0 & \dots & & \\ 0 & T_2 & 2(T_1+T_2) & T_1 & 0 & \dots & \\ \vdots & & & & & & \\ \dots & 0 & T_{n-1} & 2(T_{n-1}+T_{n-2}) & T_{n-2} & & \\ \dots & & & \dots & \dots & 0 & 1 \end{bmatrix} \begin{bmatrix} p'_0 \\ p'_1 \\ p'_2 \\ \vdots \\ p'_{n-1} \\ p'_n \end{bmatrix} = \quad (22)$$

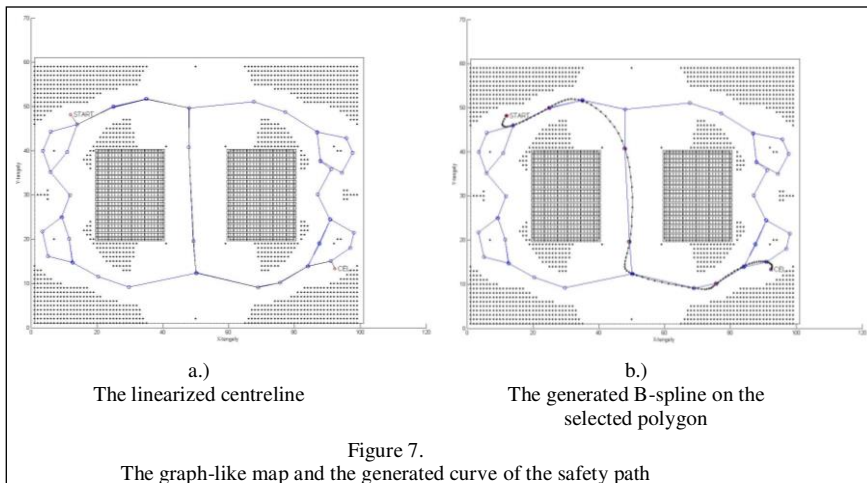
$$\begin{bmatrix} v_{start} \\ 3[T_0/T_1(p_2 - p_1) + T_1/T_0(p_1 - p_0)] \\ 3[T_1/T_2(p_3 - p_2) + T_2/T_1(p_2 - p_1)] \\ \vdots \\ 3[T_{n-2}/T_{n-1}(p_n - p_{n-1}) + T_{n-1}/T_{n-2}(p_{n-1} - p_{n-2})] \\ v_{end} \end{bmatrix}$$

$$p(t_j) = \sum_{i=-1}^{n+1} p_i N_i^d(t_j) = p_j \quad (23)$$

3.3 Case Study 2 - Path Planning in Single Agent's Domain

In the following, simple simulation results are presented for the path planning in single agent's domain. The first one illustrates the safe path generation, while the other is an example of fast path creation.

3.3.1 The “Safe Path” Generation



As it can be seen in Figure 7, in this case the safest path is generated on the centreline of the AN. The complexity of the path is calculated through the Cost function with the following form:

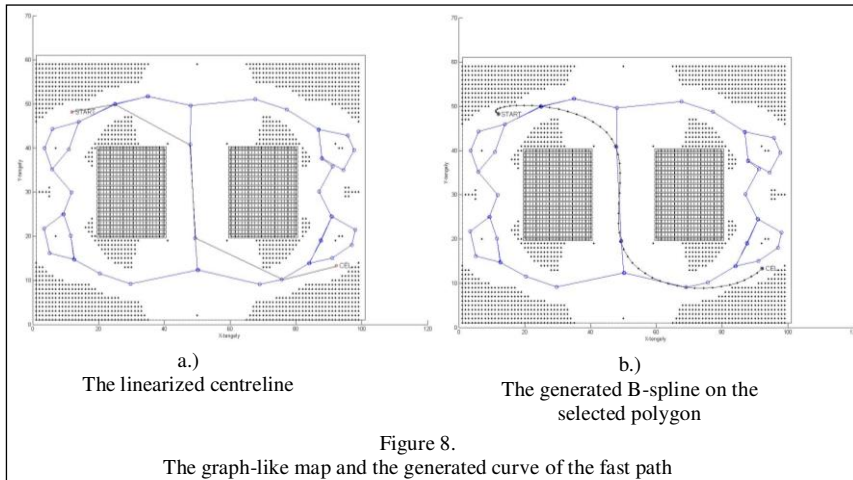
$$Cf_{safety} = \underbrace{\min(w_{(g)}SSG_{(g)})}_{\text{the shortest segments to the "centerline"}} + \min(w_{(h)}CCG_{(h)}) + \min\left(\sum_i Ws_{(i)} + \sum_j Wn_{(j)}\right) \Bigg|_{\substack{SG(g) \rightarrow SG(\min) \\ CG(h) \rightarrow CG(\min)}} + \min(Cf_{g \times h \times k}) \quad (24)$$

The parameters and results of the calculations are summarized in Table 2.

Table 2
The calculated results of the “safety” path

Parameters (supposed)		Calculated results	
Velocity	3 [m/s]	Nr. of nodes	12
Acceleration	1 [m/s]	Execution's time	65,322 [s]
Deceleration	1 [m/s]	Length	120,97 [m]
Orientation's changing	1 [s]	Complexity	835,07

3.3.2 The “Fast Path” Generation



The cost function of the fast path can be as:

$$Cf_{fast} = \min(Cf_{g \times h \times k}) + \underbrace{w_{(g)}SSG_{(\min)} + w_{(h)}CCG_{(\min)}}_{\text{Weighting of thesegments between the visiblenodes}} \quad (25)$$

The parameters and results of the calculations are summarized in Table 3.

Table 3
The calculated results of the “fast” path

Parameters (supposed)		Calculated results	
Velocity	3 [m/s]	Nr. of nodes	6
Acceleration	1 [m/s]	Execution's time	61,483 [s]
Deceleration	1 [m/s]	Length	110,35 [m]
Orientation's changing	1 [s]	Complexity	654,79

3.3 Path Planning and Optimization in Multi-Agent Domain

There is a large amount of problems in path planning in a multi-agent domain. The first, as mentioned before, is the problem of homogeneity of the platform. Let us suppose that the area of navigation contains a lot of spaces for opening several multi-lane paths.

In the case of agents with equal dimensions, the lanes can be identically set with the same width to make the path planning easier. The traffic control can follow two strategies: 1) selected agents can wander only on the selected lanes, 2) agents can change the lanes if the selected lane is free of other agents. This strategy needs some centralized control, because the agent has no information about the

occupancy of the other lanes. In our opinion, the lanes should be divided into more segments and the occupancy of the segments could be monitored in the so called “segment’s occupancy table” belonging to the central traffic control.

In case of agents with different dimensions and different localization’s systems, the situation is more complicated. The ideal case would be dynamically changing the lane-width in the different segments, what is hardly realistic, but not impossible (theoretically). The second (more realistic) possibility is to fit the lane-width to the biggest agent in the system. In this way, we are back at the previous, static lane-width system.

Outside of this, the path optimization in the multi-agent domain should be solved in the same way as in the single agent system, i.e., by the topological graph of the environment, with the only difference that the topological path will have more sub-branching or, in dynamically changing segmentation, the topological graph will change dynamically as well.

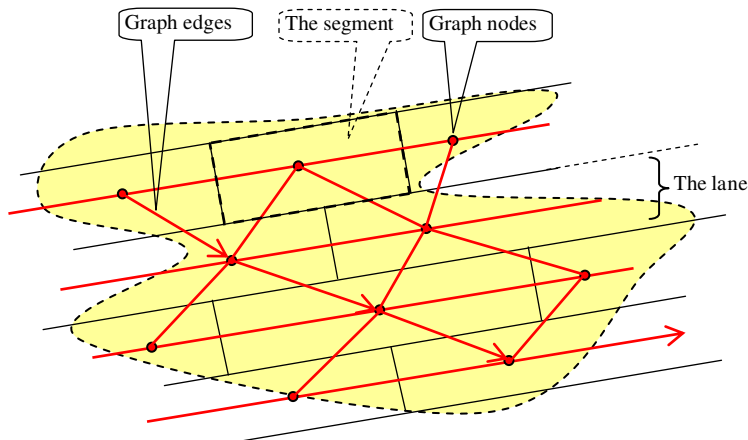


Figure 9.
An extracted part of the multi-lane work space

The regulations regarding the weighting of the graph, which were stated in Sub-subsection 3.2.1.a, are valid in this case too, except that in the multi-agent case we have to think in the space-time continuum due to the occupation of different segments in different time intervals. This time factor increases the computation and the dimensionality of the problem.

Conclusions

In the research field of mobile-robot systems, a large amount of papers have been published related to intelligent navigation or parking systems [10]. Among the most significant approaches in parking navigation is the use of a hybrid navigation structure with elements of computational intelligence (CI) [11]. The first papers dealt with the single agent’s systems. Later on multi agent systems (MAS) have come into the focus, where the agents were defined in a different way. A good

example for the extended agent's definition can be found in [12], where the basic classification of the agents is extended by the functional-computational aspect. The next direction of research in MAS concerns the cooperation and/or the self-organization of the agents. This is possibly one of the most recent fields of research regarding multi-agent systems. In [13] the agent's cooperation is evaluated based on the agent's performance. The self-organization can be found not only in multi-agent systems but in manufacturing systems too [14]. After or parallel with agents cooperation, swarm technology, inspired by the behaviour of ants and bees has started to spread [15]. However, in this paper the use of the expression *swarm-technology* is avoided, replaced by such expressions like cooperation, collaboration, or self-organization, which seem more suited to the situation.

This paper introduces a new method for potential field (PF) building on partly centralized multi-agent's domain. The 'partly centralized' expression is because the PF is built-up on a host computer, however the agents share their actual positions with each other (and certainly also with the remote host computer). The presented strategy is analysed, evaluated, and illustrated through a case study.

Furthermore a new path planning process is proposed in this paper (see section 3: The path planning process). Firstly, the theorems of optimal path planning are introduced in single agent's domain, then analysed and evaluated through another case study. Afterwards, the author shows that the new formulas developed and used in single agent's system can be validated, with the burden of higher computational demands, in MAS, too.

Acknowledgement

This work was sponsored by the Hungarian National Scientific Fund (OTKA 105846). The project was realised through the assistance of the European Union, with the co-financing of the European Social Fund, TÁMOP-4.2.1.B-11/2/KMR-2011-0001.

References

- [1] M. K. Sahota, A. K. Mackworth: Can Situated Robots Play Soccer? (Mar. 04. 1999);
URL: <http://www.cs.ubc.ca/spider/mack/links/papers/ai94sm/ai94sm.ps>
- [2] M. K. Sahota, A. K. Mackworth, R. A. Barman, S. J. Kingdon: Real-Time Control of Soccer-Playing Robots Using Off-Board Vision, in: IEEE International Conference on Systems, Man, and Cybernetics, 1995, pp. 3690-3693
- [3] H. Kitano, M. Tambe, P. Stone, M. Veloso, S. Coradeschi, E. Osawa, H. Matsubara, I. Noda, M. Asada: The Robocup Synthetic Agent Challenge 97, in: International Joint Conference on Artificial Intelligence (IJCAI97), 1997

-
- [4] J. A. Iglesias, A. Ledezma, A. Sanchis: Caos Coach 2006 Simulation Team: An opponent Modelling Approach, Computing and Informatics, Vol., pp. 1-23, V 2008-jan-17
- [5] A. E. Yilmaz: Swarm Behaviour of the Electromagnetics Community as regards Using Swarm Intelligence in their Research Studies, Acta Polytechnica Hungarica, ISSN 1785-8860, Vol. 7, No. 2, pp. 81-93, 2010
- [6] I. Nagy: Behaviour Study of a Multi-agent Mobile Robot System during Potential Field Building, Acta Polytechnica Hungarica, Vol. 6, No. 4, pp. 111-136, 2009
- [7] J. Liu, J. Wu: Multi-Agent Robotic Systems, CRC Press LLC, ISBN 0-8493-2288-X, 2001
- [8] T. Lozano-Perez: Spatial Planning: a Configuration Space Approach, in IEEE Trans. on Computers 32/1983
- [9] Nagy I.: Pozicionáló pontosságon alapuló közel idő-optimalis pályatervezési eljárás mobilrobotokhoz (Localization Error Based Near Time-optimal Path Planning Process, for Mobile Robots), PhD Thesis, pp 61-84, Budapest University of Technology and Economics, Hungary, 2010, In Hungarian
- [10] Gy. Mester: Intelligent Mobile Robot Motion Control in Unstructured Environments, Acta Polytechnica Hungarica, Journal of Applied Sciences, Vol. 7, Issue No. 4, pp. 153-165, Budapest, Hungary, 2010
- [11] J. Vaščák: Navigation of Mobile Robots Using Potential Fields and Computational Intelligence Means, Acta Polytechnica Hungarica, ISSN 1785-8860, Vol. 4, No. 1, pp. 63-74, 2007
- [12] J. Kelemen: Agents from Functional-Computational Perspective, Acta Polytechnica Hungarica, ISSN 1785-8860, Vol. 3, No. 4, pp. 37-54, 2006
- [13] B. Frankovič, T-T. Dang, I. Budinská: Agents' Coalitions Based on a Dynamic Programming Approach; Acta Polytechnica Hungarica, ISSN 1785-8860, Vol. 5, No. 2, pp. 5-21, 2008
- [14] J. Somló, I. J. Rudas: General Solution for the Self-Organizing, Distributed, Real-Time Scheduling of FMS- Automatic Lot-Streaming Using Hybrid Dynamical Systems, Acta Polytechnica Hungarica, ISSN 1785-8860, Vol. 8, No. 6, pp. 155-180, 2011
- [15] J. Dréo, P. Siarry: A New Ant Colony Algorithm Using the Heterarchical Concept Aimed at Optimization of Multim minima Continuous Functions, in Proceedings of the Third International Workshop on Ant Algorithms (ANTS'2002) Vol. 2463 of LNCS, M. Dorigo, G. Di Caro and M. Sampels, ed.s, Berlin: Springer-Verlag, pp. 216-221, 2002

A New Approach for LED Plant Growth Units

Ramazan Şenol, Kubilay Taşdelen

Suleyman Demirel University, Faculty of Technology, 32260, Isparta Turkey
ramazansenol@sdu.edu.tr, kubilaytasdelen@sdu.edu.tr

Abstract: This study aims to enable plant production even during sunless periods using a LED plant growth unit by controlling input variables such as temperature, soil humidity, atmospheric humidity, light intensity, wind speed, level of carbon dioxide in greenhouses and output variables such as lighting, cooling, heating, ventilation, irrigation by means of fuzzy logic control (FLC). It is expected that these indoor tests will provide means to grow plants such as tomato, pepper or cut flowers especially in regions that have sunless and cold winter months like Isparta. To this end, the design of the control unit, development of the Fuzzy rule base, and outline and simulations of the LED plant growth unit have been examined. The study focused on the factors affecting the greenhouse control such as ambient temperature, outside temperature soil humidity, CO₂ production, wind speed, light intensity, heating, cooling, ventilation, irrigation, the LED plant growth unit as well as on the Fuzzy designs for lighting. The LED plant growth unit has been operated with direct current supply (DC). The findings of the indoor tests carried out with the designed LED plant growth unit for pepper and aromatic chamomile are presented.

Keywords: LED plant growth unit; Intelligent light system; Greenhouse Automation

1 Introduction

Fluorescent lamps were used through long years in the development of plant growth units which were launched for the purpose of growing plants indoors or in greenhouses even at the times of no daylight. In recent years, more efficient and economic growth units started to be developed thanks to the developments in LED technology. Obtaining crops is not possible especially in the greenhouses where cut flower is grown, in the regions that have sunless and cold winter months. This situation creates a negative economic impact on the producers planting in the greenhouses. In recent years, LED products have come into our lives swiftly thanks to the innovations and changes in LED technology in a large number of sectors from informatics to lighting. Higher definition and resolution TVs or monitors, more efficient and economic lighting units have been rapidly spreading. The usage of LED units instead of traditional lighting units becomes not only economic, but also decorative. LED lighting units supercede fluorescent or

energy-saving lamps thanks to their longevity and low negative health effects. The increase in LED choice for lighting especially in offices and factories has reached a considerable level. Furthermore, LED plant growth units were swift to supercede fluorescent and halogen lamps. Formerly, LED plant growth units did not look promising because of low lighting efficiency. Nevertheless, thanks to recent technological developments and better longevity and lighting efficiency in LED lighting units, LED plant growth units came to the fore again. In fact, studies have been performed within the scope of NASA's Advanced Exploration Systems (AES) at Kennedy Space Center's Space Life Sciences Laboratory. The main purpose of a greenhouse is to improve the environmental conditions in which plants are grown. In greenhouses provided with the appropriate equipment, these conditions can be further improved by means of climate control [1]. Modern greenhouse and computerized climate control modules have become inseparable nowadays. Computerized climate control is an intrinsic part of present day modern greenhouse [2]. Some of the advantages of FLC systems in greenhouses are improvements in crop quality, harvest, energy saving [3], as well as in the reduction of the human factor [4]. The main environmental factors affecting the greenhouse climate control are as follows: temperature, relative humidity, of the inside air; vapor pressure deficit, transpiration [5], sunlight, CO₂ generation, wind speed [6] and lighting. The Output Unit Models for the greenhouses are heating system, cooling system, irrigation systems, mechanical fan, fog cooling and Lighting System [1].

In this study, a fuzzy controlled greenhouse model was set ,and the performance of the growth lamp designed with LEDs of different wave lengths and colors was examined. Parameters such as soil humidity, ambient temperature and humidity, exterior ambient temperature and humidity, wind speed, radiation doses under interior ambient and growth unit and interior carbon dioxide level were measured and processed as fuzzy rule-based. Accordingly, heating, ventilation, irrigation and shadowing of the greenhouses and scaling the light level of the LED growth unit were experimented. All measurement and control parameters were recorded on the MMC card found on the control unit. The performance of the developed control unit and the LED growth unit and its effect on pepper were examined indoors.

2 Material and Method

2.1 Modeling The Greenhouse

The greenhouse controller block diagram, which is integrated into the system model recommended by Javadikia et al 2009, is seen in Figure 1 [1].

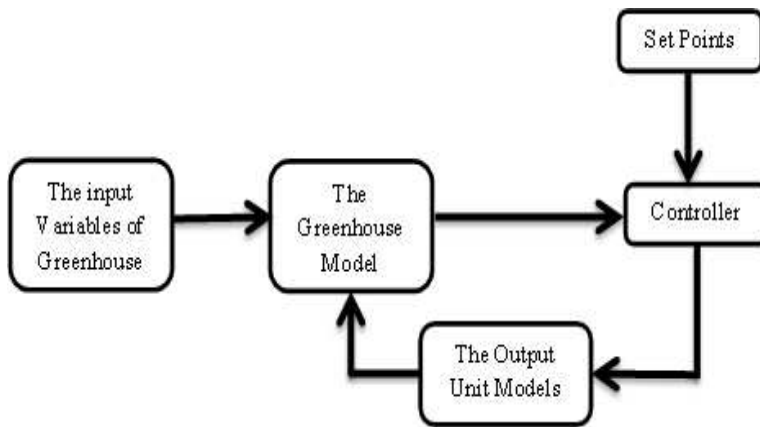


Figure 1
Greenhouse controller block diagram

The total area of the prototype greenhouse is set to 2 square meters. In the set model, input variables are light intensity, temperature, air humidity, soil humidity, wind speed and carbon dioxide level. As for output variables, identification of the light intensity of the LED plant growth unit, irrigation, heating, cooling, and ventilation are handled. Shadowing is not considered in the developed model. Since the aim of the model is to provide artificial light into the greenhouse especially during sunless periods, the need for shadowing is eliminated. However, taking summer into consideration, an output was designed on the control card output for controlling the shadowing unit. Chao and Gates [7] reviewed recent models for greenhouses, from which we take the following dynamic equations for interior air temperature. Note that conversion of sensible heat to latent heat is accounted for by using a “net” sensible heat term in each equation. A greenhouse dynamic equation is [1];

$$\rho C_p V \frac{\partial T}{\partial t} = (q_h + \alpha S A_f) - \rho C_p \dot{V} (T - T_{out}) - U A_s (T - T_{out}) \quad (1)$$

Variables in these equations are defined as:

A_f = floor area (m²)

A_s = surface area (m²)

α = building net solar heating efficiency

C_p = specific heat of air [J (kg °C)⁻¹]

q_h = heater output (W)

ρ = air density (kg m⁻³)

S = solar irradiance (W m⁻²)

T = interior air temperature (°C)

T_{out} = outside air temperature (°C)

U = overall building thermal conductance (W m⁻² °C⁻¹)

V = building volume (m³)

\dot{V} = volumetric ventilation rate (m³ s⁻¹)

2.2 Traditional Climate Control

This control system is based on a heater actuator which is turned on and turned off by a thermostat whenever the temperature error is oversteps the fixed regulation band. The humidity depends on the internal air temperature and the ventilation rate. This last variable is regulated by opening the windows of the greenhouse, based on the measured wind-speed. This also avoids some dangerous situations such as high wind speed in the external environment [8].

2.3 Fuzzy Logic Climate Control

As known from the Fuzzy Logic principles an FLC acts as a non-linear system implementing a human-based reasoning for the computation of their output values [8]. Fuzzy knowledge-based systems are one of the most successful applications of fuzzy sets and fuzzy logic methods. This is mainly due to the flexibility and simplicity by which knowledge can be expressed using fuzzy rules as well as to the theoretical developments in this field [9]. The fuzzy rule base consists of a collection of fuzzy IF–THEN rules. The basic configuration of a fuzzy logic system for a greenhouse is shown in Figure 2. The features and Fuzzy linguistic expressions of input/output system variants are given in Table 1 and Table 2.

Table 1
The Fuzzy linguistic expressions of input /output system variants

Parameters	Type	Fuzzy Linguistic expressions
Ambient Temperature	Input	Very Low, Low, Medium, High, Very High
Inside Temperature	Input	Very Low, Low, Medium, High, Very High
Air Humidity	Input	Very Low, Low, Medium, High, Very High
Soil Humidity	Input	Very Low, Low, Medium, High, Very High
CO ₂	Input	Very Low, Low, Medium, High, Very High
Wind Speed	Input	Very Low, Low, Medium, High, Very High
Lighting	Input	Very Low, Low, Medium, High, Very High
Heating System	Output	Very Low, Low, Medium, High, Very High
Cooling System	Output	Very Low, Low, Medium, High, Very High
Irrigation System	Output	Very Low, Low, Medium, High, Very High
LED plant Growth Unit	Output	Very Low, Low, Medium, High, Very High
Mechanical Fan	Output	Very Low, Low, Medium, High, Very High

Table 2
The Features of input /output system variants

Parameters	Min	Max	Denomination
Ambient Temperature	-20	40	°C
Inside Temperature	-20	50	°C
Air Humidity	0	100	%
Soil Humidity	0	100	%
CO ₂	0	2000	ppm
Wind Speed	0	10	m/s
Lighting	0	20000	Lux
Heating System	0	3	kW
Cooling System	0	20	Micron
Mechanical Fan	0	50	°
Irrigation System	0	20	Lt
LED plant Growth Unit	0	20000	Lux

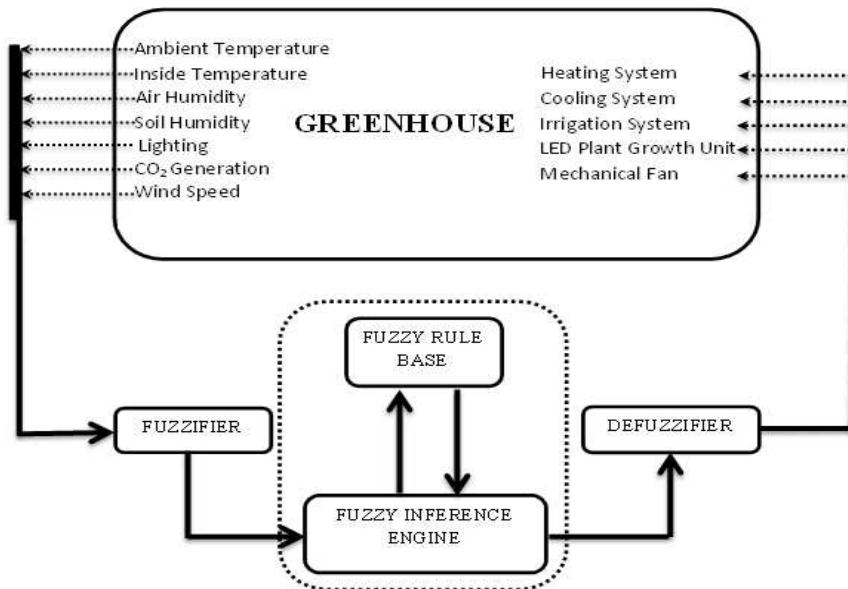


Figure 2
The Fuzzy control system model designed for the greenhouse system

For all the Fuzzy inferences, the Mamdani inference model was preferred as it is both easy and suitable for the greenhouse model. The triangle fuzziness method was chosen. Reference situations for tests were chosen according to growing conditions. Relying on expert opinion, the value of soil humidity was determined

to be 70%, the need for light as 10000 Lux, ambient temperature in the greenhouse as 24 °C. Fuzzification of the input signs which belong to these specified parameters is given in Figure 3.

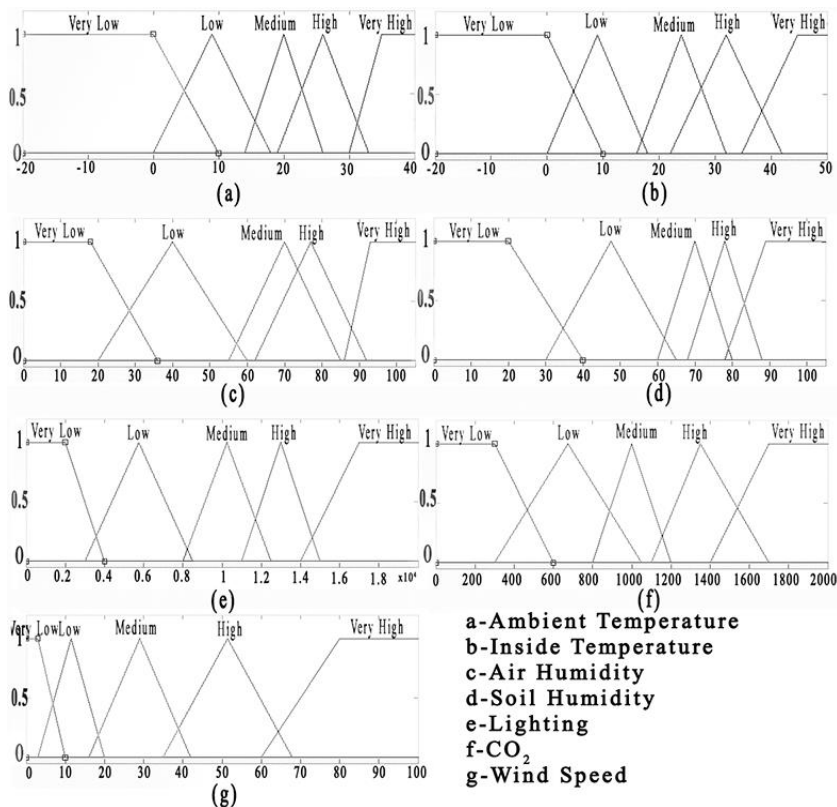


Figure 3

Fuzzification of input operating conditions

Fuzzification of the output signs for the specified output parameters (heating, cooling, ventilation, lighting, irrigation) is given in Figure 4. Since the tests were carried out indoors, parameters such as the measurement of the wind speed and the level of light which comes into the greenhouse from the outside were not considered. Wind speed and level of light parameters which exist on the rule base were deactivated during the experiments. How the exterior light intensity that comes into the greenhouse affects the output of the LED plant growth unit is given in Table 3. The control logic of the LED plant growth unit is mentioned in the control section.

Table 3
Effect of light intensity to LED plant growth unit output parameters

Light Intensity	LED plant growth unit output
Very Low	Very High
Low	High
Medium	Medium
High	Low
Very High	Very Low

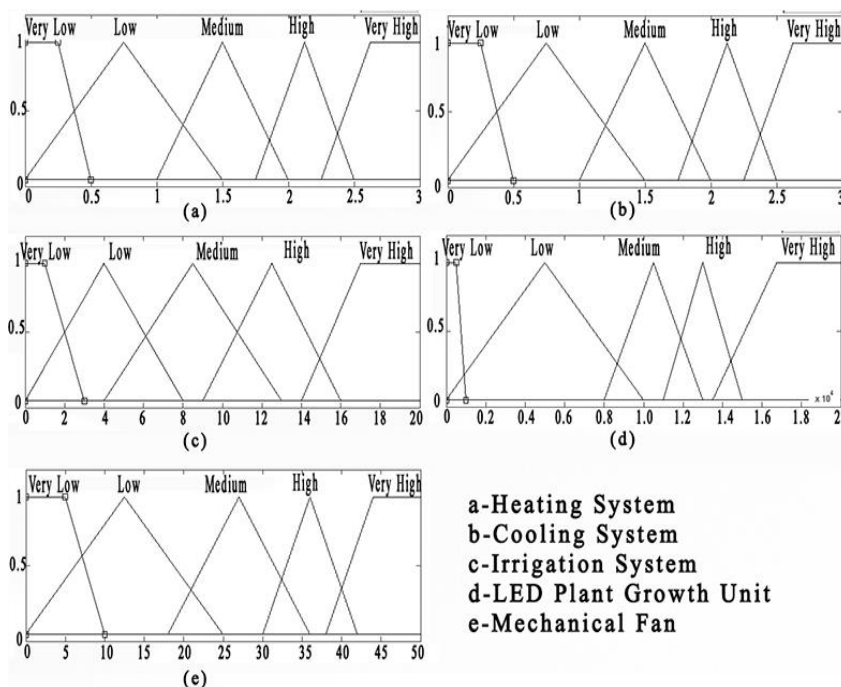


Figure 4
Fuzzification of output operating conditions

2.4 LED Plant Growth Unit

The designed LED plant growth unit is composed of Royal Blue, Blue, UVA, Far Red and Red LEDs. Total electric power consumption of the unit which is composed of power LEDs of 3 W, 5 W and 10 W is 217 W. Direct current fans used for cooling increases this value to 220 W. Power LEDs were installed on the aluminum PCBs, whose features are given in Table 4.

Table 4
Features of the aluminum PCB

Power LED PCB	Model 1	Model 2
Diameter	100mm	120mm
LED Pieces	9	12
Ground Color	White	White
Number of PCB	1	6

Power LED layout for settlement in Figure 5 shows the design for obtaining an effective lighting design and effective air cooling. Thanks to the established lighting layout, a light source which has a wave length of 380-385 nm with Ultra Violet UVA, 455-457.5 nm with Royal Blue power led, 460-475 nm with Blue power led, 615-630 nm with Red power led, and 660 nm with Far Red power led, was set. Electrical features of the power LEDs that were used are given in Table 5. Emission spectra of red (R) and blue (B) LEDs is given in Figure 6a.

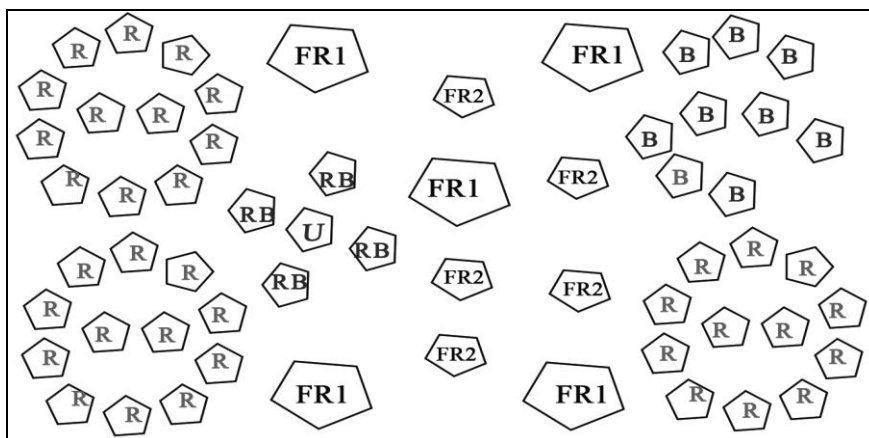


Figure 5

The settlement of the power LEDs which have different wavelengths in the LED plant growth unit

Table 5

Electrical features of the power LEDs which have different wave lengths in the LED plant growth unit

<i>Index</i>	<i>RB</i>	<i>B</i>	<i>U</i>	<i>R</i>	<i>FR1</i>	<i>FR2</i>
Name	Royal Blue	Blue	Ultra Violet UVA	Red	Far Red	Far Red
Power (Watt)	3	3	5	3	10	3
Pieces	4	9	1	36	5	5
Rate of Radiation	5,53	12,44	2,30	49,76	23,04	6,91
Wavelength (nm)	455 - 457.5	460 - 475	380 - 385	615 - 630	660	660

Intensity (Lm)	30 - 40	25 - 32	400 – 600 (MW/sq)	65 - 75	300 320	70 - 80
Viewing Angle (Degree)	120	140	115-125	140	180	120
Forward Voltage (V)	3.4 - 3.6	3.2 - 4.0	6.5 - 7.5	2.2 – 3.0	7.0 – 9.0	2.7 – 3.0
Average Forward Current (mA)	700	700	750	700	1000	750

Power LEDs were soldered onto the aluminum PCBs as shown in Figure 5 with special thermal paste, the features of which are given in Table 6. Aluminum PCBs were mounted on the aluminum coolers with special thermal paste, the features of which are given in Table 7. Thermal grease helps to disperse the heat from aluminum PCB to the heat sink effectively. It has a high temperature resistance. It is non-toxic, tasteless and non-corrosive. The heat on the surface is rejected from the surface due to the DC fans which were mounted on the back surface of aluminum coolers.

Table 6
The features of Gold Thermal Grease Paste

<i>Gold Thermal Grease Paste</i>	
Thermal Conductivity (W/m-k)	> 3
Thermal Resistance ($^{\circ}\text{C-in}^2/\text{W}$)	< 0.123
Color	Gold

Table 7
White Thermal Compound Grease

<i>Thermal Compound Grease Paste</i>	
Thermal Conductivity (W/m-k)	> 0.65
Thermal Resistance ($^{\circ}\text{C-in}^2/\text{W}$)	< 0.262
Color	White

LED plant growth unit's height is 2 meters from the ground. The sides of the closed area were covered with Mylar film and was aimed for more effective lighting. The Mylar film has 175 micron in thickness, high reflectance, very high level of thermo stability, and further, is easy to clean. Mylar Film, commonly used in wall covering material by the indoor cultivators, is a reflective product. It also enables the use of each watt of energy spent by the lighting unit. In the case of using aluminum foil as the wall covering material, the zigzags on the aluminum foils cause extremely hot spots and these hot spots could have a lens effect, focusing the light on certain parts of the plant resulting in burn spots. Holding a smooth structure, Mylar film does not result in hot spots and is preferred for indoor studies.

2.5 Control Unit

PIC microprocessor 18F4550 which was produced by Microchip Company was chosen as the controller in the control unit. Sensors were connected to the ports of controller. These include one temperature sensor (DS18B20) to measure outer ambient temperature, one humidity sensor (SHT11) to measure soil humidity and temperature, one humidity sensor (SHT11) to measure in-greenhouse ambient humidity and temperature, one photo diode (S1223) to measure the level of light coming from outside into the greenhouse, one photo diode (S1223) to measure the total level of light coming from outside and LED plant growth unit into the greenhouse and one Carbon dioxide sensor (MG811) to measure the level of carbon dioxide in the greenhouse. The measured light values were amplified with the opamp and applied to the controller. The spectral sensitivity of the photo diode (PD) from the S1223 datasheet is shown in Figure 6b. The connection was made by the mosfets to enable the outputs of heating, cooling, irrigation, ventilation system and the output of the LED plant growth unit light control to the ports of the controller which was directed as output. Thanks to the mosfets output units on the control card, the parameters such as heating, cooling, ventilation, irrigation, lighting can be controlled according to PWM.

Schematic representation of the control system is given in Figure 7. Thanks to the LCD indicator on the control card, the instant values of the system in the greenhouse can be monitored. All the components of the system can be monitored from a distance by computer connection. Temperature, humidity, irradiation values and heating, cooling, irrigation, ventilation and lighting event times are recorded on the MMC unit on the card. The parameters such as irrigation, ventilation, heating and lighting can be controlled using PWM.

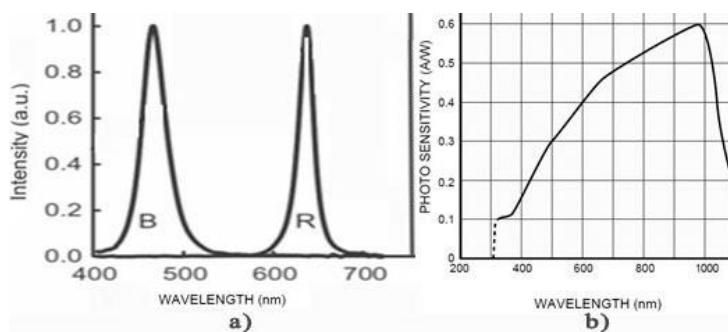


Figure 6

a) Emission spectra of red (R) and blue (B) LEDs

b) The spectral sensitivity curve of the photodiode (PD) from the S1223 datasheet is shown

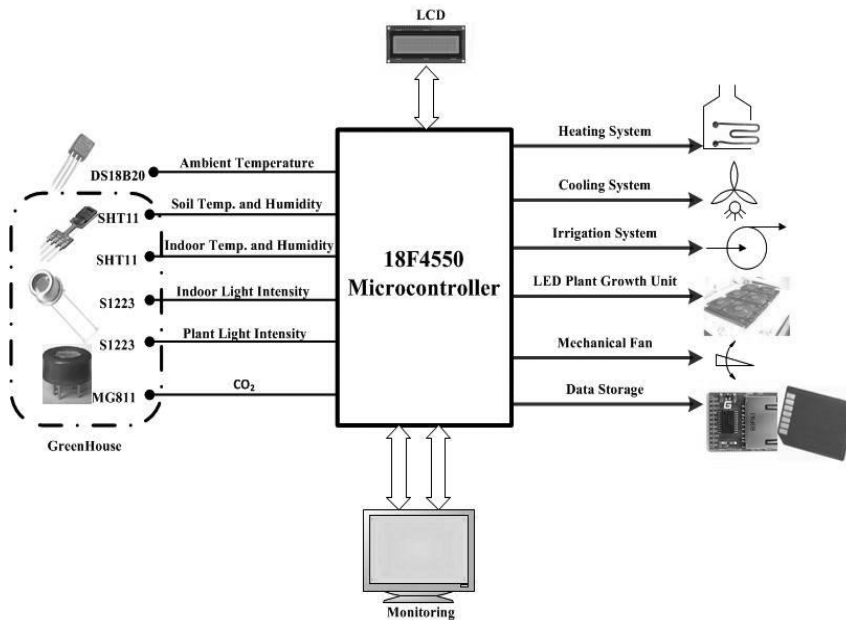


Figure 7

Schematic representation of the control system

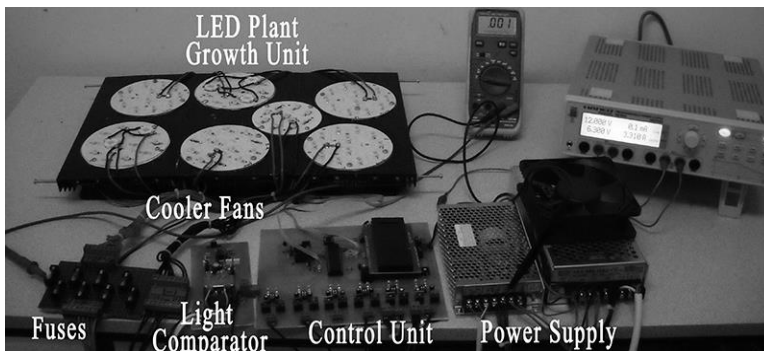


Figure 8

LED plant growth unit and control equipment

A scene from the test period of the LED plant growth unit and control card is given in Figure 8. The programmable Hameg HMP2020 power supply was used for current tests. Almemo UVA probe head FLA 603 UV12, lux probe head FLA 603 and an irradiation unit that were developed using S1223 photodiodes were used for radiometry measurements. Almemo FHAD 46 series humidity sensor was used for the calibration of SHT11 sensor which was used for humidity and temperature and DS18B20 sensor. SHT11 sensor used for soil humidity and

temperature was mounted into a pointed copper tube. Holes were made on the pointed side of the copper tube and then it was placed into soil. The back part of the copper tube was insulated to make sure it was not affected by the outer conditions.

2.6 Experiments

The growth chamber model for LED plant growth unit is given in Figure 9. For three weeks pepper plants were grown in a 2-square-meter closed area that was 2 meters high, with an average day temperature of 25 °C and a night temperature of 19 °C. The sides and ground of the closed area were covered with Mylar film and pepper and aromatic chamomile were placed in it. The parameters such as humidity and temperature values, soil temperature and humidity, light intensity, the level of carbon dioxide in the area were measured and saved in MMC. Plants were exposed to 16 hours of lighting every day. The average indoor light intensity was 10000 Lux. All operation conditions and measured values were recorded on an MMC card in real time with the integration of the real time clock (DS1307) of the control card. While ventilation should be carried out using a mechanical fan in a real greenhouse, it was instead provided with the help of direct current fans in the constructed mechanism. A mini DC pump, the water hole diameter of which was 4 mm, was used for drip irrigation. In addition, the atomized system involving a pump and nozzles was used to balance the ambient humidity. This system atomized water to the interior area when the humidity was low.



Figure 9

The appearance of the testing apparatus

LED plant growth unit was supplied in constant supply mode during the experiments. In other words, each led in the LED plant growth unit and the features given in Table 5 had constant current supply. Thus, there was constant light, which has a wave length varying between 380 nm and 660 nm, of 10K Lux. The growth values of pepper and aromatic chamomile are given in Figures 10 and 11. In Figure 12, pepper and aromatic chamomile growth phase periods in the 19.04.2013 and 10.05.2013 labeled a-b-c and d-e-f.



Figure 10
Pepper plant growth

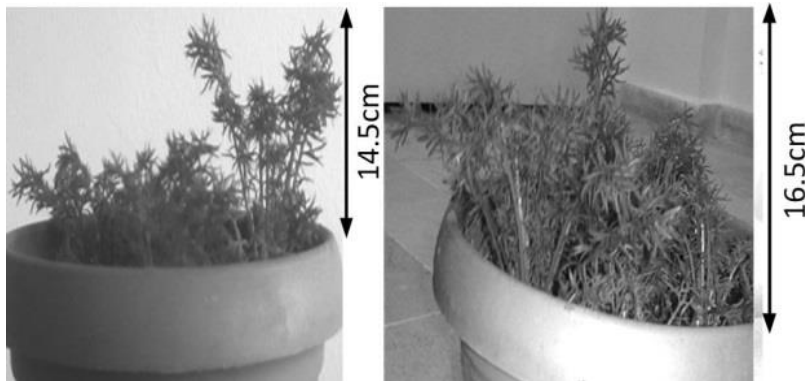


Figure 11
Aromatic Chamomile plant growth

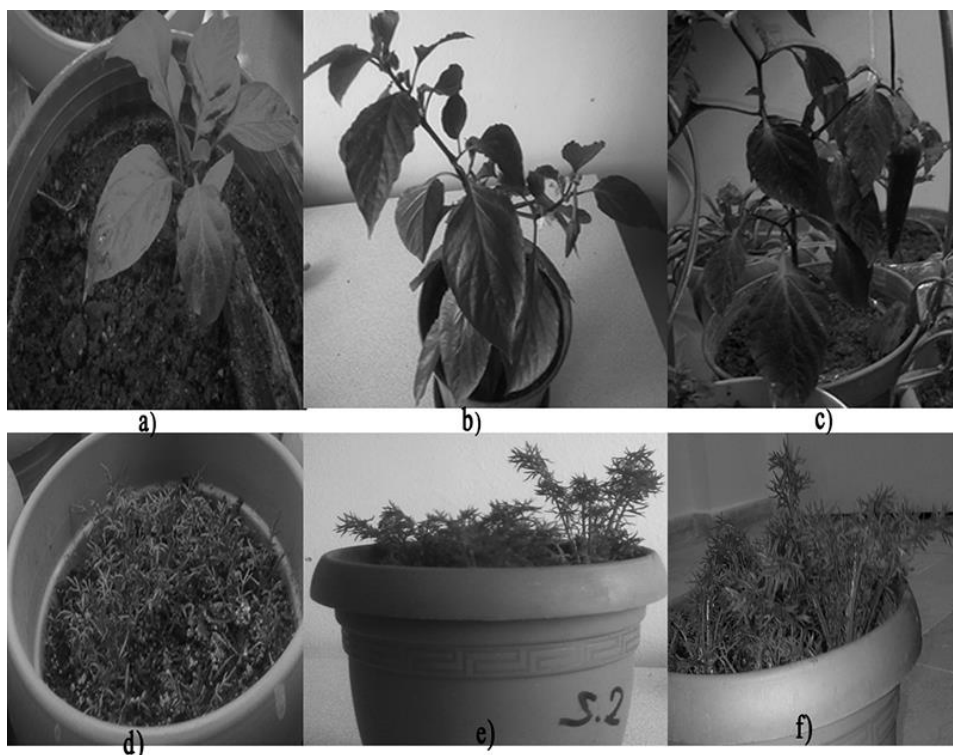


Figure 12

Pepper and Aromatic Chamomile plant growth

- a) 19.04.2013 pepper, b) 03.05.2013 pepper, c) 10.05.2013 pepper, d) 19.04.2013 Aromatic Chamomile, e) 03.05.2013 Aromatic Chamomile, f) 10.05.2013 Aromatic Chamomile

Conclusions

Fuzzy control can reduce the financial costs in the greenhouses. While the quality of the crops is increased, energy costs are reduced in a greenhouse controlled via fuzzy logic method. The indoor plant growth cabin with fuzzy logic-based control suggested in the study was designed for the purpose of growing plants in the greenhouses when there is not enough light during winter months. In the indoor experiments, only the parameters such as light, temperature, humidity, carbon dioxide were taken as input. In the rule base, the fuzzy logic method was applied in accordance with the working conditions of a real greenhouse. Output parameters were irrigation, ventilation and lighting. Factors like heating and cooling were not considered in the controlled indoor environment. The results that were obtained from pepper and aromatic chamomile are presented above.

Since the main objective of the study is to ensure carnation production in greenhouses during winter, later experiments shall involve greenhouse conditions

for growth of carnation. Alternate energy sources like soil source heat pump as well as biomass shall be used to produce heating energy needed during winter.

In the study, a DC constant supply condition was considered. As for the ongoing designs, new growth units are worked on to examine two different working conditions simultaneously. The upcoming studies will discuss the experiments conducted with existing control card and control mechanism on the plants that are tested by one LED plant growth unit with PWM output and by another LED plant growth unit with constant DC supply. Thus, the development process and crop yield of the plants which are grown in PWM mode and with DC constant supply will be examined. Finally, the effect of different PWM parameters on plants will be studied.

References

- [1] Javadikia, P., Tabatabaeefar, A., Omid, M., Alimardani, R., Fathi, M. (2009) Evaluation of Intelligent Greenhouse Climate Control System-based Fuzzy Logic in Relation to Conventional Systems. International Conference on Artificial Intelligence and Computational Intelligence, pp. 146-150
- [2] Straten, G. V. (1999) Acceptance of Optimal Operation and Control Methods for Greenhouse Cultivation. Annual Reviews in Control, Vol. 23, pp. 83-90
- [3] Seginer, I., Zlochín, I. (1997) Night-Time Greenhouse Humidity Control with a Cooled Wetness Sensor. Agricultural and Forest Meteorology, Vol. 85, pp. 269-277
- [4] Collewet, C., Rault, G., Quéllec, S., Marchal, P. (1998) Fuzzy Adaptive Controller Design for the Joint Space Control of an Agricultural Robot. Fuzzy Sets and Systems, pp. 1-25
- [5] Joliet, O., Hortitrans (1994) A Model for Predicting and Optimizing Humidity and Transpiration in Greenhouse, Journal of Agricultural Engineering. Vol. 57, No. 1, pp. 23-37
- [6] Körner, O., Challa, H. (2003) Process-based Humidity Control Regime for Greenhouse Crops. Computers and Electronics in Agriculture, pp. 1-20
- [7] Chao, K., Gates, R. S. (1996) Design of Switching Control Systems for Ventilated Greenhouses, Trans ASAE, Vol. 39, No. 4, pp. 1513-1523
- [8] Caponetto, R., Fortuna, L., Nunnari, G., Occhipinti, L. (1998) A Fuzzy Approach to Greenhouse Climate Control, Proceedings of the American Control Conference, Philadelphia, Pennsylvania, pp. 1866-1870
- [9] Salgado, P., Cunha, JB. (2005) Greenhouse Climate Hierarchical Fuzzy Modelling. Control Engineering Practice 13, 613-628

Productive Entrepreneurship in the EU and Its Barriers in Transition Economies: A Cluster Analysis

Zsuzsanna K. Szabo, Emilia Herman

“Petru Maior” University of Tg. Mures
1 N. Iorga, 540088 Tg. Mures, Romania
zsuzsanna.szabo@ea.upm.ro, emilia.herman@ea.upm.ro

Abstract: A wide-spectrum of registered entrepreneurial activities can be observed in transition economies. However, the outcomes are not reflected in the projected economic growth. This article examines the entrepreneurial performance of transition economies in the European context and presents a research approach on the relationship between economic development, institutions and entrepreneurship in order to identify needs to eliminate barriers to productive entrepreneurship. The authors present a cluster analysis of EU Member States. In this respect, the scientific approach is a necessity. The findings of the study can be useful for policymakers to formulate policies in concordance with priorities.

Keywords: productive entrepreneurship; transition; value creation; cluster analysis

1 Introduction

Entrepreneurship is considered the “main driver of economic growth” [12]. It is also widely acknowledged that entrepreneurship has a positive impact on different indicators measuring the level of economic development. Moreover, entrepreneurship is a topic that concerns potential entrepreneurs who are interested in starting their own businesses as well decision makers who are willing to formulate adequate policies aiming to enhance a more favorable environment for businesses. Entrepreneurship has developed greatly over the last 20 years and it continues to grow. Entrepreneurship was studied in its multidimensionality and a tremendous number of research papers have been published. Entrepreneurship scholars identified a large variety of entrepreneurial activities across different societies all over the world, such as formal/informal, legal/illegal and necessity/opportunity entrepreneurship, respectively.

This paper focuses on the entrepreneurial activities output by investigating the entrepreneurship impact on economic development. In this respect, we concentrate on the efficiency and quality of the entrepreneurial activities. The main purpose of the study is to analyze the connection between entrepreneurial activities and value creation.

In his 1990 fundamental paper, Baumol, distinguished between productive, unproductive, and even destructive entrepreneurship [5]. He claimed that while the level of entrepreneurship was constant over time and across the phases of development, the quality of entrepreneurship varied considerably. According to Baumol, entrepreneurial differences were determined by institutions, not by the degree of the underlying entrepreneurial spirit. Baumol's theory was recognized as a significant contribution to the economics of entrepreneurship literature [26]. A theoretical and empirical exploration of the productive, unproductive and destructive entrepreneurship was published in 2008 by Sauka [22]. The conceptual framework developed by Sauka, also presents a fundamental contribution to the entrepreneurship literature. It opens a research direction with the aim to reduce the differences between the outputs of entrepreneurial activities between countries. Sauka measured productive entrepreneurship in terms of growth on societal and venture level. The environment, in which the entrepreneurial process is taking place, determines the quality of the individuals' skills, abilities and transformation in outputs [23], [24]. To assure productive entrepreneurship, the role of entrepreneurial orientation (EO) was recognized as significant. Sauka [22] and Miller [20] proposed the following dimensions of EO: Innovativeness, proactiveness and risk-taking. Later, in 1996, another two dimensions were introduced: competitive aggressiveness and autonomy [19]. Innovation is considered the engine of growth, being an important element of development achievements [14]. Its impact on the growth of the innovative SME's is significant, as confirmed by official data [12]. Therefore, *innovative entrepreneurship* started to be considered a key factor of modern economic development [12]. Productive entrepreneurship generates economic wealth through innovation and by filling gaps in the market. Douhan and Henrekson [8] confirm a strong positive relationship between productive entrepreneurship and an economy's innovativeness as well as its ability to adapt. Entrepreneurial behavior (EB) is treated in various ways in literature. Research papers prove the role of institutions in the output of entrepreneurial activity and underline the difference between quality and quantity entrepreneurship. Estrin *et al.* [10]; Aidis and Sauka [1] determined specific types of EB in transition countries.

This article examines the performance of entrepreneurial activities in transition economies, in the European context, to identify the barriers which must be eliminated through adequate policies in order to catch up with developed economies. We will analyze the entrepreneurial activity through the generated output, in order to determine needs, to eliminate the barriers for productive entrepreneurship.

2 Research Questions, Hypotheses and Objectives

A reduced number of research studies, which focus on productive, unproductive and destructive entrepreneurship, have been published. Entrepreneurship exists all over the world, but the importance of entrepreneurship does not consist only in the quantitative presence of entrepreneurship, but in the entrepreneurial activities impact on economic development. The conceptual framework of productive entrepreneurship was developed by Sauka, who underlined the importance of analyzing the firms' activities output on both, venture and societal levels [22]. Researchers started to focus on the efficiency of entrepreneurship and studies were published which treated the quantity and quality of entrepreneurship separately. In order to measure entrepreneurship, the Global Entrepreneurship Index was introduced by Acs and Szerb in 2009 [2], and was continuously developed and renamed as the Global Entrepreneurship and Development Index (GEDI) by the same scientists [3]. It is widely recognized that technology and innovation have a positive impact on the entrepreneurial performance and have a significant role in the social and economic development through the created output. At the same time, significant differences can be observed in innovation capacity and performance between EU Member states [27]. Estrin et al. [10] present the most important role of institutions in "the rising SME contribution to employment and value added (output)." Based on the literature, three main institutions are considered relevant for entrepreneurship: property rights [17]; state-sector [5] and financial sector [16], [6], and all of them are considered barriers to entrepreneurship. We believe that, in order to reduce the gap between developed and transition economies, and transform the entrepreneurial activity in a productive way, it is necessary to make a detailed analysis of entrepreneurial activities and study the financial, institutional, human capital, socio-cultural factors and their impacts on the entrepreneurial activities output both within and across societies. The study is focused on the following research topics.

Question 1: To evaluate the performance of the entrepreneurial activity in transition economies, we will first determine a comparative view of entrepreneurship in the EU. We are interested in studying the relationship between transition economies and developed economies as it relates to entrepreneurship and the implications for socio-economic development and seeing whether there is a meaningful difference or not. We will measure the intensity via TEA-Total early-stage Entrepreneurial Activity [15], and the entrepreneurial performance via GEDI methodology.

H1: The total early-stage Entrepreneurial Activity (TEA) has an increasing tendency in transition economies.

H2: The efficiency of entrepreneurship is determined by the level of stages of economic development.

H3: GEDI and GEM-TEA Index measure different aspects of entrepreneurship.

Question 2: We will explore the entrepreneurship in its multidimensionality using 12 variables which highlight economic development, entrepreneurship, institutional development, innovation and technological readiness. To gauge the economic performance various indicators such as GDP/capita, the labor productivity and the Global Competitiveness Index (GCI) were used. Innovation capacities and performance will be measured by the Summary Innovation Index (SII) and a nation's or community's degree of preparation to participate in and benefit from information and communication technology developments via NRI index. The institutional environment will be expressed by the Ease of Doing Business Rank (DB) and the Index of Economic Freedom. Entrepreneurship will be defined by GEDI, Necessity-Driven Entrepreneurial Activity indicator (TEA necessity) and Improvement-Driven Opportunity Entrepreneurial Activity (TEA opportunity), as a percentage of Total early-stage Entrepreneurial Activity. Innovative entrepreneurship will be analyzed by SMEs introducing product or process innovations and SMEs introducing marketing or organizational innovations as a percentage of SMEs. We will realize a cluster analysis of EU member states.

H4: The EU Member States can be enrolled in different clusters based on the entrepreneurial performance.

Question 3: We are interested to see the connection between the intensity of entrepreneurial activity and the generated output from it. It is widely acknowledged that the generated output has an impact on the economic development. In the pursuit of studying whether the entrepreneurial activity in transition economies is productive or not, we will analyze the efficiency of entrepreneurship and we will compare the output on both the venture and societal level between EU member states.

H5a: The output on both the venture and societal level shows high differences between transition and developed economies.

H5b: In transition economies, entrepreneurship is productive on the societal level, having a significant role in the generation of employment.

Question 4: In order to improve the outputs of the different types of entrepreneurial activities, we will study the different aspects of entrepreneurial activities using both individual and institutional data. Some researchers show that the institutional environment has a considerable impact on the output of entrepreneurial activities. Sauka [22] studied how environment and institutions can moderate the entrepreneurial orientation and entrepreneurial behavior having impact on outputs. We will compare the results of transition economies relative to their peer countries in the same cluster. A comparative study between clusters will be realized as well. The aim of this investigation is to identify the barriers for transition economies and provide policy suggestions on how to encourage productive entrepreneurship. Entrepreneurial attitudes have a fundamental impact

on factor driven economies, the entrepreneurial activity on the efficiency driven economies and the entrepreneurial aspiration on innovation driven economies.

H6: The position of the transition economies regarding the connection between innovation and economic development measured by GDP/capita is far from the position of the developed economies. Within the cluster, the situation is comparatively similar. The low level of innovative capacity presents a barrier to productive entrepreneurship.

H7: The high quality of institutions can be expected to have a significant role on the quality of entrepreneurial activity, and thus on the level of the economic development. The institutional environment presents an obstacle to productive entrepreneurship in transition economies.

H8: On the venture level, large enterprises are more productive. The increasing number of large enterprises in transition economies should be pursued aggressively because of its strong relationship within economic development.

3 Methodology and Data

We used publicly available databases such as GCI, Global Competitiveness Index (2007-2013), introduced by Xavier Sala-i-Martin in 2004, countries rank published annually by World Economic Forum, using different indicators grouped by 12 pillars [29]; SII, Summary Innovation Index (2012-2013) - the Innovation Union Scoreboard divided the EU Member States into four groups based on their summary innovation performance [12]; NRI, Network Readiness Index (2012-2013), defined as a nation's or community's degree of preparation to participate in and benefit from information and communication technology developments [30]; Ease of Doing Business Rank [28]; Index of Economic Freedom, according to The Heritage Foundation [21], covering all aspects of economic environment, consisting of four pillars of economic freedom care and involving both individuals and governments (Rule of Law, Limited government, Regulatory efficiency, Open markets); GEM, Global Entrepreneurship Monitor, an ongoing multinational project created to investigate entrepreneurship [15], [32]; EUROSTAT database [13]; GEDI, Global Entrepreneurship and Development Index, which captures the multidimensional nature of entrepreneurship, the qualitative and quantitative aspects of entrepreneurial activity, using both individual and institutional data, [4]. The different types of used indicators characterizes the entrepreneurial activity, the business environment from different points of view and, in this way, they sustain the methodology giving a strong fundamental base for this study.

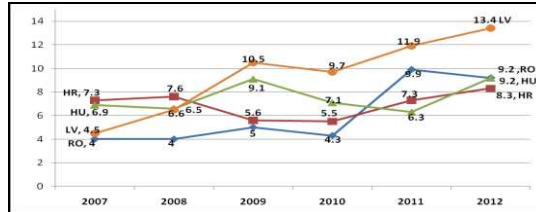
In the pursuit of obtaining a comparative view of the performance of entrepreneurship, we used the Principal Component Analysis (PCA). PCA is a

useful multivariate statistical technique that is used to identify patterns in data, and express the data in a way that highlights similarities and differences [25]. PCA is an advantageous method because it reduces the dimensionality of a data set consisting of a large number of interrelated variables to a few factors or principal components, while retaining as much as possible of the variation present in the data set [18]. In this study, the principal component analysis with Varimax rotation and Kaiser Normalization is used to transform the set of originally mutually correlated variables into a new set of independent variables. Based on the entrepreneurship performance of the transition economies in the European context, we will establish a classification of the European countries using cluster analysis. Cluster analysis finds peer countries and identifies relatively homogenous groups of countries based on the selected variables/principal components. The principal components obtained by PCA became the basis for cluster analysis, which led to the identification of the homogeneous groups of countries. Therefore, at first we used the hierarchical cluster analysis, using Ward's method and the Euclidian distance in order to determine the number of clusters. This method was followed by the k-means cluster analysis [11]. K-means cluster analysis is a commonly used procedure to identify relatively homogeneous groups of cases based on selected characteristics. It was proven that principal components (PCA) are actually the continuous solution of the cluster membership indicators in the K-means clustering method. Thus, the PCA automatically performs data clustering according to the K-means objective function, the solution to Kernel K-means is given by Kernel PCA components [7]. Descriptive statistics was used to thoroughly study the internal and external interpretation of the results obtained using the principal components analysis, as well as the cluster analysis. To verify the relationships suggested by the hypotheses, regression analysis was employed. The quality of prediction is measured by the value R^2 . To measure the strength of association between two ranked variables, the Spearman's rank-order correlation was used. For data processing, the SPSS software package was used.

4 Results and Analysis

Regarding hypothesis *H1*, longitudinal data was used and we can observe, as can be seen in Figure 1, that in transition economies the total early-stage Entrepreneurial Activity (TEA) has an increasing tendency. Differences can be observed among countries, for some of them the increasing tendency is more accentuated than for the others. On the other hand, these countries did not record performance on venture-level, in terms of GDP/capita and labor productivity, [13]. Some transition economies such as Poland, Slovakia and Bulgaria are missing because of data availability for the period of 2007-2010.

Next, we used cross-sectional data to measure the entrepreneurial activity outputs and their impact on economic development. A study on the performance of entrepreneurship is required because, from the competitiveness point of view, transition countries lag behind developed economies.

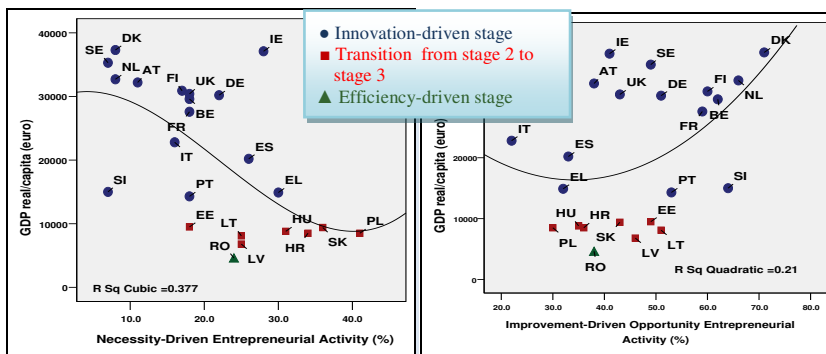


Source: [32]

Figure 1

Total early-stage Entrepreneurial Activity (TEA)

To analyze the impact of the stages of the economic development on entrepreneurial activity efficiency, hypothesis *H2* was tested. To see the relationship between Necessity-Driven Entrepreneurial Activity indicator (calculated as percentage of those involved in Total early-stage Entrepreneurial Activity-TEA) and the stage of economic development, measured by GDP/capita, we calculated the Spearman correlation coefficient ρ . The calculated $\rho = -0.619$ indicates a moderate negative relationship, as can be seen in Figure 2a.



Source: Own calculations based on data provided by [13], [29], [32]

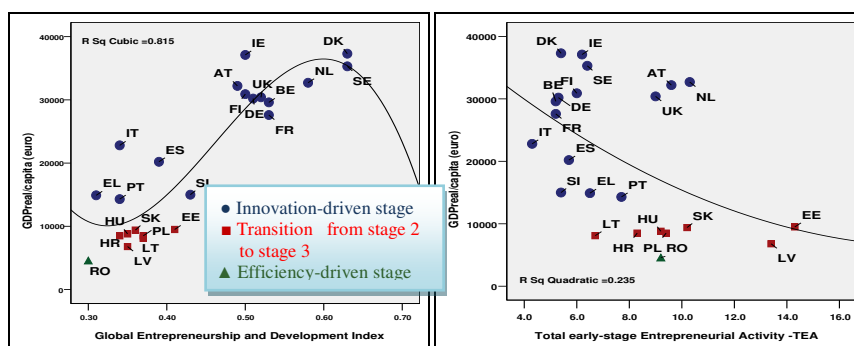
Figure 2

- (a) Negative moderate correlation between “necessity entrepreneurship” and economic development
- (b) Positive moderate to low correlation between “opportunity entrepreneurship” and economic development

In the case of Improvement-Driven Opportunity Entrepreneurial Activity, the calculated Spearman correlation coefficient is $\rho = +0.398$, which indicates that the correlation is a moderate to low positive (Figure 2b). Thus, it is confirmed that necessity driven entrepreneurship decreases with the evolution of the stages of the economic development and the opportunity driven entrepreneurship has a high

impact on the growth of the GDP. The efficiency of entrepreneurship, measured as output on venture level, increases with the evolution of the stages of economic development.

Examining results of testing H3, a significant relationship is revealed between GEDI and economic development (Spearman correlation coefficient $\rho = +0.797$, $R^2 = 0.803$, $p < 0.001$). A negative moderate to low relationship between GEM-TEA index and economic development was indicated by the calculated Spearman correlation coefficient: $\rho = -0.409$, $R^2 = 0.235$, $p < 0.1$). Our results highlight that GEDI and GEM-TEA index measure different aspects of entrepreneurship as can be seen in Figures 3a and 3b. It can be noticed that GEDI is focused on the quality and TEA on the quantity of entrepreneurial activity.



Source: Own calculations based on data provided by [4], [13], [29], [32]

Figure 3

- (a) Positive relationship between GEDI and economic development in EU23 countries
- (b) Negative moderate to low relationship between TEA and economic development, in EU23 countries

In order to test hypothesis **H4**, we selected indicators from publicly available databases. We used a descriptive analysis of the considered indicators to highlight the heterogeneity of the entrepreneurial activity of European countries. A study on the quality of entrepreneurship needs a complex analysis. We used 12 variables (Table 1) and we analyzed 23 EU member states (Luxemburg, Malta, Czech Republic, Bulgaria, Cyprus data missing) focusing on the following: economic development, entrepreneurship, institutional development, innovation and technological preparedness.

The number of valid cases for this set of variables (N) is 23. PCA requires a strong relationship between the variables included in the analysis. The correlation matrix obtained based on our own calculation fulfilled the requirements. Starting from the significant positive or negative correlations, identified between the initial variables, using PCA (Rotation method: Varimax with Kaiser Normalization; rotation converged in 3 iterations), the information of 12 of the variables can be represented by two components. The two components explain 80.03% of the total variance in the variables which are included in the components.

Table 1
Variables included in the analysis PCA and cluster. Descriptive Statistics

Variables	N	Minimum	Maximum	Mean	Std.Deviation
Global Entrepreneurship and Development Index- GEDI	26	.30	.63	0.428	0.101
GDP/capita	26	3700	37300	19500.0	11348.83
TEA opportunity- TEA opp.	23	22.00	71.00	46.609	12.911
TEA necessity-TEA-nec	23	7.00	41.00	21.130	9.550
Network Readiness Index - NRI	26	3.86	5.98	4.777	0.665
Global Competitiveness Index - GCI	26	3.93	5.54	4.688	0.511
Summary Innovation Index- SII	26	.19	.75	0.469	0.173
SMEs introducing product or process innovations - SMEs-PP	26	13.17	57.00	33.844	12.639
SMEs introducing marketing or organizational innovations - SMEs-Mk	26	16.31	60.55	36.049	10.465
Index of Economic Freedom – IEF	26	55.40	76.10	68.496	5.424
Ease of Doing Business Rank- DB	26	1.00	26.00	13.500	7.649
Labor productivity-LP	26	44.30	142.60	91.642	24.478

Source: Own calculations based on data [4], [12], [13], [21], [28], [29], [30], [32]

The first principal component (PC1), which explains 67.41% of total variance, includes seven variables (Table 2). Six of these variables can be specific to an efficient and productive entrepreneurship, having a positive impact on national competitiveness: institutional variables (DB, IEF), NRI, GEDI, GCI and TEA opportunity-improvement driven opportunity entrepreneurial activity. This component (PC1) is negatively correlated with the TEA necessity-driven entrepreneurial activity. Thus, the necessity driven entrepreneurship cannot create economic development measured by GDP/capita. The second principal component (PC2) explains 12.62% of total variance and includes five variables (Table 2): the innovativeness of entrepreneurs (measured by the number of SMEs with marketing and process innovation), the innovation performance (SII), labor productivity and economic development (measured by GDP/capita). All variables have a positive contribution to the creation of the component.

Table 2
Principal Components for EU countries
(Rotated Component Matrix)

The results of the cluster analysis: Final
cluster centers and ANOVA

Table 3

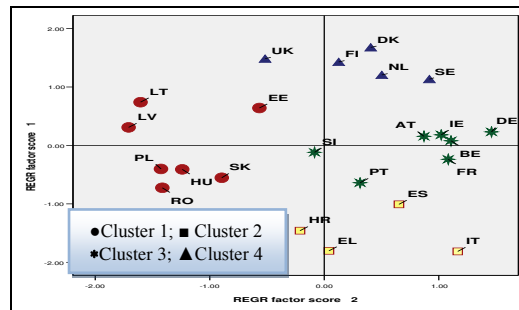
Initial variables	PC 1	PC2	Final Cluster Centers					
			Cluster 1	Cluster 2	Cluster 3	Cluster 4		
DB	0.910	0.165						
IEF	0.858	0.107						
NRI	0.845	0.479						
GEDI	0.755	0.573						
GCI	0.752	0.564						
TEAop	0.686	0.210						
TEAnec	-0.524	-0.500						
SMEmk	0.163	0.889						
SMEspro	0.157	0.881						
LP	0.259	0.841						
GDP	0.515	0.792						
SII	0.621	0.752						
			ANOVA					
			Cluster		Error		F	Sig.
			Mean Square	df	Mean Square	df		
PC1			6.202	3	0.179	19	34.72	0.00
PC2			5.683	3	0.261	19	21.81	0.00

Source: Own calculations

The overall MSA (Measure of Sampling Adequacy) for the set of variables included in the analysis was 0.808, which exceeds the minimum requirement of 0.50 for overall MSA. PCA requires the probability associated with Bartlett’s Test of Sphericity to be less than the level of significance. The probability associated with the Bartlett test is <0.001 which satisfies this requirement. The Cronbach’s Alpha for each component (0.797 and 0.948) is higher than the minimum acceptable level (0.60). To define the number of clusters in which the 23 countries will be classified, we used the *hierarchical cluster analysis, Ward’s method and Euclidean distance*. Then, we used the *k-means analysis* to actually form the clusters. The results of the Snedecor’s F-distribution (ANOVA) can be seen in Table 3. The formed clusters are statistically significant (significance level is smaller than 0.01). The analyzed 23 EU Member States were enrolled in four clusters, as can be seen in Figure 4. Cluster 1 includes *Baltic States and CEE states* (Estonia, Latvia, Lithuania, Poland, Hungary, Romania and Slovakia). Cluster 2 named by us “*southern cluster*” includes Greece, Italy, Spain and Croatia. Cluster 3 named “*continental cluster*” groups Austria, Belgium, Germany, France, Ireland, Slovenia and Portugal. Cluster 4, the “*northern cluster*”, includes Sweden, Denmark, Finland, Netherlands and United Kingdom.

Countries enrolled in the *northern cluster* can be characterized by a very high productive entrepreneurship. It can be noticed that these countries (except the United Kingdom) are distributed mainly in relation to the positive meaning of the variables that form the PC1. The Nordic EU countries recorded a high GEDI value from 0.5 to 0.63. Sweden together with Denmark, having a GEDI of 0.63 points

and are the EU leaders, ranked in the 2nd and 3rd places (after the USA) out of 118 countries. In the case of these countries, the level of opportunity-driven entrepreneurship is also high. The values of SII and NRI are higher than in other countries. Denmark, Finland and Sweden are “innovation leaders” in Europe. The position of the United Kingdom, in the 2nd quadrant, is due to the lower value of the PC2 variables. In the case of the innovative SMEs as a percent of total SMEs (technological innovation), the United Kingdom represents only 21.26% in comparison with Sweden where this value is 47.38% [12]. In the countries mentioned above, the institutional environment is favorable to the development of efficient businesses. In the Ease of Doing Business Rank, these countries are ranked between 5-14 (except the Netherlands ranked 28th out of 189 countries) and, at the same time, the Index of Economic Freedom, which has a positive impact on the quality of entrepreneurship, is also high.



Source: Own calculations based on data [4], [12], [13], [21], [28], [29], [30], [32].

Figure 4

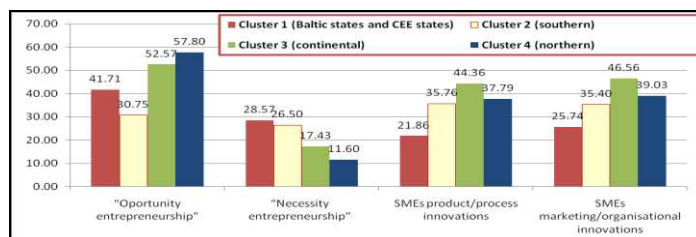
Clusters of entrepreneurial activity efficiency in EU obtained by PCA

Countries in the *continental* cluster can be characterized by a medium toward high productive entrepreneurship. Countries from this cluster, except Slovenia are on the right side of Figure 4, being characterized by a high value of the variables included in PC2. In these countries, the level of the innovative entrepreneurship is the highest, both technological innovations and non-technological innovations. After SII, 5 countries out of 7 included in the cluster are “innovation followers”. Germany is an “innovation leader” and Portugal a “moderate innovator”. Slovenia is placed in the third quadrant, but close to the origin because the level of innovative SMEs is low, almost 60% of the value calculated in the case of Germany. The Improvement-Driven Opportunity Entrepreneurial Activity indicator has high value not so far from the northern cluster average. This cluster was operating in 2011 at 84% from GEDI average of the *northern* cluster. Comparatively with the northern cluster, the institutional quality, technological readiness (measured by NRI) and competitiveness present a deficiency. In these respects, these countries are behind the northern cluster countries.

Countries which belong to the Southern Cluster can be characterized by an entrepreneurial activity having low level venture output, with low impact on economic development, measured by GDP/capita. This group of countries is characterized by the lowest GEDI overall, having the lowest entrepreneurial aspirations sub-index. Within this cluster, the countries show heterogeneity. Croatia and Greece are situated very close to PC1 in a negative sense and tend to be closer to Cluster 1. This means that “necessity entrepreneurship” is more accentuated than in Italy and Spain. Italy’s position in quadrant 4 and outside the “correlation circle” is due to the high value of GDP/capita, SMEs introducing marketing or organizational innovations as a percentage of SMEs and SII value, comparatively with the peer countries in the cluster. Moreover, it is differentiated with an early-stage of Entrepreneurial Activity. Based on SII, all peer countries are “Moderate innovators”. According to GCI [29], Croatia is in transition from stage 2 (Efficiency-driven) to stage 3 (Innovation-driven) and the other peer countries are Innovation-driven economies.

Cluster 1, which consists of the Baltic States and CEE States, shows the highest level of necessity entrepreneurship. This cluster is very far from the PC2 (-1.26). Thus, some of the indicators such as labor productivity, economic development and innovativeness have the lowest values. A low level of economic performance can be observed. The GDP/capita average is only 23.8% of the GDP/capita realized by the countries from the northern cluster and the labor productivity is 62%. Concerning innovation among peer countries, heterogeneity can be observed. Estonia has the highest level of innovativeness among peer countries, being “Innovation follower”; followed by “Moderate innovators” countries such as Hungary, Lithuania, Slovakia; and “Modest innovators” as Romania, having below 50% of the EU27 innovation performance. Estonia has the highest number of innovative SMEs and the impact on the economic development is also the highest among peer countries. The Baltic States are situated in the 2nd quadrant because in these countries the necessity entrepreneurship is lower than in the CEE countries. Regarding competitiveness, based on GCI, 6 countries from this cluster are enrolled as economies in transition from stage 2 to stage 3, and the 7th, Romania, is considered an efficiency-driven economy.

Making an analysis among clusters, it can be noticed that countries acknowledged as having productive entrepreneurship are all situated in the northern cluster and have the highest level of opportunity entrepreneurship. The Baltic and CEE countries have the highest level of necessity entrepreneurship among clusters, as can be seen in Figure 5.

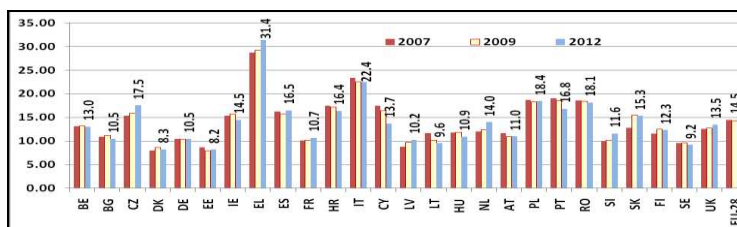


Source: Own calculations based on data provided by [12], [32]

Figure 5

Comparative analysis of entrepreneurial activity among clusters

Regarding hypothesis **H5a**, the results indicate that entrepreneurship can have a positive impact on the national economy and in this respect we have to analyze the output not only at venture level. Sauka emphasized that the link between the degree of entrepreneurial activity and economic growth should not be limited to venture-level performance but rather be measured by employment rate at national level. Different indicators are proposed to measure the entrepreneurship contribution at societal level, [22]. We used longitudinal data to analyze the evolution of self-employment in EU28. The output at societal level measured by employment shows also high differences between transition and developed economies, but countries which belong to the 4th cluster, as can be seen in Figure 6, are not situated in the last places in this case. Self-employment does not have a significant impact on national and global markets, but its role in the national economy cannot be contested. In EU member states, a strong negative relationship was identified between self-employment and the density of large enterprises ($\rho = -0.513$, $p < 0.01$).

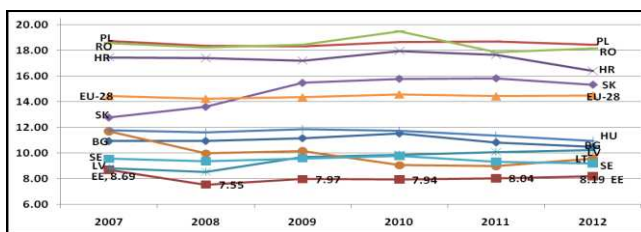


Source: Own calculations based on data provided by [13]

Figure 6

Self-employment in EU28 (2007-2012)

In transition economies, the entrepreneurial activity can be considered productive at the societal level, thus hypothesis **H5b** is confirmed. Moreover, transition economies continue to offer, at least on the same level self-employment, as can be observed in Figure 7. The obtained results sustain the affirmation that the main contribution of SMEs to economic development can be measured through employment generation and innovativeness, and the affirmation that the importance of entrepreneurship is reflected in total SME output at societal level [22].



Source: Own calculations based on data provided by [13]

Figure 7

Self-employment rate in transition countries, Sweden (EU leader by GEDI) and EU28, 2007-2012

Furthermore, hypotheses **H6**, **H7** and **H8** will be tested regarding barriers to productive entrepreneurship, to formulate tasks to reduce the distance of the transition economies to the northern cluster. To become closer to the northern cluster which is characterized by very high productive entrepreneurship, improvements at both the individual and institutional levels must be made. Different conditions must be fulfilled by these countries to make their enrolment in the innovation-driven stage possible. It is well-known that productive entrepreneurship needs a favorable institutional environment but, on the other hand, productive entrepreneurship gives a venture-level performance, hence has a positive impact on economic development and permits its enrolment in a superior economic stage. To determine the barriers to productive entrepreneurship, we examine the constituent pillars of the indicators used in this study. The GEDI methodology focuses on quality, thus for our purpose, this is most important. Analyzing its pillars [4], all transition economies have a low value (on a scale 0-1), on the process innovation pillar (Table 4), suggesting the true value of hypothesis **H6**.

Table 4

‘Efficiency’ of National System of Entrepreneurship and Pillars of GEDI

	‘Efficiency’ relative to the EU leaders of NSE*	Worst Three GEDI Pillars		
HU	55.56%	Risk Capital	Process Innovation	Opportunity Perception
PL	58.73%	Opportunity Start-up	Risk Capital	Process Innovation
SK	57.14%	Quality of Human Resources	Opportunity Perception	Process Innovation
BG	49.21%	Risk Capital	Process Innovation	Technology Level
HR	53.97%	Process Innovation	Risk Capital	Opportunity Perception
RO	47.62%	Technology Level	Risk Capital	Process Innovation

*NSE- National System of Entrepreneurship

Source: Based on data provided by [4]

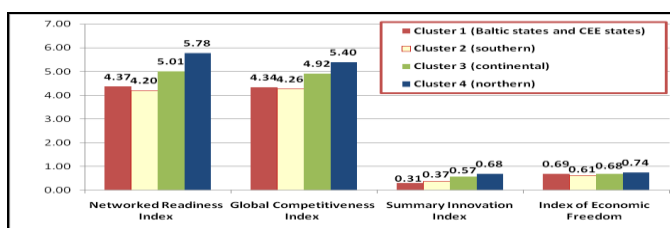
The main cause for this extremely reduced level of the *Process Innovation* pillar is determined by the very low level of public-private investment in R&D, as it can be noticed in Table 5.

Table 5
Barriers to productive entrepreneurship

	Public R&D expenditures as % of GDP		Business R&D expenditures as % of GDP		Ease of Doing Business Rank		Index of Economic Freedom	
	2007	2011	2007	2011	2009 Rank (181 countries)	2013 Rank (189 countries)	2007	2011
BG	0.31	0.26	0.14	0.30	45	58	62.7	65
HU	0.47	0.43	0.49	0.75	41	54	64.8	67.3
PL	0.39	0.53	0.17	0.23	76	45	58.1	66
RO	0.31	0.31	0.22	0.17	47	73	61.2	65.1
SK	0.28	0.43	0.18	0.25	36	49	69.6	68.7
HR	0.47	0.42	0.33	0.34	41	89	53.4	61.3
SE	0.92	1.03	2.47	2.34	17	14	69.3	72.9
EU-27	0.66	0.75	1.18	1.27				

Source: Own construction based on data provided by [12], [21], [28]

Testing of hypothesis *H6* indicates a strong relationship between SII and GDP/capita ($\rho = +0.925$, $p < 0.001$); and a strong relationship between SII and GCI ($\rho = +0.897$, $p < 0.001$). Therefore, innovation can be considered a main driver of productive entrepreneurship. Figure 8 shows that the Baltic States and the CEE States have a very low level of SII compared to the northern cluster.



Source: Own calculations based on data provided by [12], [21], [29], [30]

Figure 8

Competitiveness, technological readiness, innovation and institutional environment among clusters

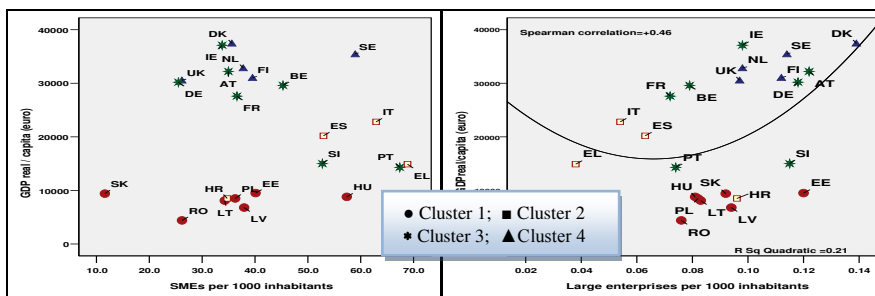
Testing of hypothesis *H7* indicates a strong relationship between indicators having an important role in the quality of entrepreneurial activity, as can be seen in Table 6. The impact of the quality of institutions on productive entrepreneurship is also shown in Figure 8. We can observe that countries from the northern cluster have the highest value on the quality of institutions.

Table 6
Institutional environment and productive entrepreneurship in EU countries * $p < 0.001$

ρ^* Pearson correlation coefficient	GEDI	GCI	NRI
Ease of Doing Business rank	0.717	0.742	0.836
Index of Economic Freedom	0.675	0.727	0.758

Source: Own calculations based on data provided by [4], [21],[28], [29], [30]

Regarding hypothesis **H8**, we started our research looking for an answer to the following issue: Why is the intensity of the entrepreneurial activity not reflected in venture-level performance in the case of transition economies? We studied the relationship between the density of SME's and GDP/capita and the density of large enterprises and GDP/capita in the EU countries (Figure 9a and 9b). As for the relationship between the average density of SMEs and the level of development of the countries, data in Figure 9a show that no statistically significant relationship was identified between the two indicators, in 2011, at the level of the EU countries.



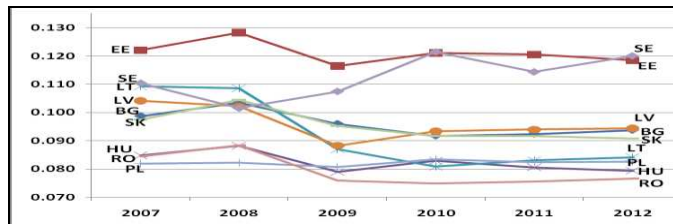
Source: Own calculation based on data provided by [13], [31]

Figure 9

- (a) The density of SMEs and economic development, EU, 2011- statistically insignificant relationship
- (b) Positive relationship between the density of large enterprises and economic development, EU, 2011

Therefore, the existing gaps on the level of economic development cannot be explained by disparities in the entrepreneurial activity, expressed by the density of SMEs. The study regarding the relationship between the density of large enterprises and GDP/capita (Figure 9b) shows that in countries with a low density of large enterprises, the GDP/capita is reduced as well (the case of transition economies). In developed economies, especially northern countries, the high density of the large companies is accompanied by a high level of GDP/capita. Labor productivity is higher in large companies than in SME's, because of the scale economies, the intensive use of capital, as well as a higher degree of technology compared to the existing one in SME's.

Figure 10 illustrates that in countries with a very low level of GDP/capita, the density of large enterprises is also reduced and longitudinal data show that this tendency is not increasing. Hence, hypothesis H8 is confirmed.



Source: Own calculation based on data provided by [13], [31]

Figure 10

Density of large enterprises (over 250 employees)

5 Discussion and Conclusions

The hypotheses in this study have been successfully supported by empirical data. Specifically, hypothesis H4 indicates that EU Member States should be enrolled in clusters because of the strong relationships between the variables which characterize the entrepreneurial activities performance. The EU member countries were grouped based on the efficiency of the entrepreneurial activity, our research being focused on productive entrepreneurship. The name of clusters was given by the countries geographical position within the cluster. We identified, for the analyzed, countries the main factors which have a significant impact on high output, starting with the differences between the clusters and then by exploring the frame of the cluster, countries with the greatest distance from the centre of the cluster.

Within the *Northern Cluster*, are the countries with the best performance in the EU, leaders in the world, related to the considered indicators, they being ranked in the first places. These countries are the most innovative and competitive, with the highest density of large enterprises, high quality of institutions and a high number of innovative SME's. In this cluster, the United Kingdom is at the furthest distance from the centre. This can be explained by the low level of innovative SME's from the total SME's. In the United Kingdom, the necessity driven entrepreneurship is the highest compared to its peer countries and the entrepreneurial aspiration is not sufficiently developed. Longitudinal data show that self-employment is increasing. The density of SME's and large enterprises is the lowest in the cluster.

Regarding the *Continental Cluster*, the enrolled countries show lower level of productive entrepreneurship than those grouped in the northern cluster. The general characteristics of the cluster presented in Section 4, indicate the national priorities for these countries. In this cluster, we have to analyze separately the case of Slovenia (SI) and Portugal (PT) situated at the greatest distance from the centre

of the cluster. In the case of SI, the worst position within the cluster can be explained by the lowest level of economic development, measured by GDP/capita, and by the quality of entrepreneurial activities, having a low GEDI value, the NRI and GCI have the lowest level in the cluster which points out that the technological environment, its use and competitiveness must be improved. The position of PT in the cluster reveals the need to improve the quality of entrepreneurship; the GEDI value has the lowest level in the cluster. PT has a better position because the share of innovative SME's is higher. The position of Ireland in the cluster, is central, but our results show some special characteristics such as the highest level of necessity entrepreneurship, the lowest density of SME,s and the highest density of large enterprises. Labor productivity has the highest position in the cluster which explains the fact that the GDP/capita is at the highest level in EU23 after Denmark.

Countries in the *Southern Cluster* manifest the highest dispersion in relation to the PC2 variables; this cluster is very far from PC1. Croatia (HR) belongs to this cluster, but it can be characterized by the highest level of necessity entrepreneurship and also improvement driven entrepreneurship related to its peer countries. However, the entrepreneurial activity has the lowest impact because of the lowest level of labor productivity. HR needs to improve the innovative performance having the lowest level of SII, the technological environment and its use. In the case of HR, GCI through its pillars needs to be analyzed to detect why it shows the lowest level. Italy (IT) has the lowest level of improvement entrepreneurship in the EU and the highest GEDI value compared to its peer countries which explains the highest level of economic output in the cluster. Greece (EL) presents the lowest GEDI value and has the highest level of self employment. The results show that IT and EL have the highest density of SMEs, but the percentage of innovative SMEs is the lowest in the cluster, having a lower impact on economic development.

Transition economies are situated in the 1st cluster [9]. Concerning productive entrepreneurship, these countries lag behind other EU Member states. The Baltic States and CEE countries must be treated in a different way. The low level of output measured by GDP/capita and labor productivity is a common characteristic. In Baltic States, the improvement driven entrepreneurship is higher than in CEE countries. Based on our own calculations, Romania (RO) has the lowest level of necessity entrepreneurship. In this respect, it is situated close to the Baltic States. In Hungary (HU), the density of SMEs is very high and can be compared with the situation of Sweden, but unfortunately, the entrepreneurial activities are unproductive. Estonia (EE) followed by Latvia (LV) has the highest density of large enterprises, but the contribution of GDP/capita is at a very low level. The main problem, in transition economies, is innovativeness and the very low number of innovative SMEs. The quality of institutions is also lower in CEE countries than in Baltic States.

6 Recommendations

The main purpose of this paper is to identify the transition economies barriers to productive entrepreneurship in the European context. Therefore, recommendations will be formulated relative to this aspect.

Transition economies must formulate policies which encourage and sustain the improvement of entrepreneurial activities efficiency to increase the venture level output. The obtained results demonstrate that, between the transition countries, there are differences which indicate that a different treatment is needed; the priorities are different in each and every country. The low level of the values on the *Risk Capital pillar* reflects that business financing and undercapitalization is a critical weakness of transition countries' start-ups and new ventures.

Croatia was enrolled in the continental cluster because the share of innovative SME's is higher than in the other transition economies, and labor productivity is the highest after Slovakia (SK). The quality of institutions has to be improved. Moreover, there is a need to improve the quality of entrepreneurial activities. The low value of NRI shows that the nation's degree of preparation to participate in and benefit from information and communication technology developments has to be increased.

Estonia, according to the analyzed indicators, is the leader of the transition economies. The country should increase the labor productivity through the improvement of the quality of entrepreneurial activities.

Latvia, having the lowest GEDI value between the Baltic States, needs to improve the quality of entrepreneurial activities. The innovative capacities have to be ameliorated. Labor productivity needs to be increased.

Lithuania needs to improve the entrepreneurial attitudes, the innovative capacities and the quality of institutions.

Hungary needs to improve the quality of entrepreneurial activities; 'the Efficiency' relative to the EU leaders of National System of Entrepreneurship (NSE) is 55.56%. The worst GEDI pillars, which need improvement, are risk capital, process innovation and opportunity perceptions. The quality of institutions requires improvement. The number of innovative SME's needs to be increased, and policies that ameliorate innovative capacities are required.

Poland needs to improve the innovative performance. The quality of entrepreneurial activities has to be improved; 'the Efficiency' relative to the EU leaders of NSE is 58.73%. The worst GEDI pillars are opportunity start-up, risk capital and process innovation. Poland requires policies to reduce the necessity driven entrepreneurship.

Romania needs to improve the entrepreneurial activities performance, 'the Efficiency' relative to the EU leaders of NSE is 47.62%, the lowest percentage

between transition economies. The GEDI value shows that entrepreneurial attitudes and abilities are not sufficiently developed; the actual level of quality is not able to produce high output. The GEDI value and its sub-indexes show that Romania has to increase the technology level, risk capital and process innovation. It needs to be analyzed why the improvement driven entrepreneurship produces the lowest level of GDP/capita between EU states. In this respect, a comparative analysis is required with Slovakia, Croatia, Estonia, since they have approximately the same density of SMEs but with significantly higher output than in the case of Romania. The density of large enterprises has to be increased and policies to develop the labor productivity are required. In Romania, the entrepreneurial activities are the most unproductive. The quality of the institutions and environment has to be assessed. Policies are needed to improve the quality of institutions. Romania has the lowest value of DB, EFI compared to its peer countries.

Slovakia needs to improve the quality of entrepreneurial activities; ‘the Efficiency’ relative to the EU leaders of NSE is 57.14%. The worst GEDI pillars are quality of human resources, opportunity perception, and process innovation. The entrepreneurial activities are the most productive between transition economies. Thus, it can be considered the best practice example. The number of SMEs has to be extended.

Bulgaria was not enrolled in the cluster analysis because of the missing GEM data. Based on GEDI, ‘the efficiency’ relative to the EU leaders of NSE is 49.21%. It has to improve risk capital, process innovation, and technology level. It also needs to improve the quality of institutions. Policies to improve the labor productivity are required, in this respect it is situated on the last place. Moreover, it needs to improve the innovative capacities.

Future research. The findings in this paper highlight the status of performance of transition economies’ entrepreneurial activities, in the European context. The authors identified obstacles to productive entrepreneurship. The primary factors contributing to the movement between clusters should be examined. According to this study, EU Member States require special and different treatment. To formulate policies in concordance with priorities, the prioritization of the needs would be an interesting topic for future research.

References

- [1] Aidis, R., Sauka, A.: Entrepreneurship in a Changing Environment. Analyzing the Impact of Transition Stages on SME Development. RENT (2005) Welter edition, online publication, www.ecsb.org
- [2] Ács, Z. J., Szerb L.: The Global Entrepreneurship Index (GEINDEX), Foundations and Trends in Entrepreneurship (2009) Vol. 5, No. 5, pp. 341-435
- [3] Acs, Z. J., Szerb, L.: The Global Entrepreneurship and Development Index, Conference 2010 on “Opening Up Innovation: Strategy, Organization and

- Technology” at Imperial College London Business School, June 16-18
- [4] Ács, Z. J., Szerb L., Autio, E.: *Global Entrepreneurship and Development Index 2013*, Edward Elgar Publishing Limited. London
 - [5] Baumol, W. J. *Entrepreneurship: Productive, Unproductive, and Destructive* *Journal of Political Economy* (1990) Vol. 98, No. 5, pp 893-921
 - [6] Chilea D. *L’espace fiscal Europeen*, *The Juridical Current*, No. 4, 2009, pp. 38-50
 - [7] Chris, D., Xiaofeng, H.: *K-Means Clustering via Principal Component Analysis*. 21st International Conference on Machine Learning, pp. 1-9, Banff, Canada (2004) University of Texas Arlington
 - [8] Douhan, R., Henrekson, M.: *Productive and Destructive Entrepreneurship in a Political Economy Framework*. Stockholm, Sweden; Research Institute of Industrial Economics; IFN Working Paper (2008) No. 761
 - [9] *EBRD Transition Report. Integration across borders*, European Bank for Reconstruction and Development, 2012
 - [10] Estrin, S., Meyer, EK., Bychkova, M.: *Entrepreneurship in Transition Economies*, *Oxford Handbook of Entrepreneurship* (2008) Oxford University Press
 - [11] Everit, B. S., Landau, S., Leese, M., Stahl, D. *Cluster Analysis*, 5th ed. Wiley, 2011
 - [12] EU. *The Innovation Union Scorebord*. Research and IUS EC, 2013, Jan. 9
 - [13] Eurostat database, 2013. Retrieved November 10, 2013. http://epp.eurostat.ec.europa.eu/portal/page/portal/statistics/search_database
 - [14] Fagerberg, J., Sapprasert, K.: *National innovation systems: The emergence of a new approach*. *Science and Public Policy* (2011) 38(9), Nov, pp 669–679
 - [15] *Global Entrepreneurship Monitor (GEM) Reports*; Retrieved Nov. 2, 2013, from <http://www.gemconsortium.org/docs/cat/1/global-reports>
 - [16] Gros, D., Steinherr, A.: *Economic Transition in Central and Eastern Europe: Planting the Seeds*. Cambridge: Cambridge University Press; 2004
 - [17] Harper, A. D.: *Foundations of Entrepreneurship and Economic Development*, New York: Routledge, 2003
 - [18] Jolliffe, I. *Principal Component Analysis*, 2nd ed. New York: Springer; 2002
 - [19] Lumpkin, G., Dess, G. *Clarifying The Entrepreneurial Orientation Construct and Linking It To Performance*; *Academy of Management Review* (1996) pp. 135-172
 - [20] Miller, D.: *The Correlates of Entrepreneurship in Three Types of Firms*.

- Management Science (1983) pp. 770-791
- [21] Miller, T., Holmes, K. R., Feulner, E. J.: Index of Economic Freedom. Promoting Economic Opportunity and prosperity, The Heritage Foundation and Dow Jones & Company, Inc; 2013
- [22] Sauka, A.: Productive, Unproductive and Destructive Entrepreneurship: A Theoretical and Empirical Exploration. Michigan: The William Davidson Institute At The University Of Michigan, 2008
- [23] Simonová, S.: Identification of Data Content Based on Measurement of Quality of Performance. E+M *Ekonomie a Management* (2012) pp. 128-137
- [24] Smallbone, D., Welter, F.: Conceptualising Entrepreneurship in a Transition Context. *International Journal of Entrepreneurship and Small Business*, Vol. 3, Nr. 2, 2006, pp. 190-206
- [25] Smith, I. L.: A tutorial on Principal Components Analysis, 2002, Febr 26
- [26] Sobel, R. S: Testing Baumol: Institutional Quality and the Productivity of Entrepreneurship. *Journal of Business Venturing*, 2008, 23; pp. 641-655
- [27] Szabo, K. Z., Soltés, M., Herman, E.: Innovative Capacity and Performance of Transition Economies: Comparative Study at the Level of Enterprises. *E&M Economics and Management* (2013) pp. 52-67
- [28] World Bank-WB. *Doing Business: Smarter Regulations for SMEs*, International Bank for Reconstruction and Development, 2013
- [29] World Economic Forum; *The Global Competitiveness Report 2013-2014*
- [30] WEF, *The Global Information Technology Report*, 2013
- [31] ***http://ec.europa.eu/enterprise/policies/sme/facts-figures-analysis/performance-review/index_en.htm
- [32] *** GEM database <http://www.gemconsortium.org/key-indicators>
- [33] ***http://ec.europa.eu/enterprise/policies/sme/promoting-entrepreneurship/index_en.htm

Enhancing Student Satisfaction Based on Course Evaluations at Budapest University of Technology and Economics

Zsuzsanna Eszter Tóth, Tamás Jónás

Department of Management and Corporate Economics, Faculty of Economic and Social Sciences, Budapest University of Technology and Economics
Magyar tudósok körútja 2, H-1117 Budapest, Hungary
tothzs@mvt.bme.hu, jonas@mvt.bme.hu

Abstract: The Department of Management and Corporate Economics ran an extended survey including a questionnaire and various problem solving techniques among students on five different business courses in 2011, in order to acquire deeper knowledge about the factors influencing student (dis)satisfaction and to lay the foundation for long-term course improvement actions. According to PDCA logic, we repeated the student satisfaction measurement process in 2012 to assess the effectiveness of short-run improvement actions. This article summarizes our main results and highlights the improvement actions needed in the long run. Improving student satisfaction is a must for all courses, as the financial issues of the faculty and the departments are strongly affected by student course ratings.

Keywords: higher education; student satisfaction; brainstorming; cause and effect diagram; PDCA; quality improvement actions

1 Introduction

Recent changes in the Hungarian higher education system precipitate structural reorganizations, finance issues of the system and increasing competition among institutions. The fundamental structural changes of the Hungarian higher education system make it imperative to address the issue of quality. In many educational fields students are required to pay tuition fees and this places a greater focus on the value and the quality of the education they receive. Under these circumstances, institutions have to undertake competitive strategies in order to face the strong rivalry from other Hungarian and European universities. In this competitive framework, only those institutions which provide high quality educations and environments for their students can survive. These effects can be measured by assessing overall student satisfaction.

At Budapest University of Technology and Economics (BME) active students have been asked to evaluate each course they have attended during the term since 1999. These measurements are the focus of our research. The main purpose of this study is to better understand the factors influencing student (dis)satisfaction by using a course evaluation questionnaire and various quality management tools. Based on our results, quality improvement actions were set and their effectiveness was evaluated by repeating the same student satisfaction measurement in the following academic year. This work aims to compare and understand the results of these measurements. According to the PDCA logic we end up with a new improvement plan for the forthcoming academic year and summarize the limits of our research.

2 Literature Review

The issue of quality in higher education is rather complex, not simply because the interpretation of quality is subjective, but because the educational service is a very complex activity and we do not know all the factors that can influence the outcomes [1]. At the same time, it should be taken into consideration, that various stakeholders are involved in higher education [2], from single students, who are the primary consumers [3], to all students, parents, staff, employers, business and legislators as secondary consumers [4]. In order to improve quality in a higher educational context such institutions should be established which utilize the voice of customers, students and users in the day-to-day operation of higher education.

Higher education institutions are increasingly aware that they need to deal with many competitive pressures, as they are part of a service industry. They have, therefore, put greater emphasis on student satisfaction. Student satisfaction is a short-term attitude that results from evaluating their experience of the education service [5]. As a consequence, institutions have been paying more attention to meeting the expectations and needs of their students [6]. The higher the service quality, the more satisfied the customer [7]. Accordingly, satisfaction is based on customer expectations and perception of service quality [8] [9]. What counts in higher education is the perceived quality of service [10]. Owlia and Aspinwall [11] give a possible explanation of service quality dimensions in higher education. The mechanisms for measuring the service quality of courses and programs depend on the applied research instruments (e.g. student feedback questionnaires). Most institutions apply different variables, questionnaires, evaluation methods, and most of them are developed internally without the consideration of reliability or validity [4] [12] [13].

The issue of quality in higher education has received increased attention in the last decade in Hungary [14]. However, the change is slower than in the rest of Europe. As in other European countries, higher education has become a mass-market

service, characterized by an increasing number of students and an increasingly diverse number of institutions. Due to the recent reform in Hungary, tuition-free state institutions have been rapidly raising tuition charges, as state student aid has dropped significantly. In this context, the issue of quality has become more important. The follow-up of European trends since the 1990's has resulted in continuous changes in the Hungarian higher education sector, which has been unprepared [15]. Although legislation has existed for almost 20 years, Hungarian higher education reveals very few substantive results. From time to time, individual and isolated improvement actions come to light in order to break through institutional and individual disinterest and demotivation [15]. Polónyi's [1] research suggests that according to the labor market the quality of higher education embeds in the practice-orientation of education, lecturers, notes and students, rather than in academic criteria. The feedback of employers regarding graduate students' skills should be taken into consideration as well [16]. Higher education institutions have a responsibility to its students, to equip them with practical knowledge. According to Topár [17], the philosophy of TQM could lay the foundation for well-functioning quality management systems, in the long run, as TQM encourages universities to concentrate on their core activity and inspires educational institutions to embed quality into the institutional culture [18]. The approach of addressing quality and continuous improvements has also been motivated by the launch of the Hungarian Quality Award of Higher Education in 2007. However, only a few institutions performed well, which was due to the immaturity of institutions in self-assessment, to the lack of a "quality culture" and a missing set of quality management tools/techniques. In recent years, the HEFOP 3.1.1 program aimed at special issues of quality improvement in the higher education sector. Several consortiums worked on adopting the EFQM Model in higher education, which resulted in the proposal of UNI EFQM and UNI CAF models [19]. The recent TÁMOP 4.1.4 08/1-2009-0002 Program – titled Quality Improvement in Higher Education – launched a number of projects to fulfill quality improvement targets. Although the program has finished, most of the results are still to be disseminated.

The concept of the student as a customer is now commonplace in higher education [3]. Yorke [20] argues that this supplier/customer relationship is not as clear as in the case of other service relationships, because students are also "partners" in the learning process. Sirvanci [21] identified four different roles for students: product-in-process, internal customers for facilities, laborers in the learning process and internal customers for the delivery of course materials. From this multiple role of students model it is clear why customer identification is a complicated and confusing issue in the case of higher education. As students are the customers of the educational service they should measure the quality of the output and be the judge of quality, similarly to the customers in the industrial context [22].

Student satisfaction is about evaluating the educational services provided by institutions that frame their academic life [23]. Student satisfaction surveys are

commonly used as feedback to determine the delivery of education. A number of studies have been conducted to measure student satisfaction at university level all over Europe [23]. Rowley [24] summarized four reasons for collecting student feedback: to provide students with the opportunity to offer their opinion regarding the courses in order to lay the foundation for improvements; to express their level of satisfaction with teaching and learning; to encourage students to give feedback and to use the results as benchmarks; and to provide indicators that have an impact on the reputation of the institution in the marketplace and in the labor market.

The student is now recognized as the principal ‘stakeholder’ of the Hungarian higher education as well. Student feedback of some sort is usually collected by most institutions, though there is little standardization on how this is collected and what is done with it. There is still little understanding of how to use and to act upon the collected data. As market forces grow, attracting and keeping students satisfied, becomes increasingly important in Hungary too. Therefore, student satisfaction surveys can serve two purposes. First, they can serve as a tool for planning and implementing continuous improvement activities. Second, they can be considered as managerial tools, guiding higher education institutions to adapt to the changing circumstances of this market [23].

3 Understanding the Voice of Students at BME

During our research we followed the steps for a TQM-based course evaluation process as proposed by Venkatraman [25]. Table 1 shows the alignment of the course evaluation process with the phases of the PDCA cycle, needed to understand the opinion of students and to enhance their satisfaction (see Table 1).

Table 1
Course evaluations steps reflecting the PDCA logic [25] [26]

PDCA Cycle	Steps of the course evaluation process
Plan	1. Select the courses to be evaluated.
	2. Describe the purpose and structure of course evaluations.
	3. Conduct course evaluations to obtain primary student inputs.
	4. Prepare an evaluation report of the findings based on the questionnaire.
	5. Conduct brainstorming sessions and construct cause and effect diagrams with student involvement to obtain secondary student inputs.
	6. Conduct an improvement action plan based on primary and secondary student inputs.
Do	7. Implement improvement actions dedicated for the forthcoming semester.
Check	8. Check the effectiveness of improvement actions with repeated course evaluations at the end of the semester.
Act	9. Act upon the results regarding the courses.

With the objective of understanding students' opinions concerning the quality of an educational service, we surveyed students on five courses in 2011, using a survey that was built for this particular purpose. The survey consists of a questionnaire containing 11 questions. Students were asked to express their opinions in two dimensions, namely, scoring the importance and the performance related to each question using the ordinal scale from 1 to 6 – a score of 1 being the lowest, and 6 the highest value, both in terms of the importance and performance dimensions (see Table 2).

Table 2
The survey questionnaire

Importance (1: Not important at all, 6: Very important)						Question	Performance (1: Minimum, 6: Maximum)					
1	2	3	4	5	6	1. How much do you find the topic highlighted in title of subject needful to establish your management and business knowledge?	1	2	3	4	5	6
1	2	3	4	5	6	2. How much do you feel so that the subject – considering the time frame given to the course – discussed the related sub-topics at appropriate level with appropriate importance?	1	2	3	4	5	6
1	2	3	4	5	6	3. In general, how much do you find the subject recommendable and fitting to the syllabus?	1	2	3	4	5	6
1	2	3	4	5	6	4. How much did the academic (lecturer) seem well-prepared?	1	2	3	4	5	6
1	2	3	4	5	6	5. How much did you find the teacher's lectures understandable and logical?	1	2	3	4	5	6
1	2	3	4	5	6	6. How much did you feel – considering the nature of subject – the teacher being vivid and thrilling?	1	2	3	4	5	6
1	2	3	4	5	6	7. How much did you find the supplementary materials and teaching aids prepared by the lecturer appropriately comprehensive and substantial?	1	2	3	4	5	6
1	2	3	4	5	6	8. How much did you feel the supplementary materials and teaching aids prepared by the lecturers well structured and easy to follow?	1	2	3	4	5	6
1	2	3	4	5	6	9. How much did the supplementary materials and teaching aids prepared by the lecturers help you following the lectures, making notes, and learning the subject?	1	2	3	4	5	6
1	2	3	4	5	6	10. How much were the examining circumstances correct and fair?	1	2	3	4	5	6
1	2	3	4	5	6	11. How much did you find the lecturer's examining method suitable to measure your real knowledge?	1	2	3	4	5	6

The performance dimension of a question reflects how much the students are satisfied with the educational performance in the particular field addressed, while the importance category is used to express the importance of a particular topic. The measurement was repeated with the same questionnaire in 2012, in the case of the Business Statistics course. The evaluated courses and the level of education for each course are summarized in Table 3.

Table 3

The evaluated courses, the level of education, response rates and Cronbach's Alpha coefficients (2011)

Course	Level	Questionnaires handed out	Filled questionnaires	Response rate	Cronbach's Alpha for Performance	Cronbach's Alpha for Importance *
Business Statistics	B.Sc.	253	104	41%	0.8826	0.8747
Innovative Enterprises	B.Sc.	215	91	42%	0.8140	0.8758
Quantitative Methods	MBA	95	45	47%	0.8396	0.9067
Quantitative Methods	M.Sc.	210	111	53%	0.8813	0.8634
Quality Management	B.Sc.	205	101	49%	0.8175	0.7693

Each question of our questionnaire was defined with the purpose of measuring educational performance. Therefore, the internal consistency of survey items is expected based on performance scores. Every student who answered the survey had the opportunity to assign an importance score to each question based on his or her personal perceptions. In comparison with the performance score, whose sum represents the student's aggregate perception of the educational performance, the importance score does not have such an interpretation. On the other hand, the product of importance and performance scores assigned by a student to a survey question expresses his or her individually weighted perception of performance for the survey item.

3.1 Survey Results from 2011

The two-dimensional survey approach is built on the consideration that topics having higher importance scores should have higher performance values as students rightly expect higher service level in the areas which they consider more important. The average importance and average performance scores were calculated for each survey question with the purpose of determining how the importance and performance categories relate to each other. Figure 1 shows the total sum of importance scores and the total sum of performance scores for each question.

Taking the five analyzed courses together into consideration, the biggest disconnects between the importance and performance dimensions are in the areas addressed by Question 5, 8, 9, 10 and 11.

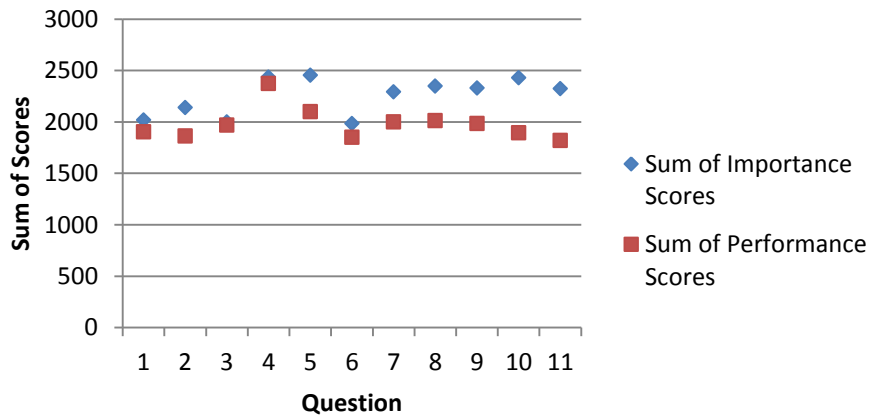


Figure 1
Total scores for importance and performance of questions

3.2 Brainstorming

Based on these five questions of course evaluation, the following three questions were raised for the brainstorming session.

1. How do you think the professor could develop the comprehension and logical structure of his/her classes? (Q5)
2. What ideas come to your mind as regards the notes and educational supplementary material? (Q8, Q9)
3. In your opinion, what would be the best exam system and conditions that could be used to assess realistically and fairly the students' knowledge about a given subject? (Q10, Q11)

Six groups of students were asked to brainstorm as many ideas as they could to respond to our three questions. The two groups involved, each of which consisted of 7 to 9 students, collected their answers separately from their own brainstorming sessions. After combining and harmonizing the answers for the three questions, the answers were divided into four categories according to the type of skill needed to be developed by the lecturer. Table 4 shows the definition of the skills.

It should be noted that the areas wherein improvements are needed cannot always be clearly assigned to one category. Nevertheless, students suggested some development ideas which would require the improvement of several areas. For example, some issues could be realized, partly, by developing the pedagogical and methodological abilities and partly by improving the technical and organizational conditions.

In regard to ideas emerging from the first brainstorming question, students listed mainly the pedagogical/didactical preparedness and methods used by lecturers as problems. The inaccurate didactical, education technological and methodological knowledge of lecturers is mainly due to their lack of teaching qualifications and inappropriate teaching techniques. The intensification of this knowledge would be an important aspect while improving the quality of courses. The development of pedagogical skills could also contribute to resolve noted problems concerning human.

Table 4
Definition of skills and their relation to service quality dimensions [11]

Type of skill	Definition	Related service quality dimensions proposed by Owlia and Aspinwall [11]
S: subject knowledge	It is the specific professional knowledge of the lecturer which refers to the fundamental knowledge of the taught discipline and to the up-to-datedness of the lecturer on the specific topic. This kind of knowledge enables the lecturer to transfer the essential knowledge to students and familiarize them with the specific field of study.	Reliability, Performance, Completeness, Flexibility
H: human skills	Human skills are the human attributes of the lecturer which depend on the lecturer himself/herself and consistent with the generally expected norms. These skills enable the lecturer to endear a specific discipline to students.	Responsiveness, Access, Competence, Courtesy, Communication
P: pedagogical / didactic skills	It covers the professional teaching knowledge and the relating practical skills which enables the lecturer to plan and structure the lectures during the semester. This includes grabbing the attention of students, motivating them, keeping their interest and curiosity, motivating students. The appropriate compilation of exams and homework belong to this skill as well.	Responsiveness, Access, Competence, Courtesy, Performance, Flexibility, Redress, Communication
T: technical / organizational skills	These are education-related technical and organizational conditions including e.g. the appropriate technical equipment of classrooms (projector, computer, sound system, etc.), ergonomics of rooms and their equipment (chairs, tables and their placement, heating-cooling and shading system, etc.), or even the service quality of administrative departments (Dean's offices, offices of academic affairs etc.).	Communication, Tangibles, Redress

In answering the second brainstorming question ideas regarding technical skills had to be taken into consideration. Some of the deficiencies could be resolved by developing the computer skills of lecturers. The other group of listed ideas (video records, audio books) would require a bigger financial investment from the university. Based on students' feedback lecturers should improve their presentation skills and put greater emphasis on demonstrating practical examples and case studies.

The third brainstorming question addressed the issue of evaluation. Most of the ideas can be associated with pedagogical and technical skills. Students require more stringency at exams and consistent penalties for cheating. Students would need written, richly explained evaluations, more practical examples, more consultations, trial exams, etc. They also want more precise and more thorough evaluations.

3.3 Survey Results from 2011 – Business Statistics Course

Figure 2 shows a considerable gap between averages of importance and performance scores in the case of some questions. The conclusion that there is a lack of an expected strong positive correlation between the average scores of the two survey dimensions is also supported by the correlation coefficient of 0.1328 calculated for averages of importance and performance scores. Based on these initial results, we focused on the questions with the largest gaps between averages of their importance and performance scores. Table 5 shows the numerical results of the initial analysis.

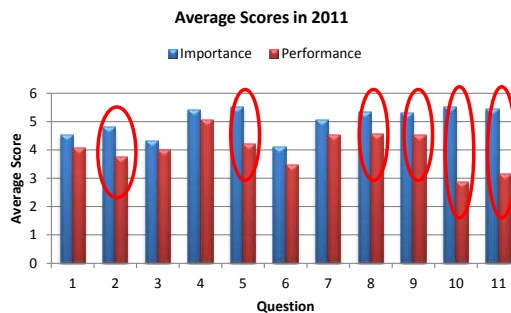


Figure 2

Averages of importance and performance scores in 2011

In order to narrow the scope of improvement activities, we focused on survey questions representing top 80% of sum of importance-performance differences. The rows highlighted in Table 5 and the bars marked in Figure 2 indicate these questions (see Table 2).

Based on the ideas of the brainstorming session and on the survey results of Business Statistics in 2011, we constructed a cause and effect matrix (Table 6) with the involvement of a group of Business Statistics students in order to set immediate goals. In the matrix Y stands for the outputs (effects) and X for the inputs (causes). Students ranked the outputs by giving importance values to the questions in the questionnaire. The ranking of inputs were determined with student involvement.

The results of the cause and effect analysis confirm the conclusions of the brainstorming session. The three fields addressed by the questions are strongly interrelated, as a number of problems raised by the students, can be solved easily by the lecturer and the department responsible for the courses.

Table 5

Difference between the importance and performance average scores for each question

Question	Average Importance	Average Performance	Average Importance - Average Performance
1	4.5294	4.0784	0.4510
2	4.8137	3.7549	1.0588
3	4.3235	3.9902	0.3333
4	5.4216	5.0784	0.3431
5	5.5098	4.2255	1.2843
6	4.1188	3.4608	0.6580
7	5.0490	4.5294	0.5196
8	5.3333	4.5490	0.7843
9	5.3137	4.5196	0.7941
10	5.5196	2.8725	2.6471
11	5.4554	3.1471	2.3084

3.4 Actions Defined

Based on the initial statistical analyses of survey data from 2011 and on the results of brainstorming and the cause and effect matrix, the following actions were defined and implemented on the Business Statistics course in 2012 in the spirit of the PDCA logic.

- Lecturers took part in the Lecturers' programme organized by the Institute of Continuing Engineers Education at BME in order to improve their pedagogical skills (related survey questions: 5, 8, 9, 10, 11)
- Regular consultations emphasising the most important theoretical topics and their relations, as well as, discussing the critical steps of the taught calculation methods, were held one day before each midterm exam (related survey questions: 10, 11)
- Additional, comprehensive consultation materials were prepared for each consultation. The consultation materials were made available for students in presentation slides (related survey questions: 8, 9, 10, 11)
- Well-defined theoretical topics with outlines of required answers were prepared for each midterm exam consultation (Related survey questions: 8, 9, 10, 11)
- The typical calculation exercises required in the midterm exams were summarised and overviewed during the consultations (related survey questions: 5, 8, 9)

- The weights of different sub-topics in the midterm exams were deliberately harmonized with the time spent on discussing and lecturing the corresponding sub-topic (related survey questions: 2)
- The entire course was taught by one lecturer, instead of two or three lecturers teaching, dedicated blocks of the course (related survey questions: 2, 8, 9)

Table 6
Cause and effect matrix

Output (Variable Y)	The subjects discuss the related sub-topics at appropriate level with appropriate importance (Q2)	The lectures are understandable and the logic of the teacher is clear (Q5)	The supplementary materials and teaching aids are well-structured and easy to follow (Q8)	The supplementary materials and teaching aids support the understanding of lectures and the preparation for exams (Q9)	The examining circumstances are correct and fair (Q10)	The chosen examining method is suitable to measure the knowledge (Q11)		
Output ranking	3	4	1	2	6	5		
Input (Variable X)							Rank	Rank %
Classroom teaching materials	3	10	5	10	1	4	100	14,75%
Supplementary teaching materials (e.g. notes, materials for consultation, sample tests, case studies, theses)	4	9	7	9	1	4	92	13,57%
Student motivation in classrooms (extra points, homework, team assignments)	1	6	1	7	0	2	51	7,52%
Lecturer skills and motivation	2	4	2	3	2	3	55	8,11%
Classroom equipment	0	3	1	4	5	2	60	8,85%
Curriculum	8	6	3	4	1	1	67	9,88%
Structure of a lecture	7	8	5	4	1	1	72	10,62%
IT background of lectures (e-learning, multimedia techniques, up to date software, servers, learning sites)	3	6	3	6	1	4	71	10,47%
Evaluation/Examination (type (i.e. oral or written), equipment, supervision)	0	0	0	0	10	10	110	16,22%

4 Impact of Improvement Actions

After implementation of the improvement actions discussed above, we conducted the same survey at the end of the Business Statistics course in 2012, to see how the actions taken impacted students' satisfaction. The response rate was 43%. The Cronbach's alpha coefficient was, based on performance scores, 0.8482 and based on product of importance and performance scores it was 0.8722. These two figures support the consistency of the survey used in 2012.

4.1 Comparison of Survey Results from 2011 and 2012

Figure 3 shows the average scores for each survey question in 2011 and 2012.

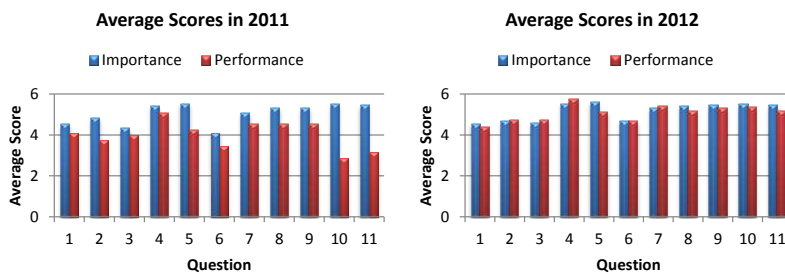


Figure 3
Average scores in 2011 and 2012

The importance and performance scores can be considered as random variables, and so their averages can be taken as point estimates of their expected values. The graphs in Figure suggest two hypotheses. On the one hand, we may assume that the gaps between expected values of importance and performance scores significantly decreased from 2011 to 2012 especially in the case of questions that the actions taken are related to. On the other hand, the average importance scores suggest that there was no significant change in the means of importance scores, that is, students' opinion about importance of topics addressed by survey questions did not change significantly. The graphs in Figure 4 – which show the year-to-year importance and performance averages – also support the idea of setting the hypotheses above.

The hypothesis that the means of importance scores did not change significantly can be formally stated in the following hypotheses pairs.

$H_0(i)$: for question i , mean of importance score in 2011 is equal to mean of importance score in 2012 ($i=1, \dots, 11$)

$H_a(i)$: for question i , mean of importance score in 2011 is different from mean of importance score in 2012 ($i=1, \dots, 11$)

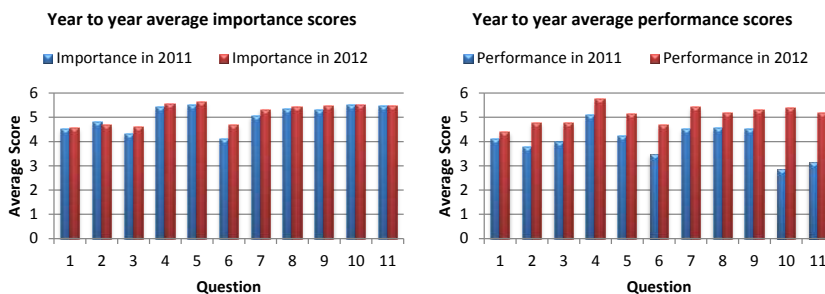


Figure 4

Year-to-year average importance and performance scores

As the sample size in 2011 and 2012 was 102 and 97, respectively, based on the central limit theorem, each $H_0(i)$ hypothesis was tested against the $H_a(i)$ hypothesis by applying the two samples z-test as an approximate statistical test at significance level of 0.05. The inputs and results of conducted tests are summarized in Table 7. We can see from Table 7, that except for question 6, the calculated p-values are greater than the set significance level of 0.05. Hence, except for question 6, the null-hypothesis for each question can be accepted vs. the alternative hypothesis. In other words, the change from 2011 to 2012 in students' opinion about the importance of topics addressed by survey questions is statistically insignificant; the only one exception is question 6.

Table 7

Inputs and p-values of tests on equality of importance score means in 2011 and 2012

Question	Average in 2011	Average in 2012	Standard Deviation in 2011	Standard Deviation in 2012	z-value	p-value
1	4.5294	4.5567	1.3402	1.3147	0.1450	0.8847
2	4.8137	4.6701	1.1234	1.1701	0.8825	0.3775
3	4.3235	4.5979	1.1954	1.3437	1.5193	0.1287
4	5.4216	5.5361	0.8837	0.7914	0.9639	0.3351
5	5.5098	5.6186	0.8052	0.7136	1.0094	0.3128
6	4.1188	4.6701	1.1983	1.2806	3.1319	0.0017
7	5.0490	5.3196	1.0843	0.9077	1.9122	0.0559
8	5.3333	5.4330	0.9047	0.8024	0.8230	0.4105
9	5.3137	5.4639	0.9008	0.8424	1.2154	0.2242
10	5.5196	5.4948	0.8870	1.0320	0.1811	0.8563
11	5.4554	5.4742	0.8963	0.8303	0.1534	0.8781

From the year-to-year average performance scores visible in Figure 4, we may assume that there was a significant increase from 2011 to 2012 in mean of performance score for each question. Based on this assumption, we can set the following $H_0^{(i)}$ null- and $H_a^{(i)}$ alternative hypotheses pairs:

$H_0^{(i)}$: for question i , mean of performance score in 2011 is equal to mean of performance score in 2012 ($i=1, \dots, 11$).

$H_a^{(i)}$: for question i , mean of performance score in 2011 is less than mean of performance score in 2012 ($i=1, \dots, 11$).

As we discussed, the sample sizes allow us to use the two samples z-test as an approximate method to test the hypotheses stated above. The inputs and results of statistical tests are summarized in Table 8.

Table 8
Inputs and p-values of tests on equality of performance score means in 2011 and 2012

Question	Average in 2011	Average in 2012	Standard Deviation in 2011	Standard Deviation in 2012	z-value	p-value
1	4.0784	4.3918	1.2483	1.2124	-1.7961	0.0362
2	3.7549	4.7526	1.3456	0.9686	-6.0247	0.0000
3	3.9902	4.7423	1.3679	0.9712	-4.4889	0.0000
4	5.0784	5.7629	1.1831	0.5357	-5.2995	0.0000
5	4.2255	5.1340	1.2341	0.9961	-5.7277	0.0000
6	3.4608	4.6701	1.1576	1.2806	-6.9768	0.0000
7	4.5294	5.4021	1.0873	0.8498	-6.3250	0.0000
8	4.5490	5.1546	1.0775	1.0035	-4.1052	0.0000
9	4.5196	5.2990	1.3105	1.0425	-4.6541	0.0000
10	2.8725	5.3711	1.4534	0.8935	-14.6876	0.0000
11	3.1471	5.1546	1.4240	0.9280	-11.8384	0.0000

Each p-value in Table 8 is less than 0.05 and so for each survey question the null-hypothesis is rejected and the alternative hypothesis is accepted at significance level of 0.05. It means that the mean of performance score for each survey question increased significantly from 2011 to 2012.

We have previously seen in Table 7, that changes in mean of importance score can be considered significant only in the case of Question 6. We do not know the exact reasons for the observed increase in mean of this score, but taking the nature of this question into account, we may assume that the increase in educational performance has positively impacted students' opinion about importance of topic addressed by the question. We plan to investigate this phenomenon more deeply in future research activities.

The correlation coefficient between the average importance and performance score for 2012 is 0.8669. The same correlation coefficient for 2011 was 0.1328, that is, the stochastic relationship between the importance and performance categories is much stronger in 2012 than in 2011.

4.2 Further Actions Planned

In the light of our continuous improvement philosophy and following the PDCA cycle of course evaluation (see Table 1), the following actions are considered as having the potential to improve the educational performance of the Business Statistics subject in the future.

The entire curriculum is large and comprehensive; indeed, the lecture notes provided to students contain close to 200, A4 pages. We need to review the structure of the curriculum and the lecture notes to ensure that the consecutive topics are in a logical and consistent order so that there is no topic which requires knowledge that is introduced later on. Calculation exercises are part of the lectures. Based on feedback from students and their representatives, it would be definitely more effective if the calculation exercises were discussed in smaller groups within seminars. Defining optional project exercises based on cases from different companies would challenge the students to solve some real-life problems using the tools and techniques learnt during the course. These changes are to come in the forthcoming term (in the academic year 2013/2014), now that we are in the phase of revising the whole course based on the aforementioned ideas. The applied pedagogical methods need a thorough review [27], as the brainstorming sessions highlighted these skills as urgent issues.

Conclusions

In our research, we studied the quality of teaching and learning at BME, that led to student (dis)satisfaction. Student satisfaction is of high importance in our faculty, as the average student satisfaction, with courses taught, serves as an influential factor when planning the budget of a department. The results could also serve as inputs, when evaluating the performance [28] and enhancing the loyalty and satisfaction of the academic staff [29].

This kind of questionnaire structure and the validation of the presented dual approach would not only highlight the areas that need to be improved, but also students' involvement in improvement actions could have more impact. The feedback students provide is also useful to the Chairperson of the course or the Dean, allowing comparisons to be made between the courses and arrangements to improve teaching performance. The results may have implications for management responsible for resource allocations to various areas of the University services and infrastructure. Our aim is to take the necessary steps towards long term improvements and analyzes, regularly, as to whether the actions have solved the most critical problems. This approach ensures that the voice of students is fully integrated into quality improvement efforts and contributes to a better understanding of the students' requirements.

References

- [1] Polónyi, I. (2008): "A felsőoktatás minőségügye" (Quality in Higher Education), *Educatio*, 2008/1, pp. 5-21

-
- [2] Tam, M. (2001): "Measuring Quality and Performance in Higher Education", *Quality in Higher Education*, Vol. 7, No. 1, pp. 47-54
 - [3] Hill, F. M. (1995): "Managing Service Quality in Higher Education: the Role of the Student as Primary Consumer", *Quality Assurance in Education*, Vol. 3 No.3, pp. 10-21
 - [4] Rowley, J. (1997): "Beyond Service Quality Dimensions in Higher Education and towards a Service Contract", *Quality Assurance in Education*, Vol. 5, No. 1, pp. 7-14
 - [5] Elliott, K. M. and Healy, M. A. (2001): "Key Factors Influencing Student Satisfaction related to Recruitment and Retention", *Journal of Marketing for Higher Education*, Vol. 10, No. 4, pp. 1-11
 - [6] DeShields, O. W., Kara, A. and Kaynak, E. (2005): "Determinants of Business Student Satisfaction and Retention in Higher Education: Applying Herzberg's Two-Factor Theory", *International Journal of Educational Management*, Vol. 19, No. 2, pp. 128-139
 - [7] Parasuraman, A., Zeithaml, V. and Berry, L. (1988), "SERVQUAL: a Multiple-Item Scale for Measuring Consumer Perceptions of Service Quality", *Journal of Retailing*, Vol. 64 (Spring): pp. 12-40
 - [8] Johnston, R. and Lyth, D. (1991): "Service Quality: Implementing the Integration of Customer Expectations and Operational Capability", in Brown, S. W., Gummesson, E., Edvardsson, B. and Gustavsson, B. (Eds), *Service Quality: Multidisciplinary and Multinational Perspectives*, Lexington Books, Lexington, MA
 - [9] Cronin, J. J. Jr, Taylor, S. A. (1992): "Measuring Service Quality: a Re-Examination and Extension", *Journal of Marketing*, Vol. 56, pp.55-68
 - [10] Bemowski, K. (1991): "Restoring the Pillars of Higher Education", *Quality Progress*, pp. 37-42
 - [11] Owlia, M. S. and Aspinwall, E. M. (1996): "A Framework for the Dimensions of Quality in Higher Education", *Quality Assurance in Education*, Vol. 4, No. 2, pp. 12-20
 - [12] Ramsden, P. (1991): "A Performance Indicator of Teaching Quality in Higher Education: The Course Experience Questionnaire", *Studies in Higher Education*, 16, 129-150
 - [13] Oldfield, B. M., Baron, S. (2000): "Student Perceptions of Service Quality in a UK University Business and Management Faculty", *Quality Assurance in Education*, Vol. 8, No. 2, pp. 85-95
 - [14] Csizmadia, T., Enders, J., Westerheiden, D. F. (2008): "Quality Management in Hungarian Higher Education: Organisational Responses to Governmental Policy", *Higher Education*, Vol. 56, No. 4, pp. 439-455

- [15] Bálint, J. (2008): "Működnek-e a minőségfejlesztési rendszerek a felsőoktatásban?" (Do the Quality Improvement Systems Work in the Higher Education Sector?), *Educatio*, 2008/1, pp. 94-110
- [16] Farkas, A., Nagy, V. (2008): "Student Assessment of Desirable Technical Skills: a Correspondence Analysis Approach", *Acta Polytechnica Hungarica*, Vol. 5, No. 2, pp. 43-57
- [17] Topár, J. (2008): "Felsőoktatási intézmények minőségbiztosítása", (Quality Assurance in Higher Education Institutions), *Educatio*, 2008/1, pp. 76-93
- [18] Lomas, L., (2004): "Embedding Quality: the Challenges for Higher Education", *Quality Assurance in Education*, Vol. 12, No. 4, pp. 157-165
- [19] Szintay, I., Veresné Somosi, M. (2007): "A felsőoktatás egy javasolt minőségirányítási modellje"(A Proposed Quality Management Model for Higher Education), *Magyar Minőség*, 2007/3, pp. 26-30
- [20] Yorke, M. (1999): "Assuring Quality and Standards in Globalised Higher Education", *Quality Assurance in Education*, Vol. 7, No. 1, pp. 14-24
- [21] Sirvanci, M. (1996): "Are Students the True Customers of Higher Education?", *Quality Progress*, Vol. 29, No. 10, pp. 99-102
- [22] Zairi, M. (1995): "Total Quality Education for Superior Performance", *Training for Quality*, Vol. 3, No. 1, pp. 29-35
- [23] Wiers-Jenssen, J., Stensaker, B. and Groggaard, J. B. (2002): "Student Satisfaction: towards an Empirical Deconstruction of the Concept", *Quality in Higher Education*, Vol. 8, No. 2, pp. 183-195
- [24] Rowley, J. (2003): "Designing Student Feedback Questionnaires", *Quality Assurance in Education*, Vol. 11, No. 3, pp. 142-149
- [25] Venkatraman, S. (2007): "A Framework for Implementing TQM in Higher Education Programs", *Quality Assurance in Education*, Vol. 15, Iss: 1, pp. 92-112
- [26] Tóth, Zs. E., Jónás, T., Bérces, R., Bedzsula, B. (2011): "Course Evaluation by Importance-Performance Analysis and Improving Actions at the Budapest University of Technology and Economics", 15th QMOD Conference on Quality and Service Sciences: From Learnability and Innovability to Sustainability. Poznan, Lengyelország, 2012.09.05-2012.09.07
- [27] Suplicz, S. (2009): "What Makes a Teacher Bad? Trait and Learnt Factors of Teachers' Competencies", *Acta Polytechnica Hungarica*, Vol. 6, No. 3, pp. 125-138
- [28] Stoklasa, J., Talasořva, J., Holeček, P. (2011): "Academic Staff Performance Evaluation – Variants of Models", *Acta Polytechnica Hungarica*, Vol. 8, No. 3, pp. 91-111

- [29] Krajcsák, Z. (2013): "Attitűdök és elvárások az alkalmazotti elkötelezettség ötfaktoros modelljében", *Marketing és menedzsment*, Vol. 47, No. 4, pp. 86-94

An analysis of Expected Population States in the Space of Population States: the Case Study of Three-Element Populations

Iwona Karcz-Duleba, Andrzej Cichon

Institute of Computer Engineering, Control and Robotics, Janiszewskiego St.
11/17, 50-372 Wrocław, Wrocław University of Technology, Poland
iwona.duleba@pwr.wroc.pl, andrzej.cichon@pwr.wroc.pl

Abstract: In this paper, an analysis of phenotypic evolutionary search with proportional selection and Gaussian mutation is presented. Evolution is regarded in the space of population states where population is considered as a whole. This approach enables theoretical studies of expected states for small populations. In this paper, three-element populations are examined. The expected states of populations cannot be calculated explicitly due to overwhelming complexity. Therefore, they are approximated numerically. A study of the expected states dynamics and its dependence on several parameters is also provided. It appears that the population moves around, in a fitness landscape, as a compact cluster of individuals and quickly locates neighborhoods of optima.

Keywords: evolutionary computation; small populations; space of population states; population dynamics

1 Introduction

Due to complexity, high-dimensionality and non-linearity, a theoretical study of evolutionary algorithms is rather difficult. Therefore, some simplifying assumptions have to be accepted. One of several possibilities is to consider infinite (or very large) populations [1, 2, 3]. The opposite approach is to consider populations composed of only a few individuals [4, 5]. A population can be represented in two different ways: either regarding its individuals in the space of their types, or concerning the whole population in a space of population states (a space of all possible populations). The second approach is specific for modeling evolutionary algorithms as Markov chains [6, 7] or dynamical systems [1].

In this paper, we will focus on finite, small populations evolving under proportional selection and Gaussian mutation in a real-valued space of population

states. In the real-world applications, populations are not infinite. Moreover, small populations have better exploration properties in search for the global optimum of multidimensional and multimodal quality functions. Nonetheless, using small populations in an evolutionary process has some disadvantages. Such populations behave more chaotically and are unable to maintain diversity for many generations. They cannot penetrate as large areas within a search space as more numerous ones. Also, small size of a population may lead to genetic drift which can result in reduction of a fitness value. Theoretical studies of small populations are scarce and mainly devoted to evolution strategies (ES) [8]. The presented population states approach facilitates the study of very small populations' dynamics in landscapes of one-dimensional unbounded fitness functions. These states allow us to analyze averaged (deterministic) evolution of the whole population instead of non-deterministic behavior of its elements. The expected values locate position of the averaged population and evolution may be interpreted as the population's trajectory in the space of states. Somewhat similar approaches were successfully applied to study the evolution of an ensemble of binary-coded populations in a phase space, that is a space of all possible sets of gene sequences [9], as well as to describe the averaged (macroscopic) evolutionary dynamics of simple genetic algorithm using statistical mechanics-based methods [10].

Thus far, the simplest possible case of two-element populations with one real-valued trait (gene) was studied [4, 5]. Expected values of consecutive population states were calculated and the asymptotic behavior of evolution was examined. We argue that it would be informative to extend the previous analyses to more numerous populations. Therefore, in this paper, estimation of expected values of population state for three-element populations is provided and the mean-value dynamics is evaluated.

The rest of the paper is organized as follows. In Section 2, a formal description of the considered evolution model is presented. Calculations of expected population state for three-element populations are provided in Section 3, followed by the expected dynamics studies in Section 4. Section 5 concludes this paper.

2 Model of Phenotypic Evolution

A one-dimensional version of the model of phenotypic asexual evolution, based on Darwinian theory of evolution, is regarded in the paper [11]. An m -element population $P = \{\mathbf{x}_1, \mathbf{x}_2, \dots, \mathbf{x}_m\}$ evolves in an unbounded one dimensional ($n = 1$) continuous real-valued search space, so the k^{th} individual is described by one trait (*type*) $\mathbf{x}_k = \{x_{k,1}\} = x_k$, and corresponding quality index (*fitness*) $q(x_k): \mathbb{R} \rightarrow \mathbb{R}^+$. Evolution of successive generations of individuals is ruled by two mechanisms: 1) Proportional selection (also called soft, or roulette-wheel selection) where a

parent is chosen randomly with probability proportional to its fitness, 2) Gaussian mutation producing the offspring individual by adding independent random variables, normally distributed with identical standard deviation σ to the parental traits. The model is simple but demonstrates essential properties of an evolutionary process and allows one to obtain some theoretical results for infinite [3], as well as finite (small) populations [4, 5].

Evolving populations are usually studied in a *space T of individuals' types*. In this space, when the location of i^{th} generation P^i is known, a conditional distribution of a new individual's position in the $(i+1)^{\text{st}}$ generation is given by:

$$f_T^{i+1}(\mathbf{x} | P^i) = \sum_{k=1}^m \alpha(\mathbf{x}_k^i) g(\mathbf{x}, \mathbf{x}_k^i) = \sum_{k=1}^m \alpha_k^i N_k^i, \quad (1)$$

where $\alpha(\mathbf{x}_k^i) = \alpha_k^i = q(\mathbf{x}_k^i) / \sum_{j=1}^m q(\mathbf{x}_j^i)$ is the relative quality of the k^{th} individual,

$$g(\mathbf{x}, \mathbf{x}_k^i) = N_k^i = N(\mathbf{x}_k^i, \sigma)(\mathbf{x}) = \frac{1}{\sigma\sqrt{2\pi}} \exp\left(-\frac{(\mathbf{x} - \mathbf{x}_k^i)^2}{2\sigma^2}\right)$$

describes a normal distribution of mutation, $q(\mathbf{x})$ denotes a non-negative fitness function, σ stands for the standard deviation of mutation.

The population as a whole is considered in a *space of population states S* . The structure of this space is seemingly more complex than the typically studied space T . The dimensionality of S depends on the population size and it is equal to $\dim S = mn$ (compared to $\dim T = n$). In the case of one-dimensional search spaces, $\dim S = m$ and $S = \mathbb{R}^m$. Additionally, as the population is insensitive to ordering of its individuals, an equivalence relation U has to be defined in S to identify all the points corresponding to permutations of individuals within the population. Consequently, the population state is reduced to a point in the quotient (factor) space $S_U = S/U = \mathbb{R}^m/U$. In this study, the relation U arranges individuals within population in a decreasing manner based on the values of their traits. Thus, in the case of three-element population, in the quotient space S_U the population state becomes an ordered tuple $\mathbf{s} = \{x_1, x_2, x_3\}$, where $x_1 \geq x_2 \geq x_3$.

When a state \mathbf{s}^i of population in the i^{th} generation is known, the probability distribution $\tilde{f}_{S_U}^{i+1}(\mathbf{s} | \mathbf{s}^i)$ of the population state in S_U in the next generation can be determined. The distribution is a product of m individual distributions (1) considered in the space T :

$$\tilde{f}_{S_U}^{i+1}(\mathbf{s} | \mathbf{s}^i) = m! \prod_{j=1}^m f_T^{i+1}(x_j | \mathbf{s}^i) = m! \prod_{j=1}^m \sum_{k=1}^m \alpha(\mathbf{x}_k^i) N(\mathbf{x}_k^i, \sigma)(x_j) = m! \prod_{j=1}^m \sum_{k=1}^m \alpha_k^i N_{jk}^i. \quad (2)$$

Once the distribution (2) is defined, the expected value of next population state can be computed. Unfortunately, because of the restriction of the population state to the quotient space S_U , straightforward calculations of the expectations are only possible for two-element populations [4, 5]. For this simplest case, an expected asymptotic behavior of evolution was studied and some essential aspects of the process were discovered, namely rapid unification of initially widely diversified populations and a slow motion towards the optima of the quality function. For more numerous populations, expected values have to be approximated numerically.

3 Expected Value of Population State of Three-Element Population

Determining the expected value of the population state of a three-element population is one of the main objectives of this paper. To obtain the value, several triple definite integrals need to be calculated with integrand given in the multiplicative form of normal distribution functions with different parameters. As an illustrative example, x_1 coordinate of the expected state is given by:

$$\begin{aligned} E^{i+1}[x_1 | s^i] &= \int_{-\infty}^{+\infty} \int_{-\infty}^{x_1} \int_{-\infty}^{x_2} x_1 \tilde{f}_{S_U}^{i+1}(x_1, x_2, x_3 | s^i) = \\ &= \int_{-\infty}^{+\infty} \int_{-\infty}^{x_1} \int_{-\infty}^{x_2} x_1 \left(3! \prod_{j=1}^3 \sum_{k=1}^3 \alpha_k N_{jk} \right) dx_3 dx_2 dx_1 = 3! \int_{-\infty}^{+\infty} \int_{-\infty}^{x_1} \int_{-\infty}^{x_2} x_1 (\alpha_1 N_{11} + \alpha_2 N_{12} + \alpha_3 N_{13}) \cdot \\ &\cdot (\alpha_1 N_{21} + \alpha_2 N_{22} + \alpha_3 N_{23}) \cdot (\alpha_1 N_{31} + \alpha_2 N_{32} + \alpha_3 N_{33}) dx_3 dx_2 dx_1, \end{aligned} \quad (3)$$

and, for simplicity, the generation number i was omitted within integrals. It is worth noticing that limits of integration of two inner integrals do not range from minus to plus infinity. Instead, the upper limits are constrained, since the values are calculated in a quotient space being a reduced real space (\mathbb{R}^m / U) .

Let us first denote the component integral $I_1(p, r, s)$ as:

$$I_1(p, r, s) = 3! \alpha_p \alpha_r \alpha_s \int_{-\infty}^{+\infty} \int_{-\infty}^{x_1} \int_{-\infty}^{x_2} x_1 N_{1p} N_{2r} N_{3s} dx_3 dx_2 dx_1,$$

where p, r, s take values from the set $\{1, 2, 3\}$ (with repetitions). In order to obtain just a single coordinate of the expected state, 27 such integrals need to be calculated. Having performed some exhaustive computations, we finally obtained the following form of I_1 :

$$I_1(p, r, s) = \frac{3}{2\pi} \alpha_p \alpha_r \alpha_s \left(\frac{1}{b} \sqrt{\frac{\pi}{2}} \exp\left(-\frac{b^2(x_p^i - x_r^i)^2}{2}\right) \operatorname{erfc}\left(\frac{b(2x_s^i - x_p^i - x_r^i)}{\sqrt{6}}\right) + \right. \\ \left. + x_p^2 \pi \left[\operatorname{erfc}\left(\frac{b(x_s^i - x_r^i)}{\sqrt{2}}\right) - \operatorname{erf}\left(\frac{b(x_r^i - x_p^i)}{\sqrt{2}}\right) - \frac{b}{\sqrt{\pi}} I_1(p, r, s) \right] \right), \quad (4)$$

where: $I_1(p, r, s) = \int_{-\infty}^{+\infty} \exp(-b^2(x_2 - x_r^i)^2) \operatorname{erf}(b(x_2 - x_p^i)) \operatorname{erf}(b(x_2 - x_s^i)) dx_2$, $b = (\sqrt{2}\sigma)^{-1}$, and $\operatorname{erf}(x)$, $\operatorname{erfc}(x)$ are error function and complementary error function derived from normal distributions.

$I_1(p, r, s)$ can only be evaluated analytically for $p = r = s$. If $p = r$ or $r = s$, the integral can be calculated using the approximation $\operatorname{erf}^2(x) \approx 1 - \exp(-x^2 \pi^2 / 8)$. For $p \neq r \neq s$, $I_1(p, r, s)$ has to be computed numerically.

Ultimately, expected value of coordinate x_1 can be expressed as a sum of:

$$E^{i+1}[x_1 | \mathbf{s}^i] = \sum_{p=1}^3 \sum_{r=1}^3 \sum_{s=1}^3 I_1(p, r, s). \quad (5)$$

Expected values of coordinates x_2 and x_3 are calculated correspondingly:

$$E^{i+1}[x_2 | \mathbf{s}^i] = \sum_{p=1}^3 \sum_{r=1}^3 \sum_{s=1}^3 I_2(p, r, s), \quad (6)$$

$$E^{i+1}[x_3 | \mathbf{s}^i] = \sum_{p=1}^3 \sum_{r=1}^3 \sum_{s=1}^3 I_3(p, r, s), \quad (7)$$

and their component integrals are given in Appendix 1. All calculations and simulations were performed using *Mathematica* software [12].

4 Dynamics of Expected States of Three-Element Populations

With given values of the expected states, an expected long-term behavior of the evolving three-element populations can now be analyzed. Simulations of the expected states were carried out in landscapes of different quality functions: unimodal triangle and Gaussian, both symmetrical and asymmetrical. Similarly, multi-modal functions in the form of bimodal Gaussian fitness with different

heights and various distances between optima were considered (all the functions are listed in Appendix 2). In these landscapes, population dynamics and the influence of several parameters (standard deviation of mutation σ , fitness function asymmetry, and distance between optima) was analyzed. In order to study population diversity, random and homogeneous initial populations were examined.

Expected states are a good estimation of random population behavior. In Fig. 1, locations of coordinates x_1, x_2, x_3 averaged over 50, 100 and 500 runs are presented along with expected states coordinates calculated with Eqns. (5)–(7) in the course of 30 generations. The fitness function is shown in the right panel. It can be noticed that the averaged behavior closes the expected state trajectories — the approximation accuracy is acceptable for less than 100 runs.

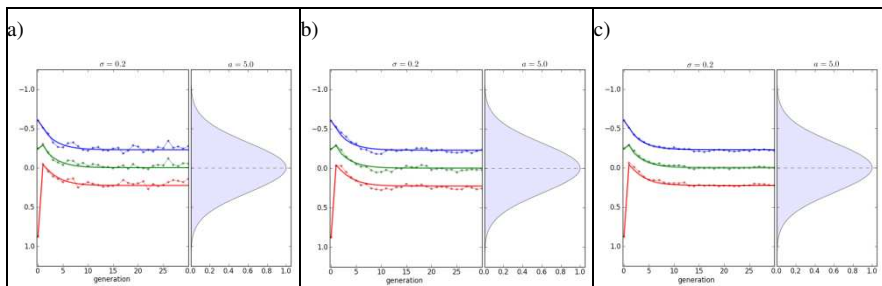


Figure 1

Random evolution of three-element populations averaged over: a) 50; b) 100; c) 500 runs (dotted lines) along with the expected states coordinates (solid lines). The red, green, and blue colors correspond respectively to coordinates x_1, x_2, x_3 of consecutive states. Parameters on the upper side of the plots specify the value of the standard deviation of mutation (σ) used in the simulations, as well as the α parameter of unimodal Gaussian fitness function (cf. Appendix 2)

At first, we will examine expected states trajectories in a landscape of the unimodal Gaussian fitness function with the optimum located at $(0,0,0)$. Five trajectories of 30 generations starting from different random initial states are presented in Fig. 2 followed by Euclidean distances between consecutive states d_s in Fig. 3, and Euclidean distances between the states and the optimum d_o in Fig. 4 together with a steady state distance from optimum versus σ plot (for the distances definitions see Appendix 3).

Based on the simulations, the following observations can be made:

- At the beginning, differences in subsequent locations of trajectory points are large, thus Euclidean distances between successive states d_s are large (jumps of trajectories) (Fig. 3),

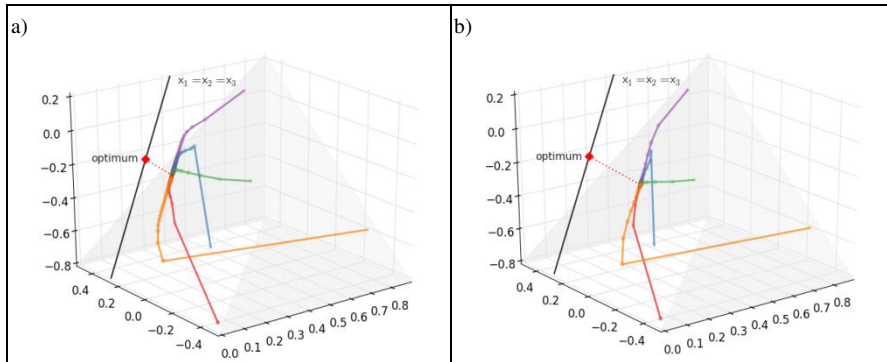


Figure 2

Five expected trajectories of three-element populations starting from different initial states. Coordinates correspond to the values of $E[x_1]$, $E[x_2]$, $E[x_3]$; identity line $x_1 = x_2 = x_3$ and the optimum are depicted. a) $\sigma=0.1$; b) $\sigma=0.2$

- Just after a few generations, the differences become much smaller, so distances d_s decrease (small steps of trajectories),
- Subsequent states are located along a line parallel to the *identity line* $x_1 = x_2 = x_3$ called *evolutionary channel* [5]; the distance between the channel and the identity line depends on σ (Fig. 2),
- Expected states do not change, i.e., trajectories starting from different initial states converge to one point (a steady state, or equilibrium point),
- The rate of convergence to the steady state depends on the standard deviation of mutation σ ,
- Steady states are not located exactly at the optimum,
- Distances between subsequent states and the optimum d_o quickly decreases to a value depending on the standard deviation σ ; the bigger the σ , the larger the distance to the optimum in the steady state (Fig. 4).

Trajectories of expected values of three-element populations for various unimodal fitness functions: Gaussian and triangle, in their symmetrical and asymmetrical forms are presented in Fig. 5. An influence of the standard deviation of mutation on “shift” of expected steady states from the optimum in a landscape of unimodal asymmetrical Gaussian fitness function is shown in Fig. 6.

Independently of the fitness form, initially diversified population converges rapidly (in two–three generations) and forms a cluster with a radius close to σ , as in Fig. 2, Fig. 5 d-f, and Fig. 7 d-f. When the initial population is homogeneous, it becomes instantly diversified by the mutation operator and, in the following generations, forms the cluster as well (Fig. 5 a-c), (Fig. 6), (Fig. 7 a-c), (Fig. 8 a).

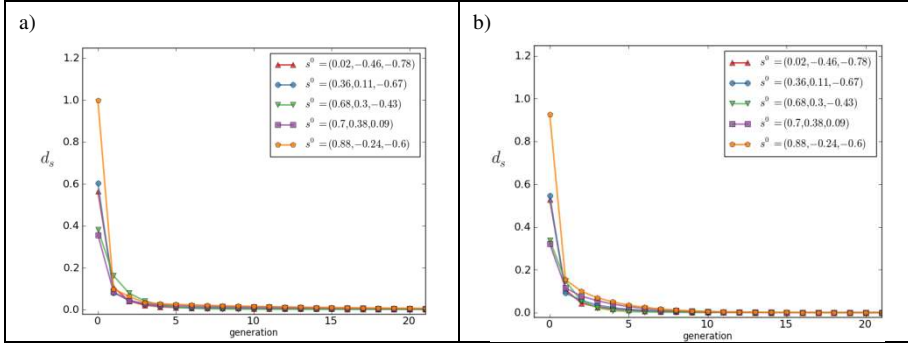


Figure 3

Distances between successive states d_s for five trajectories starting from different initial states given in Fig. 2. a) $\sigma=0.1$; b) $\sigma=0.2$

In the case of an initially homogeneous population, $x_1^0 = x_2^0 = x_3^0 = x^0$, thus $q(x_1^0) = q(x_2^0) = q(x_3^0)$, and it is possible to calculate directly on the expected values using (5)–(7):

$$E^1[x_1 | s^0] \approx x^0 + 0.85\sigma, \tag{8}$$

$$E^1[x_2 | s^0] \approx x^0, \tag{9}$$

$$E^1[x_3 | s^0] \approx x^0 - 0.85\sigma. \tag{10}$$

Coordinate x_2 remains unchanged, while the other two differ from their initial positions by about σ — a homogeneous population is spread out by the operation of mutation. The case will be also discussed later on.

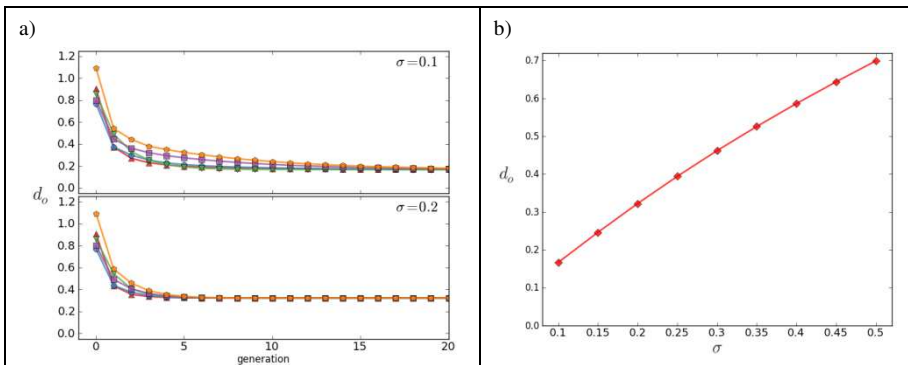


Figure 4

- a) Distances between successive states and the optimum d_0 for five trajectories starting from different initial populations plotted in Fig. 2 and specified in Fig. 3, for $\sigma=0.1$ and $\sigma=0.2$.
- b) A steady state distance from the optimum d_0 versus σ

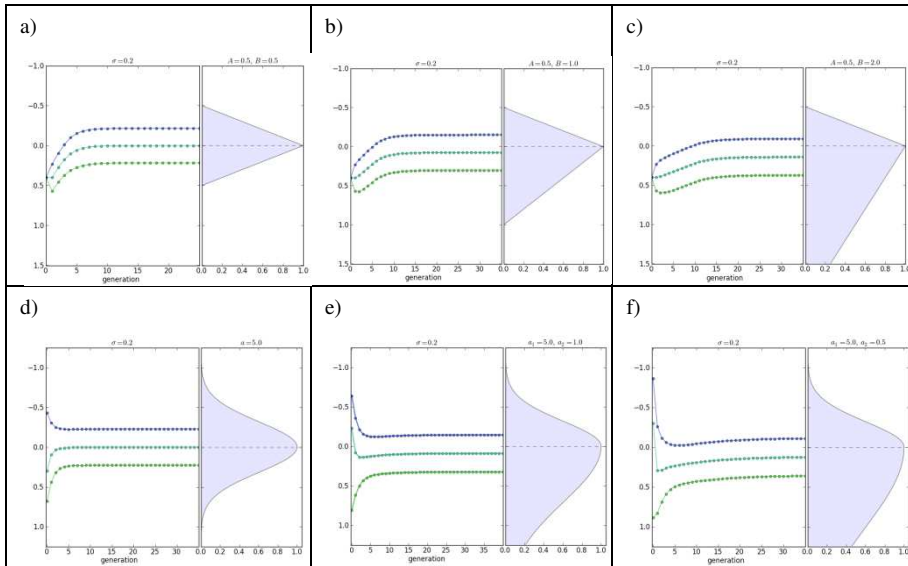


Figure 5

Evolution of expected values of three-element populations in the landscapes of unimodal symmetrical (a, d) and asymmetrical (b, c, e, f) fitness functions: a)-c) triangle; d)-f) Gaussian; $\sigma=0.2$

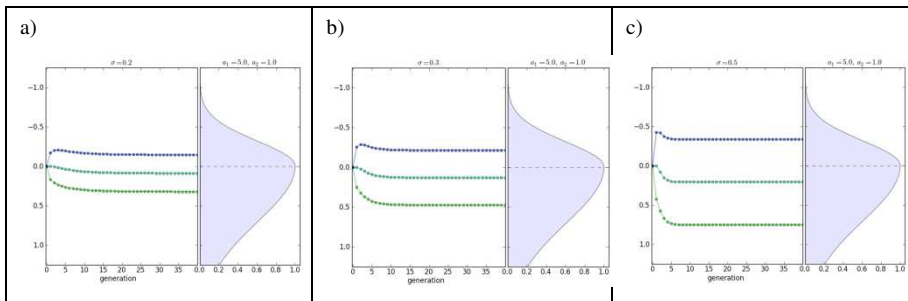


Figure 6

Influence of standard deviation of mutation on "shift" of expected steady states in a landscape of unimodal asymmetrical Gaussian fitness function: a) $\sigma=0.2$; b) $\sigma=0.3$; c) $\sigma=0.5$

When unimodal fitness function is symmetrical, $E[x_1 | s^i]$ and $E[x_3 | s^i]$ are situated symmetrically on the slopes of the function in equal distances from the optimum, while $E[x_2 | s^i]$ is located at the optimum (which is good news for the optimum seekers) (Fig. 5 a, d). Asymmetry in the fitness landscape affects the expected states: they are shifted towards the slope with a "bigger mass": the greater the asymmetry, the greater the displacement (Fig. 5 b, c, e, f). Moreover, the magnitude of the shift depends on σ : the attraction strength increases along with the value of σ (Fig. 6).

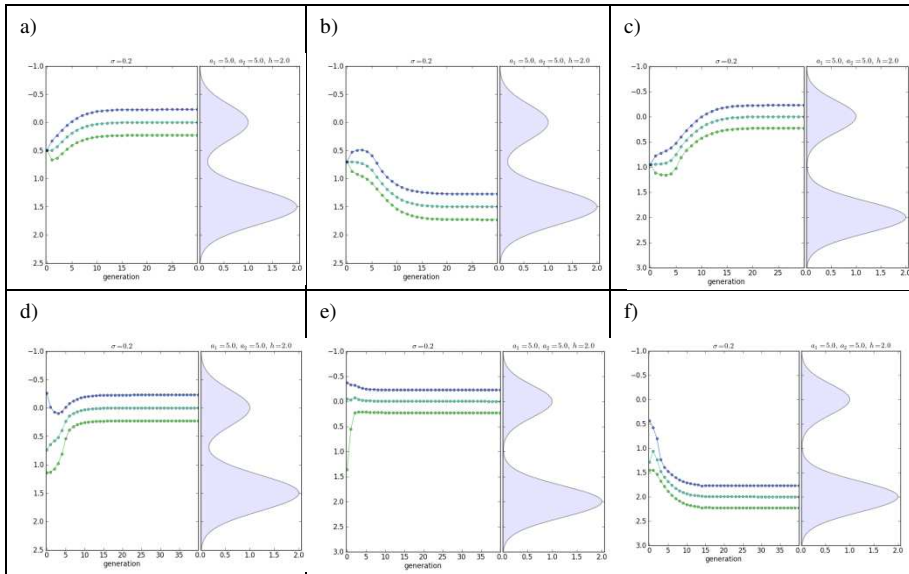


Figure 7

Evolution of expected values of three-element populations in a landscape of bimodal Gaussian fitness functions. Homogenous initial population (a-c) lies in a basin of attraction of the local (a, c) and the global (b) optimum. Random initial population (d-f) in a basin of attraction of the local (d, e) and the global (f) optimum. Functions represent different distances between optima: a), b), d) $d=1.5$; c), e), f) $d=2$; $\sigma=0.2$

Now, let us discuss the case of bimodal fitness functions. The considered functions have got two basins of attraction corresponding to the local and the global optimum. Evolution of expected values of three-element populations in a landscape of bimodal Gaussian fitness functions with different distances between optima d for homogenous and random initial populations are shown in Fig. 7. Expected states trajectories for uniformly distributed initial states are presented in Fig. 8a, followed by Euclidean distances between successive states and the optimum in Fig. 8b.

The expected population converges to the vicinity of one of the optima and its trajectory depends both on the initial population state and σ . As to the evolution of expected states over unimodal fitness landscape (cf. Fig. 2), additional observations for homogeneous initial state can be noted:

- Immediately, in the first generation, population is diversified and its expected state is pushed away from the identity line (jumps of trajectories),
- Subsequent states are located along the evolutionary channel; the channel is more distinct than in the case of initially diversified population (Fig. 2),

- Distances between consecutive states in the channel are small and converge to zero,
- Trajectories converge to the local/global optimum when starting within a basin of attraction of the local/global optimum (Fig. 7 a-c), (Fig. 8a),
- Distances between subsequent states and the optimum decrease rapidly (Fig. 8b),
- Distances of steady states from related optimum are the same for local and global ones.

A border between basins of attraction of both optima, displayed in Fig. 9, is situated on the saddle and its accurate position depends on a distance between optima d and on the standard deviation of mutation σ . With the increasing value of σ , the strength of the global optimum attraction intensifies: a population is more dispersed and more easily attracted. The initially diversified population (Fig. 7 d-f) may converge to local or global optimum in the initial-state-dependent manner.

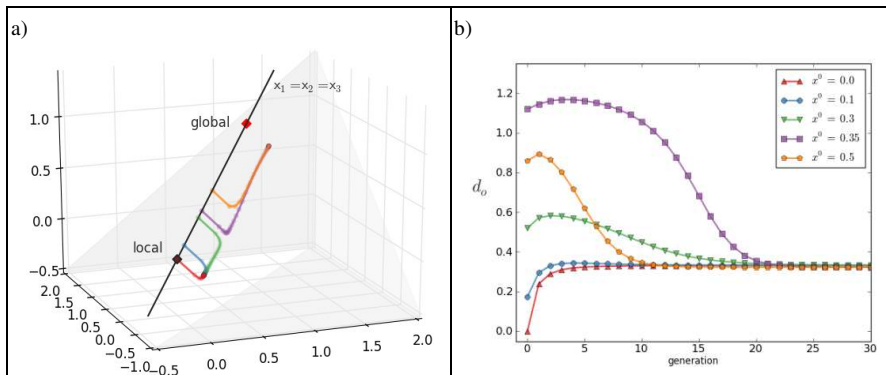


Figure 8

a) Trajectories of expected values of three-element populations starting from different homogeneous initial states in a landscape of bimodal fitness function. b) Distances between successive states and the optimum d_o for five trajectories given in the left panel. Two upper lines (for $x^0 = 0.35$, and $x^0 = 0.5$) correspond to trajectories attracted by the global optimum, three lower ($x^0 = 0.0$, $x^0 = 0.1$, $x^0 = 0.3$) correspond to trajectories attracted by the local optimum; $\sigma=0.2$

Analogously to unimodal fitness functions, the expected population in the steady state forms a cluster in the vicinity of the optimum. However, expected coordinate $E[x_2 | s^i]$ is not located exactly at the optimum any more but it is moved by the influence of the other hill. The shift of population's steady state from the optimum is presented in Fig. 10. A value of the shift is a function of the distance between optima d and the standard deviation of mutation. Clearly, the global optimum attracts populations much stronger than the local one, and consequently the shift on the local hill towards the global one is much bigger than the other way around.

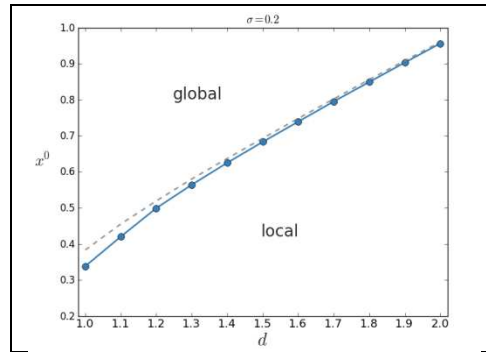


Figure 9

Border between basins of attraction of the global and the local optimum as a function of distance between optima d . Dotted line indicates saddle minimum. Homogeneous initial population, $\sigma=0.2$.

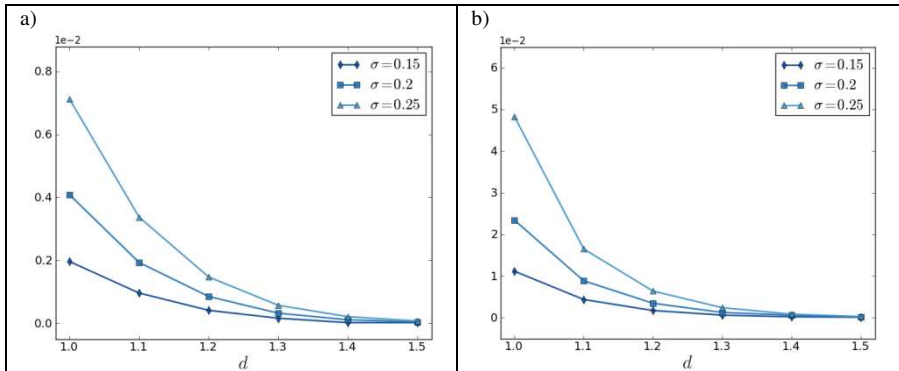


Figure 10

Shift of population's steady state from the optimum versus distance between optima d for: a) the global optimum; b) the local optimum

5 Summary

The work presented herein for expected states of three-element populations, facilitates understanding of the rules of artificial evolution, hence, may be useful in improving efficiency of evolutionary algorithms. The following conclusions are justified:

- Initially diversified (random) populations quickly converges to a cluster with a radius close to σ . Thus, efforts of many practitioners to widely diversify initial populations, in order to avoid premature convergence, may be abortive,

- Initially homogenous populations quickly disperse to a cluster with a radius close to σ ,
- Expected states of populations in the cluster slowly move along the evolutionary channel and converge to a steady state near the optimum,
- Although the steady state is placed at some distance from the optimum, expected values of second coordinate $E[x_2 | s^i]$ locate the optimum for symmetrical fitness functions. This distance depends on the standard deviation of mutation, σ , and the fitness function,
- The shift of expected population from the optimum may indicate bigger mass in the shift direction, i.e., asymmetry of unimodal function or a saddle in multi-modal landscape. These observations may be useful for identification of black-box or grey-box fitness functions.

The examined behavior of three-element populations is qualitatively very similar to that of two-element systems [4, 5], thus we presume that obtained results can be extended for more numerous (but still small) populations. Preliminary simulations of evolution of more numerous populations in the quotient space of population states revealed that properties discussed herein are accurate. In the future, more dimensional type spaces should be examined using the population space paradigm. Simulations of a conventional evolution in more dimensional types spaces T ($n > 1$) confirmed a similar population behavior: unification of diversified population, progress along evolutionary channel and fluctuation in a neighborhood of the optimum. In more numerous populations and in multidimensional spaces, no analytical formulas for expected values exist (as in the simplified models). Presumably, numerical simulations will become more cumbersome, as integrals needed to obtain the expected values, are more complex.

Appendix 1: Component integrals for coordinates x_2 and x_3

Component integrals for $E^{i+1}[x_2 | s^i]$ and $E^{i+1}[x_3 | s^i]$ are given by:

$$I_2(p, r, s) = \frac{3}{2\pi} \alpha_p \alpha_r \alpha_s \left[\frac{1}{b} \sqrt{\frac{\pi}{2}} \left[\exp\left(-\frac{b^2(x_r^i - x_s^i)^2}{2}\right) - \exp\left(-\frac{b^2(x_r^i - x_p^i)^2}{2}\right) \right] + \right. \\ \left. + x_r^i \pi \left[\operatorname{erfc}\left(\frac{b(x_s^i - x_r^i)}{\sqrt{2}}\right) - \operatorname{erf}\left(\frac{b(x_r^i - x_p^i)}{\sqrt{2}}\right) - b\sqrt{\pi} I_2(p, r, s) \right] \right]$$

$$I_3(p, r, s) = \frac{3}{2\pi} \alpha_p \alpha_r \alpha_s \left(-\frac{1}{b} \sqrt{\frac{\pi}{2}} \exp\left(-\frac{b^2(x_r^i - x_s^i)^2}{2}\right) \operatorname{erfc}\left(\frac{b(x_r^i + x_s^i - 2x_p^i)}{\sqrt{6}}\right) + x_s^2 \pi \left[\operatorname{erfc}\left(\frac{b(x_s^i - x_r^i)}{\sqrt{2}}\right) - \operatorname{erf}\left(\frac{b(x_r^i - x_p^i)}{\sqrt{2}}\right) - \frac{b}{\sqrt{\pi}} I_3(p, r, s) \right] \right)$$

where:

$$I_2(p, r, s) = \int_{-\infty}^{+\infty} x_2 \exp\left(-b^2(x_2 - x_r^i)^2\right) \operatorname{erf}\left(b(x_2 - x_p^i)\right) \operatorname{erf}\left(b(x_2 - x_s^i)\right) dx_2,$$

$$I_3(p, r, s) = \int_{-\infty}^{+\infty} \exp\left(-b^2(x_2 - x_r^i)^2\right) \operatorname{erf}\left(b(x_2 - x_p^i)\right) \operatorname{erf}\left(b(x_2 - x_s^i)\right) dx_2,$$

$$\text{and } b = (\sqrt{2}\sigma)^{-1}.$$

Appendix 2: Fitness functions

Triangle fitness function with parameters A, B

$$f(x) = \begin{cases} x/A + 1 & \text{for } x \in [-A, 0), A > 0 \\ -x/B + 1 & \text{for } x \in [0, B), B \geq A \\ 0 & \text{otherwise} \end{cases}.$$

Unimodal Gaussian fitness function parameterized with A and B

$$f(x) = \begin{cases} \exp(-Ax^2) & \text{for } x \leq 0 \\ \exp(-Bx^2) & \text{for } x > 0 \end{cases},$$

for a symmetric version: $f(x) = \exp(-ax^2)$.

Bimodal Gaussian fitness function composed of two unimodal hills with different heights (h) and distance between optima d

$$f(x) = \exp(-a_1x^2) + h \exp(-a_2(x-d)^2).$$

Appendix 3: Definitions of Euclidean distances d_s and d_o

The values of distances between consecutive states d_s , and between consecutive states and the optimum d_o are calculated as Euclidean metrics. For the given coordinates of successive states $s^0, s^1, s^2, \dots, s^i$ in m -dimensional space S_U , the optimum x^* , and the number of generations i , we get:

$$d_s^k(s^k, s^{k+1}) = \|s^k - s^{k+1}\| = \left(\sum_{j=1}^m (s_j^k - s_j^{k+1})^2 \right)^{1/2}, \text{ for } k = 0, \dots, i-1,$$

and

$$d_o^k(s^k, x^*) = \|s^k - x^*\| = \left(\sum_{j=1}^m (s_j^k - x_j^*)^2 \right)^{1/2}, \text{ for } k = 0, \dots, i.$$

References

- [1] M. D. Vose. The Simple Genetic Algorithm. Foundations and Theory. MIT Press, 1999
- [2] S. Voget. Theoretical Analysis of GA with Infinite Population Size. Complex Systems, 10(3), 1996, pp. 167-183
- [3] I. Karcz-Duleba. Dynamics of Infinite Populations Evolving in a Landscape of Uni- and Bimodal Fitness Functions. IEEE Transactions on Evolutionary Computations, 5(4), 2001, pp. 398-409
- [4] I. Karcz-Duleba. Asymptotic Behavior of Discrete Dynamical System Generated by Simple Evolutionary Process. Journal of Applied Mathematics and Computer Science, 14(1), 2004, pp. 79-90
- [5] I. Karcz-Duleba. Dynamics of Two-Element Populations in the Space of Population States. IEEE Transactions on Evolutionary Computations, 10(2) 2006, pp. 199-209
- [6] A. E. Nix, M. D. Vose. Modeling Genetic Algorithms with Markov Chains. Annals of Mathematics and Artificial Intelligence, 5, 1992, pp. 79-88
- [7] T. E. Davis, J. C. Principe. A Markov Chain Framework for the Simple Genetic Algorithm. Evolutionary Computation, 1(3), 1993, pp. 269-288
- [8] H.-G. Beyer. The theory of evolution strategies. Berlin, Springer-Verlag, 2001
- [9] A. Prügel-Bennett. Modelling Evolving Populations. Journal of Theoretical Biology, 185(1), 1997, pp. 81-95
- [10] J. L. Shapiro. Statistical Mechanics Theory of Genetic Algorithms. Theoretical Aspects of Evolutionary Computing, 2001, pp. 87-108

- [11] R. Galar. Evolutionary Search with Soft Selection. *Biological Cybernetics*, 60, 1989, pp. 357-364
- [12] A. Cichon. Expected State of Three-Element Populations. (in Polish) Technical Report of Institute of Computer Engineering, Control and Robotics, No. 21, 2013. English excerpt of the report and *Mathematica* source code are available at http://iwona.duleba.staff.iiar.pwr.wroc.pl/Acta_files/index.html

Use of Computer Simulation in Estimation of GSM Base Station Output Power

Mladen Mileusnić, Tomislav Šuh, Aleksandar Lebl, Dragan Mitić, Žarko Markov

Institute for Telecommunications and Electronics, IRITEL A.D. BELGRADE
Batajnički put 23, 11080 Belgrade, Serbia
E-mail: mladenmi@iritel.com, suh@iritel.com, lebl@iritel.com, mita@iritel.com,
Zarko.Markov@iritel.com

Abstract: In this paper we present how computer simulation can be used to estimate the mean output power and the probability cumulative distribution function of one base station output power in GSM. The basis of the method is adding the simulation of random distance between the mobile station (MS) and base transceiver station (BTS) to the known method of telephone traffic simulation. The simulation is a suitable method for the estimation of base station output power, especially in the case when it is not easy to calculate the output power's dependence on these factors. A couple of numerical examples present the results of these simulations.

Keywords: computer simulation; random number generation; probability distribution function; GSM; base transceiver station; output power; telephone traffic

1 Introduction

The use of radio links and mobile communication is quickly increasing, which is why energy saving is of growing importance in this field. There are at least reasons for energy saving. The first one is growing cost of energy, and the second one is environmental preservation because of the detrimental effect of increased energy production [1] [2]. The program of energy saving is called *GREEN Radio (Globally Resource-optimized and Energy-Efficient Networks)*. This program has several directions, but for this paper the most important direction pertains to telephone traffic characteristics that are used to save energy. This direction is often also called *TANGO (Traffic-Aware Network planning and Green Operation)*. Energy consumption, i.e. instantaneous consumption of electrical power of one base station (*Base Transceiver Station, BTS*) in the network of mobile telephones (GSM), depends on different factors: number of carriers, i.e. number of traffic (TCH) channels, distribution of surface users' density in the cell, influence of intra-cell connections, influence of half-rate connections, influence of

the limited number of traffic sources, and influence of the environment on signal attenuation.

The first carrier (BCCH) always has constant, i.e. greatest, power [3], and it is not considered in this paper. In the channels of other carriers the power is adjusted according to the instantaneous needs, i.e. in this case power control exists.

The density of surface users is important, because the distance between the base station and the user determines the base station output power for that channel. It is clear that less power is needed if more users are situated near the base station.

Intra-cell connections are established between the users, situated in the same cell [4]. The influence of intra-cell connections is seen as the increase of power per connection when the part of intra-cell traffic increases because each intra-cell connection seizes two channels.

On the contrary to the influence of intra-cell connections, influence of half-rate connections [5] decreases emission power per connection. In this paper it is considered that the results, obtained for full-rate connections, are conservative, i.e. that they are on the safe side in relation to the model with half-rate connections.

The influence of a limited number of traffic sources (Engset model) increases model efficiency. Unfortunately, this increase is less than the decrease of efficiency caused by intra-cell connection establishment [6].

The environmental influence on signal attenuation is such that the signal is attenuated as a function of the distance between the user and the base station at a degree between two and five.

One of the important factors is instantaneous number of mobile telephone connections, i.e. instantaneous value of telephone traffic. Minimizing of the transmitter power leads to the minimizing of self-interference in the system, i.e. to maintenance of requested quality of service (*Quality of Service*, QoS) in the conditions of optimal output emission power in BTS. The third component of the problem of battery backup in BTS, which is used if the primary power source of the electric power network is interrupted, or if alternative energy source is used. If all these reasons are considered, it is necessary to know the output power of BTS as a function of all factors, that influence the emission power in the corresponding cell. As the accurate calculation of this dependence is sometimes very complex, in this paper we present the method for this dependence determination by computer simulation. The method is proved by simulation of one simple case: we consider a group of traffic channels containing two to four carriers (14 to 30 TCH channels), signal attenuation is related to the square of the distance between the user and the base, there are no intra-cell and half-rate connections, users' density distribution is uniform in the whole cell, there is a great number of users in the model (Erlang model).

Section 2 deals with model presentation. This section also gives some important assumptions and the list of designations, which are used in the paper. Section 3 presents the process of simulation, and Section 4 gives the results of simulation.

2 Model, Assumptions and Designations

Let us consider one BTS with dynamic power control in a GSM network [3] [7]. The network uses FDMA (*Frequency Division Multiple Access*) and TDMA (*Time Division Multiple Access*), implemented within each carrier. The number of carriers used in one BTS is denoted by N_f , and the number of time slots used on each carrier by N_s ($=8$). The number of traffic channels, N_t , used for telephone connection establishment is slightly lower than the total number of channels, i.e. $N_t < N_c = N_f \cdot N_s$, because some of the channels are used for signalling. The offered traffic to all traffic channels in BTS is given by A . The total served (handled) traffic is Y . The call loss (or blocking), caused by lack of idle traffic channels, is denoted by B .

A distribution function of random variables will be denoted by F . For example: let us consider the random variable X with one of its values x . As it is well known, the (cumulative) probability distribution function (CDF) of a random variable X , $F_X(x)$, presents the probability that X is less or equal to x :

$$F_X(x) = P(X \leq x)$$

The probability density function of X is denoted by $f_X(x)$ and it is, for continuous random variables, equal to the derivative of the distribution function $F_X(x)$.

The output power of one traffic channel (W) is defined as mean power during the useful part of GSM burst.

The output power of one traffic channel as part of total BTS power is $\omega = W/8$.

The mean output BTS power is mean value of power as sum of all traffic channels powers, $W_{Bm} = \sum \omega_i$, $i=1,2,\dots,N_t$, Fig. 1.

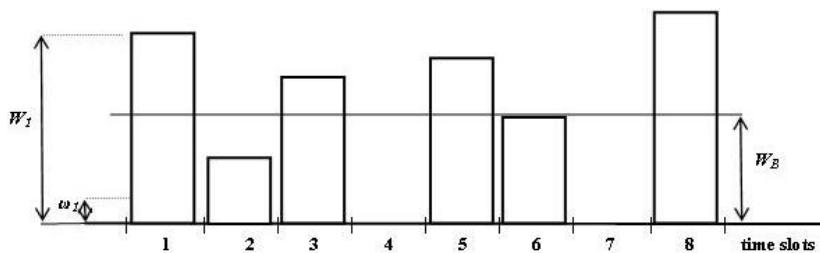


Figure 1

Symbolic presentation of output power for one BTS with 8 traffic channels: W_1 - output power of first traffic channel, ω_1 - output power of first channel as part of mean BTS output power, $\omega_1 = W_1/8$, W_{Bm} - mean output power of BTS, $W_{Bm} = \sum \omega_i$, $i=1,2,\dots,8$

We shall make some assumptions, which simplify the model, but do not decrease the quality of analysis.

A1. The output power of the BTS is adjusted for all active traffic channels on all carriers only according to the user's distance.

A2. Mobile stations (MS) are uniformly distributed in the cell area. The cell area is the circle with radius R . This assumption is adopted in order to enable calculations. Generally, users can be arbitrary distributed.

A3. The output power of one channel (W) depends on the random distance, (D), between MS and BTS:

$$w = g(d) \quad (1)$$

where $w_{max} = g(R)$ is the largest emission power of one channel.

The distance between BTS and MS, D , is a random variable and its distribution function:

$$F_D(d) = P(D \leq d) \quad (2)$$

represents probability that the distance is less or equal to some value d . This assumption means that output power of one traffic channel is continuous random variable (as also D), which is in practice not completely true, because the output power changes in steps of 2 dB. The distribution density of random variable D is $f_D(d)$.

A4. The number of users, i.e. mobile stations N_{ms} in one cell, which is overlaid by the considered base station, is much higher than the number of traffic channels, i.e. $N_{ms} \gg N_t$. This assumption allows us to use the well-known Erlang model for traffic calculations, [7], section 2.4.4. As in A2, this assumption is adopted in order to make calculation easier. The model can also be Engset if this assumption is not valid.

3 Simulation

Computer simulation of telephone traffic process has been well-known for a long time. A detailed description of this process can be found in [8] and [9], although these are not the oldest references from this area. This method, called roulette method or Monte Carlo method, is first used for the determination of call loss in telephone systems, where it was not always easy to derive mathematical formulas for the calculation. The interesting characteristic of the method is the following one: the real process in telephone system happens in continuous time, and the computer simulation happens in discrete moments of time. This inconsistency makes no problem for the determination of time-relations in queueing systems, [10].

The simulation of telephone traffic in a fully available group, as in the group of radio channels in one GSM cell, is based on the generation of a random number RN1 with uniform distribution in the interval $(0, A+N_t)$.

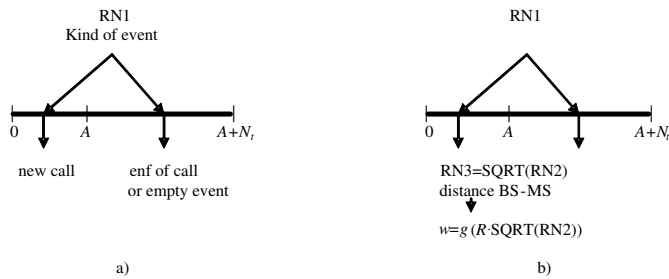


Figure 2
Simulation principle

The new call is generated if it is $0 < RN1 < A$, and the end of the connection on channel K ($K=1,2,\dots,N_i$) happens if channel K is busy and if the generated number is situated in the interval $K-1 < RN1 < K$, Fig. 2a). If it is $K-1 < RN1 < K$, and channel K is free, this is an empty event. It is obvious that in this process of simulation the main random variable is the number of instantaneous connections j in the system.

In order to determine the characteristics of output power of channel with power control in GSM by simulation, the process of traffic simulation must be upgraded in such a way that, for the new call, the random distance between MS and BTS, is generated, Fig. 2b). According to the assumption A2, the cumulative distribution function (CDF) of the distance is calculated in the following way. The probability that MS-BTS distance is equal or smaller than x is the the probability that the location of MS is in the circle with radius x , i. e.

$$F_D(x) = P(d \leq x) = \frac{\pi \cdot x^2}{\pi \cdot R^2} = \frac{x^2}{R^2}, \quad 0 \leq x \leq R \quad (3)$$

The desirable distribution of random numbers in this simulation can be obtained from the uniform distribution by inverse transform method, [11] or [12]. In the case of uniform users' density in the cell, equation (3), it is necessary to generate numbers with the inverse quadratic distribution. So, the random numbers, which determine the distance between BTS and MS, are calculated as the square root of the uniformly distributed random numbers. It means that random distance BTS-MS (d) can be obtained in simulation from the random number RN2, which has the uniform distribution in the range (0,1), by implementing the operation $d=R \cdot RN3=R \cdot \text{SQRT}(RN2)$, as presented in [11] or [12]. Finally, the output power of one connection in simulation process is obtained as the random variable w , which is the function of the random distance BTS-MS, according to (1).

A flow chart of the program for simulation is presented in Fig. 3. Steps in simulation are: 1. random number (RN1) generation, 2. multiplication of this number by $A+N_i$, 3. decision whether generated random number RN1 means the new call or connection interruption, 4. new call – are there free channels, 5. seizing of free channel L , 6. random number (RN2) generation, 7. and 8. determination of random distance BTS-MS in the new connection using channel L , 9. calculation of the power for the new connection on channel L , 10. increase of

total power by the value of the power of new connection, 11. generated random number corresponds to the channel K , 12. checking whether channel K is busy, 13. release of channel K , if it is busy, 14. decrease of total power by the power of channel K .

The mean value of output power and CDF of the probability of output power for one active channel and for the group of channels in one BTS can be obtained using the simulation, whose flow chart is presented in Fig. 3.

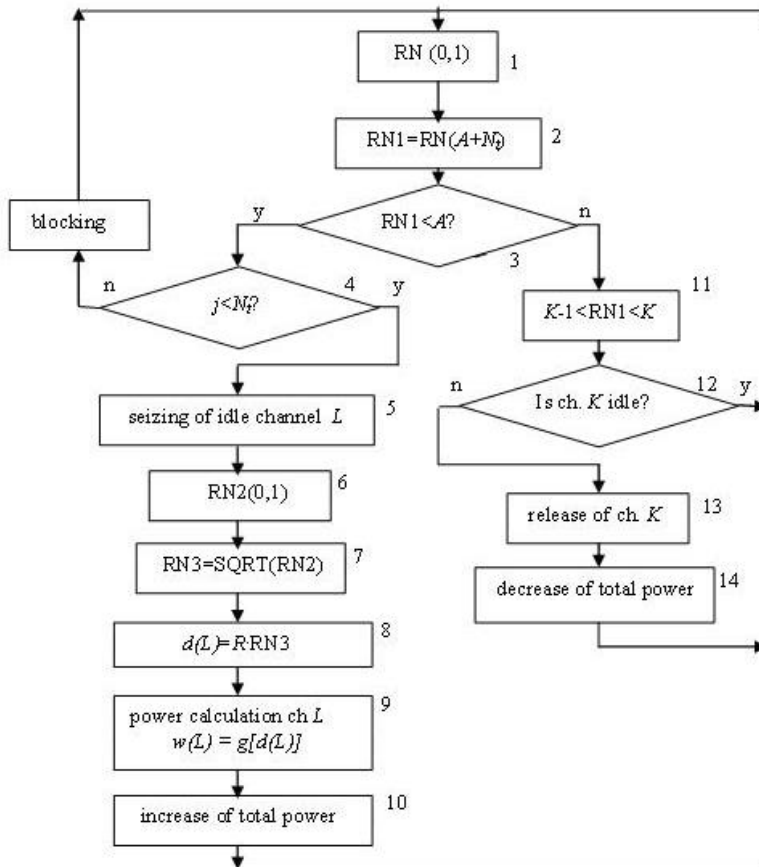


Figure 3
Flow chart of simulation

4 Example

Let us consider a GSM cell where the dependence of output power on the distance between BTS and MS is presented by the quadratic function, i.e.:

$$w = a \cdot d^2 \quad (4)$$

For independent random variable, the distance BTS-MS, d , we can define CDF $F_D(x)$ as expressed by (3). The output power of one busy channel, w , as the function of random variable d , has the CDF $F_W(y)$, according to [13, section 5.3, equation (5.9)]:

$$\begin{aligned} F_W(y) &= 0, & y &\leq 0 \\ F_W(y) &= P\{w \leq y\} = P\left\{-\sqrt{\frac{y}{a}} \leq d \leq \sqrt{\frac{y}{a}}\right\} = \\ &= P\left\{0 \leq d \leq \sqrt{\frac{y}{a}}\right\} = F_D\left(\sqrt{\frac{y}{a}}\right) = \frac{y}{a \cdot R^2}, & 0 \leq y &\leq w_{\max} \\ F_W(y) &= 1, & w_{\max} &\leq y \end{aligned} \quad (5)$$

because it is always $d > 0$.

Let us suppose that for the considered cell we have $R=10$ km and $w_{\max} = g(R)=40$ W, (class 4). The CDF of the probability of output power w and ω for one active channel are obtained by calculation and simulation and presented in Fig. 4.

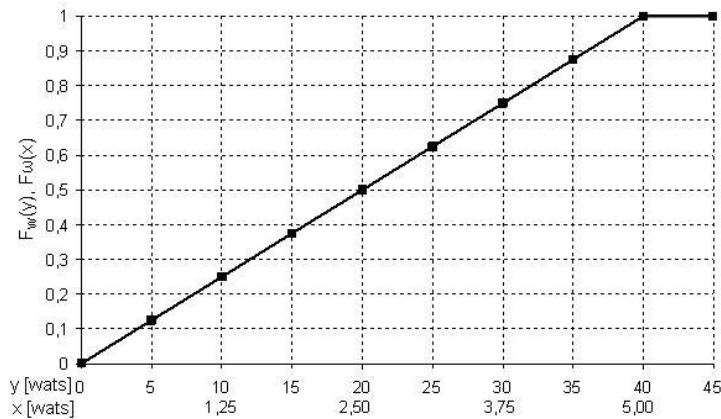


Figure 4

CDF of the probabilities of w and ω for one active channel

From Fig. 4 and equation (5) can be concluded that mean output power of one active channel is $w_m = 0.5 \cdot w_{\max}$.

The mean output power of one BTS, W_{Bm} , is the sum of mean powers of all active traffic channels in all states. This sum depends on mean output power of one active channel and on traffic, i.e. on the number of active channels. It is the sum of probabilities that j ($j=1,2,\dots,N_t$) channels are occupied, according to truncated Poisson distribution, [14], that holds for Erlang group, $ERL(j,A,N_t)$, multiplied by $j \cdot \omega_m$ i. e. by the mean output power of these j channels:

$$W_{Bm} = \sum_{j=1}^{N_t} j \cdot \omega_m \cdot ERL(j, A, N_t) \quad (6)$$

where $\omega_m = w_{mT}/8$. It is obvious that the value of mean power of BTS depends on traffic, and that it can be in the range $0 \leq W_{Bm} \leq N_t \cdot w_{mT}/8$.

From telephone traffic theory it is known that the equation

$$\sum_{j=1}^{N_t} j \cdot ERL(j, A, N_t) = Y = (1 - B) \cdot A \quad (7)$$

presents the value of served traffic in Erlang model, [14]. That's why the mean output power of one BTS is $W_{Bm} = \omega_m \cdot (1 - B) \cdot A$.

Fig. 5 presents mean output power of one BTS as the function of the value of offered traffic for the values: $N_t=14$, $N_t=22$ and $N_t=30$. These values are obtained by the calculation and by simulation. In the simulation the number of connections per channel was at least 1000. In all cases of simulation from Fig. 4 and Fig. 5 differences between the values obtained by the calculation and simulation are negligible.

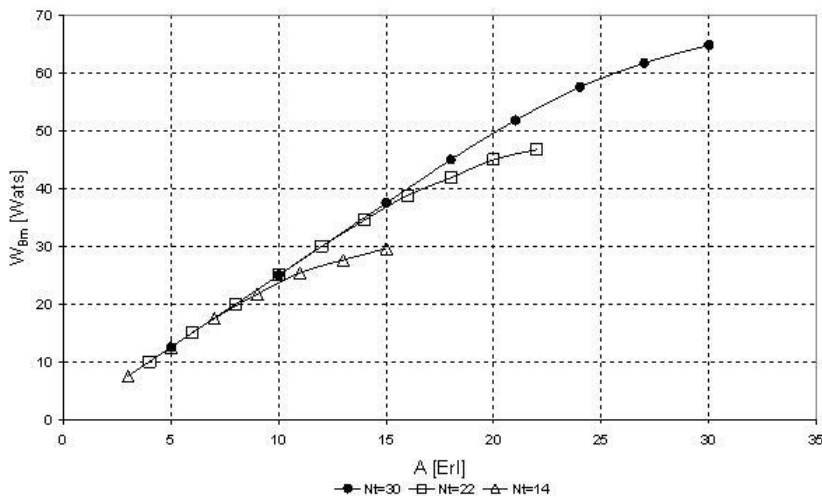


Figure 5

Mean output power of one BTS in the function of traffic, $N_t = 14, 22$ and 30 channels

Figs. 6a) and 6b) present CDF of output power of one BTS, $F_{WB}(w)$, which is obtained by simulation with $R=10$ km, $w_{max} = g(R)=40$ W. The system is simulated for the group of 14 channels, and for two values of offered traffic: $A=5$ Erl (low traffic) and $A=13$ Erl (heavy traffic). The call loss in the first case is negligible ($B=0.05\%$), and in the second case the traffic load is great and it causes great call loss ($B=15\%$).

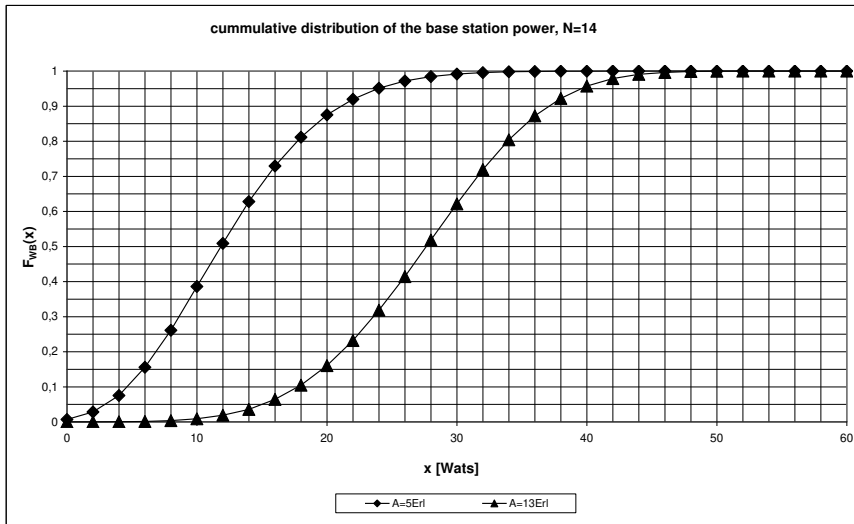


Figure 6a)

CDF of output power for one BTS with $N_c=14$ channels, $A=5$ Erl and $A=13$ Erl

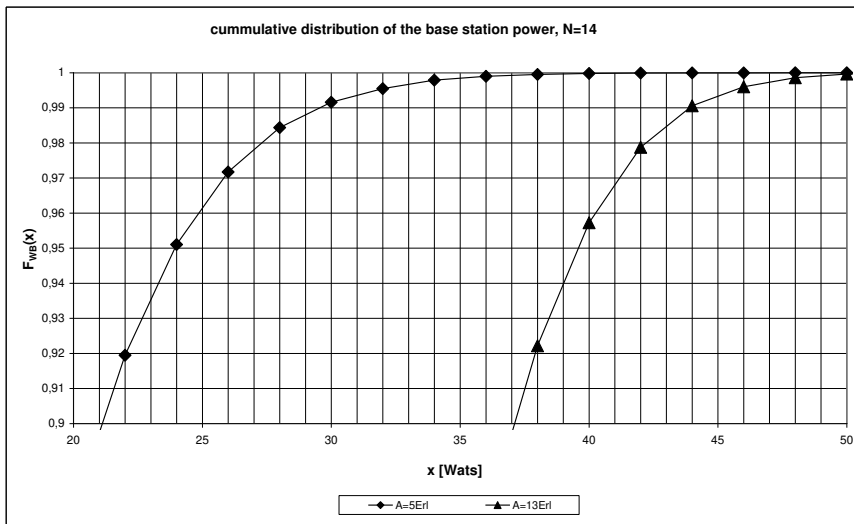


Figure 6b)

CDF of output power for one BTS with $N_c=14$ channels, $A=5$ Erl and $A=13$ Erl (detailed)

Figs. 7a) and 7b) present CDF of output power of one BTS, $F_{WB}(w)$, in the similar GSM cell as in Figs. 6, but for $N_f=22$ channels. In this case the low traffic (which causes traffic loss $B=0.05\%$) is 10.2 Erl, and heavy traffic 21.9 Erl ($B=15\%$).

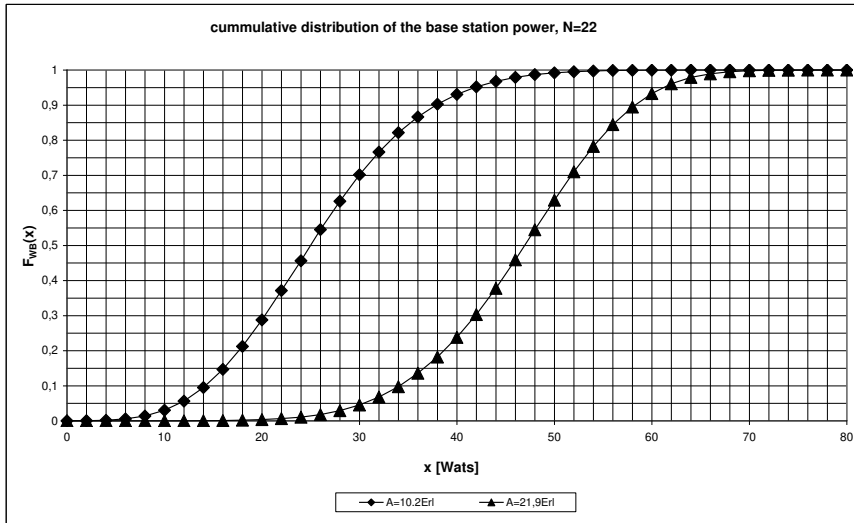


Figure 7a)

CDF of output power for one BTS with $N_f=22$ channels, $A=10.2$ Erl and $A=21.9$ Erl

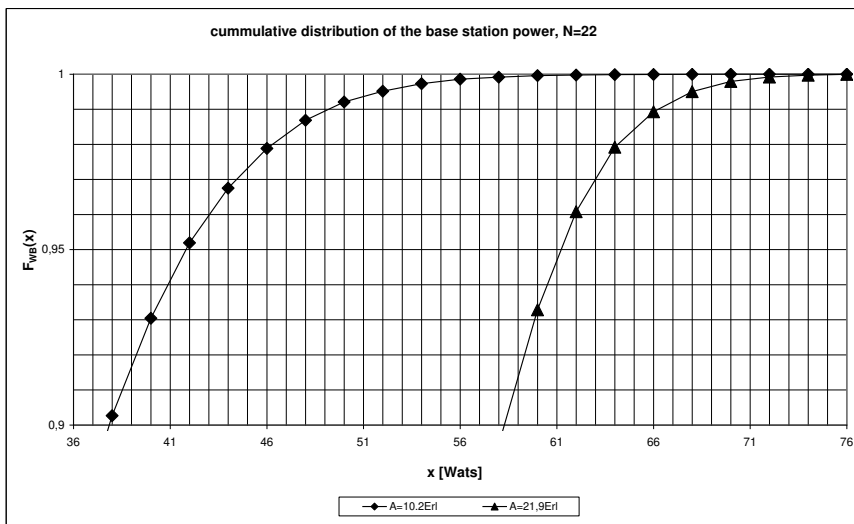


Figure 7b)

CDF of output power for one BTS with $N_f=22$ channels, $A=10.2$ Erl and $A=21.9$ Erl (detailed)

Figs. 8a) and 8b) present CDF of output power of one BTS, $F_{WB}(w)$, in the case when $N_f=30$. In this case the low traffic (which causes traffic loss $B=0.05\%$) is 15.9 Erl, and heavy traffic 21.9 Erl ($B=15\%$).

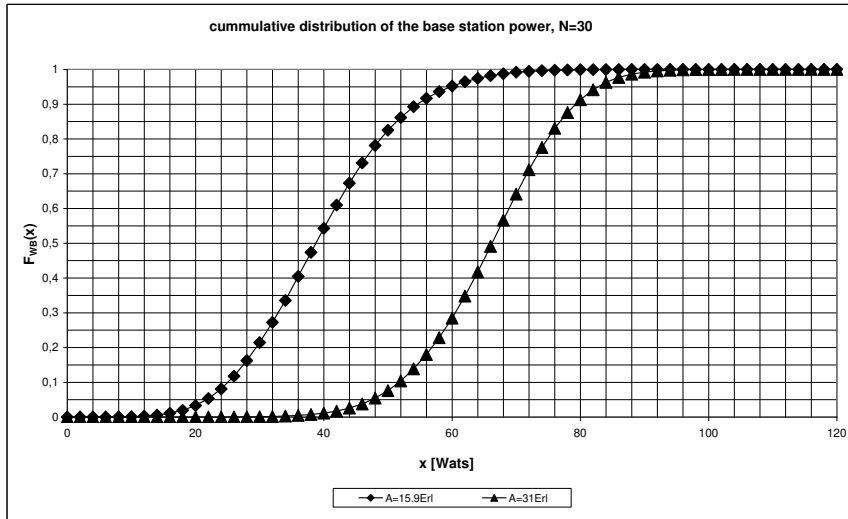


Figure 8a)

CDF of output power for one BTS with $N_f=30$ channels, $A=15.9$ Erl and $A=31$ Erl

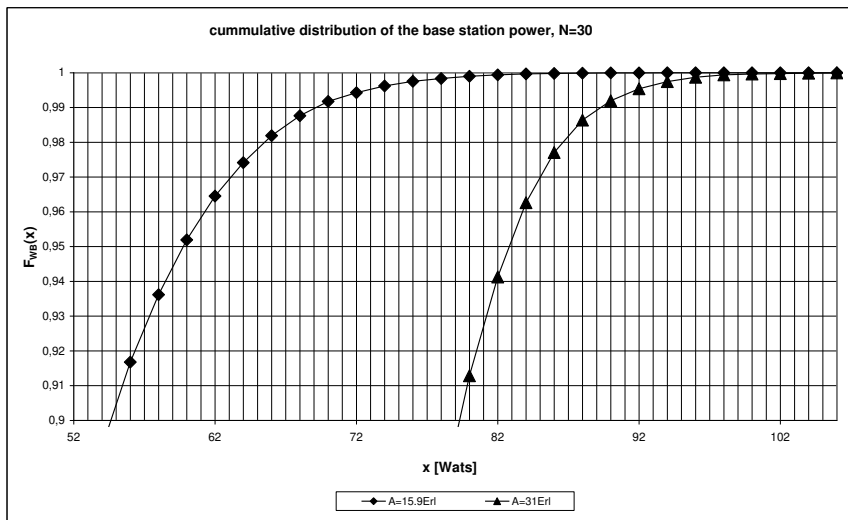


Figure 8b)

CDF of output power for one BTS with $N_f=30$ channels, $A=15.9$ Erl and $A=31$ Erl (detailed)

From the detailed Figs. 6b), 7b) and 8b) we can conclude how much power is necessary to satisfy 95% connections. So, from the detailed Fig. 6b), presented for 14 channels, it can be seen that, in the case of smaller offered traffic (5 Erl), the mean power of 24 W is satisfactory for 95% of connections, while in the case of greater traffic (13 Erl) it is necessary to provide 39.6 W for the same goal. From Fig. 7b) it follows that, for 22 channels, the power of 42 W satisfies 95% of connections in the case of smaller offered traffic (10.2 Erl), and 61 W is necessary for greater offered traffic (21.9 Erl). The corresponding values for 30 channels, from Fig. 8b), are 60 W for smaller offered traffic (15.9 Erl) and 83 W for greater offered traffic (31 Erl).

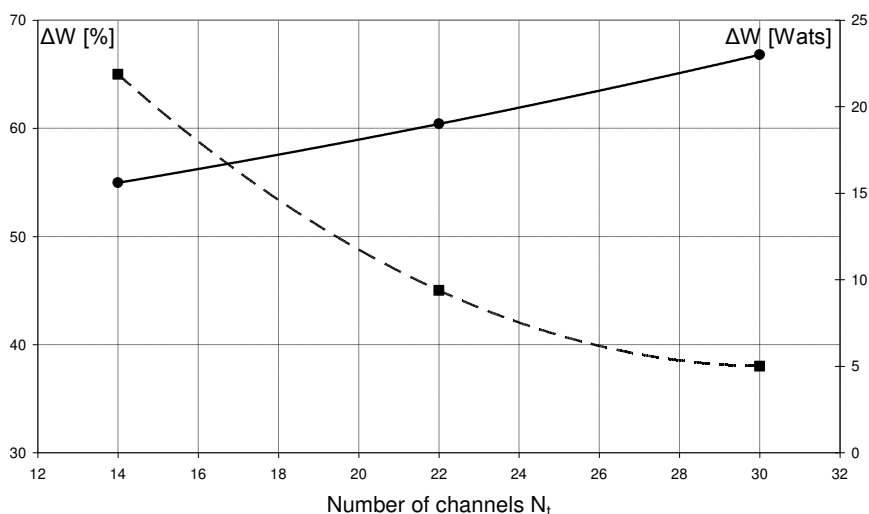


Figure 9

Difference of necessary power for 95% of connections in the case of small and great traffic as the function of the number of traffic channels

Fig. 9 presents the dependence of difference of necessary power (ΔW) for 95% of connections in the case of great and small traffic from the number of channels. The difference is presented as the absolute value (ΔW [Watts]) and as the relative value (ΔW [%]). The relative value of the difference is calculated in relation to the smaller traffic.

Remark: the method of simulation is verified comparing the results obtained by simulation with the results of measurements presented in [15]. Unfortunately, the results of measurements from [15] are for a network without power control. That's why this model is a very simple case.

Conclusion

The program for the simulation of telephone traffic can be upgraded in order to estimate the output power of one BTS in GSM. The program takes into account all

components, which can have influence on the output power in real situation: the number of traffic (TCH) channels, offered traffic, the distribution of surface users' density in the cell, the influence of intra-cell connections, the influence of half-rate connections, the influence of a limited number of traffic sources, and the environmental influence on signal attenuation. The program can be used to estimate the mean output power of one BTS and the CDF of the probability of output power. The calculation of CDF of total output power of one BTS can be very complex, because it requires the calculation of the probability density function for the sum of random values for each channel's power (convolution). That's why this simulation method is very important, especially in the case when the dependence of output power on the distance between MS and BTS is expressed by a complicated function. The main condition enabling the implementation of this simulation, is that the distribution function of the distance between MS and BTS. If CDF of the distance between MS and BTS is a complicated function, its inverse function can be obtained by mathematical programs, as MATLAB or MATHEMATICA.

The other important implementation of the simulation is to determine the BTS output power for very complex models, where it is difficult to obtain the results by calculation. These are the models with intra-cell traffic, the Engset model, models with complex distribution of users' density in the cell, and models with a different environmental influence on signal attenuation.

The credibility of the results of this paper's simulations are supported by comparison of its results to direct calculations.

References

- [1] Niu, Z.: Advances in Green Communications and Networks, VTC2012-Spring
- [2] Choi, J.: Green Radio, Approaches and Performance Analysis, (2012): <http://ccit.kaist.ac.kr/Lecture%20Notes/Green%20Radio%202.pdf>, August 2012
- [3] Heine, G.: GSM Networks: Protocols, Terminology and Implementation, Artech House, 1999
- [4] Jovanović, P., Šuh, T., Lebl, A., Mitić, D., Markov, Ž.: Influence of Intra-cell Connections on the Traffic Calculation of Radio Resources in Mobile Network, *Frequenz*, Vol. 67, Issue 9-10, September 2013, pp. 315-320
- [5] Winands, E. M. M., Wieland, J., Sanders, B.: Dynamic Half-Rate Connections in GSM, *AEU*, Vol. 60, Issue 7, July 2006, pp. 504-512
- [6] Šuh, T., Jovanović, P., Lebl, A., Mitić, D., Markov, Ž.: Comparison of the Influence of Intra-Cell Traffic and Finite Number of Mobile Phones on the Determination of Number of Channels in the BTS of GSM Network, *Frequenz*, Vol. 68, Issue 3-4, March 2014, pp. 171-176

- [7] Eberspächer, J., Vögel, H.-J. and Bettstetter, Ch.: GSM, Switching, Services and Protocols, John Wiley & Sons, 1999
- [8] Olsson, K. M.: Simulation on Computers. A Method for Determining the Traffic-Carrying Capacities of Telephone Systems, TELE, Vol. XXII, No. 1, 1970
- [9] Kosten, L.: Simulation in Teletraffic Theory, 6th ITC, Munich, 1970
- [10] Rodrigues, A. and de los Mozos, J. R.: Roulette Model for the Simulation of Delay-Loss Systems, ITT Electrical Communication, Vol. 47, No. 2, 1972
- [11] Jeruchim, M. C., Balaban, Ph. and Shanmugan, K. S.: Communication Systems, Modeling, Methodology and Techniques, Kluwer Academic Publishers, second edition, section 7.2.2., 2002
- [12] Akimaru, H., Kawashima, K.: Teletraffic, Theory and Application, Springer, section 7.3.3., 1992
- [13] Papoulis, A.: Probability, Random Variables, and Stochastic Processes, McGraw-Hill, 1965
- [14] Iversen, W. B.: DTU Course 34340, Teletraffic Engineering and Network Planning, Technical University of Denmark, 2011
- [15] Colombi, D., Thors, B., Persson, T., Wiren, N., Larsson, L. E., Jonsson, M., Tomevik, C.: Downlink Power Distribution for 2G and 3G Mobile Communication Networks, Radiation Protection Dosimetry, Vol. 157, No. 4, March 2013, pp. 477-487

Nonlinear Modeling of a Switched Reluctance Motor using LSSVM - ABC

Jebarani Evangeline Stephen¹, Selvaraj Suresh Kumar², Jayaraj Jayakumar³

¹ Department of Electrical and Electronics Engineering, Karunya University, Karunya Nagar, Coimbatore 641 114, Tamil Nadu, India; jeba_eva@karunya.edu

² Department of Electronics and Communication Engineering, Dr. N. G. P Institute of Technology, Dr. N. G. P Nagar, Kalapatti Road, Coimbatore 641 048, Tamil Nadu, India; hod_ece@drngpit.ac.in

³ Department of Electrical and Electronics Engineering, Karunya University, Karunya Nagar, Coimbatore 641 114, Tamil Nadu, India; jayakumar@karunya.edu

Abstract: To enhance the performance of a Switched Reluctance Motor (SRM), it is essential to build a precise model of the machine. Due to its double salient structure, the model is nonlinear. It is complicated to develop a simple mathematical model for such nonlinear systems. However, owing to the advancements in kernel based learning methods for statistical learning and structural risk minimization, the use of Least Square Support Vector Machine (LSSVM) for function estimation is powerful and accurate, with less computations needed. The accuracy of the regression model and generalization ability depends upon the proper selection of hyperparameters of LSSVM. It is necessary to employ a meta-heuristic technique for the optimal values of hyperparameters. This paper presents a nonlinear flux modeling of SRM based on LSSVM regression optimized by Artificial Bee Colony (ABC) algorithm. The training and testing sample data are obtained by 2D FEA using MagNET software. It was analyzed that the tuning by ABC algorithms offers a high degree of accuracy when compared to the values obtained by Particle Swarm Optimization (PSO), Differential Evolution (DE) and Genetic Algorithm (GA).

Keywords: Switched Reluctance Motor; Magnetic Characteristics; Modeling; Least Square Support Vector Machine regression; Artificial Bee Colony Algorithm

1 Introduction

Switched Reluctance Motors are a smart alternative to the conventional induction motors and to the variable speed motor drive applications because of its high efficiency, low cost, rugged structure, fault tolerant capability and wide range of speed operations. Due to its doubly salient structure and magnetic saturation, its

flux linkage characteristics and torque characteristics are highly nonlinear and dependent on the rotor position and phase current [1]. It is difficult to model the SRM with accuracy due to its nonlinearity. To accurately model the SRM, there are three methods:

- 1) Analytical modeling
- 2) Finite-Element Analysis (FEA) method
- 3) Direct or Indirect measurement techniques.

The mathematical expression for flux linkage was developed using (i) the geometrical data of the machine [2-4] (ii) the magnetic equivalent circuit [5-6] and (iii) data from the FEA method [7-11]. A simple and traditional look up table approach is used to calculate the flux and torque values. The intermediate values of current and rotor position could be obtained using interpolation [12-17]. As the above method is time consuming and involves intensive computation, there is a possibility for tradeoff in accuracy. The nonlinear model of SRM was also developed with the traditional neural network (NNs) such as Back Propagation, Radial Basis Function, Polynomial Neural Network, Pi-Sigma Neural Network, etc. [18-22] Regardless of its advancement, the neural network model suffers from the local minima solution, possibility of over fitting and dependency on quality and quantity of data.

In order to overcome the drawbacks of artificial neural networks, Support Vector Machine (SVM) was proposed. Like ANNs, SVM also can be used to solve both classification and regression problems. An SVM is a classifier derived from the statistical learning theory and was first introduced by Vapnik. In regression problems, a non-linear function is learned by a linear learning machine in a kernel induced feature space, while the capacity of the system is controlled by a parameter that does not depend on the dimensionality of the space [23]. The process of employing SVMs in regression problems is referred to as Support Vector Regression (SVR). The SVM has the capacity to prevent over fitting by the generalization theory. It can be formulated as a quadratic programming problem with linear inequality constraints. The Least Squares Support Vector Machine (LSSVM) is a least square version of SVM which considers the inequalities for classical SVM. As a result, the solution of LSSVM follows directly from solving a system of linear equations instead of quadratic programming, which makes LSSVM faster than SVM with reduced computational time [24-27]. LSSVM could also be used for classification and regression [23]. However, the accuracy of the regression model using LSSVM relies on the values of the hyper-parameters used. In the past, several reports were available for LSSVM based forecasting model, which is used in wide range of applications [29-34]. In this paper, the flux characteristics of the SRM are forecasted and the hyper-parameters are optimized using optimization techniques like Genetic Algorithm (GA), Particle Swarm Optimization (PSO) [35-37].

A four phase, 500W, 8/6 SRM was used for the present study. The static characteristics of the machine were analyzed using a 2-D finite element method with MagNET software. In this paper, the nonlinear modeling of the Switched Reluctance Motor characteristics based on the LSSVM - ABC has been studied. The hyper-parameters of the model were optimally selected using Artificial Bee Colony (ABC). The paper has been organized as follows: the mathematical model of SRM is briefed in section II. In section III, the basics of LSSVM and Artificial Bee Colony algorithm are discussed. In Section IV, the implementation of forecasted model using LSSVM – ABC is discussed. The results of the parameter optimization are given in section V.

2 Mathematical Model of SRM

The SRM is doubly salient with an unequal number of rotor and stator poles. Torque is produced by the tendency of the rotor poles to align with poles of the excited stator phase and is independent of the direction of the phase current. The mathematical model of the SRM for flux and torque is very difficult to calculate due to its nonlinearity [1]. When neglecting the mutual inductance between the winding, the voltage equation for each phase is written as:

$$v = Ri + \frac{d\psi}{dt} \quad (1)$$

where v is the voltage applied across the phase winding, Ri is the voltage drop due to winding resistance and ψ is the total flux-linkage of the coil. If the saturation effect is neglected, the relation between flux (ψ) and current (i) is defined as follows:

$$\psi = L(\theta, i)i \quad (2)$$

Where $L(\theta, i)$ is the phase inductance of the winding. Due to the double saliency of the machine, the inductance varies with the rotor position θ and current i .

The general expression for the torque produced by one phase at any given rotor position θ is:

$$T_{ph}(\theta, i) = \left(\frac{\partial W(\theta, i)}{\partial \theta} \right)_{i=constant} \quad (3)$$

Where w is the co-energy. Co-energy can be calculated as:

$$W(\theta, i) = \left(\int_0^i \psi(\theta, i) di \right)_{\theta=constant} \quad (4)$$

Total instantaneous torque is given by the sum of the individual phase torques.

$$T_e(\theta, i) = \sum_{i=1}^{N_{ph}} T_{ph}(\theta, i) \quad (5)$$

Where N_{ph} is the number of phases in the machine. The electromagnetic dynamic model of the motor and the load are expressed as shown in (6)

$$T_e - T_l = J \frac{d^2\theta}{dt} + B \frac{d\theta}{dt} \quad (6)$$

where T_l is the load torque, J is the moment of inertia of rotating masses and B is the viscous friction coefficient. The load torque is a function of the angular speed, depending on the type of load.

3 Methodology

3.1 Least Square Support Vector Machine for Regression

A Russian scientist Vladimir N. Vapnik introduced the Support Vector Machine (SVM) based on the Statistical Learning Theory (SLT) and the Structural Risk Minimization principle. In SVM, the solutions are obtained by solving the set of nonlinear equations using Quadratic Programming (QP) and thereby avoiding the local minima. Suykens proposed a modified version of SVM known as Least Square Support Vector Machine (LSSVM) which transforms the quadratic optimization problem into a set of linear constraints. This can be specifically described as follows [24].

Consider the given set of training data (D)

$$D = \{(x_k, y_k) | k = 1, 2, \dots, N\} \quad (7)$$

Where N is the number of training data pairs, $x_k \in R^n$ is the regression vector and $y_k \in R$ is the output. The regression model is formulated by a nonlinear mapping function $\varphi(\cdot)$ which maps the input data to a higher dimensional feature space.

$$y = \omega^T \varphi(x) + b \quad (8)$$

Where ω and b are the weight vector and bias respectively. The LSSVM can be used as both a classifier and function estimation. When it is used for function estimation, the quadratic loss function is taken as the cost function for optimization. The standardized cost function of LSSVM is

$$\min J(\omega, e) = \frac{1}{2} \omega^T \omega + \frac{1}{2} \gamma \sum_{k=1}^N e_k^2 \quad (9)$$

subject to the constraint

$$y_k = \omega^T \varphi(x_k) + b + e_k, k = 1, 2, \dots, N \quad (10)$$

Where e_k is the desired error and γ is regularization parameter, which equates the model's complexity and training error. A lagrangian is formulated to solve the above constrained optimization problem.

$$L(\omega, b, e, \alpha) = J(\omega, e) - \sum_{k=1}^N \alpha_k \{\omega^T \varphi(x) + b + e_k - y_k\} \quad (11)$$

Where α_k is the lagrange multiplier and it is otherwise known as support value. The above equation can be solved by partially differentiating with respect to each variable and when equated to zero. With the removal of ω and e , the Karush – Kuhn – Trucker (KKT) system is obtained as:

$$\begin{bmatrix} 0 & 1 \\ 1^T & z + \gamma^{-1}I \end{bmatrix} \begin{bmatrix} b \\ \alpha \end{bmatrix} = \begin{bmatrix} 0 \\ y \end{bmatrix} \quad (12)$$

with

$$y = [y_1, \dots, y_N]$$

$$1 = [1_1, \dots, 1_N]^T$$

$$0 = [0, \dots, 0]$$

$$\alpha = [\alpha_1, \dots, \alpha_N]$$

$$Z = \{Z_{kj} | k = 1, \dots, N\}, Z_{kj} = \varphi(x_k)^T \varphi(x_j) = K(x_k, x_j), j = 1, \dots, N$$

Where $K(x_k, x_j)$ is the kernel function and must satisfy Mercer's condition. The commonly used kernel functions are linear, polynomial, radial basis function (RBF) kernel and multi-layer perceptron (MLP). In this paper, RBF kernel is used.

$$K(x, x_k) = \exp\left(-\frac{\|x - x_k\|^2}{2\sigma^2}\right) \quad (13)$$

In the above equation, σ is the kernel or bandwidth parameter.

The LSSVM regression function can be defined as:

$$y(x) = \sum_{k=1}^N \alpha_k K(x, x_k) + b \quad (14)$$

The performance of the LS-SVM depends on a value of regularization parameter and the kernel parameters. These parameters determine the accuracy and generalization ability of LS-SVM model. Therefore, it is essential to optimize these parameters [28].

3.2 Artificial Bee Colony (ABC) for Parameter Optimization of LSSVM Model

To obtain the optimal hyper-parameters for LSSVM, the Artificial Bee Colony Algorithm (ABC) proposed by Karaboga is used [38-41]. It is a swarm based meta-heuristic algorithm used for numerical optimization. The method of the ABC algorithm imitates the foraging behavior of a honey bee swarm. In the bee colony,

certain tasks are performed by specialized individuals. The principal task of the specialized bees is to identify the best food source which gives the maximum nectar amount in a self organized manner. The ABC model consists of three essential groups of bees: employed bees, onlooker bees and scout bees. The size of a colony depends on the number of employed bees and onlooker bees. The number of food sources/nectar sources equals half of the colony size. The aim of the whole colony is to maximize the nectar amount. Employed bees search for the food sources (solution) and each solution is a D-dimensional vector where D refers to the number of optimization parameters. The nectars' amount (fitness value) is computed. The information obtained is shared with the onlooker bees which are waiting in the hive (dance area). The onlooker bees exploit a nectar source based on the information shared by the employed bees. The onlooker bees also determine the source to be abandoned and allocate its employed bee as scout bees. The task of the scout bees is to find the new valuable food sources. They search the space near the hive randomly.

The steps of the ABC algorithm are as follows:

1. Initialization Phase
2. Employed Bees Phase
3. Onlooker Bees Phase
4. Scout Bees Phase
5. Memorize the best solution achieved so far
6. **until** (cycle = maximum cycle number) proceed step2 else stop

Initialization Phase: The D-dimensional vector of the population of food sources are initialized ($m = 1 \dots SN$, SN: Colony size) by scout bees and control parameters are set. Since each food source is a solution to the optimization problem, each vector holds n variables ($n = 1 \dots D$, D: no of parameters to be optimized) which are to be optimized so as to minimize the objective function.

$$x_{mn} = l_n + rand(0,1) * (u_n - l_n) \quad (15)$$

Where l_n and u_n are the lower and upper bound of the parameter x_{mn} respectively.

Employed Bees Phase: Employed bees search for new food source (\vec{V}_m) having higher nectar amount within the neighborhood of the food source (\vec{x}_m) in their memory. The neighbor food source (\vec{V}_m) can be determined using the formula:

$$V_{mn} = x_{mn} + \varphi_{mn}(x_{mn} - x_{kn}) \quad (16)$$

Where k and n are the randomly selected index for new solution and φ_{mn} is a random number within the range [-1, 1]. Once the new solution is obtained, the fitness is calculated and the best solution is selected based on greedy selection method. The fitness value of the solution fit_m is calculated using the formula

$$fit_m = \left\{ \begin{array}{ll} \frac{1}{1+fit_m(\vec{x}_m)} & \text{if } fit_m(\vec{x}_m) \geq 0 \\ 1 + abs(fit_m(\vec{x}_m)) & \text{if } fit_m(\vec{x}_m) < 0 \end{array} \right\} \quad (17)$$

Where $fit_m(\vec{x}_m)$ is the objective function value of solution \vec{x}_m .

Onlooker Bees Phase: Employed bees share their food source information with onlooker bees waiting in the hive and then onlooker bees probabilistically choose their food sources depending on the information. The onlooker bee exploits a food source based on the probability of fitness. The probability of fitness can be calculated by using the formula:

$$p_m = \frac{fit_m}{\sum_{m=1}^{SN} fit_m} \quad (18)$$

Once a food source for an onlooker bee is chosen, a neighborhood is determined and its fitness value is computed and best solution is selected based on greedy selection methods.

Scout Bees Phase: Scout bees randomly choose their food sources. Employed bees whose solutions cannot be improved become scout bees and their solutions are abandoned. Then, the converted scouts start to search for new solution.

4 Experiment

4.1 Measurement of Flux Linkage

In nonlinear characteristics of the SRM, the value of flux and torque varies with the rotor position and phase current. Therefore, the knowledge about the values of flux and torque is essential for better control of the motor. Therefore, the flux and torque profiles of the machine can either be obtained using numerical computation or experimentally. Finite Element Analysis (FEA) is a powerful technique for obtaining the numerical solutions to the considered machine structure. The FEA can be conveniently used to obtain the magnetic vector potential values throughout the motor in the presence of complex magnetic circuit geometry and nonlinear properties of magnetic materials. This vector potential value A determines the magnetic field inside the motor using the Poisson's equation.

$$\frac{\partial}{\partial x} \left(\gamma \frac{\partial A}{\partial x} \right) + \frac{\partial}{\partial y} \left(\gamma \frac{\partial A}{\partial y} \right) = -J \quad (19)$$

Where γ is the magnetic reluctivity and J is the current density vector. A 2D static field analysis was been carried out using a FEA based CAD package called MagNET. Since the number of rotor poles are six, the magnetic circuit becomes the same every 60° when only one phase is excited. The unaligned and aligned condition of stator and rotor poles occurs at every 30° interval. For the machine

considered, the aligned condition of the rotor occurs at 60° whereas, it is in unaligned position at 31° . At a rotor position θ , the co-energy, torque and the flux linkage in the excited phase are noted down for different values of winding current.

4.2 Data Preparation

The specification of the four phase 8/6 SRM is given in Table 1. Since all the phases of the machine are identical to each other, it is sufficient to consider the data of one phase for analysis. For training data set of flux linkage characteristics, the rotor position θ and current i ranges from $[0-5A]$ and $[31^\circ- 60^\circ]$ respectively. For testing data set, the rotor position θ and current i with an interval of 3° and $0.5A$ were considered for the analysis of the proposed model. To improve the accuracy of prediction model, input for training and testing data set, are normalized by Min-Max normalization procedure. In the Min-Max normalization, a linear transformation is performed on the original data values and values are mapped in the new interval $[new_maxA, new_minA]$ using the formula (20).

$$v' = \frac{v-minA}{maxA-minA}(new_maxA - new_minA) + new_minA \quad (20)$$

450 pair of samples were chosen for the training set and 154 pair of samples were considered for testing.

Table 1
Specification of the SRM

Parameter	Value
Rated Output Power	500 [W]
Coil Voltage	150 [V]
Rated Current	3 [A]
Rated Speed	4000 [rpm]
Rated torque	4.5 [Nm]
Number of stator poles	8
Number of rotor poles	6

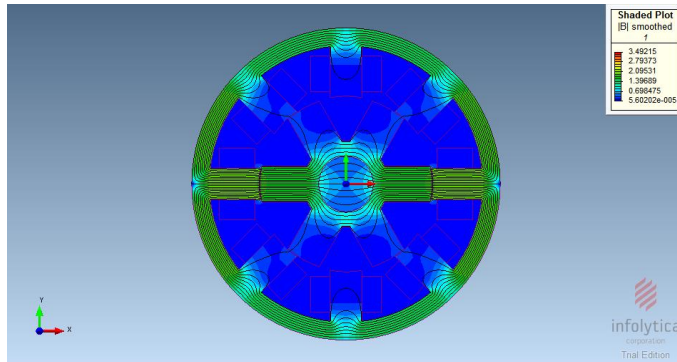


Figure 1
Field distribution of SRM

4.3 Parameter Tuning

In LSSVM regression, only two parameters have to be tuned (i.e. kernel parameter σ and regularization parameter γ). The model performance and generalization ability depends upon these parameters. These parameters cannot be tuned separately. The main idea is to find the optimal parameter values with minimum prediction error. The prediction error can be calculated using leave-one-out cross validation on the training set. The optimization ranges for these parameters are defined arbitrarily. The following optimization algorithms have been used for tuning the parameters: Genetic Algorithm (GA), Particle Swarm Optimization (PSO), Differential Evolution (DE) and Artificial Bee Colony (ABC).

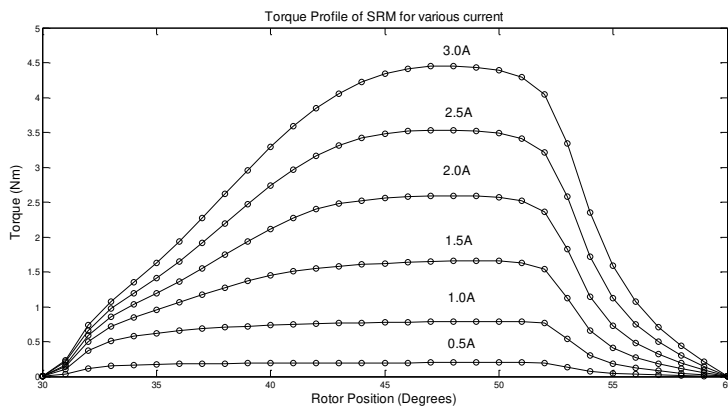


Figure 2
Torque Profile of SRM for various current

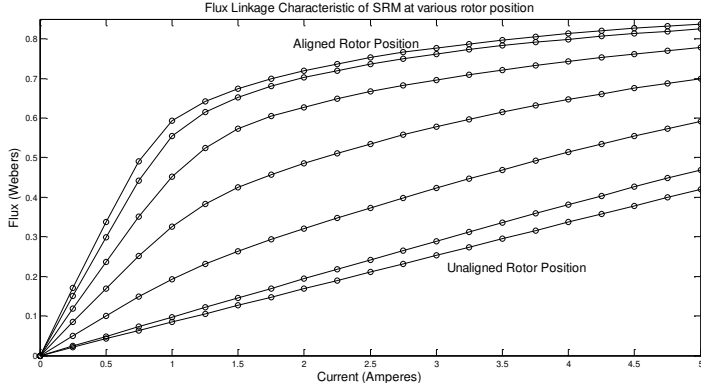


Figure 3

Flux linkage characteristics of SRM

4.4 Performance Evaluation

To obtain the perfect fit of the proposed regression model, the Mean Absolute Percentage Error (MAPE) is used as the objective function for the optimization process. i.e., MAPE is used as main performance indicator. In addition, normalized mean square error (NMSE) is also used to evaluate the prediction error during the cross validation.

$$\text{MAPE} = \frac{1}{n} \left[\sum_{i=1}^n \left| \frac{y_t - \hat{y}_t}{y_t} \right| \right] \quad (21)$$

$$\text{NMSE} = \left(\frac{\sum_{i=1}^n (y_t - \hat{y}_t)^2}{\sum_{i=1}^n (y_t - \bar{y}_t)^2} \right) \quad (22)$$

Where y_t and \hat{y}_t is the actual value and forecasted values respectively, \bar{y}_t is the average of actual data and n is the number of data. For a good fit, the value of MAPE and NMSE should be closer to zero.

5 Result

The proposed algorithm was implemented using MATLAB R2010a and the relevant codes were developed and processed on a 3.0 GHz Intel Pentium IV PC with 2.0 GB RAM under the Windows XP environment. In order to verify the efficiency of the proposed regression model, the results were compared with other prediction models such as LSSVM, LSSVM-GA, LSSVM-PSO and LSSVM-DE. The hyper parameters of the LSSVM are well tuned using the ABC algorithm. The minimal fitness value (shown in Figure 4) was achieved after 11 iterations with the value of $C=3545.88$ and $\sigma^2=0.04512$ with a mean absolute error of 0.066% and mean relative error of $0.379 \times 10^{-3}\%$.

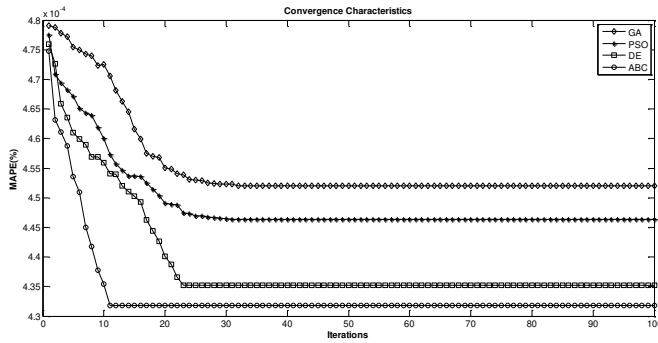


Figure 4
Convergence Characteristics

Table 2 (a)
Comparison of optimized parameters and its performance indicators

Model	Method	C	σ^2	MAPE	NMSE
Flux Linkage	LSSVM	3173.08	0.05890	5.310×10^{-4}	2.337×10^{-5}
	LSSVM - GA	3384.71	0.04835	4.521×10^{-4}	1.885×10^{-5}
	LSSVM - PSO	3534.92	0.04796	4.463×10^{-4}	1.857×10^{-5}
	LSSVM - DE	3539.63	0.04591	4.352×10^{-4}	1.774×10^{-5}
	LSSVM - ABC	3545.88	0.04512	4.318×10^{-4}	1.741×10^{-5}

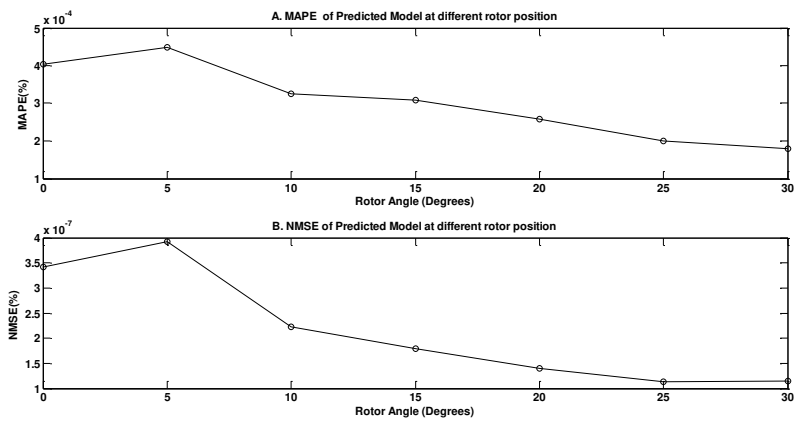


Figure 5
(a). MAPE (%) of predicted output at different rotor position (b). NMSE of predicted output at different rotor position

Table 2 (b)
Comparison of errors for the optimized parameters

Model	Method	C	σ^2	Average Absolute error (%)	Average Relative error (%)
Flux Linkage	LSSVM	3173.08	0.05890	0.082	0.656×10^{-3}
	LSSVM - GA	3384.71	0.04835	0.070	0.619×10^{-3}
	LSSVM - PSO	3534.92	0.04796	0.069	0.577×10^{-3}
	LSSVM - DE	3539.63	0.04591	0.067	0.493×10^{-3}
	LSSVM - ABC	3545.88	0.04512	0.066	0.379×10^{-3}

Due to the fine tuning of LSSVM parameters by LSSVM–ABC, it is observed from Table 2 that the value of MAPE is decreased to $4.318 \times 10^{-4}\%$ and NMSE is decreased to $1.741 \times 10^{-5}\%$. The MAPE absolute error at various rotor positions are shown in Figure 5(a) and the NMSE at rotor position is shown in Figure 5(b). As the value of mean absolute error is less with LSSVM-ABC, the proposed regression model gives a high degree of accuracy and the output is highly precise.

Conclusions

Apposite values for regularization parameters are essential to Least Squares Support Vector Machines (LS-SVM) which result in better learning and generalization abilities. This paper presents a novel parameter optimization method for LS-SVM based on an Artificial Bee Colony (ABC) algorithm. The LSSVM – ABC gives better forecast of flux values of the SRM at various rotor angles. Due to the ability for global search, ABC algorithm does not to consider LS-SVM dimensionality and complexity. The proposed method proves to be an effective approach for fitting the values with an improved statistical result.

Acknowledgement

The authors wholeheartedly thank the management of Karunya University (Karunya Institute of Technology & Sciences), Coimbatore for providing necessary facilities. The authors would like to acknowledge the support and guidance given by Mr. R. Karthikeyan, Associate Professor, Sri Venkateswara College of Engineering, Sriperumbadur, Chennai during the FEM analysis of SRM using MagNET.

References

- [1] T. J. E. Miller: Electronic Control of Switched Reluctance Machines, Newnes Power Engineering Series, Newnes Publishers, Oxford, 2001
- [2] S. A. Hossain, I. Husain: A Geometry Based Simplified Analytical Model of Switched Reluctance Machines for Real-Time Controller Implementation, IEEE Transactions on Power Electronics, Vol. 18, No. 6, 2003, pp. 1384-1389

-
- [3] V. Radun: Analytically Computing the Flux Linked by a Switched Reluctance Motor Phase When the Stator and Rotor Poles Overlap, IEEE Transactions on Magnetics, Vol. 36, No. 4, 2000, pp. 1996-2003
- [4] H. C. Lovatt: Analytical Model of a Switched-Reluctance Motor, IEE Proceedings on Electrical Power Applications, Vol. 152, No. 2, 2005, pp. 352-358
- [5] J. M. Kokernak, D. A. Torrey: Magnetic Circuit Model for the Mutually Coupled Switched Reluctance Machines, IEEE Transactions on Magnetics, Vol. 36, No. 2, 2000, pp. 500-507
- [6] M. A. Preston, J. P. Lyons: A Switched Reluctance Motor Model with Mutual Coupling and Multi-Phase Excitation, IEEE Transactions on Magnetics, Vol. 27, No. 6, 1991, pp. 5423-5425
- [7] C. Roux, M. M. Morcos: A Simple Model for Switched Reluctance Motors, IEEE Power Engineering Review, Vol. 20, No. 10, October 2000, pp. 49-52
- [8] I. A. Viorel, L. Strete, I. Husain: An Analytical Model of Switched Reluctance Motor Based on Magnetic Field Analysis Results, Proceedings of 3rd International Symposium on Electrical Engineering and Energy Converters, Suceava, Romania, 2009, pp. 97-100
- [9] C. Ong, M. Molloam: Predicting the Steady-State Performance of a Switched Reluctance Machine, Proceedings of Conference Record of the 1989 IEEE Industry Applications Society Annual Meeting, Vol. 1, 1989, pp. 529-537
- [10] E. Afjei, K. Navi, S. Ataei: A New Two Phase Configuration for Switched Reluctance Motor with High Starting Torque, Proceedings of 7th International Conference on Power Electronics and Drive Systems, PEDS '07, 2007, pp. 517-520
- [11] S. F. Ghousia, Narayan Kar: Performance Analysis of an 8/6 Switched Reluctance Machine using Finite-Element Method, Proceedings of IEEE Power Engineering Society General Meeting, 2007, pp. 1-7
- [12] B. Fahimi, G. Suresh, J. Mahdavi, M. Ehsami: A New Approach to Model Switched Reluctance Motor Drive Application to Dynamic Performance Prediction, Control and Design, Proceedings of 29th Annual IEEE Power Electronics Specialists Conference PESC-98, Fukuoka, Vol. 2, 1998, pp. 2097-2102
- [13] H. P. Chi, R. L. Lin, J. F. Chen: Simplified Flux Linkage Model for Switched Reluctance Motors, IEE Proceedings of Electrical Power Applications, Vol. 152, No. 3, 2005, pp. 577-583
- [14] J. M. Stephenson, J. Corda: Computation of Torque and Current in Doubly Salient Reluctance Motors from Nonlinear Magnetization Data, Proceedings of Institution of Electrical Engineers, Vol. 126, No. 5, 1979, pp. 393-396

- [15] D. W. J. Pulle: New Database for Switched Reluctance Drive Simulation, Proceeding of IEE proceedings B on Electric Power Applications, Vol. 138, No. 6, 1991, pp. 331-337
- [16] D. A. Torrey, J. H. Lang: Modeling a Nonlinear Variable Reluctance Motor Drive, Proceeding of IEE proceedings B on Electric Power Applications, Vol. 137, No. 5, 1997, pp. 314-326
- [17] P. Chanchaoensook, M. F. Rahman: Dynamic Modeling of a Four-phase 8/6 Switched Reluctance Motor using Current and Torque Look-up Tables, Proceeding of 28th Annual Conference of the Industrial Electronics Society, Vol. 1, 2002, pp. 491-496
- [18] C. Elmas, S. Sagiroglu, I. Colak, G. Bal: Modeling of a Nonlinear Switched Reluctance Drive based on Artificial Neural Networks, Proceedings on 5th International Conference on Power Electronics and Variable-Speed Drives, London, 1994, pp. 7-12
- [19] W. Z. Lu, A. Keyhani, A. Fardoun: Neural Network based Modeling and Parameter Identification of Switched Reluctance Motors, IEEE Transactions on Energy Conversion, Vol. 18, No. 2, 2003, pp. 284-290
- [20] T. Lachman, T. R. Mohamad, C. H. Fong: Nonlinear Modeling of Switched Reluctance Motors using Artificial Intelligence Techniques, IEE Proceedings on Electric Power Applications, Vol. 151, No. 1, 2004, pp. 53-60
- [21] Yan Cai, Qingxin Yang, Yanbin Wen, Lihua Su: Nonlinear Modeling and Simulating of Switched Reluctance Motor and its Drive, Proceedings of the 2nd International Conference on Computer and Automation Engineering (ICCAE), Singapore, Vol. 3, 2010, pp. 465-469
- [22] R. Vejian, N. C. Sahoo, R. Gobbi: Mathematical Modeling of Flux Linkage Characteristics of Switched Reluctance Motors using Polynomials Neural Networks, Proceedings of IEEE International Power and Energy Conference, Kuala Lumpur, 2006, pp. 378-382
- [23] V. Vapnik: The Nature of Statistical Learning Theory, Springer-Verlag, New York, 1995
- [24] J. A. K. Suykens, T. Van Gestel, J. De Brabanter, B. De Moor, J. Vandewalle: Least Squares Support Vector Machines, World Scientific, Singapore, 2002
- [25] J. Valyon, G. Horváth: Extended Least Squares LS-SVM, International Journal of Computational Intelligence, Vol. 3, 2007, pp. 234-242
- [26] L. Jun: Identification of Dynamic Systems using Support Vector Regression Neural Networks, Journal of Southeast University, Vol. 22, No. 2, 2006

- [27] Bahman Mehdizadeh, KamyarMovagharnejad: A Comparative Study Between LS-SVM Method and Semi Empirical Equations for Modeling the Solubility of Different Solutes in Supercritical Carbon dioxide, *Chemical Engineering Research and Design*, Vol. 89, No. 11, 2011, pp. 2420-2427
- [28] Xie, Chunli, Cheng Shao, Dandan Zhao: Parameters Optimization of Least Squares Support Vector Machines and its Application, *Journal of Computers*, Vol. 6, No. 9, 2011, pp. 1935-1941
- [29] P. Pingfeng, H. Weichiang: Forecasting Regional Electricity Load based on Recurrent Support Vector Machines with Genetic Algorithms, *Electric Power Systems Research*, Vol. 74, No. 3, 2005, pp. 417-425
- [30] Yuansheng Huang, Jiajia Deng: Short-term Load Forecasting with LS-SVM Based on Improved Ant Colony Algorithm Optimization, *Journal of Computational Information Systems*, Vol. 6, No. 5, 2010, pp. 1431-1438
- [31] ZurianiMustaffa, YuhaniYusof: A Hybridization of Enhanced Artificial Bee Colony-Least Squares Support Vector Machines for Price Forecasting, *Journal of Computer Science*, Vol. 8, No. 10, 2012, pp. 1680-1690
- [32] ZurianiMustaffa, YuhaniYusof: Optimizing LSSVM using ABC for Non-Volatile Financial Prediction, *Australian Journal of Basic and Applied Sciences*, Vol. 5, No. 11, 2011, pp. 549-556
- [33] L. Yu, H. Chen, S. Wang, K. K. Lai: Evolving Least Squares Support Vector Machines for Stock Market Trend Mining, *IEEE TransactionsonEvolutionary Computation*, Vol. 13, No. 1, 2009, pp. 87-102
- [34] Fazeli, Hossein, Reza Soleimani, Mohammad Ali Ahmadi, Ramin Badrnezhad, Amir H. Mohammadi: Experimental Study and Modeling of Ultrafiltration of Refinery Effluents, *Energy & Fuels*, Vol. 27, No. 6, 2013, pp. 3523-3537
- [35] S. Linyun, L. Hui, L. Zhen: Modeling of Switched Reluctance Motors based on LS-SVM, *Chinese Society for Electrical Engineering*, Vol. 27, No. 6, 2007, pp. 26-30
- [36] Wanfeng Shang, Shengdun Zhao, YajingShen: Application of LSSVM with AGA Optimizing Parameters to Nonlinear Modeling of SRM, *Proceeding of 3rd IEEE Conference on Industrial Electronics and Applications*, Singapore, 2008, pp. 775-780
- [37] Qianwen Xiang, Yukun Sun, Xiaofu Ji: Modeling Inductance for Bearingless Switched Reluctance Motor based on PSO-LSSVM, *Chinese Control and Decision Conference (CCDC)*, Mianyang, 2011, pp. 800-803
- [38] DervisKaraboga, B. Basturk: A Powerful and Efficient Algorithm for Numerical Function Optimization: Artificial Bee Colony (ABC) Algorithm, *Journal of Global Optimization*, Vol. 39, No. 3, 2007, pp. 459-471

- [39] Dervis Karaboga: Artificial Bee Colony Algorithm, Scholarpedia, 5(3):6915
- [40] Dervis Karaboga: A Comprehensive Survey: Artificial Bee Colony (ABC) Algorithm and Applications, Artificial Intelligence Review, March 2012
- [41] Dervis Karaboga, Bahriye Akay: A Comparative study of Artificial Bee Colony Algorithm, Applied Mathematics and Computation, Vol. 214, 2009, pp. 108-132

A New Approach for Designing Gear Profiles using Closed Complex Equations

Bálint Laczik¹, Peter Zentay², Richárd Horváth²

¹Department of Manufacturing Science and Technology, Budapest University of Technology and Economics, Egry József u. 1, H-1111 Budapest, Hungary, laczik@goliat.eik.bme.hu

²Óbuda University Donát Bánki Faculty of Mechanical and Safety Engineering, Népszínház u. 8, H-1081 Budapest, Hungary, zentay@actel.hu, horvath.richard@bgk.uni-obuda.hu

Abstract: The literature solely uses the homogeneous transformation matrix method for solving the problems of rotations and translations, for gear contact problems. In this paper a different approach is introduced, using complex algebra for designing the profiles of gear teeth. We intend to present the general theory and technique of designing the generating gear rack and the meshing counter profile of arbitrary profile gears. For the illustration of the practical use of his method we shall present the design steps of a gear, with a cosine profile, a general involute gear and the profile of the lobes of a Root blower pump. These examples will properly illustrate the applicability of the presented design process.

Keywords: gear profile; meshing theory; envelope; complex function

1 Introduction

One of the important machine elements, from the beginning of the technical era, is the gear. It has been used since the dawn of time in ancient Persia, Greece and the Roman age, usually for operating water pumps. These gear designs were not very efficient, mostly using the pin and crown gearing principle [1].

The first general application of the analytical tooth profile can be related to the works of L. Litvin [2]. His homogeneous matrix transformation method became increasingly popular from the time that the calculations could be performed by computers. New results for the classical problems were made possible with the help of computer aided mathematical deductions. The paper describes the representation of the gear contact principles using a complex algebraic method [2, 3, 4]. The solution of the equations is used for the generation of the gear profile, the contact line and also the generating gear rack tool profile. The practical use of

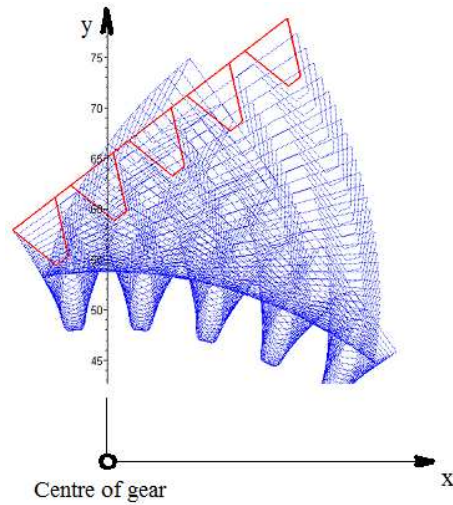


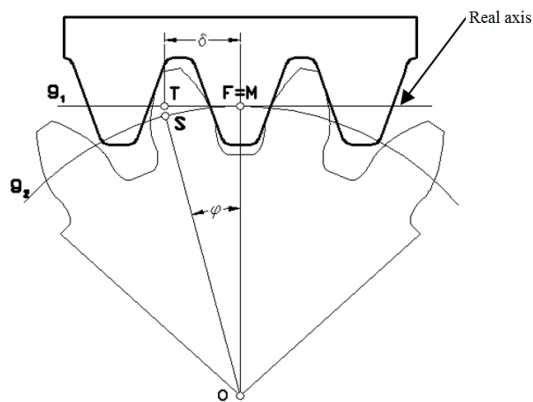
Figure 2

Generating the involute gear with the rack

The non-slip rolling of the profile of the rack (its straight line) on the centre of the gear can be constructed from the following two motion elements (see: Fig. 3a to 3c):

I. The first motion is: the rack moves from the starting position 1 with the distance of $\delta = r \cdot \varphi$ in the direction of the real axis (position 1').

II. The second motion when the rack moves by a rotation around the origin with the angle φ to the position 1''. (Assuming plain rolling the gear centre g_2 is the arc length $MS = r \cdot \varphi$ and the length of the rolling straight line g_1 is $TM = \delta$. From the figure the following equation can be obtained: $MS = TM$. (See: Fig. 3a).



a) Starting position of the Rack

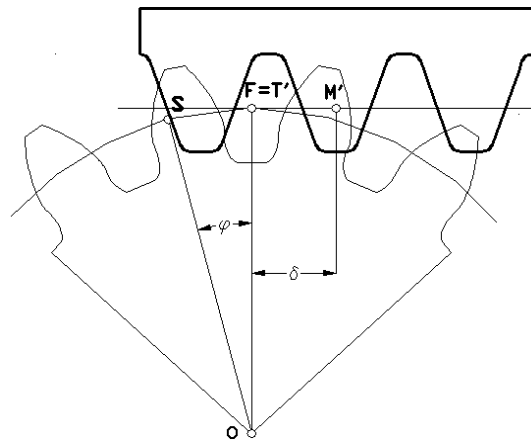
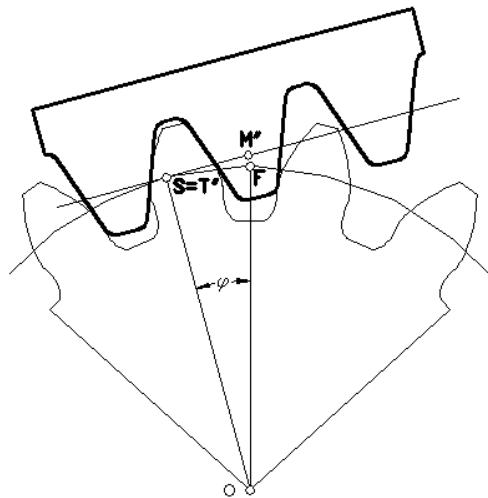
b) 1st motion element of rollingc) 2nd motion element of rolling

Figure 3

The motion elements of gear generation

Fig. 3a) illustrates the starting position of the rack, Fig. 3b) the 1st and Fig. 3c) the 2nd motion element of the rolling. With the use of the motion elements (I and II) the shape enveloped by the motion of the rack and the gear profile meshing with it can be determined in a general way. Let the rack profile be given with a complex function with the parameter u , according to the following equation:

$$z = z_1(u) + I \cdot z_2(u) \quad (1)$$

The complex transformation formula of the motion elements I -II is given by the following formula:

$$w = (z_1(u) + I \cdot z_2(u) + r \cdot \varphi) \cdot e^{(I \cdot \varphi)} \quad (2)$$

where r is the radius of the pitch curve, and z_1 and z_2 are the real and imaginary parts of the rack profile function.

During the roll the following differential equation is valid for the border form (2) (the gear teeth) generated by the rack given by equation (1). The real and the imaginary parts of the function are $R(w)$ and $I(w)$. During the roll the following differential equation is valid for the border form (2) (the gear teeth) generated by the rack given by equation (1). The real and the imaginary parts of the function are $R(w)$ and $I(w)$.

$$\tan(\alpha) = \frac{\frac{\partial}{\partial \varphi} I(w(u, \varphi))}{\frac{\partial}{\partial \varphi} \operatorname{Re}(w(u, \varphi))} = \frac{\frac{\partial}{\partial u} I(w(u, \varphi))}{\frac{\partial}{\partial u} \operatorname{Re}(w(u, \varphi))} \quad (3)$$

By expanding the differential equation (3) the following formula is gained:

$$\frac{\left(\frac{d}{du} z_2(u)\right) \cdot \cos(\varphi) + \left(\frac{d}{du} z_1(u)\right) \cdot \sin(\varphi)}{\left(\frac{d}{du} z_1(u)\right) \cdot \cos(\varphi) - \left(\frac{d}{du} z_2(u)\right) \cdot \sin(\varphi)} - \frac{-z_2(u) \cdot \sin(\varphi) + r \cdot \sin(\varphi) + \cos(\varphi) \cdot z_1(u) + \cos(\varphi) \cdot r \cdot \varphi}{r \cdot \cos(\varphi) - \sin(\varphi) z_1(u) - \sin(\varphi) \cdot r \cdot \varphi - z_2(u) \cdot \cos(\varphi)} = 0 \quad (4)$$

An analytic (closed form) solution of the differential equation (4) can be obtained for the variable φ :

$$\varphi = \frac{-\left(\frac{d}{du} z_2(u)\right) \cdot r + \left(\frac{d}{du} z_2(u)\right) \cdot z_2(u) + z_1(u) \cdot \left(\frac{d}{du} z_1(u)\right)}{r \cdot \left(\frac{d}{du} z_1(u)\right)} \quad (5)$$

The expression can be further simplified using the following substitutions:

$$z_1(u) = F_1, z_2(u) = F_2, \frac{d}{du} z_1(u) = f_1, \frac{d}{du} z_2(u) = f_2 \quad (6)$$

The variable φ can be expressed with the formula of the rack (1), and its derivatives according to u . In this way a very simple formula is obtained for the variable φ :

$$\varphi = -\frac{-f_2 \cdot r + f_2 \cdot F_2 + F_1 \cdot f_1}{r \cdot f_1} \quad (7)$$

The gear tooth profile is expressed as a complex equation which is dependent on the parameter u , in this way by substituting the variable φ into the two-parameter equation the solution can be obtained in a closed form:

$$K = \left(F_1 + F_2 \cdot I - \frac{-f_2 \cdot r + f_2 \cdot F_2 + F_1 \cdot f}{f_1} \right) \cdot e^{\left(\frac{I(-f_2 \cdot r + f_2 \cdot F_2 + F_1 \cdot f)}{r \cdot f_1} \right)} \quad (8)$$

To obtain a proof of the line of action the theorem of Willis is used. The equation of the profile tangent at the point given by the parameter u - with complex coordinates $z_1(u) + I \cdot z_2(u)$ - for the line of action is:

$$t = z_1(u) + I \cdot z_2(u) + \lambda \cdot \left(\left(\frac{d}{du} z_1(u) \right) + I \cdot \left(\frac{d}{du} z_2(u) \right) \right) \quad (9)$$

The equation of the normal of the profile at the same point is:

$$k = z_1(u) + I \cdot z_2(u) + \lambda \cdot \left(\left(\frac{d}{du} z_2(u) \right) - I \cdot \left(\frac{d}{du} z_1(u) \right) \right) \quad (10)$$

According to the theorem of Willis the profile normal crosses the point with the following coordinates $0 + I \cdot r$. Using this theorem the equation of connection can be formulated in the following way:

$$z_2(u) - \lambda \cdot \left(\frac{d}{du} z_1(u) \right) = r \quad (11)$$

The connection can be expressed by solving equation (11) according to λ :

$$\lambda = \frac{z_2(u) - r}{\frac{d}{du} z_1(u)} \quad (12)$$

The next step is to substitute the value of λ into the real part of equation (10):

$$\delta = z_1(u) - \frac{(z_2(u) + r) \cdot \left(\frac{d}{du} z_2(u) \right)}{\frac{d}{du} z_1(u)} \quad (13)$$

The profile normal belonging to the parameter u of the rack, meshes the rolling straight (line) of the rack at the point $x = \delta$. The u parameter point of the rack will roll into the main point after the value of $-\delta$. The complex equation of the connecting line can be expressed with the function of the rack:

$$M = z_1(u) - \delta + I \cdot z_2(u) \quad (14)$$

3 Applications of the Theory

In this chapter, three examples will be shown to illustrate the application of the presented method, by generating different geometry gears such as a cosine profile gear, the profile of the lobes of a Roots blower and also generating a general involute gear. These examples show that this analytical method can be easily used for very different problems, for designing conventional and non-conventional gears.

3.1 Generating a Cosine Gear Profile

Using the method herein, an example of generating a gear and its generating rack that has a cosine profile is shown. The advantages of this profile and a manufacturing method were described in [5]. A different and simpler method is given for the generating process.

The rack profile is described by the following equation:

$$z = u + I \cdot \left(r + 10 \cdot \sin\left(\frac{u}{5}\right) \right) \quad (15)$$

In this example the radius of the pitch circle of the gear is $r = 50 \text{ mm}$. Substituting the values of r , the number of teeth (N) and the expression (15) into equation (2) provides the following formula:

$$w = \left(u + \left(50 + 10 \cdot \sin\left(\frac{u}{5}\right) \right) \cdot I + 50 \cdot \varphi \right) \cdot e^{(\varphi \cdot I)} \quad (16)$$

The coordinate values for the abscissa and the ordinate of the real $R(w)$ and imaginary $I(w)$ part of w are assigned to variables as $X = R(w)$ and $Y = I(w)$.

The values of the coordinates are evaluated by partial derivation of X and Y according to u and φ shown in (17):

$$\begin{aligned} \frac{\partial}{\partial u} X &= \cos(\varphi) - \sin\left(\frac{u}{5} + \varphi\right) - \sin\left(-\frac{u}{5} + \varphi\right) \\ \frac{\partial}{\partial \varphi} X &= -\sin(\varphi)u - 50 \cdot \sin(\varphi) \cdot \varphi - 5 \cdot \sin\left(\frac{u}{5} + \varphi\right) + 5 \cdot \sin\left(-\frac{u}{5} + \varphi\right) \\ \frac{\partial}{\partial u} Y &= \cos\left(-\frac{u}{5} + \varphi\right) + \cos\left(\frac{u}{5} + \varphi\right) + \sin(\varphi) \\ \frac{\partial}{\partial \varphi} Y &= -5 \cdot \cos\left(-\frac{u}{5} + \varphi\right) + 5 \cdot \cos\left(\frac{u}{5} + \varphi\right) + \cos(\varphi)u + 50 \cdot \cos(\varphi) \cdot \varphi \end{aligned} \quad (17)$$

Using equation (3) a differential equation of the profile is defined that is made equal to zero (18):

$$\frac{\frac{\partial}{\partial \varphi} I(w(u, \varphi))}{\frac{\partial}{\partial \varphi} \operatorname{Re}(w(u, \varphi))} - \frac{\frac{\partial}{\partial u} I(w(u, \varphi))}{\frac{\partial}{\partial u} \operatorname{Re}(w(u, \varphi))} = 0 \quad (18)$$

By expanding equation (18) the following equation is obtained:

$$\frac{\cos\left(-\frac{u}{5} + \varphi\right) + \cos\left(\frac{u}{5} + \varphi\right) + \sin(\varphi)}{\cos(\varphi) - \sin\left(\frac{u}{5} + \varphi\right) - \sin\left(-\frac{u}{5} + \varphi\right)} - \frac{-5 \cdot \cos\left(-\frac{u}{5} + \varphi\right) + 5 \cdot \cos\left(\frac{u}{5} + \varphi\right) + \cos(\varphi)u + 50 \cdot \cos(\varphi) \cdot \varphi}{-\sin(\varphi)u - 50 \cdot \sin(\varphi) \cdot \varphi - 5 \cdot \sin\left(\frac{u}{5} + \varphi\right) + 5 \cdot \sin\left(-\frac{u}{5} + \varphi\right)} = 0 \quad (19)$$

Equation (19) can be solved analytically. The closed form solution according to φ can be given as:

$$\varphi = -\frac{2 \cdot \cos\left(\frac{u}{5}\right) \cdot \sin\left(\frac{u}{5}\right)}{5} - \frac{u}{5} \quad (20)$$

This solution can be further simplified using the following trigonometric identity:

$$2 \cdot \cos\left(\frac{u}{5}\right) \cdot \sin\left(\frac{u}{5}\right) = \sin\left(\frac{2u}{5}\right) \quad (21)$$

The formula of the gear profile (w) can be determined using the simplified formula of equation (21):

$$w = \left(\left(50 + 10 \cdot \sin\left(\frac{u}{5}\right) \right) I - 10 \cdot \sin\left(\frac{2 \cdot u}{5}\right) \right) e^{\left(\left(\frac{\sin\left(\frac{2u}{5}\right)}{5} \frac{u}{50} \right) I \right)} \quad (22)$$

The contact curve of the cosine gears can be formulated using equation (14) as:

$$M = -20 \cdot \cos\left(\frac{u}{5}\right) \cdot \sin\left(\frac{u}{5}\right) + \left(50 + 10 \cdot \sin\left(\frac{u}{5}\right) \right) I \quad (23)$$

The generated gear, the contact and the enveloping rack are shown in Fig. 4. The teeth profile of the cosine rack is obtained from the calculation. The gear described in [8] has a cosine profile on the generated gear, however, the profile on the rack is a complicated curve which is difficult to manufacture accurately. The method described above is simpler because the rack profile is a cosine curve that is easier and cheaper to manufacture accurately. The profile of the generated gear teeth is better suited for a proper gear.

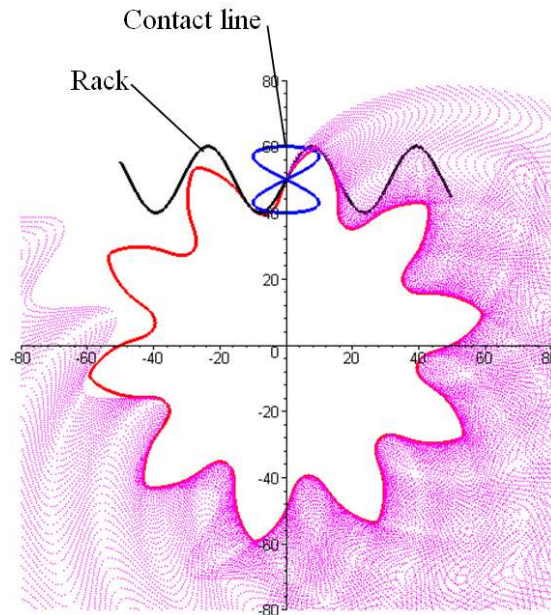


Figure 4

The full profile of the generated cosine gear enveloped by the rack and the contact line

3.2 Generating the Profile of the Lobes of the Roots-Blower

Another example of the presented theory is shown, where a rack profile is generated which can envelope the shape of the lobes of a Roots blower [6, 7]. The lobes of the blower consist of semicircles with the radius of $\rho = \frac{\pi}{2}$. The lobes connect tangentially to each other. In the case when the number of lobes is two, the radius of the acting pitch circle is $r = \frac{4\rho}{\pi}$. The equation of the profiles applied to semicircles according to (1) is:

$$p(u) = \begin{cases} -\sqrt{\rho^2 - (u - \rho)^2} & \text{if } u < 2 \cdot \rho \\ \sqrt{\rho^2 - (u - 3 \cdot \rho)^2} & \text{otherwise} \end{cases} \quad (24)$$

Applying the Fourier series on the parametric formula (24) the following formulae can be generated (25):

$$A_j = \frac{\int_0^{2\pi} p(u) \cdot \sin(j \cdot u) du}{\pi} \quad (25)$$

$$B_j = \frac{\int_0^{2\pi} p(u) \cdot \cos(j \cdot u) du}{\pi}$$

Using these equations the formula of the rack profile can be given by the following expressions:

$$z_1(u) = u \quad (26)$$

$$z_2(u) = \frac{B_0}{2} + \left(\sum_{i=1}^n (A_{2i-1} \cdot \sin((2i-1) \cdot u) + B_{2i} \cdot \cos(2i \cdot u)) \right)$$

Using the formula (6) for (26):

$$F_1 = z_1(u) \quad (27)$$

$$F_2 = r + z_2(u)$$

Using formulae (7) and (8) on (27) will generate the complete contour of the Roots-blower. The rolling of the rack can be presented by using equation (2). Fig. 5 shows the result of the whole motion of the generating process and the generated lobe. Fig. 6 shows the joined pair of lobes in its housing. The inside curvature of the housing has a radius of $R = r \cdot \sqrt{2}$. The movement of the rack will also generate additional profile elements which have a valid shape according to equation (8) but are never realized on a real work piece (see Fig. 6). These parts of the curve will be cut off by the generating tool. Nevertheless they are theoretically interesting because, they meet all the requirements expressed by differential equation (3).

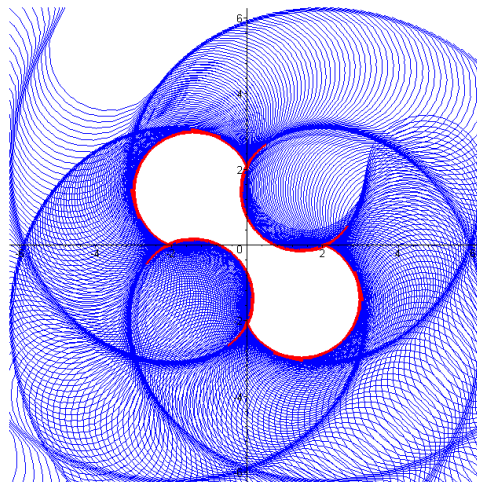


Figure 5

The generation of the profile of a Roots-blower lobe

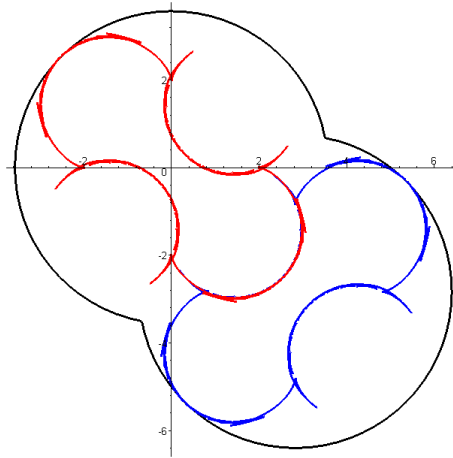


Figure 6

The profiles of the Roots-blowers according to the solution of the model.

3.3 Generating the Profile of a Standard Involute Gear

The last example, illustrates the design process of a general involute gear using our proposed method. The real differences between the mathematical point of view of gears and that of those realized at tooth generation, can be shown in more detail on involute gears using the method herein. The parametric equation of the rack (characterized by modulus $m=2$, basic angle α , addendum high h_1 and dedendum h_2 the depth factors on the tool) is the following:

$$p(u) = \begin{cases} \frac{u}{\tan(\alpha)} & \text{if } u < h_1 \cdot \tan(\alpha) \\ h_1 & \text{if } u < \pi \cdot h_1 \cdot \tan(\alpha) \\ \frac{\pi - u}{\tan(\alpha)} & \text{if } u < \pi + h_2 \cdot \tan(\alpha) \\ -h_2 & \text{if } u < 2 \cdot \pi - h_2 \cdot \tan(\alpha) \\ \frac{u - 2 \cdot \pi}{\tan(\alpha)} & \text{otherwise} \end{cases} \quad (28)$$

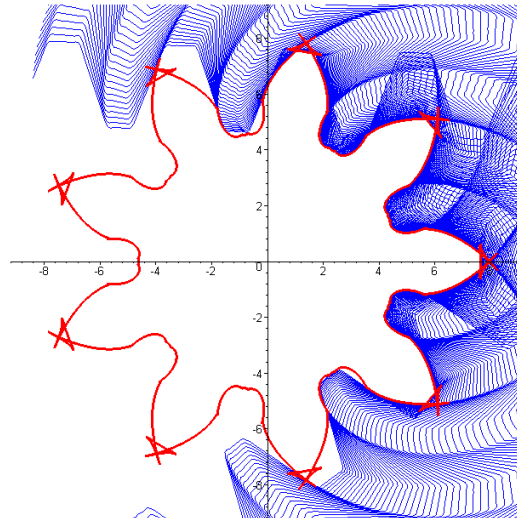
The Fourier series of the rack is generated according to equations (25) and (26). In general when the module of the gear is not two ($m \neq 2$) and the profile displacement factor is not zero ($\zeta \neq 0$), in the Fourier series (26), the following equation holds:

$$\hat{u} = \frac{2u}{m} \quad (29)$$

Carrying out the substitution (28) and (29) into (6) the formula for the rack profile is the following:

$$\begin{aligned} F_1 &= z_1(\hat{u}) \\ F_2 &= r + \frac{m}{2} \cdot z_2(\hat{u}) + \xi \cdot m \end{aligned} \quad (30)$$

The process of translation and complex rotations is again carried out according to (7) and (8) to obtain the full gear profile. The results of the process can be seen in Fig. 7a a gear contour in the case of nine teeth $N = 9$, $m = 1.34$, $\alpha = 20^\circ$, $h_1 = 1.25$, $h_2 = 1$, $\xi = 0.2$ can be seen together with the generating tool movement. From Fig. 7 it is easy to see that profile generated according to formula (8) is wrong because, the number of teeth is too few, so undercuts will appear. Tooth sharpening can be partially seen on top of the generated teeth. In Fig. 7b a variant of the previous solution can be seen, where no profile displacement ($\xi = 0$) was used.



a)

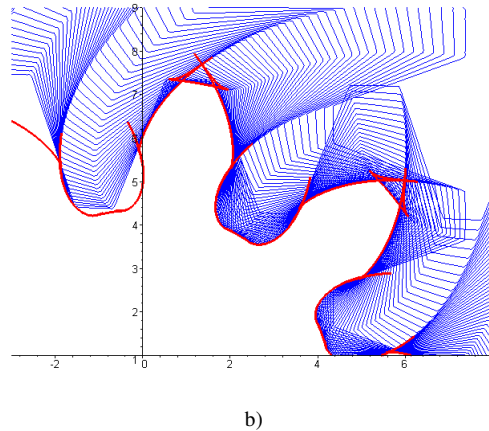


Figure 7

Full (a) and partial (b) involute profiles with different values of undercut

Conclusion and further remarks

The method developed in this work is “manufacturing friendly”. As it was seen, the non-conventional tooth profile and the rack (the tooth profile generating tool) are generated easily. This method uses complex algebra and complex functions that can be used for generating other general gear tooth profiles not described here. The demonstrated profiles were only shown here as examples, but an almost infinite variation of profiles can be generated with this method, as long as the tooth profile can be described by a suitable Fourier series.

References

- [1] H.-CHR. GRAF SEHERR-THOSS: Die Entwicklung der Zahnradtechnik, Springer Verlag Berlin-Heidelberg-New York (1965)
- [2] Faydor, L. Litvin, Alfonso Fuentes: Gear Geometry and Applied Theory, Cambridge University Press (2004)
- [3] Laczik, B.: Design and Manufacturing of Non-Circular Gears by Given Transfer Function, *ICT 2007 Conference*, Miskolc, Hungary (2007) 101-109
- [4] Laczik, B.: Re-Discovery of the Non-Circular Gears, *Manufacturing 2008 Conference*, Budapest, Hungary (2008) 21-28
- [5] Shanming Luo, Yue Wub, Jian Wang: The Generation Principle and Mathematical Model of a Novel Cosine Gear Drive, *Mechanism and Machine Theory* 43 (2008) 1543-1556

- [6] Shih-Hsi Tong, Daniel C. H. Yang: On the Generation of New Lobe Pumps for Higher Pumping Flowrate, *Mechanism and Machine Theory* 35 (2000) 997-1012
- [7] Ligang Yao, Zhonghe Ye, Jian S. Dai, Haiyi Cai: Geometric Analysis and Tooth Profiling of a Three-Lobe Helical Rotor of the Roots blower, *Journal of Materials Processing Technology* 170 (2005) 259-267
- [8] Laczik, B., Zentay, P., Horváth, R.: Modelling the Gear Generating Process with Complex Functions, *7th International Conference on Mechanical Engineering*, Budapest, Hungary (2010) 496-501

The Influence of Thickeners on the Rheological and Sensory Properties of Cosmetic Lotions

Tereza Moravkova, Petr Filip

Institute of Hydrodynamics, Acad. Sci. Czech Rep., Pod Patankou 5,
166 12 Prague 6, Czech Republic, e-mail: moravkova@ih.cas.cz, filip@ih.cas.cz

Abstract: Two empirical models were proposed for a description of rheological characteristics of four eye creams, differing only in the thickener component that preserves the chemical structure of these cosmetic lotions. Coupling between selected sensory variables (such as softness when removing cream from the pot and the “spreadability” on the back of the hand) and rheological parameters was carried out for both models. A close coupling (and hence mutual substitution) between the rheological and sensory parameters enabled evaluation of the sensory parameters by the rheological ones and thus, saving time and money consuming sensory assessment by fast instrumental rheological analysis. It was shown that a proper choice of an empirical model substantially broadens the range of these substitutions.

Keywords: cosmetic lotion; eye cream; empirical rheological modelling; sensory analysis

1 Introduction

Cosmetic lotions are the emulsions formed in principle by two immiscible liquids. They are prone to various instabilities such as creaming, sedimentation, flocculation, Ostwald ripening, coalescence and phase inversion summarized in Tadros [1]. To prevent emulsion from the appearance of the instabilities, various admixtures (in very limited volumes), namely emulsifiers and thickeners are added into the emulsions. Emulsifiers exhibit two favorable properties - a decrease in interfacial tension between both liquids and a stabilization of the dispersed phase against coalescence. Thickeners, on the other hand, partially inhibit the reaction between the chemicals contained in the emulsion and simultaneously modify, to a higher extent, than emulsifiers, the rheological characteristics.

The principal aim of sensory analysis is to differentiate between consumer-friendly and negative attributes of the materials such as cosmetic lotions. No wonder that sensory analysis dominates in the process of their production (see Lukic et al. [2]). This methodology of sensory evaluation of cosmetic products follows three principal points: suitable choice of evaluated variables, suitable

choice of the corresponding absolute or universal scales, and suitable choice of a professional panel (expensive). Gilbert *et al.* [3, 4] have presented a method of Spectrum Descriptive Analysis reflecting an accurate sensory description of products by rating each attribute on chosen scales. This method allows for comparison of the relative intensities within a product or among additional products.

However, sensory analysis has several drawbacks. The evaluation is subjective and very time and money consuming; since, it requires the service of a professional panel. The current discussion revolves around substituting the sensory analysis by rheological measurements that would provide a model flow curve approximating the relation shear stress τ vs. shear rate $\dot{\gamma}$, where shear viscosity η represents a related factor

$$\tau = \eta \cdot \dot{\gamma} \quad (1)$$

The number of parameters in such empirical models usually range from two (the power-law model) to five (the Carreau-Yasuda model), see Macosco [5]. However, the cosmetic lotions quite often exhibit viscoplastic behavior, i.e. the so called yield stress is present, a value of which is necessary to exceed for passage from the static form of cosmetic lotion to its spreadable phase. In the case of yield stress, the number of adjustable parameters in the empirical models is raised by one in respect to the plasticity of the studied material. Yield stress τ_0 can be expressed either explicitly (as e.g. in the three-parameter Herschel-Bulkley model) or implicitly. If there are found tight relations between the individual sensory parameters (pouring from the bottle, softness when removing cream from the pot, ease of spreading, or thickness) and adjustable parameters appearing in the empirical rheological models, then an evaluation of the sensory parameters by their rheological, adjustable counter-parts, can represent a time and money saving approach for improving the final product. Scott Blair [6] was the first who applied this approach in 1939.

There are a series of empirical models that describe the behavior of emulsions or suspensions, including the well-known, Einstein's theoretically based model, for dilute suspensions. However, their applicability is often restricted either to low percentage participation of one component with respect to the other, or the proposed models are directly tailored for the final material. This is caused by complexity of the emulsions viscosity and depends on a number of factors. Pal [7] that summarize ten entry factors: shear rate, time, viscosity of continuous and dispersed phase, density of continuous and dispersed phase, particle (droplet) radius, concentration of particles, thermal energy and interfacial tension. In addition, there is an influence of other factors. Danov [8] proposed an analytical expression for the viscosity of dilute emulsions in the presence of emulsifiers. Experimental determination of emulsion viscosity is very well elaborated and its measurement is very accurate to a fraction of a percent.

Coupling between rheological and sensory properties was recently studied by Karsheva et al. [9], Nakagawa and Ueda [10], Reeve and Amigoni [11], Ibanescu et al. [12], Moravkova and Stern [13]. The study of influence of a solid ingredient on both rheological and sensory properties is relatively rare. Danov [8] proposed an analytical expression for the viscosity of dilute emulsions in the presence of emulsifiers as already mentioned above. Lukic et al. [2] studied four water-in-oil creams differing in only one emollient component. The samples were submitted to rheological, sensory and textural characterization. The results indicated that certain alteration restricted to the oil phase induced a change in all investigated characteristics. Obtained correlation between physical measurements and certain sensory attributes confirmed that textural analysis, as a fairly simple measurement, can be used as a surrogate for rheological measurements. Abu-Jdayil et al. [14] analyzed the influence of the Dead Sea salt content in cosmetic emulsions to its rheological properties and stability. Karsheva and Georgieva [15] studied an effect of plant extracts and thickeners on flow properties of phytocosmetic formulation comparing two oily cosmetics gels (with different gelling components) to a cosmetic cream. For a description of its consistency they applied the power law model, specifically behavior of the consistency index K .

The objective of this study is to specify the influence of a small change in the composition of a cosmetic emulsion (eye creams) to its rheological and textural properties. The composition of four eye creams differ only in the thickener used, all other components are identical. For the rheological description there were proposed two empirical models and for each of them an analysis relating the adjustable and sensory parameters was carried out. It was shown that coupling between these groups of parameters strongly subject to a choice of an empirical model. This indicates that a suitable model should be carefully selected either from the existing ones or tailored with respect to a type of studied emulsion.

2 Experimental

2.1 Materials

Four samples of eye creams, labeled cr1, cr2, cr3, and cr4, were prepared using the laboratory homogenizer SilentCrusher M (Heidolph, Schwabach, Germany). This homogenizer enables individual adjustment of speed from 5000 to 26000 rpm and is suitable for quantities from 0.8 to 2000 ml.

The composition of the samples and suppliers is contained in Table 1 (without thickeners). Total amount of each sample was 2 kg and afterwards filled in 50 ml containers. All four samples differed only in a type of the thickener (mostly 0.3 wt.%), only cr3 deviates negligibly in other components, see Table 2.

Table 1
Ingredients of the samples

Ingredients (INCI name - International Nomenclature of Cosmetic Ingredients)	Ingredient	Supplier	Content [wt.%] cr1-4	
details in Table 2	Thickener	details in Table 2		
Polyglyceryl -3- Methylglucose Distearate	Tego care 450	Degussa	3	
Glyceryl Stearate	Cutina GMS V	Cognis	2	
Cetearyl Alcohol	Lanette O	Cognis	1	
Caprylic/Capric Triglyceride	ACE CCT	ACE Trade	7	
Cetyl Ricinoleate	Tegosoft CR	Evonik- Goldschmidt	4	
Persea Gratissima (Avocado) Oil	Avocado oil	M&H	4	
Macadamia Ternifolia Seed Oil	Macadamia oil	M&H	6	
Panthenol	Panthenol 75 L	Roche Vitamins	0.5	
Tocopheryl Acetate	Vitamin E acetat	Roche Vitamins	1	
2-Bromo-2- Nitropropane-1,3- Diol, Methylchloroisothia- -zolinone, Methylisothia- zolinone	Euxyl K 145	Schülke&Mayr	0.15	
Sodium Lactate, Sodium PCA, Glycine, Fructose, Urea, Niacinamide, Inositol, Sodium Benzoate, Lactic Acid	Lactil GDS	Evonik- Goldschmidt	0.5	
Parfum	Fragrance	Charabot	0.1	
Aqua	Water, distilled		cr1,2,4 cr3	70.45 70.39

While xanthan gum and carrageenan are of natural origin, polyacrylamide and carbomer represent synthetic thickeners. The usage of the thickeners is almost identical, only carbomer is presented in lower concentration because neutralization by triethanolamine is required.

Table 2
Thickeners contained in the samples

Sample	Thickener	Thickener (trade name)	Supplier	Content [wt.%]
cr 1	polyacrylamide	Sepigel 305	Seppic	0.3
cr 2	xanthan gum	Keltrol CG-SFT	CP Kelco	0.3
cr 3	carbomer with	Carbopol Ultrez 20	Lubrizol	0.12
	triethanolamine	TEA		0.24
cr 4	carrageenan	Genuvisco CI 123	CP Kelco	0.3

2.2 Devices

Rheological measurements were carried out with a rotational rheometer RheoStress 300 (Thermo Scientific, Karlsruhe, Germany). A cone-and-plate system with Sensor: C35/1° Ti (cone diameter 35 mm, cone angle 1°) was used. In contrast to a plate-and-plate arrangement, the chosen cone-and-plate arrangement respects non-Newtonian course of measured characteristics, and hence provides more responsible data. All measurements were carried out at 25°C.

2.3 Methodology

Both rheological and sensory approaches were applied to characterize the samples. These two approaches are not mutually independent, but coupled. As already mentioned above, sensory analysis is time and cost demanding, in addition, there is a certain influence of evaluation panel subjectivity. Evaluation from the sensory analysis can be, to some extent, replaced by the rheological characterization, which represents a substantially cheaper and effective solution. To verify the possibility for an acceptable replacement of selected sensory parameters by rheological means, for the problem (thickener alteration), the following steps were carried out:

- Rheological measurement determining a relation between shear stress and shear rate (flow curve) in the range of shear rate 10^{-2} - 600s^{-1} . Such experiments range among classical routine measurements, when using any standard rotational rheometer. In contrast, to sensory analysis requiring skilled and qualified panelists, staff using a rotational reometer can be acquainted with the mentioned type of measurements in a short span of time (hours)

- Sensory evaluation was carried out under standard conditions, as specified by the ISO standards (ISO 8589, ISO 8586.1, ISO 6658). Nineteen trained panelists completed a special questionnaire concerning 14 parameters (including color, shine, appearance of the surface, feeling during rub in, fragrance, frequency of the use of eye creams etc.). Each parameter was rated on a category scale with pre-defined descriptive terms. The four most important parameters (softness when removing cream from the container, ease of spreading on the face and on the back of the hand, and feeling on the skin after absorption) were rated on a graphical unstructured scale as well. For these four sensory parameters there were adjusted their counter-equivalent rheological qualities measured by the rotational rheometer.

The following section presents data processing of both rheological and sensory measurements and the possibilities of their coupling.

3 Results

3.1 Rheological Analysis

The experiments relating shear stress τ and shear rate $\dot{\gamma}$ for eye creams cr1-4 were carried out, see Figs. 1-4. It is apparent that the small change in the compositions of eye creams cr1, cr2, cr3, and cr4 results in substantially different behavior of flow curves. This confirms a non-negligible impact of the thickeners used on the overall manifestation of the individual products.

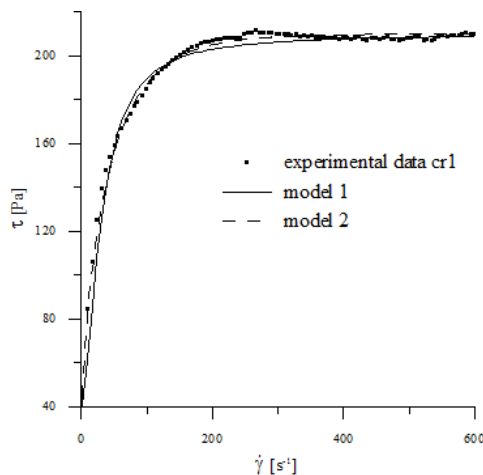


Figure 1

Approximation of the flow curve of cr1 by models 1 and 2

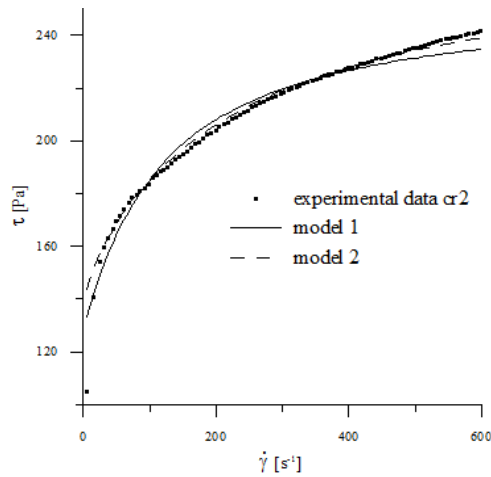


Figure 2

Approximation of the flow curve of cr2 by models 1 and 2

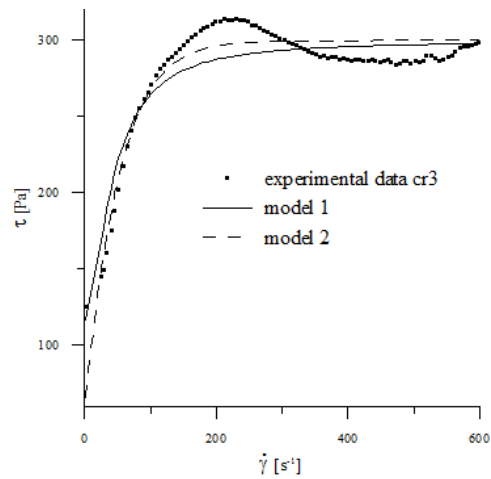


Figure 3

Approximation of the flow curve of cr3 by models 1 and 2

Two empirical models were proposed for a description of flow behavior of the individual eye creams. The two models differ not only in their algebraic forms but also in a number of adjustable parameters. Naturally, emphasis is paid to the relatively simple algebraic structure of both models, usage of well-known monotonous functions (powers, hyperbolic functions), unambiguous determination of the entry parameters, and overall simplicity of evaluation of the individual parameters. The required attributes of newly proposed empirical models are presented in more detail for example in David and Filip [16].

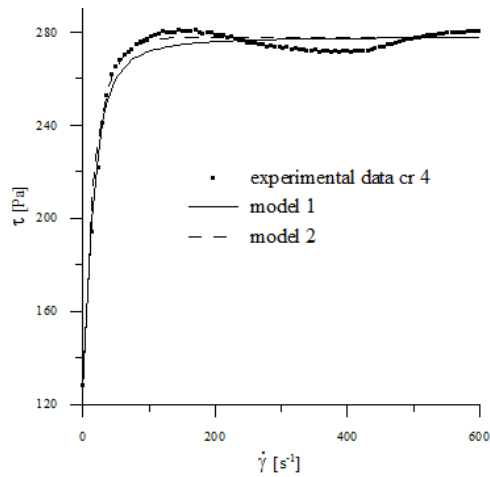


Figure 4
Approximation of the flow curve of cr4 by models 1 and 2

The 5-parameter model 1 is of the form

$$\tau = a_1 - \frac{b_1}{c_1 + d_1 \dot{\gamma}^{e_1}} \quad (2)$$

and the 4-parameter model 2 is of the form

$$\tau = a_2 \cdot \tanh(b_2 \dot{\gamma}^{c_2} + d_2) \quad (3)$$

Optimization of the parameters with respect to the individual eye creams is summarized numerically in Table 3 and graphically in Figs. 1-4. As can be seen, the average deviations of both model curves from the experimental points are quite similar.

Table 3
The parameters of the models 1 and 2

Eye cream	Parameters of model 1					Parameters of model 2			
	a_1	b_1	c_1	d_1	e_1	a_2	b_2	c_2	d_2
cr 1	210	340	2.0	0.007	1.66	210	0.050	0.70	0.18
cr 2	254	400	3.2	0.020	1.06	254	0.013	0.70	0.60
cr 3	300	550	3.0	0.005	1.70	300	0.016	0.94	0.22
cr 4	278	300	2.0	0.022	1.66	278	0.060	0.80	0.48

3.2 Sensory Analysis

The results of the sensory analysis involving all assessed parameters evaluated at category scales are presented in Table 4. Each category contained descriptive terms, and the trained evaluators marked one or more category on a scale. The most frequent descriptions are introduced in the last column of Table 4.

Table 4
Results of the sensory analysis

Assessed property	Descriptive terms	Most frequent descriptions
frequency of the use of eye cream	daily, very often, often, sometimes, rarely, never	daily, often
surface of the cream	smooth, grainy, bubbles, separated oil/water, other in-homogeneity	smooth, bubbles
shine of the cream	very shiny, shiny, matt, uneven	very shiny, shiny
color of the cream	bright white, white, blue-ish, greenish, ivory, grey, brownish, uneven, spots	white, bright white
fragrance	extremely nice, very nice, nice, neutral, unpleasant, unsavory	nice, neutral
softness when removing cream from the pot	very hard, hard, adequately hard, soft, too soft, sticky	adequately hard, soft, hard
spreadability on the back of the hand	optimal, satisfactory, bad, very bad	bad, satisfactory
fragrance during spreading	extremely nice, very nice, nice, neutral, unpleasant, unsavory	neutral, nice
intensity of the fragrance	light, optimal, intensive, too intensive	optimal, light
spreadability on the face	optimal, satisfactory, bad, very bad	satisfactory, bad
feelings during rub in	cooling, smooth, warm, rough, scratchy, burning, drying out	cooling, smooth
absorption	very quick, good, difficult, very difficult	difficult, very difficult
feeling on the skin after absorption	extremely nice, very nice, nice, neutral, unpleasant, unsavory	neutral, nice, unpleasant
interest in using the sample	daily, very often, often, sometimes, rarely, never	often, daily

Spreadability of the cream is evaluated at two places – on the face and on the back of the hand due to different body temperature. This dual assessment of spreadability was proved to be useful (see Moravkova and Stern [13]).

Four properties boldfaced in Table 4 (softness when removing cream from the pot - SRE, spreadability on the face - SprFa, spreadability on the back of the hand - SprH, and feeling on the skin after absorption - Feel) range to the most important features studied in the creams. Their more detailed evaluation is presented in Table 5. Only these properties will be discussed in the following. All other properties introduced in Tab. 4 serve only for more complete sensory characterization of the creams studied.

Table 5
Results of the sensory analysis, selected parameters (mean values, evaluated at scale 0-100)

	SRE – softness when removing cream from the pot	SprFa – spreadability on the face	SprH – spreadability on the back of the hand	Feel – feeling on the skin after absorption
100 responds to	very soft	optimal	optimal	very pleasant
cr1	37	79	80	69
cr2	43	81	80	63
cr3	73	61	53	63
cr4	65	55	52	58

The results of the sensory analysis confirmed the influence of the thickeners on the important sensory characteristics. Considering the spreadability (on both places), the samples cr1 and cr2 received more positive assessment than cr3 and cr4. The opposite distribution occurs in the SRE (softness when removing cream from the pot) category, where creams cr3 and cr4 were evaluated as softer compared to cr1 and cr2. The assessment of the feeling on the skin (Feel) gives similar values for all the four eye creams.

3.3 Correlation between Rheological and Sensory Measurements

Table 6
Correlation coefficients among the rheological (model 1) and sensory parameters (significant relations are bold)

	a_1	b_1	c_1	d_1	e_1
SRE – softness when removing cream from the pot	0.9397	0.4895	0.1420	-0.0642	0.4810
SprFa – spreadability on the face	-0.7631	-0.0938	0.2570	-0.1119	-0.6294
SprH – spreadability on the back of the hand	-0.8473	-0.2656	0.1065	-0.0204	-0.5998
Feel – Feeling on the skin after absorption	-0.7503	0.0963	-0.0636	-0.6910	0.0338

The linear relations between the sensory variables and the rheological parameters were determined. The individual correlation coefficients for all relations are summarized in Tables 6 and 7. The selected linear approximations for which the correlation coefficients indicate statistically significant coupling between the sensory and rheological analyses are depicted in Figs. 5-7 for the eye creams cr1, cr2, cr3, and cr4. It follows that the tightest relations are for the following couples: (a_1 , softness when removing cream from the pot), (a_2 , softness when removing cream from the pot), (c_2 , softness when removing cream from the pot).

Table 7
Correlation coefficients among the rheological (model 2) and sensory parameters
(Significant relations are bold)

	a_2	b_2	c_2	d_2
SRE – softness when removing cream from the pot	0.9397	-0.0802	0.9349	-0.0896
SprFa – spreadability on the face	-0.7631	-0.3376	-0.7517	0.0659
SprH – spreadability on the back of the hand	-0.8473	-0.1773	-0.8509	0.1003
Feel – Feeling on the skin after absorption	-0.7503	-0.1083	-0.3815	-0.6167

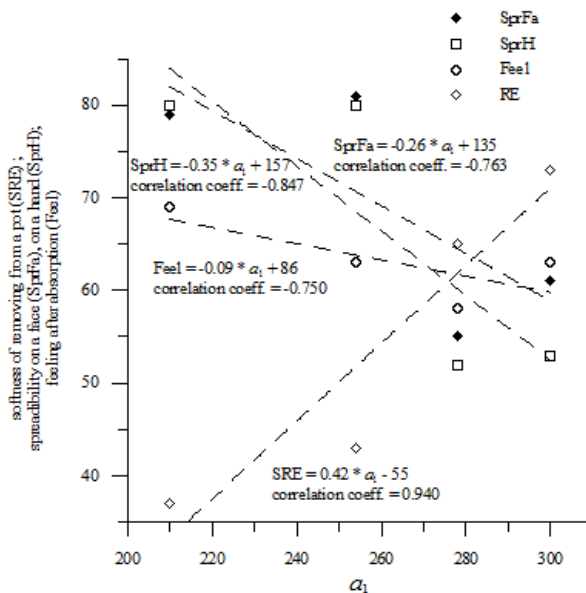


Figure 5

Relationships between sensory parameters and parameter a_1

Thus, the parameters a_1 , a_2 and c_2 provide an alternative to subjective sensory analysis because they can directly estimate two sensory variables from the rheological measurements, namely the softness when removing cream from the pot and the spreadability on the back of the hand.

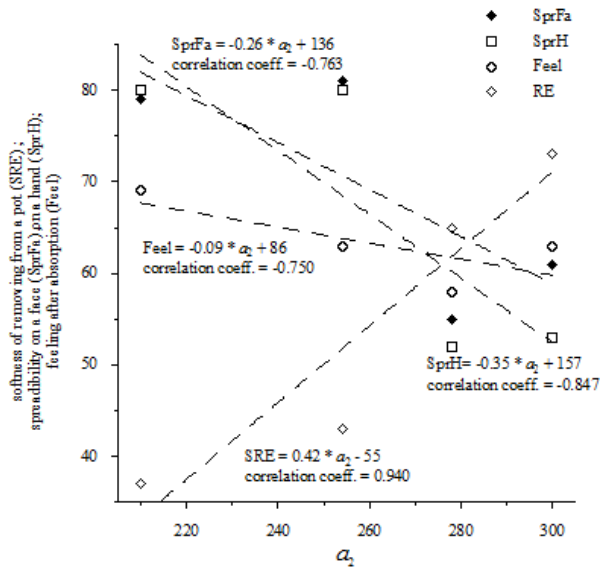


Figure 6

Relationships between sensory parameters and parameter a_2

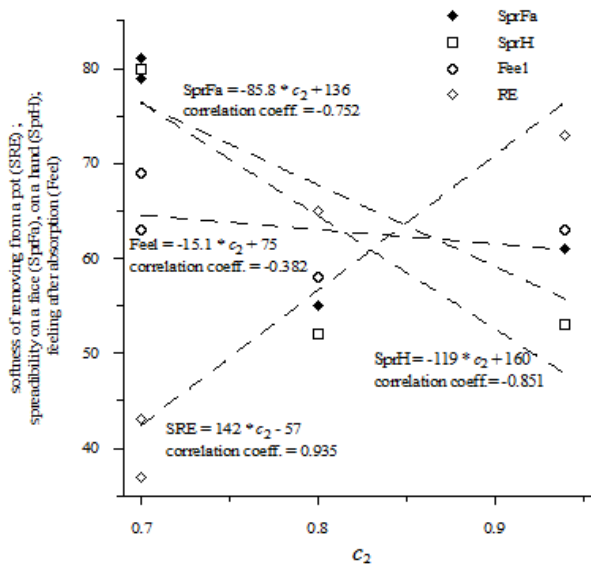


Figure 7

Relationships between sensory parameters and parameter c_2

Conclusions

A proper choice of a rheological model, can significantly help with a closer coupling of sensory variables and model parameters. An algebraic form of the rheological models belongs to a category of materials, to which the models are applied. A usage of standard empirical models (for example a classical power law model or viscoplastic Herschel-Bulkley one), represents a routine that makes it possible to proceed. However, if we want to obtain a closer coupling, a proposal of a new model with a better description of flow behavior of specific category of materials seems to be more promising.

This was confirmed in this present study of the characterization of four eye creams. In this case, two empirical models were proposed. Their rheological efficiency with respect to the description of the experimental data τ vs. $\dot{\gamma}$, is almost identical in spite of the different numbers of parameters (model 1: 5 parameters, model 2: 4 parameters). We found that the efficiency of model 2, concerning correlation of the rheological parameters, with the sensory variables is better. This is documented by the fact that softness, when removing cream from the container and spreadability on the back of the hand, can be checked independently, by two rheological parameters a_2 and c_2 in duplicated. Moreover, model 2 ensures easier evaluation because of the lower number of parameters being four.

However, either model under study, exhibits balanced efficiency from both the rheological and sensory point of view, and proves the possibility to substitute chosen sensory variables of four eye creams by their corresponding model parameters. It means that no panelists are required for the evaluation of sensory variables which are coupled with the rheological parameters. This significantly simplifies the procedure of the continuous checking of eye-cream production and reduces a pre-testing phase of new slightly modified recipes for new products.

The rheological experiments, as presented above, can be carried out using any standard rotational rheometer. These measurements can be classified as routine thus not requiring any special training of staff. As a result, evaluation of sensory variables by their rheological counter-parts, represents a remarkable time and money saving process.

Acknowledgement

The authors wish to acknowledge the Grant Agency CR for the financial support of Grant Project No.103/09/2066.

References

- [1] T. F. Tadros, *Rheology of Dispersions*, 2010, Wiley-VCH, Weinheim
- [2] M. Lukic, I. Jaksic, V. Krstonosic, N. Cekic, S. Savic, *A Combined Approach in Characterization of an Effective w/o Hand Cream: the*

- Influence of Emollient on Textural, Sensorial and in Vivo Skin Performance, *International Journal of Cosmetic Science* 34 (2012) 140-149
- [3] L. Gilbert, C. Picard, G. Savary, M. Grisel, Impact of Polymers on Texture Properties of Cosmetic Emulsions: a Methodological Approach, *Journal of Sensory Studies* 27 (2012) 392-402
- [4] L. Gilbert, G. Savary, M. Grisel, C. Picard, Predicting Sensory Texture Properties of Cosmetic Emulsions by Physical Measurements, *Chemometrics and Intelligent Laboratory Systems* 124 (2013) 21-31
- [5] Ch. W. Macosco, *Rheology: Principles, Measurements, and Applications*, 1994, Wiley-VCH, New York
- [5] G. W. Scott Blair, Psycho-Rheology in the Bread Making Industry, *Cereal Chemistry* 16 (1939) 707-711
- [7] R. Pal, Scaling of Relative Viscosity of Emulsions, *Journal of Rheology* 41 (1997) 141-150
- [8] K. D. Danov, On the Viscosity of Dilute Emulsions, *Journal of Colloidal and Interface Science* 235 (2001) 144-149
- [9] M. Karsheva, S. Georgieva, S. Alexandrova, Rheological Behavior of Sun Protection Compositions during Formulation, *Korean Journal of Chemical Engineering* 29 (2012) 1806-1811
- [10] Y. Nakagawa, T. Ueda, The Application of Rheology in the Development of Unique Cosmetics, *Nihon Reoroji Gakkaishi* 38 (2010) 175-180
- [11] P. Reeve, S. Amigoni, Rheology: a Precious Tool for Cosmetic Formulation, *Actualite Chimique* 323-24 (2008) 89-98
- [12] C. Ibanescu, M. Danu, A. Nanu, M. Lungu, B. C. Simionescu, Stability of Diperse Systems Estimated using Rheological Oscillatory Shear Tests, *Revue Roumaine de Chimie* 55 (2010) 933-940
- [13] T. Moravkova, P. Stern, Rheological and Textural Properties of Cosmetic Emulsions, *Applied Rheology* 21 (2011) 35200
- [14] B. Abu-Jdayil, A. H. Mohameed, A. Bsoul, Determination of optimal Dead Sea Salt Content in a Cosmetic Emulsion using Rheology and Stability Measurements, *Journal of Cosmetic Science* 59 (2008) 1-14
- [15] M. Karsheva, S. Georgieva, Flow Properties of Phytocosmetic Formulations. Effect of Plant Extracts and Thickeners, *Comptes Rendus de l' Academie Bulgare des Sciences* 63 (2010) 1725-1732
- [16] J. David, P. Filip, Phenomenological Modelling of Non-Monotonous Shear Viscosity Functions, *Applied Rheology* 14 (2004) 82-88

Petri Nets to B-Language Transformation in Software Development

Štefan Korečko, Branislav Sobota

Department of Computers and Informatics, Faculty of Electrical Engineering and Informatics, Technical University of Košice, Letná 9, 041 20 Košice, Slovakia, stefan.korecko@tuke.sk, branislav.sobota@tuke.sk

Abstract: Petri nets and B-Method represent a pair of formal methods, for computer systems engineering, with interesting complementary features. Petri nets have nice graphical representation, valuable analytical properties and can express concurrency. B-Method supports verified software development. To gain from these complements, a mapping from Petri nets to the language of B-Method has been defined and its correctness proved. This paper presents, by means of a case study, the usefulness of incorporation of Petri net designs in a software application developed by B-Method. Modifications of this mapping intended for the Event-B method and treatment of concurrency are also discussed.

Keywords: Petri nets; B-Method; Event-B; refinement; software development; concurrency

1 Introduction

Petri nets (PN) [8] are a formal language able to naturally express behaviour of non-deterministic, parallel and concurrent systems. PN offer an easy to understand graphical notation and analytical methods, which, for example, allows one to derive invariant properties from the structure of the net. There are many types of PN with different expressional and modelling power. PN can be used for modelling, analysis and simulation of systems from various areas, including network protocols, operating systems, workflow management and business processes [5] and robotic manufacturing systems [18, 19]. On the other hand, the B-Method (B) [1] is a state based, model-oriented formal method intended for software development. Its strength lies in a well-defined development process, which allows one to specify a software system as a collection of components called B-machines and refine such an abstract specification to a concrete one. The concrete specification can be automatically translated to ADA, C or another programming language. An internal consistency of the abstract specification and correctness of each refinement step are verified by proving a set of predicates called proof obligations (POBs). The whole development process, including proving, is supported by an industrial-strength software tool called Atelier B.

Important properties of these methods are complementary: in PN invariant properties can be derived from the structure of the net; in B we have to specify invariants manually. B has verified development process but is intended only for sequential systems; PN can express concurrency but lack a development process. This led to an idea of integration of these methods. The idea was realized in the form of semantics-preserving mappings from the language of B-Method (B-language) to Coloured Petri nets [14] and from Evaluative Petri nets (EvPN) to the B-language [13, 15]. The second mapping transforms each EvPN to a computationally equivalent (bisimilar) B-machine. Its formal definition and proof of correctness was presented in [13, 15] and it has even also been shown that it can be used for an additional analysis of PN in B-Method [16]. However, its usefulness for software development has yet to be treated. Therefore, in this paper we present a case study that demonstrates how a B-machine, obtained by the second mapping, can be used as a component of a software system, developed by B-Method. We also outline an approach to reflect concurrent aspects of PN models in B and describe how the mapping can be adapted for a new version of B, called Event-B. The case study uses Place-transition nets, which can be regarded as a subclass of EvPN, so both PN and the mapping are treated to this extent only.

The rest of the paper is organized as follows. Sections 2 and 3 provide necessary information about Place-transition (PT) nets and B. Section 4 defines the mapping from PT nets to B-Method and shows its application to both the “classical” B and Event-B. Section 5 presents the case study and section 6 discusses the approach to reflect concurrent aspects. Section 7 describes related work and in the conclusions we deal with plans for future research and development.

2 Place-Transition Nets

Place-transition nets (PT nets) [8], also called Generalised Petri nets [10], are one of the most commonly used and researched type of PN. A PT net is defined [10] as a 5-tuple

$$N=(P, T, pre, post, m_0), \quad (1)$$

where $P=\{p_1, \dots, p_k\}$ is a finite set of places, $T=\{t_1, \dots, t_n\}$, is a finite set of transitions, $pre: P \times T \rightarrow \mathbb{N}$ is a preset function, $post: P \times T \rightarrow \mathbb{N}$ is a postset function and $m_0 \in \mathbb{N}^{|P|}$ is the initial marking. \mathbb{N} is the set of natural numbers, including 0.

PT net is usually depicted as an oriented graph with places (circles or ellipses) and transitions (bold lines or rectangles) as vertices (Fig. 1). Arcs are defined by the functions pre and $post$: When $pre(p, t) \neq 0$, then there is an arc from p to t , when $post(p, t) \neq 0$, then there is an arc from t to p . If the value of $pre(p, t)$ or $post(p, t)$ is greater than 1 then it is written next to the corresponding arc. For example, in the net in Fig. 1 we have $pre(p_2, t_1)=10$, $pre(p_1, t_1)=0$, $post(p_1, t_1)=1$ and $post(p_4, t_2)=1$.

With each transition t we can associate two sets: a set of pre-places of t ($\bullet t$) and a set of post-places of t ($t \bullet$). They are defined as follows:

$$\bullet t = \{p \mid p \in P \wedge pre(p,t) \neq 0\}, \quad t \bullet = \{p \mid p \in P \wedge post(p,t) \neq 0\}. \quad (2)$$

A *marking* of PT net N is a function $m: P \rightarrow \mathbb{N}$. Value of $m(p)$ is the number of tokens in the place p . Markings represent states of a Petri net. Markings are often written as vectors, $m = (m(p_1), \dots, m(p_k))$. For example the initial marking of the net from Fig. 1 is $m_0 = (0, 10, 0, 10)$. A transition $t \in T$ is enabled (feasible) in marking m , if and only if

$$\forall p \in \bullet t : m(p) \geq pre(p,t), \quad (3)$$

When t is enabled, it can be executed (fired). The result of its execution is a new marking $m'(p) \in \mathbb{N}^{|P|}$:

$$m'(p) = m(p) - pre(p,t) + post(p,t), \quad (4)$$

A marking, which can be reached from the initial marking of some PT net N by firing some sequence of enabled transitions, is called a *reachable marking* of N .

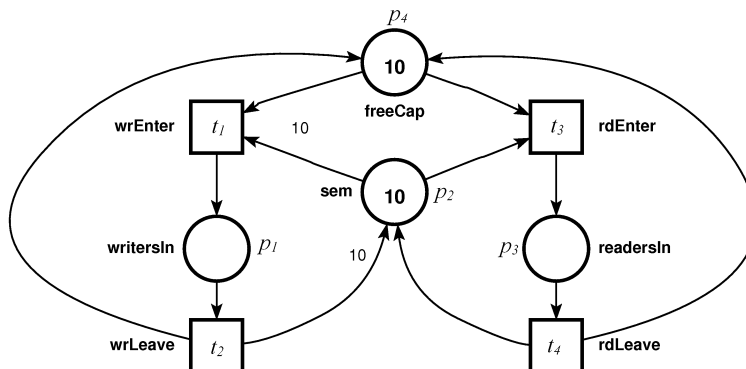


Figure 1

PT net representing limited variant of RW problem

An example of PT net can be seen in Fig. 1. The net specifies a solution of a limited variant of the so-called readers-writers (RW) problem. The RW problem can be described as follows: We have shared contents (a library) that can be accessed concurrently by two kinds of processes: readers, which only read the contents and writers, which also modify it. The problem is to ensure that no reader will access the contents while some writer is modifying it. In the limited variant of the problem, the library capacity, that is, the maximal number of processes accessing concurrently, is limited. The capacity is set to 10 in our example. The number of tokens in *writersIn* is the number of writers in the library (i.e. of processes modifying it) and the number of tokens in *readersIn* is the number of

readers in the library. Firing of *wrEnter* means that a writer process started accessing the library and *wrLeave* that it finished accessing the library; *rdEnter* and *rdLeave* have similar meaning for readers. We mentioned earlier that a handful of analytical methods are available for PN. One of them is a computation of so-called place invariants and by applying it to our net we get equations (5) and (6), which hold in any reachable marking *m* of the net. The equations prove that the net has required properties, such as the mutual exclusion of readers and writers.

$$m(\text{writersIn}) + m(\text{freeCap}) + m(\text{readersIn}) = 10 \quad (5)$$

$$10 \cdot m(\text{writersIn}) + m(\text{sem}) + m(\text{readersIn}) = 10 \quad (6)$$

3 B-Method

As it was written above, the *B-Method* (*B*) [1] allows us to specify a software system as a collection of *B-machines* and to refine such an abstract specification to an implementable one, while providing formal means to prove that both abstract specification and its refinements are consistent. All components in B are written in its own *B-language* (also called B-AMN), which is based on Zermelo-Fraenkel set theory and E.W. Dijkstra's Guarded Command Language [9].

Table 1
General structure of B-machine (left) and Refinement (right)

MACHINE <i>M(p)</i>	REFINEMENT <i>R(p)</i>
CONSTRAINTS <i>C</i>	REFINES <i>M</i>
SETS <i>St</i>	SETS <i>St1</i>
CONSTANTS <i>k</i>	CONSTANTS <i>k1</i>
PROPERTIES <i>Bh</i>	PROPERTIES <i>Bh1</i>
VARIABLES <i>v</i>	VARIABLES <i>w</i>
DEFINITIONS <i>D</i>	DEFINITIONS <i>D1</i>
INVARIANT <i>I</i>	INVARIANT <i>J</i>
ASSERTIONS <i>A</i>	ASSERTIONS <i>A1</i>
INITIALISATION <i>T</i>	INITIALISATION <i>T1</i>
OPERATIONS	OPERATIONS
$y \leftarrow op(x) =$	$y \leftarrow op(x) =$
PRE <i>P</i> THEN <i>S</i> END	PRE <i>P1</i> THEN <i>S1</i> END
...	...
END	END

Each B-machine consists of several clauses (Table 1). The most important are the MACHINE clause with a name *M* of the machine and a list *p* of its formal parameters, the VARIABLES clause with a list *v* of state variables, INVARIANT with properties *I* of the state variables, INITIALISATION with an operation *T* that establishes an initial state of the machine, and OPERATIONS that contains its

operations. The B-Method obeys the encapsulation principle, so only operations of the given machine can modify its variables. We say that the machine is internally consistent if \mathbb{I} holds in each of its states. St is a list of deferred and enumerated sets. These are regarded as new types. Constants of the machine are listed in k and a predicate Bh defines properties of St and k . D is a list of macro definitions and A is a list of lemmas used to simplify proof of POBs. Only the MACHINE clause is mandatory.

Table 2
Selected generalized substitutions and their intuitive meaning

GS	meaning of GS
skip	Empty GS (do nothing).
$x := e$	Assignment of value of expression e to variable x .
$S_1 ; S_2$	Sequential composition (do GS S_1 , then GS S_2).
$S_1 \parallel S_2$	Parallel composition (do S_1 and S_2 at once).
CHOICE S_1 OR S_2 END	Do S_1 or S_2 .
PRE E THEN S_1 END	If predicate E holds, do S_1 . Otherwise, do anything.
SELECT E THEN S_1 END	If E holds, do S_1 . Otherwise, do not execute.
IF E THEN S_1 ELSE S_2 END	If E holds, do S_1 . Otherwise, do S_2 .
VAR v IN S_1 END	For any values of local variables from the list v do S_1 .
ANY v WHERE E THEN S_1 END	For any values of variables from v that satisfy E do S_1 . If no values satisfy E , do not execute.

Every operation has two parts: a header and a body. The header includes its name (op) and optional input and output parameters (x, y). The body is written in the *Generalized Substitution Language (GSL)*, a part of the B-language. GSL contains several constructs, or “commands”, called *generalized substitutions (GS)*. Some of them are listed in Table 2. The formal semantics of GSL is defined by the weakest pre-condition calculus [9]. Standardly, the body has the form of PRE GS, however if $\text{P} \equiv \text{TRUE}$ then it consists only of S. The POBs for B-machine assert that \mathbb{T} always establishes an initial state in which \mathbb{I} holds and that for each operation op it holds that if op is executed from a state satisfying \mathbb{I} and P then it always terminates in a state satisfying \mathbb{I} .

One of the valuable assets of B-Method is its verified stepwise refinement process. This means that an abstract specification, consisting of B-machines (*MM*), can be modified in one or more steps into a form of concrete, implementable, specification. There are two additional components used during the refinement process – *Refinement (RR)* and *Implementation (II)*. Structures of *MM*, *RR* (Table 1) and *II* are similar, but there are some differences. For example GS “;” and loops are not allowed in *MM* and “||”, PRE, SELECT and CHOICE are not allowed in *II*. A *RR* or *II* can refine only one *MM* or *RR* but one *MM* or *RR* can be refined by more *RR* or *II*. To refine means to modify data or operations. Interfaces (i.e.

parameters and operation headers) of a refining and a refined component have to be the same. The structure of RR can be seen in Table 1. Invariant J of the refinement R defines properties of w but also a relation between v and w . Whether J is established by $T1$ and maintained by all operations of R is, again, verified by proving the PObs.

We stated earlier that specification in B usually consists of more than one component. To access contents of one component from another, several composition mechanisms can be used. For example, SEES and USES allow different level of read-only access, INCLUDES allow to call operations of accessed component in the accessing one and IMPORTS replaces INCLUDES in implementations. These mechanisms are usually defined right after the CONSTRAINTS or REFINES clause.

3.1 Event-B

In the late 1990s a development of a new version of B-Method, called *Event-B* [2], started. Event-B was meant to be a reinvention of B-Method (now also called the classical B), based on existing experiences with the practical use of B and a wide variety of research results related to B. It has a broader scope – it is intended for computer system modelling and development in general and is not only meant for software. Specifications are called models and composition is possible via SEES and EXTENDS mechanisms. We have two types of specification components in Event-B: *Context* with sets, constants and their properties and *Machine* with everything else. Machines can be refined, and refined components are called machines, too. Operations are replaced by events and the initialisation is now one of them. Event-B uses a modified version of B-language. Most of GS have been dropped and each event has the form

$$\text{any } v \text{ where } E \text{ then } S \text{ end,}$$

where v is a list of local variables, E is a list of predicates, called guards and S is a list of (possibly multiple and non-deterministic) assignments, called actions. All its guards have to hold for an event to be executable (enabled) and when executed all its actions are run at once. On the other hand, there are some new additions to B-language that allows one to specify names and additional properties of specification components and their parts. The concept of refinement has been modified, too; in Event-B it is possible to refine one event into several events.

One may wonder how a sequential program can be described in Event-B without the sequential composition, conditional statements and loops. But the general model of an Event-B model execution is such that all its events, except of the initialisation, are executed in a loop and the loop terminates if no event is enabled. If there are more enabled events, one of them is selected non-deterministically. So, by a careful design of guards and actions we can ensure that events of a model will be executed in desired order. This is covered in more detail in [2].

4 Petri Net to B-Machine Transformation

The transformation has been originally designed for a Turing-complete low-level type of PN, called Evaluative Petri Nets (EvPN). As the type of PN used in our case study is PT nets, we present here a simplified version of the original mapping, namely the mapping π from the class PT_{cl} of PT nets to the class PT_1BM_{cl} of PT-like B-machines (Definition 1). The structure of PT-like B-machine (PT_1BM) is given in (7). In the resulting PT_1BM M , $M = \pi(N)$, there will be one state variable sv_i for each place p_i from the PT net N and one operation op_j for each transition t_j from N .

Definition 1. Let N be a PT-net $N=(P,T,pre,post,m_0)$, where $P=\{p_1, \dots, p_k\}$, $T=\{t_1, \dots, t_n\}$, and π be a mapping $\pi : PT_{cl} \rightarrow PT_1BM_{cl}$. Then the image of N under π is the PT-like B-machine M , $M = \pi(N)$, $M \in PT_1BM_{cl}$, with the structure

```

MACHINE M
VARIABLES  $sv_1, \dots, sv_k$ 
INVARIANT  $sv_1:NATURAL$  & ... &  $sv_k:NATURAL$ 
INITIALISATION  $sv_1 := iv_1 || \dots || sv_k := iv_k$ 
OPERATIONS
   $op_1 = SELECT PCond_1 THEN Sub_1 END;$ 
  ...
   $op_n = SELECT PCond_n THEN Sub_n END$ 
END

```

(7)

and elements defined as follows:

$$\forall i(1 \leq i \leq k) : iv_i = m_0(p_i) \quad (8)$$

$$\forall j(1 \leq j \leq n) : Pcond_j = prc(p_1, t_j) \& \dots \& prc(p_k, t_j) \quad (9)$$

$$\forall p, t (p \in P, t \in T) : prc(p, t) = \begin{cases} \pi_p(p) \geq pre(p, t) & \text{if } p \in^* t \\ \text{TRUE} & \text{if } p \notin^* t \end{cases} \quad (10)$$

$$\forall j(1 \leq j \leq n) : Sub_j = asg(p_1, t_j) || \dots || asg(p_k, t_j) \quad (11)$$

$$\forall p, t (p \in P, t \in T) : asg(p, t) = \begin{cases} \pi_p(p) := \pi_p(p) - pre(p, t) + post(p, t) & \text{if } p \in^* t \cup t^* \\ \text{skip} & \text{if } p \notin^* t \cup t^* \end{cases} \quad (12)$$

The π_p is an auxiliary mapping:

$$\pi_p : P \rightarrow \{sv_1, \dots, sv_k\}, \forall i(1 \leq i \leq k) : \pi_p(p_i) = sv_i \quad (13)$$

The bisimilarity between N and $\pi(N)$ is not hard to see. The construction of the INITIALISATION clause in (7) and the formula (8) ensure that the initial value of each sv_i will be the same as $m_0(p_i)$. In op_j the predicate $PCond_j$, specified according to (9) and (10), is similar to the enabling condition (3) and GS Sub_j ,

defined by (11), (12), is equivalent to the new marking computation formula (4) (both for t_j). The SELECT GS is used because it is not executable when its condition ($PCond_j$ here) is false.

4.1 B-Machine for RW Problem

The PT-like B-machine `RWlimited`, transformed from the net in Fig. 1 by the mapping π , is shown in Fig. 2. In the machine we named variables and

```

MACHINE RWlimited
VARIABLES writersIn, sem, readersIn, freeCap
INVARIANT
  writersIn:NATURAL & sem:NATURAL & readersIn:NATURAL &
  freeCap:NATURAL
INITIALISATION
  writersIn := 0 || sem := 10 || readersIn := 0 || freeCap := 10
OPERATIONS
wrEnter = SELECT sem >= 10 & freeCap >= 1 THEN
  writersIn:=writersIn+1 || sem:=sem-10 || freeCap:=freeCap-1 END;
wrLeave = SELECT writersIn >= 1 THEN
  writersIn:=writersIn-1 || sem:=sem+10 || freeCap:=freeCap+1 END;
rdEnter = SELECT sem >= 1 & freeCap >= 1 THEN
  sem:=sem-1 || readersIn:=readersIn+1 || freeCap:=freeCap-1 END;
rdLeave = SELECT readersIn >= 1 THEN
  sem:=sem+1 || readersIn:=readersIn-1 || freeCap:=freeCap+1 END
END

```

Figure 2
B-machine `RWlimited`

operations in the same way that places and transitions are named in Fig. 1. Statements “skip” and “TRUE” are omitted as for each generalized substitution S it holds that $S||\text{skip} \equiv S$ and for each predicate P that $P \wedge \text{TRUE} \equiv P$. The symbol “:” stands for “belongs to” and “NATURAL” is the set of natural numbers.

4.2 Transformation to Event-B

The concept of events in the Event-B model being executed in a loop while at least one of them is executable is essentially the same as the original concept of Petri net execution: Petri net is also firing transitions until none of them are enabled. And if more transitions are enabled simultaneously, one of them is selected randomly and fired. To adjust our transformation for Event-B we just need to rename operations to events, delete “||” and “^” symbols, add names for predicates and actions, replace SELECT by where and move the initialisation to events. We will not define the transformation formally here; we only show how the Event-B version of `RWlimited` looks like (Fig. 3).

```

machine RWlimitedEvB
variables writersIn sem
         readersIn freeCap
invariants
  @inv1 writersIn : NATURAL
  @inv2 sem : NATURAL
  @inv3 readersIn : NATURAL
  @inv4 freeCap : NATURAL
events
  event INITIALISATION
  then
    @act1 writersIn := 0
    @act2 sem := 10
    @act3 readersIn := 0
    @act4 freeCap := 10
  end

  event wrEnter
  where
    @grd1 sem >= 10
    @grd2 freeCap >= 1
  then
    @act1 writersIn :=
      writersIn + 1
    @act2 sem := sem - 10
    @act3 freeCap := freeCap-1
  end

  event wrLeave ...
  event rdEnter ...
  event rdLeave ...
end

```

Figure 3

Event-B machine RWlimitedEvB

As it can be seen, only the then...end part of an event is mandatory. The where...then...end command is semantically identical to the SELECT GS. Only INITIALISATION and wrEnter events are shown as the rest is created in the same way.

5 Application in Software Development

The form of operations introduced in Definition 1 is perfect for an analysis of Petri nets by means of B, for example to prove deadlock freeness [16]. But it is not good for software development as the SELECT GS is not feasible when its condition doesn't hold. And only completely feasible operations can be refined. Because of this, when using PT₁BM for software development we replace the form of op_j from (7) by (14) or (15). The form (15) is used if there is a need to report a success of corresponding state change back to a caller of op_j .

$$op_j = \text{IF } PCond_j \text{ THEN } Sub_j \text{ END} \quad (14)$$

$$ok \leftarrow op_j = \text{IF } PCond_j \text{ THEN } Sub_j \mid ok := \text{TRUE} \quad (15) \\ \text{ELSE } ok := \text{FALSE} \text{ END}$$

This replacement doesn't change the bisimilarity relation between markings of N and states of $\pi(N)$ as the state of $\pi(N)$ (i.e. the values of its state variables) is changed by op_j only if $PCond_j$ is true. If $PCond_j$ is false, op_j is executed but doesn't change the state of $\pi(N)$ at all.

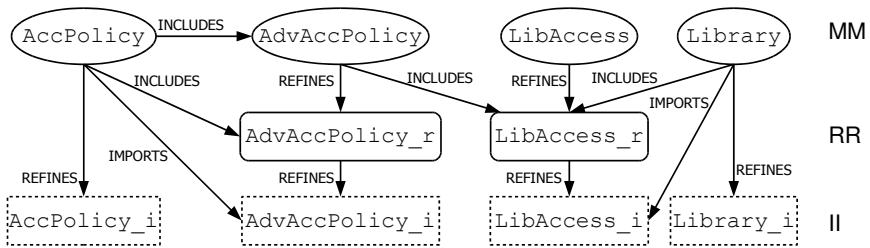


Figure 4

Components of B specification case study

In the rest of this section we present a case study that demonstrates how a B-machine, obtained from a Petri net, can be refined to a more feature-rich form and how this form can be used in other specification components in B. The structure of our specification is shown in Fig. 4. The machine translated from PT net is *AccPolicy*, which is in fact a slightly modified version of *RWlimited*. This is then included (imported) into the *AdvAccPolicy* machine, its refinement *AdvAccPolicy_r* and implementation *AdvAccPolicy_i*, in order to define a more sophisticated access policy component based on the limited RW problem solution. The *Library* machine represents shared contents and *LibAccess* with its refinement and implementation provide access to the shared contents using the policy defined by *AdvAccPolicy*.

The *AccPolicy* (Fig. 5) primarily differs from *RWlimited* in that it uses the form (15) for operations and that the abstract type *NATURAL* is replaced by an implementable type *NAT*. The second modification is an introduction of the parameter *cap*, which represents the capacity of the library and replaces the value “10” from *RWlimited*. This makes the machine more usable without affecting any of its properties. Finally, the third change is an addition of formulas equivalent to (5) and (6) to its invariant (in italic in Fig. 5). This addition was necessary for proving that variables of the machine will not exceed the limit of the type *NAT*. Fig. 5 doesn’t show bodies of *rdEnter* and *rdLeave*, as they are similar to those of the previous operations.

```

MACHINE AccPolicy (cap)
CONSTRAINTS cap:NAT & cap>0
VARIABLES writersIn, sem, readersIn, freeCap
INVARIANT
  writersIn:NAT & sem:NAT & readersIn:NAT & freeCap:NAT &
  writersIn+freeCap+readersIn=cap & cap*writersIn+sem+readersIn=cap
INITIALISATION
  writersIn := 0 || sem := cap || readersIn := 0 || freeCap := cap
OPERATIONS
ok<--wrEnter =
  IF sem >= cap & freeCap >= 1 THEN

```

```

    writersIn:= writersIn+1 || sem:= sem-cap || freeCap:=freeCap-1
    || ok:=TRUE
  ELSE ok:=FALSE END;
ok<--wrLeave =
  IF writersIn >= 1 THEN
    writersIn:= writersIn-1 || sem:= sem+cap || freeCap:= freeCap+1
    || ok:=TRUE
  ELSE ok:=FALSE END;
  ok<--rdEnter = ... END;
  ok<--rdLeave = ... END
END

```

Figure 5

B-machine AccPolicy

The crucial difference between `AccPolicy` and `AdvAccPolicy` (and corresponding refined components) is that the latter contain variables `reading` and `writing`. These are used to register processes that are currently editing or reading the shared contents. Both variables are subsets of the set `PROCESSES`, which represents all processes that could possibly access the contents. One member of `PROCESSES`, stored in the `noPr` variable, is reserved for the null process. Introduction of `reading` and `writing` allowed us to check by PObs whether our advanced procedure really obeys the access policy defined by the original PT net (and `AccPolicy`): In `AdvAccPolicy` (Fig. 6) we prove that it is impossible to write and read at the sametime, and in `AdvAccPolicy_r` (Fig. 7) we show that the number of writing and reading processes is always the same as in `AccPolicy`. Related parts of their invariants are written in italic. The operation `reqRAcc` corresponds to `rdEnter`, `reqWAcc` to `wrEnter` and `leave` unites `rdLeave` and `wrLeave`. They call the corresponding operations from `AccPolicy`. The proper order of calling is established in the refinement `AdvAccPolicy_r` since it is impossible to use the sequential composition in B-machines. The `scs` output parameter indicate whether a request to access or leave the shared contents was successful and `pr` holds assigned process id. The null process (`noPr`) is returned if the access is not granted. There are three extra operations, `canRead` and `canWrite` to return process status and `getNullPr` to get the value used as the null process. The last operation is necessary for the final stage of development as it is forbidden to read variables directly in implementations.

```

MACHINE AdvAccPolicy(prCap)
CONSTRAINTS prCap:NAT & prCap>0
INCLUDES AccPolicy(prCap)
SETS PROCESSES
VARIABLES reading, writing, noPr
INVARIANT reading <: PROCESSES & writing <: PROCESSES &
  noPr : PROCESSES & reading /\ writing = {} &
  {noPr} /\ reading = {} & {noPr} /\ writing = {}
INITIALISATION reading:= {} || writing:= {} || noPr::PROCESSES

```

```

OPERATIONS
pr,scs<--reqRAcc=
  IF PROCESSES-(reading\writing\{noPr}) /= {} THEN
    ANY pp WHERE pp:PROCESSES-(reading\writing\{noPr}) THEN
      CHOICE reading := reading \ {pp} || pr:=pp OR pr:=noPr END
      || scs<--rdEnter
    END
  ELSE scs:=FALSE || pr:=noPr END;
pr,scs<--reqWAcc=
  IF PROCESSES-(reading\writing\{noPr}) /= {} THEN
    ANY pp WHERE pp:PROCESSES-(reading\writing\{noPr}) THEN
      CHOICE writing := writing \ {pp} || pr:=pp OR pr:=noPr END
      || scs<--wrEnter
    END
  ELSE scs:=FALSE || pr:=noPr END;
scs<--leave (pr) =
  PRE pr: reading\writing THEN
    IF pr:reading THEN
      CHOICE reading := reading - {pr} OR skip END || scs<--rdLeave
    ELSE
      CHOICE writing := writing - {pr} OR skip END || scs<--wrLeave
    END
  END;
yes<--canRead (pr) = PRE pr:PROCESSES THEN
  IF pr:reading THEN yes:=TRUE ELSE yes:=FALSE END
END;
yes<--canWrite (pr) = PRE pr:PROCESSES THEN
  IF pr:writing THEN yes:=TRUE ELSE yes:=FALSE END
END;
npr <-- getNullPr = BEGIN npr:=noPr END
END

```

Figure 6
B-machine AdvAccPolicy

In Fig. 6 and the following ones the symbol “<:” means “is subset or equal”, “\ /” is the set union, “/\” the set intersection, “{ }” the empty set and “{ x }” is a set with x as its only member. The symbol “/=” stands for “not equal” and “xx: : SS” is a special kind of the ANY GS with the meaning “assign any arbitrary selected value from a set SS to a variable xx”.

```

REFINEMENT AdvAccPolicy_r(prCap)
REFINES AdvAccPolicy
INCLUDES AccPolicy(prCap)
VARIABLES reading, writing, noPr
INVARIANT card(writing)=writersIn & card(reading)=readersIn
INITIALISATION reading:= {}; writing:= {}; noPr::PROCESSES

OPERATIONS
pr,scs<--reqRAcc=
  IF PROCESSES-(reading\writing\{noPr}) /= {} THEN
    VAR acd,pp IN

```

```

acd <--rdEnter;
pp::PROCESSES-(reading\writing\{noPr});
IF acd=TRUE THEN
  reading := reading \ {pp}; pr:=pp; scs:=TRUE
ELSE scs:=FALSE; pr:=noPr END
END
ELSE scs:=FALSE; pr:=noPr END;
pr,scs<--reqWAcc=
IF PROCESSES-(reading\writing\{noPr}) /= {} THEN
VAR acd,pp IN
  acd <--wrEnter;
  pp::PROCESSES-(reading\writing\{noPr});
  IF acd=TRUE THEN
    writing := writing \ {pp}; pr:=pp; scs:=TRUE
  ELSE scs:=FALSE; pr:=noPr END
  END
ELSE scs:=FALSE; pr:=noPr END;
scs<--leave (pr)=
IF pr: reading\writing THEN
VAR acd IN
  IF pr:reading THEN
    acd <--rdLeave;
    IF acd=TRUE THEN reading := reading - {pr}; scs:=TRUE
    ELSE scs:=FALSE END
  ELSE
    acd <--wrLeave;
    IF acd=TRUE THEN writing := writing - {pr}; scs:=TRUE
    ELSE scs:=FALSE END
  END
END
ELSE scs:=FALSE END;
yes<--canRead (pr)= IF pr:PROCESSES THEN
  IF pr:reading THEN yes:=TRUE ELSE yes:=FALSE END
ELSE yes:=FALSE END;
yes<--canWrite (pr)= IF pr:PROCESSES THEN
  IF pr:writing THEN yes:=TRUE ELSE yes:=FALSE END
ELSE yes:=FALSE END;
npr <-- getNullPr = BEGIN npr:=noPr END
END

```

Figure 7

Refinement AdvAccPolicy_r

```

MACHINE Library
VARIABLES contents
INVARIANT contents:NAT
INITIALISATION contents:=0
OPERATIONS
  lcnt <-- read = lcnt:=contents;
  write(ncnt) = PRE ncnt:NAT THEN contents:=ncnt END
END

```

Figure 8

B-machine Library

The machine `Library` (Fig. 8) represents shared contents that is accessed by processes and defines operations over it. For the sake of simplicity, the content is only a natural number here.

An access to the shared contents is provided by the `LibAccess` (Fig. 9) component and its refinement. In fact, `LibAccess` defines only heads of operations and the type `RETCODE`, while the real functionality is encoded in its refinement `LibAccess_r` (Fig. 10). The reason why we have to use the refinement is the restriction on the use of “;”, again.

```
MACHINE LibAccess (lCap)
CONSTRAINTS lCap:NAT & lCap>0
SETS RETCODE={ok,failEnter, failLeave, failWrite}
OPERATIONS
  cnt, rc<--libRead= BEGIN rc::RETCODE || cnt::NAT END;
  rc<--libWrite (cnt)=PRE cnt:NAT THEN rc::RETCODE END
END
```

Figure 9

B-machine `LibAccess`

To read the contents, one has to call the operation `libRead`, which first checks whether it is possible to read by calling `reqRAcc` from `AdvAccPolicy` then reads (by calling `read` from `Library`) and, finally, calls `leave` to announce that the reading is over. For editing the `libWrite` operation is used, which works in the similar way.

We decided to not describe the four implementation components of our case study in this paper as they are similar to the corresponding refinements or machines.

```
REFINEMENT LibAccess_r (lCap)
REFINES LibAccess
INCLUDES AdvAccPolicy(lCap), Library
OPERATIONS
  cnt, rc<--libRead=
    VAR acd, prId IN
      prId,acd <--reqRAcc;
      IF acd=TRUE & prId /=noPr THEN
        cnt<--read; acd <--leave(prId);
        IF acd=TRUE THEN rc:=ok ELSE rc:=failLeave END
      ELSE cnt:=0; rc:=failEnter END
    END;
  rc<--libWrite (cnt)=
    IF cnt:NAT THEN
      VAR acd, prId IN
        prId,acd <--reqWAcc;
        IF acd=TRUE & prId /=noPr THEN
          write(cnt); acd <--leave(prId);
```

```
IF acd=TRUE THEN rc:=ok ELSE rc:=failLeave END
ELSE rc:=failEnter END
END
ELSE rc:=failWrite END
END
```

Figure 10
Refinement LibAccess_r

6 Utilization in Concurrent Environment

While the verification mechanisms of B proved to be sufficient to ensure that properties of the design (`AccPolicy` machine) are maintained in components refining and directly including it, we still cannot call the resulting implementation safe for use in a concurrent environment. B doesn't take concurrency into account, so to improve the situation, extensions to both its language and tools are necessary. The B-language can be extended by annotations allowing one to label operations that cannot be run in parallel at all or within some group of operations. Then modified compilers for B will translate these annotations to equivalent constructs of target programming languages. However, one critical question remains open: *Can the process of annotating of operations and of verifying their consistency be automated?*

The use of machines translated from Petri nets provides a partial answer here: Assuming that all concurrency issues are treated in machines transformed by π and that these machines are separately implemented (like `AccPolicy` in `AccPolicy_i`), we can automatically annotate operations in them and mark all operations that directly or indirectly call their operations as candidates for concurrent execution. However, it is very probable that the final decision about the calling operations will require certain amount of manual checking.

The automatic annotating of machines translated from PN can be easily implemented, obeying the following rule: operations created from transitions with common pre-places cannot be run at once. This is because there is a risk that their enabling conditions (*PCond* in (7)) will be evaluated at once and, as they read some common variables, will lead to faulty execution of their bodies. In machines in Fig. 2 and Fig. 5 `wrEnter` and `rdEnter` are such operations as their counterparts in Fig. 1 have common pre-places *sem* and *freeCap*. Separate and careful development of these machines is critical: we can introduce new variables and add new functionality to its refinements and implementation, but what was defined in the machine must stay intact.

Regarding the calling operations, the question is whether they call those originated from Petri nets properly. In our case study, the calling ones can be found in `AdvAccPolicy(_r)` (the first three ones) and in `LibAccess_r` (both). In the case of `AdvAccPolicy_r`, its invariants and corresponding POBs help to resolve the situation and they can be allowed to run concurrently. Operations from `LibAccess(_r)` are also the calling ones as they call the first three from `AdvAccPolicy`, but invariants and POBs are of no help here. This is because operations from `AdvAccPolicy` are called in sequence in `libRead` and `libWrite` and POBs only check states before and after an operation execution. Again, the situation can be improved by introducing annotations to define order of execution of operations in machines obtained from PN and a procedure that will check whether this order is maintained within every calling operation.

7 Related Work

The problem of Petri nets and B-Method integration attracted other researchers as well, but, to our knowledge, all of these works have been published after the initial version of our transformation [13] and approach the problem from a more or less different perspective.

The work [3] presents an encoding of PT nets and high-level PN (HLPN, tokens have values assigned in these types of PN) to the Event-B language. Each Petri net is represented by a specification consisting of two machines. The first machine contains constants, sets and variables that define the concrete Petri net. The second one contains one event for transition firing and in the case of HLPN also events for actions associated with places and transitions. The second machine is identical for all PT nets. The author uses the Atelier B version of Event-B syntax, which is much closer to the classical B-language than to the “official” version, presented in [2]. The essential difference between our approach and [3] is that we translate each transition to a separate operation (event). This is more natural and usable for software development. The author of [3] claims that his primary motivation is analysis; however our practical experience shows that the data representation chosen in [3] is usually more difficult for the Atelier B prover to handle than the one used in our approach.

In [11, 12] a mapping of a subset of the SYNTESIS scripting language, which is similar to HLPN, is presented. The target specification is the Refinement component of B-Method. In principle, the approach is close to ours: places are mapped to variables and transitions to operations. What differs is that variables in [11, 12] are sets and structure of operations is more complicated as high-level PN have individualised tokens. The purpose of the mapping is an analysis of scripts in SYNTESIS by means of B-Method. A similar transformation is used in a railway safety-related case study in [7] to translate a simple Coloured Petri net (a kind of

HLPN) specification to the Event-B language with the Atelier B syntax. The B specification in [7] uses a special machine that implements multi-sets and the purpose of this transformation is a further development of the specified system. The mapping of PN, defined in [13, 15] and used in this paper, can be quite easily modified for HLPN by adopting principles of these two approaches. However, we found the PT nets and other PN types with undistinguishable tokens (so-called low-level PN) more suitable for the role of the most abstract specification of a development. They provide analytical methods that are only hardly usable for HLPN (e.g. derivation of invariants) and an additional functionality can be added later, on the side of B-Method. On the other hand, we are aware that utilization of HLPN can lead to significant reduction in size of PN models and allow parameterisation of models that is impossible for low-level PN.

There have been also researches that combined B with other formal methods for specification of concurrent systems, primarily with the Communicating Sequential Processes (CSP) [6]. The most significant approaches are *csp2B* [4] and *CSP||B*. Both support certain subsets of CSP. The *csp2B* provides a method of transformation of CSP specifications to B-language. The transformation translates implicit states of CSP processes to variables and process events to operations and is supported by the *csp2B* tool. The *CSP||B* is a method that combines specifications in CSP and B-language in such a way that CSP controllers manage concurrently running B-machines. *CSP||B* has been introduced in [21] and further developed in subsequent works, such as [22] or [23] where it was adjusted for Event-B. Both approaches also deal formally with refinement of translated or combined specifications, so their results will be considered when designing mechanisms for maintaining some consistency aspects of B-machines created by our transformation.

Conclusions

The approach to implementation of PN specifications, shown here, looks promising and brings qualities that B doesn't provide out of the box, namely some control over concurrency aspects. PN have an easy-to-understand graphical form, so they may be more attractive for developers to use than text-based methods for concurrent systems, such as CSP. By the mapping π we have been able to properly transfer a design created and verified on the Petri nets' side to B-Method. However, as B-Method has been designed solely for development of sequential systems, its verification system is only of limited use when checking concurrency-related aspects of translated PN and components that access or refine them. Possible solution of this problem is outlined in section 6 and its realization should be one of the primary tasks for future research and development. The implementation platform will most probably be the BKPI compiler [17], developed at the home institution of authors, which can parse specifications in B-language and translate implementation components to Java and C#. Lessons learned by other teams when integrating other formal methods for concurrent systems with B (e.g. *csp2B* and *CSP||B*) will certainly be considered here. On the

PN side the demonstrated approach can also benefit from cooperation with other formalisms, for example with the linear logic [20] or artificial intelligence concepts such as cognitive maps, including their fuzzy variants [24].

Considering the strong relation between computational concepts of Petri nets and Event-B, it will also be worth to explore possibilities of incorporation of transformed PN to Event-B models. It should be also useful to integrate Petri nets in similar way to other industrially-used formal methods for software development, such as VDM or language Perfect. For the reasons mentioned in the previous section we also plan to extend the mapping π to support core features of HLPN. It is relatively easy to specify such an extension and prove its correctness, provided that the language used to handle tokens in HLPN is a subset of the B-language.

The transformation of the Evaluative PN and PT nets has been already implemented in the experimental mFDTE/PNtool2 software, which is available by request from the authors.

Acknowledgement

This work was supported by KEGA grant project No. 050TUKE-4/2012: “Application of Virtual Reality Technologies in Teaching Formal Methods”.

References

- [1] J. R. Abrial: *The B-Book: Assigning Programs to Meaning*, Cambridge University Press, Cambridge, 1996
- [2] J. R. Abrial: *Modeling in Event-B: System and Software Engineering*, Cambridge University Press, Cambridge, 2010
- [3] J. Ch. Attiogbé: *Semantic Embedding of Petri Nets into Event B*, In: *International Workshop on Integration of Model-based Methods and Tools IM FMT'09 at IFM'09 Conference*, Düsseldorf Germany, February 2009, available from: http://pagesperso.lina.univ-nantes.fr/info/perso/permanents/attiogbe/B_Petri/
- [4] M. J. Butler: *csp2B: A Practical Approach to Combining CSP and B.*, *Formal Aspects of Computing*, Vol. 12, 2000, pp. 182-196
- [5] H. Ehrig, W. Reisig, G. Rozenberg, H. Weber (Eds.): *Petri Net Technology for Communication-based Systems*, LNCS vol. 2472, Springer, 2003
- [6] C. A. R. Hoare: *Communicating Sequential Processes*, Prentice Hall, ISBN 0-13-153289-8, 1985, available from: <http://www.usingcsp.com/>
- [7] F. Defosse, P. Bon, S. Collart-Dutilleu: *Taking Advantage of some Complementary Modelling Methods to Meet Critical System Requirement Specifications*, In: *Safety and Security in Railway Engineering*, WIT Press, 2010, pp. 119-128

-
- [8] J. Desel, W. Reisig: Place/Transition Petri Nets. In: W. Reisig and G. Rozenberg (eds.) Petri Nets, LNCS Vol. 1491, Springer, 1998, pp. 122-173
- [9] E. W. Dijkstra: A Discipline of Programming, Prentice Hall, Englewood Cliffs, ISBN 0-13-215871-X, 1976
- [10] Š. Hudák: Reachability Analysis of Systems Based on Petri Nets, Elfa, Košice, 1999
- [11] L. A. Kalinichenko, S. A. Stupnikov, N. A. Zemtsov: Extensible Canonical Process Model Synthesis Applying Formal Interpretation. In: Proc. of the East-European Conference ADBIS'05, Talin, Estonia, September 2005, pp. 183-198
- [12] L. A. Kalinichenko, S. A. Stupnikov, N. A. Zemtsov: Synthesis of the Canonical Models for the Integration of Heterogeneous Information Resources. M.: IPI RAN, 2005, 87 pp (In Russian)
- [13] Š. Korečko, Š. Hudák: Implementing Petri nets via B-Method. In: Proc. of 6th International Scientific Conference Electronic Computer and Informatics, ECI 2004, September 2004, pp. 103-110
- [14] Š. Korečko, Š. Hudák, S. Šimoňák: Analysis of B-machine based on Petri Nets, Proceedings of CSE 2008 International Scientific Conference on Computer Science and Engineering, September 2008, pp. 24-33
- [15] Š. Korečko: From Petri Nets to B-Method, Technical report DCI 1/2009, Department of Computers and Informatics, Faculty of Electrical Engineering and Informatics, Technical University of Košice, 2009, available from: http://hornad.fei.tuke.sk/~korecko/pblctns/trEvPN_B.pdf
- [16] Š. Korečko, B. Sobota: Building Parallel Raytracing Simulation Model with Petri Nets and B-Method, In: Proc. of the 7th EUROSIM Congress on Modelling and Simulation, Prague, Czech Republic, 2010, ISBN 978-80-01-04589-3, 7pp
- [17] Š. Korečko, M. Dancák: Some Aspects of BKPI B Language Compiler Design, Egyptian Computer Science Journal, Vol. 35, No. 3, 2011, pp. 33-43
- [18] L. Madarász, J. Vaščák, R. Andoga, T. Karol: Decision Making, Complexity and Uncertainty: Theory and Practice, elfa s.r.o., Košice, 2010, ISBN 978-80-8086-142-1 (in Slovak)

- [19] L. Madarász, J. Živčák (Eds.): Aspects of Computational Intelligence: Theory and Applications, Topics in Intelligent Engineering and Informatics, Vol. 2, Springer, 2013
- [20] D. Mihályi, V. Novitzká, V. Slodičák: From Petri Nets to Linear Logic, In: Proc. of CSE'2008, Stará Lesná, September 2008, pp. 48-56
- [21] S. Schneider, H. Treharne: How to Drive a B Machine. In: Proc. of ZB 2000, LNCS Vol. 1878, Springer, 2000, pp. 188-208
- [22] S. Schneider, H. Treharne: Verifying Controlled Components. In: Proc. of IFM 2004, LNCS Vol. 2999, Springer, 2004, pp. 87-107
- [23] S. Schneider, H. Treharne, H. Wehrheim: A CSP Approach to Control in Event-B. In: Proc. of IFM 2010, LNCS Vol. 6396, Springer 2010, pp. 260-274
- [24] J. Vaščák, L. Madarász: Adaptation of Fuzzy Cognitive Maps – a Comparison Study, Acta Polytechnica Hungarica, Vol. 7, No. 3, 2010, pp. 109-122

A Flexible System for Request Processing in Government Institutions

Miroslav Zarić, Milan Segedinac, Goran Sladić, Zora Konjović

University of Novi Sad, Faculty of Technical Sciences,
Trg Dositeja Obradovića 6, 21000 Novi Sad, Serbia
E-mail: miroslavzaric@uns.ac.rs, milansegedinac@uns.ac.rs, sladicg@uns.ac.rs,
ftn_zora@uns.ac.rs

Abstract: This paper presents a solution for an electronic document handling system for government institutions. The proposed solution introduces a new system aimed at handling various administrative requests with minimal disruption to standard end user habits as well as minimal requirements in terms of end user training. During the development and testing phase, chosen software architecture has proved itself as robust and adaptable to requested changes. As the end user submits a request from a familiar office suite environment, usual problems, such as refusal to engage with new software and complaints about a steep learning curve are avoided. The approval of requests is executed through the standard web application. The system relies on well-defined user roles and an established workflow. The proposed solution can easily be adopted for handling various types of requests, as long as their processing fits into the deployed workflow. This system is designed with specific intention to be a low-barrier entry electronic document management system for existing administrative workers. Use of a standard office application suite for document submission allows existing users easy transition. This eliminates the need for user training and consequently reduces the disruption to the normal workflow.

Keywords: document management; workflow management; e-government; active documents

1 Introduction

E-government aims at enhancing the efficiency of governmental administrative processes, improving the quality of their services and reducing operational costs through the application of ICT (Information and Communication Technology) technologies. In this paper we present a system for handling administrative requests in a digital form (e-requests).

One of the trends in the development of e-government systems is to put emphasis on electronic document management (EDM) systems. EDM systems deal with the management of documents [1]. The document may be a part of a particular

business process, in the sense that it requires access to the document by individual staff undertaking separate activities according to a particular sequence guided by some procedural rules [2]. Workflow Management Coalition defines workflow as the computerized facilitation or automation of a business process, in whole or in part [2]. In computer science literature, business process and workflow terms are often used interchangeably; in this paper we regard them as synonyms.

Workflow management system (WfMS) is a system that completely defines, manages and executes workflows through the software in which the order of execution is driven by a computer representation of the workflow logic [2]. One of the main advantages of WfMSs is moving the focus from the automation of single process activity, to the overall management and improvement of the business processes. EDM systems are usually implemented using the document-oriented WfMS. Due to their advantages, government agencies tend to implement their services on document-oriented workflow platforms. The problem of document processing has long been recognized as a critical aspect in the enterprise productivity [3, 4, 5]. In decentralized working environments, where many people affect the contents of documents, efficient collaboration on document editing is a key feature, and a collaborative environment must take care of collisions that can arise from simultaneous access to the documents. This problem has been the focus of many research papers [6, 7, 8, 9, 10, 11, 12].

We propose an integrated system with the aforementioned characteristics through a combination of different, readily available, technologies. A standard word processing office application is used for the creation and direct submission of requests to the processing web application. Therefore, users continue to use the same application they have used for creating the printed request forms. The web application serves as a central module and as a standard access point for users involved in request processing and approval. A workflow engine is embedded in the web application. Access to the system is controlled by an authentication and authorization modules. Internal document format is XML-based, allowing for future expansions. We have observed custom business processes in different government institutions, and a case study described in this paper is developed for the local provincial government.

The rest of the paper is structured as follows. Section 2 reviews the related work. Section 3 presents basic motivations and requirements. Process description for chosen case-study is presented in Section 4. The application architecture overview is given in Section 5. At the end of the paper, a conclusion is given with some outlines for further development.

2 Related Work

This section covers two topics: research on document-based workflow systems and research on the application of office documents enriched with software components - *active documents*.

In [13], authors propose a methodology for developing hypermedia information systems on the basis of document-based workflow. The proposed methodology focuses on corporate systems that require the capability of handling complex business functions. It adopts a document-based perspective consistently through all phases. The work reported in [14, 15] addresses the problem of creating an information infrastructure and services for distributed and virtual organizations, and, particularly, the integration of two key enabling technologies, namely workflow and document management. Paper [5] proposes an XML document centric workflow management system that exploits the advantages of the XML documents, while having the full functionality of workflow management system to execute other activities. Paper [16] proposes a framework for document-driven workflow systems that requires no explicit control flow and the execution of the process is driven by input documents. The solution presented in [17] extends web-service based workflow engines with human interaction via email. A document-based dynamic workflow system, that is particularly suitable for agile business processes in which required tasks and their sequence flow may need to be determined dynamically, is proposed in [18]. Experiences in using Java Business Process Management (jBPM) for document flow are given in [19].

Any document workflow system will face the challenge of collaborative editing of document content. As stated in [12]: "Collaborative editing enables a group of people to edit documents collaboratively over a computer network." The purpose of collaboration is to achieve a common goal. Most group editing tools are using the copy/modify/merge paradigm, supported by three methods executed on a shared repository storing multi-versioned objects: checkout, commit and update. In collaborative editing two major principles of reconciling different versions of a document have become predominant: state-based merging approaches often used in versioning systems such as CVS [20], and Subversion [21], and operation based approach [22]. In recent years, since XML has become a de-facto standard format for representing structured data, special attention is given to collaborative editing of XML documents. Usage of XML documents presents a challenge and an opportunity, since most conventional operation based approaches (algorithms) such as dOPT [6], GOT [23], GOTO [24], SOCT2 [25] and similar [26, 27], view documents as linear structure. An approach to collaboration over hierarchical documents, treeOPT algorithm as well as asyncTreeOPT (for asynchronous editing) is described in [12]. In [28] collaborative editing of XML documents (in peer-to-peer environments) has been further discussed.

Term *active document* designates a document that, besides the data and structure, contains some software components (e.g., macros or scripts) [29]. Since it

combines data with processing components, an active document can embed processes such as data retrieval, data acquisition, transactions, workflows or documents archiving [30]. An overview of several case studies in which active documents are used follows.

In the United States Patent and Trademark Office (USPTO) report [31], the usage of an active Word document named *Electronic Filing System – Application Body eXtensible Markup Language, EFS-ABX*, was proposed for the creation of patent application specification in XML format. In the report the following benefits of using active Word document were identified: 1) ease of use, 2) simplified image management, and 3) simplified client side workflow. In the report [32], National Institute for Health and Clinical Excellence (NICE) has proposed active Microsoft (MS) Word 2007 documents for the creation of guidance documents in XML format. The following advantages of active MS Word 2007 documents have been identified: 1) ease of the manipulation with XML files, 2) many people have the appropriate Microsoft Office skills, 3) there is a degree of backward compatibility to MS Word 2003. Paper [33] describes an active Word document that creates an environment for editing the material in the publishing industry. The paper puts emphasis on the advantages of using XML. The research presented in the paper [34] is an example of applying active Word documents in medical practices. The paper states that the most important benefit of using Word for record keeping in medical practice is the fact that most of the doctors are already familiar with Word, so there is no need for additional training.

3 Basic Requirements and Motivation

Our case-study system is developed to improve internal e-government services for the provincial government of the Autonomous Province of Vojvodina, in the Republic of Serbia. In such an institution, there is a substantial number of documents in circulation, and their prompt handling and tracking becomes a challenging task. Furthermore, permanent storage of large quantities of paper documents, often in multiple copies, is a growing problem. These documents are commonly created using a word processing editor (commonly some office suite, usually MS Office), printed and then handed over to an employee in charge of handling specific requests. This is a starting point of a business process in which documents proceed along the chain of employees, each of them making some kind of a decision about the document and/or modification of the content. Handling requests in such a manner has not changed much for a substantial amount of time. Although this type of request processing system is common, easy to understand, and well accepted, in a digital era and e-government environment it has its shortcomings: the overall process is slow, printing a large amount of documents just for internal use is a huge waste of resources, and, as mentioned before, the storage space requirement becomes unacceptable. However, even though the

documents are already electronic at its origin, paper documents are, in some cases, still required by applicable laws or internal regulations, and they cannot be, in the near future, completely avoided and removed from the business process.

In order to alleviate some of the problems, the provincial administration was seeking an appropriate solution for electronic handling of internal requests. Such a system has to provide the same capabilities as the paper-based system, but should accelerate the whole process, automatically notify relevant participants, and make it easier for them to perform their duties. Although there are well established solutions for electronic document management, and some of them are already deployed in the provincial government, there were some special requirements that lead to the development of a specialized system. The current business model for request handling, as well as their special demands and requirements were obtained through a series of interviews with employees and managers with the following findings:

- MS Office is already in use as the standard office suite, and employees have experience with using it;
- A set of standardized request forms exists (as Word documents);
- There is an established workflow for processing internal requests;
- Regular users should experience minimal change during transition to the new system;
- The system should be able to adapt to any possible future changes in the workflow;
- The system should alert the relevant participants if a document is waiting for their attention;
- The system should allow for easy addition of new form templates;
- The system should be accessible from the local intranet.

Based on these premises and requirements, a number of different issues had to be resolved, such as document representation, appropriate document storage, appropriate way of representing the business process, and the appropriate notification of the users. After considering different options, we have come to the following conclusions:

- XML, with its inherent support for structured data, has been chosen as the format for document representation - such a choice is further supported by availability of the software for XML manipulation; In accordance with this, a native XML database will be used as the document storage module;
- It would be beneficial for the system to use MS Word to fill-in and submit electronic requests. Thus, end users would continue to use a familiar environment for filing requests. To have a modifiable process workflow, a workflow (process) engine should be used;
- Since the application core should be accessible over the intranet - it is created as a web application, and
- Apart from MS Word, other parts of this integrated system should use open-source and free software to minimize the cost of service.

A document management system, namely Alfresco, is already implemented in the provincial government institutions. However, this system is preferably used for specific purposes, usually by higher level administrative employees. On the other hand, the request processing system is intended for widespread use, as almost any administrative employee is allowed to generate a request. Alfresco is a general purpose document management system, and it has a lot of advanced functionalities, but it also takes some training for all the users to get used to it. A large base of users require additional administration in the system, with carefully crafted user groups and permissions. Since most of these functionalities are advanced, and rarely needed by ordinary users only interested in submitting the request, simplicity was the most important issue.

Although the proposed system inherits most of the features commonly present in any document management system, its main advantage is its overall simplicity. For ordinary users, creating a new request is reduced to filling out a Word document template.

All requests are transformed to a single document type – XML, simplifying later operations on the document content. Any later interaction with the system is done through a web interface. As an additional advantage, the web pages used for presenting the content to a user, are created on-the-fly by converting the request itself (in XML representation) into HTML format. Therefore, only the skeleton HTML is manually coded, while any request conforming to the defined XML schema will be properly transformed for viewing and/or editing. These two features enable easy integration of new request types to the system.

4 Process Description

Figure 1 displays the process graph in standard Business Process Modeling Notation (BPMN) notation. This graph represents a blueprint for process execution and is used to control the program execution (instead of hard coding the business logic into the application). The main concepts are nodes, transitions and tokens. Tokens are used to track the process execution. There are different types of nodes, and a *task node* is used to describe a point in the process where human intervention is required. The process execution progresses by moving the main (root) token from the start node to the end node along the possible paths defined by the graph.

One process instance (one execution of the process graph) is started when an end user submits an eRequest through the Word active document template. Users involved in the process can play different roles: *Originator, Supervisors, Director of Administration, Authorized Deputy Directors, Responsible Chief Officers, and Executors*.

choose one or more subordinate users that the request will be passed on. If *Director of Administration* assigns request to more than one of her/his *Deputies*, an implicit “dynamic forking” (when more than one approval at the same level of hierarchy is needed, but the exact number of actors is determined only at runtime) is performed, and execution path (marked with larger dashed line) is multiplied and child tokens created. The main (root) token of the process will stay in fork node until all generated child tokens are collected at the join node. The join node of this fork is presented as the last parallel gateway join node before the email *eRequest Approved Mail Notification* node.

Similar decision-making and forking is performed at the *Approval – Authorized Deputy Director* task node, when the request is assigned to multiple *Responsible Chief Officers*. The rest of the process execution is straightforward: the *Responsible Chief Officer* reviews the request, decides if it's acceptable, can approve it and pass it to his/her subordinates for execution, or can mark this part of the request handling process to be executed by himself. Finally, tasks assigned to *Executors* can only be executed. In this phase, since all necessary approvals have been obtained, the request cannot be denied final execution.

The process will make the transition to the final *eRequest Approved Mail Notification* node only when all tasks are completed. If the request has been rejected at any phase all pending tasks will be canceled upon entry to the *eRequest Rejected Mail Notification* node. After sending a mail notification to *Originator* (either with final approval and success notice, or with rejection notice) the process will enter to its final *End* state and will be archived.

Additional requests were introduced when the system went into production – the task assignment model has to be extended to support not only actors and groups, but to allow for: a) replacement for a specific user, b) reassignment of already assigned group tasks.

Replacement for specific user was needed to accommodate situations where an actor may be occupied for prolonged periods of time, and they have an opportunity to re-delegate their tasks to a registered replacement, but keep ownership of the tasks. In comparison to standard group tasks, the task stays assigned to the originally intended actor, but upon completion, the record is made that the task was performed by a replacement on their behalf. This implementation required user administration and user handling model to be extended.

The second request came into focus when it became obvious that some tasks, required to fulfill the request, can take substantial time to accomplish, and that it is possible, although rare, that one person has indeed started the task execution, but is currently unable to complete it. In the standard assignment model, tasks that were visible to the group are changed to personal tasks, when the final assignment to one actor (from the group) is performed. Other members of the group can no longer access that task, unless the assigned actor (or an administrator) returns the task to the group. Although this solution is acceptable, since the assigned actor

sometimes is not in position to do it her/(him)self, so in order to speed up the overall process execution, as well as to lower the burden on system administrators, the system is extended to allow other members of the group to see such tasks. The task is displayed alongside information to whom it is currently assigned, and when its execution was started. Other members of the group are allowed to “capture” the task and thus perform reassignment.

5 Software Architecture

In this section we'll present the global architecture of the implemented system, document structure (active documents), and software architecture of the server-side application.

5.1 Global Architecture

The global architecture of the system is presented in Figure 2. Required authentication is performed by user's operating system, wherein authentication information is stored on the LDAP (Lightweight Directory Access Protocol) server. The employee submits their request to the e-request application by using *active documents* and MS Word. An embedded macro transforms the request to XML document. Upon receiving the document, an e-request application creates an instance of the process described in the previous section and starts its execution. Users involved in request processing access the application through the web interface, and the application server consulting LDAP server performs authentication.

The server-side of the system is implemented using the Java open source technologies. The e-request application code relies on the different open source libraries such as *JBoss jBPM* workflow engine and the *Xalan XSLT* processor. The access control is performed by the *COBAC (context-sensitive access control model for business processes)* [35, 36] implementation. The received requests are stored in the *eXist* native XML database, while access control policies and workflow data are kept in the *MySQL* database. We used *Apache Tomcat* as the application server.

The system is implemented in the environment of a local area network. Access from the outside world is guarded by applied network policies. Additionally, some measures are implemented on the server side in order to protect the system from involuntary errors or malicious attacks. Wireless network access to the local network, due to the sensitivity of governmental institutions, is restricted to registered computers and users.

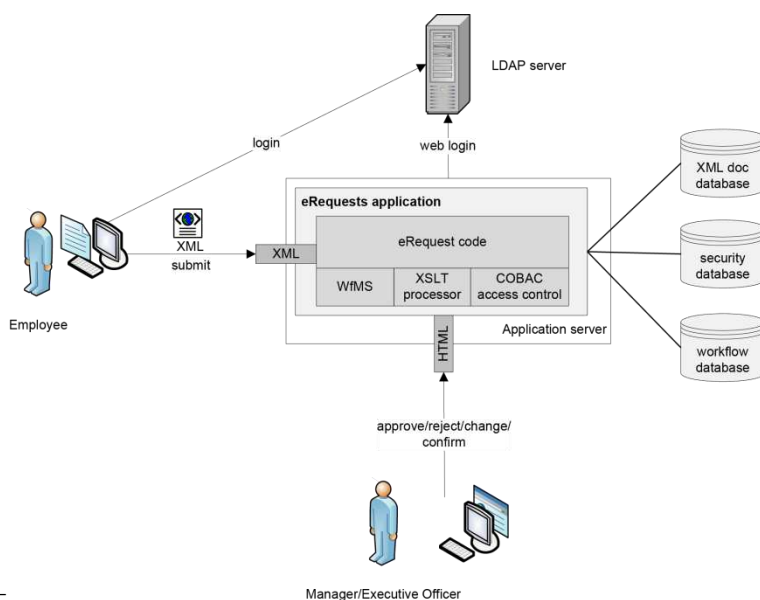


Figure 2

Global architecture

As macro-enabled Word documents (discussed in following section) are used to create requests, upon receiving the request on the server side, the XML is checked for conformance with the defined XML schema. In addition, the incoming XML string is checked for XSS-like (Cross Site Scripting) attacks. This step is necessary since XML is later transformed to HTML, and any embedded JavaScript could potentially be a threat. The SQL Injection attacks are not possible since request data is stored exclusively in the native XML database, and only process data, generated internally, is stored in the MySQL database.

Although potential for CSRF (Cross Site Request Forgery) in the restricted local network is relatively low, a proper protection is implemented on the server side. This type of attack is checked for when the request editing and/or approval phase is executed and HTTP requests are being processed.

Databases (both native XML and MySQL) are on separate servers, and access is allowed only from application server, with appropriate user credentials. Access from other networks and other computers in the local network is forbidden by applied network and server policy rules.

If outside access to the system is to be allowed in the future, it will be performed through a server in a DMZ, over an HTTPS connection. This server will be routing traffic to the application server in the local network.

5.2 Active Documents

The active documents are implemented as MS Word 2007 documents, with processing component implemented as VBA macros. Analysis of the preexisting request forms documents showed that their primary contents are: free text input fields, checkboxes, tables, and images. The active documents were designed to automate the document conversion to XML (in further text *XML requests*), according to the proposed XML Schema, and send it to the server. The overall schema is shown in Figure 3.

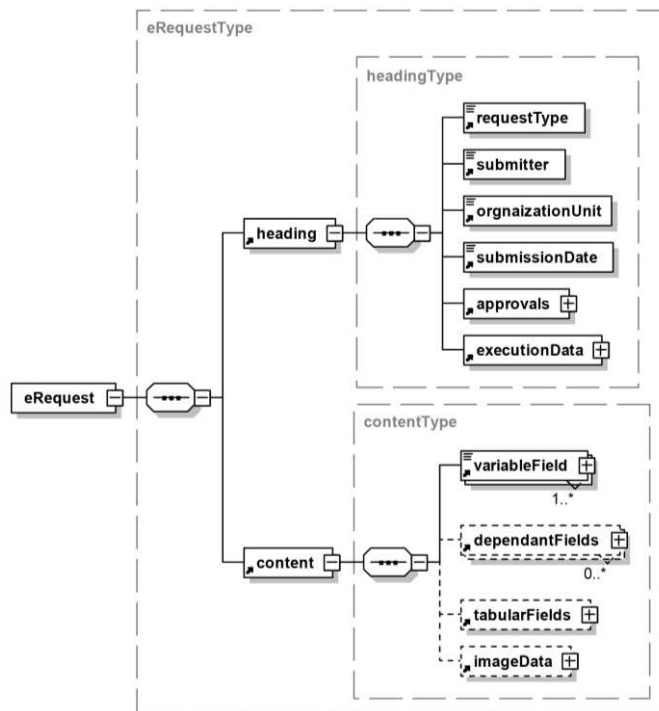


Figure 3

The overall XML Schema

Each XML request consists of two sections: *heading* and *content*. Heading contains the request submission date (*submissionDate*), the employee's data (*submitter*, *organizationUnit*), and document type (*requestType*). Other information (typed by the user into active document) is mapped to the subelements of the *content* element. When designing active documents to serve as eRequests templates, a possible solution was to use Rich Text Content Controls for free text input fields, and to map them to the XML Schema. However, such an approach tends to be inappropriate because of a vast number of forms, and the frequent need to modify them. Instead, we have simplified the documents by using two-column tables in active documents to represent text input fields. The first column contains

field names, while the second one contains field values (Figure 4). Such an approach allowed us to observe each table row as an ordered pair (*field_name*, *field_value*). Adding a new text input field to an existing form is then reduced to inserting a new row into the table. The left column is then locked to avoid accidental editing. Such an approach does not require macros to be altered for each new field.

Date:	
Time:	
Conference hall:	
Host:	
Occasion:	
Number of persons:	
Contact:	
Should be provided:	

Figure 4

Request form containing text input fields

Some forms, in addition to the text input fields, contain checkboxes. Here, a column is added to the table (Figure 5). In such a table, each row is observed as an ordered triple (*checkbox*, *field_name*, *field_value*).

<input type="checkbox"/>	Refreshments	
<input type="checkbox"/>	Lunch	
<input type="checkbox"/>	Security	
<input type="checkbox"/>	Transportation	
<input type="checkbox"/>	Parking	
<input type="checkbox"/>	Sound system	

Figure 5

Request form containing checkboxes

Some request forms contains tabular data (Figure 6). Data from tabular forms are mapped to *tabularFields* XML element, containing *rows* elements. The first *row* contains XML elements representing table columns definitions, while other table rows cells are mapped to the *variableField* elements in XML.

No.	Product name	Measuring unit	Quantity
1.	Printing paper	Package	5
2.	CD	Item	60
3.	DVD	Item	20
4.	Marker	Item	10
5.	Notebook	Item	2

Figure 6

Request form containing tabular input fields

With this approach to document processing, transformation of the request document content to XML document is achieved simply by iterating through the table rows. Additionally, some request forms can contain image elements (such as the request for printing an ID card). Therefore, it was important to support transport of image data from within the Word file to the server. To support this, Picture Content Control needs be used in the Word document, but also appropriate transformation of image binary data was needed to facilitate transport over HTTP. MS Word (2007 and higher) supports adding an optional *CustomXMLParts*. Properly bound to Picture Content Control element, it provides a Base64 representation of image binary data, which is suitable for insertion in the XML request. Upon the XML document creation, the macro sends it to the server.

5.3 Server-side Architecture

As mentioned before, Java has been used to develop server-side application. Figure 7 displays classes of the module receiving the requests sent from Word application. The central class of this module is *AcceptRequestAction* which accepts the sent XML documents. Different operations on XML documents are modeled with the *XMLUtil* class. The *LDAPService* class is used to access the employee's information (*User* class), while *COBACService* is used to perform access control as described in [35]. The *XMLDBRepository* class implements access to the native XML database. *AcceptRequestAction* uses the classes from the jBPM API to create and start a process instance, and to populate process instance with appropriate variables. The class *UserProcesses* conveys information about the processes that the user has created.

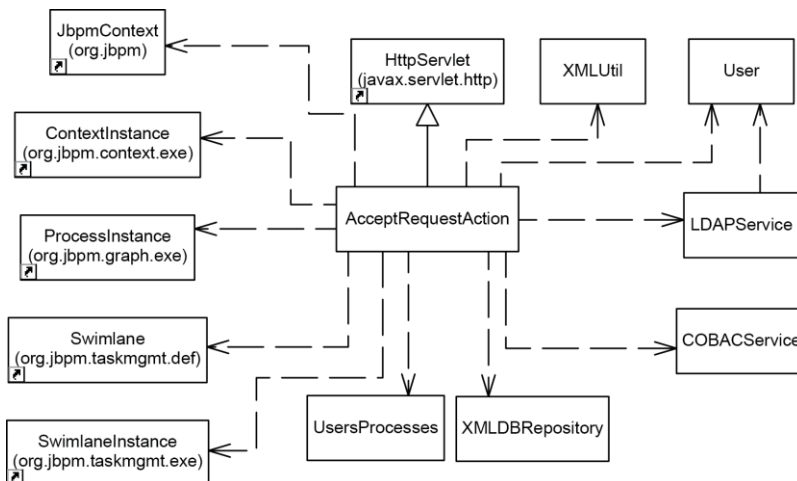


Figure 7

Classes for accepting request

Figure 8 displays classes involved in task processing, and classes involved in non-task related actions, such as searching and reviewing of requests. Since all tasks are accessed and handled through the web interface, the base class of the hierarchy – *TaskAction* – is extended from *HttpServlet* class. The class *TaskAction* contains some basic task-related functionality, and uses classes from the jBPM API to access information about the process instance. *TaskListAction*, using the jBPM API, generates the list of tasks for the current user. The *TaskViewAction* class allows the current user to access the assigned task, view the content of requests, and to make decision about it. The Loaded XML document (eRequest) is passed through an appropriate XSLT to generate the final web page. The *TaskEditAction* class, though similar to *TaskViewAction*, prepares additional variables and passes the XML document through different XSLT to generate fully editable content. *TaskProcessAction* is used to evaluate user's response to the presented task. It adds additional content to the request's XML document - the name of actor that performed the task, and his/her decision. The *ListMyRequestAction* class allows the current user to view a list of active requests he/she has submitted. This is important because content of the document is changing as document progress through workflow, and additional information about approvals and notifications/explanations are added. Additionally, the user can withdraw a request, canceling all pending process tasks, and finalizing jBPM process instance.

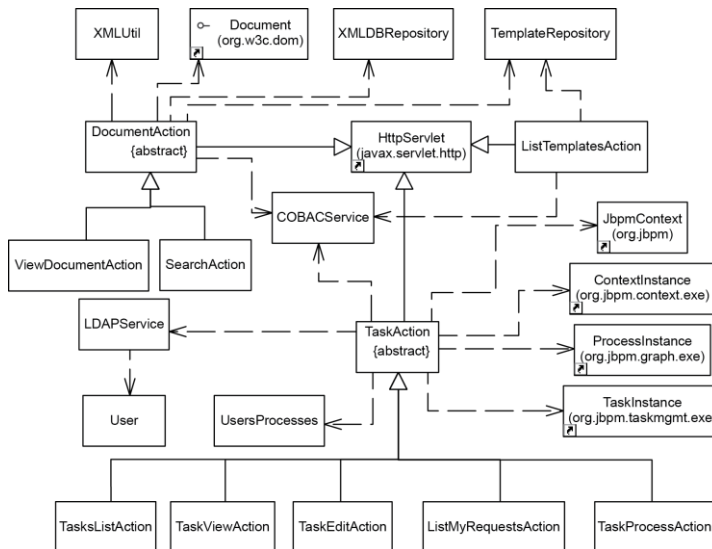


Figure 8

Classes for processing request

Actions that are not directly related to task execution are modeled through the abstract class *DocumentAction*, and its descendant classes *ViewDocumentAction* and *SearchAction*, used for document preview and for document search, respectively. A user can search document on different criteria: request type,

request status, and document originator. The Request type list is automatically generated by extracting header information from documents in repository – eliminating the need for maintenance of web application when new type of request is added to the system. The Request status list contains fixed options: active, finished – accepted, finished – rejected and withdrawn.

An additional class *ListTemplatesAction* produces a web page containing a list of macro-enabled Word documents representing eRequest template forms. The documents are stored in a dedicated folder on the server. This class scans directory and generates a list of download links on a web page.

5.3 XML Document Transformations


XML document transformation can be observed from two different standpoints: the change of XML documents content as a result of performed action, and the transformation of document content into a presentation form. The first one is a direct result of an action performed in the workflow system and the XML document content is edited. Critical operations on the XML document are node insertion, node deletion, and change of content and attribute value [28]. In our system, document editing is encapsulated in a process task-execution environment. While performing a task, users can confirm, reject or edit and confirm an eRequest. In either case a new node containing approval or rejection, with explanation and user id, will be inserted as child node of the *approval* node. In the case of editing, only certain users are allowed to change certain parts of the document in any given moment. As a result of this, most of the time, only one user will be allowed to perform her/his task over a certain part of the document. If this is the case, no conflicting (concurrent) editing will happen, and the document will be simply stored to the document repository. However, as mentioned earlier, there is a possibility of parallel tasks execution. In this case, an automatic document merger, based on document timestamp and element position in document, is performed.

Presentation layer of the web application is built by using Java Server Pages - *jsp* based dynamic pages and XSL transformations for displaying request details. Additionally, XSLT is used whenever original XML document needs to be transformed to presentation format i.e. XHTML. Hence, task processing and request document preview/modification is handled on pages generated through XSLT. Since request data is originally in XML format, this approach gives us flexibility, as only XSLT needs to be adapted if the XML format is changed in the future. Approach through XSL transformation files proved as a viable solution during development and testing phase when some changes to the originally envisioned structure of XML were requested. There are three different XSLT files used for transforming request data to three different states:

- Simple preview with no additional controls,

- Preview with controls for accepting/rejecting requests, and finally
- Transformation for editing of full content of request.

Created XSLT files convert XML documents to XHTML representations that are seamlessly integrated in overall application design. Additionally, image data is displayed in resulting XHTML by converting Base64 encoded data to image representation. Some request types contain images, allowed format is jpeg, and images are usually small so direct transformation was a feasible solution. Figure 9 displays the transformation results for editing mode. Special styles were developed to properly format the document for printing.



Republic of Serbia
Government of Autonomous Province of Vojvodina

eRequest Processing

Request for ID Card

Current User: XXXX YYYY

[Home](#) | [eRequest forms](#) | [My Requests](#) | [My Tasks](#) | [Search](#) | [Log Out](#)

eRequest No.: 121

Submitted by: Goran Sladić

Org. Unit: Provincial Secretariat for Economy

Date Submitted: 2012-04-01

Status: In Process

Implemented (executed) by:

Name: John

Family Name: Doe

Title: Mr

Organization: Provincial Secretariat for Economy

Function: Visitor


ID Card no.:

Year Issued: 2010

Place Issued: Novi Sad

Language and script to be used for printing the ID card:

Comment: None



Sample image

Reason for editing original eRequest:

Save changes and forward request

Choose executive officer:

Mary I


George

John

Ted

Cancel

Already Approved By:



2012-04-01
Edward
head of the authority

Figure 9

XSLT result for editing mode

Conclusion

In this paper we have presented an approach for the handling of administrative requests as electronic documents (eRequests). Although different DMS systems are available, and one (Alfresco) is installed in the provincial government, special requirements guided the decision to develop a new system. One of the key benefits of the implemented system is low-entry barrier for end users, achieved by using their usual workplace software environment as a tool for creation and submission of electronic requests, avoiding common uploads to different platforms and the need to train the users to work in a new environment. We have preserved their existing document templates, and enhance them to active documents.

Unlike common web forms that usually need to be completely filled out in one session, or intermediate state stored on the server, our approach allows users to work on the document, store it, continue later, and submit it when completed. Stored document with filled-in data can be later used as a starting point for a new eRequest, without the need for special template archiving mechanism. Also this approach allows administrators to easily create a new eRequest form – usually by editing an existing one and uploading it to the designated directory on the server. Some parts of the document (such as the title block) are automatically used to register a new type of request without the need to maintain special registry on the server.

To control the document processing, a workflow engine has been used. This approach gives the system a flexibility regarding possible changes in the established workflow. XML is used throughout the system to represent eRequest documents, allowing for easy manipulation and transformation.

These approaches have proven to be valuable even during the development and testing phases, when changes to the workflow were requested, as well as changes to the existing eRequest templates and creation of new eRequest forms. Initially, ten existing word templates were converted to eRequest active documents, and during this period, some were changed or removed from the system, while only one session was needed to train administrators to create new templates on their own, so they later produced ten new templates autonomously. This number will be growing as more paper requests are required to be processed through this system. Transition to electronic documents significantly reduced resource consumption in request processing (prior to introduction of this system, usual number of paper copies was 4 to 5 - this is now reduced to 1, which is archived). Annually, this amounts to a reduction of a few thousand paper sheets that no longer need to be printed and archived, and with more requests handled through the system, the difference will be even larger. Request processing time is also significantly reduced, since embedded workflow engine generates the appropriate notifications and progresses to the next task immediately upon completion of the previous one.

Further development will include adjustment of the user interface for mobile device access. This also implies that a new security layer needs to be introduced to

enhance security of the application when accessed over public wireless networks. Additionally, access control will be strengthened by introducing document and document-fragment-level access rights. For this purpose we plan to use eXtensible XML Access Control Framework [36, 37, 38]. Furthermore, ontologies will be added to increase e-requests semantics and appropriate XML elements representing this knowledge will be introduced into XML document representation.

References

- [1] International Organization for Standardization (ISO). (2001): ISO IEC 82045-1: Document Management – Part 1: Principles and Methods, ISO, Geneva, Switzerland
- [2] Hollingsworth, David: The Workflow Reference Model, Workflow Management Coalition, Cohasset, MA, USA (1995)
- [3] Baresi, L., F. Casati, S. Castano, M. G. Fugini, I. Mirbel, and B. Pernici: WIDE Workflow Development Methodology: Proceedings of the International Joint Conference on Work activities Coordination and Collaboration, San Francisco, California, USA, February 22-25, 1999, New York, NY, USA: ACM Press (1999) pp. 19-28
- [4] Casati, Fabio, Maria Grazia Fugini, Isabelle Mirbel, and Barbara Pernici: WIRES: A Methodology for Developing Workflow Applications. Requirements Engineering, Vol. 7, No. 2 (2002) pp. 73-106
- [5] Krishnan, Rupa, Lalitha Munaga, and Kamalakar Karlapalem: XDoC-WFMS: A Framework for Document Centric Workflow Management System. In H. Arisawa, Y. Kambayashi, V. Kumar, H. Mayr, and I. Hunt (eds): Lecture Notes in Computer Science 2465, Berlin: Springer (2002) pp. 348-362
- [6] Ellis, C. A. and S. J. Gibbs: Concurrency Control in Groupware Systems. SIGMOD Record, Vol. 18, No. 2 (1989) pp. 399-407
- [7] Suleiman, Maher, Michele Cart, and Jean Ferrie: Concurrent Operations in a Distributed and Mobile Collaborative Environment, Proceedings of the International Conference on Data Engineering (ICDE'98) Orlando, FL, USA, February 23-27, 1998, Los Alamitos, CA, USA: IEEE Computer Society (1998) pp. 36-45
- [8] Cobena, Gregory, Serge Abiteboul and Amelie Marian: Detecting Changes in XML Documents, Proceedings of the 18th International Conference on Data Engineering (ICDE'02), February 26-March 1, 2002, San Jose, California, USA: IEEE Computer Society (2002) pp. 41-52

-
- [9] Ionescu, Mihail and Ivan Marsic: Tree-based Concurrency Control in Distributed Groupware. *Computer Supported Cooperative Work*, Vol. 12, No. 3 (2003) pp. 329-350
- [10] Sun, David, Steven Xia, Chengzheng Sun, and David Chen: Operational Transformation for Collaborative Word Processing: Proceedings of the 2004 ACM conference on Computer supported cooperative Work (CSCW'04) Chicago, Illinois, USA, November 6-10, 2004, New York, NY, USA: ACM Press (2004) pp. 437-446
- [11] Ignat, Claudia-Lavinia and Moira C. Norrie: Flexible Collaboration over XML Documents. In Y. Luo (ed): *Lecture Notes in Computer Science*, 4101, Cooperative Design, Visualization, and Engineering, Berlin: Springer (2006) pp. 267-274
- [12] Ignat, Claudia-Lavinia and Moira C. Norrie: Multi-level Editing of Hierarchical Documents, *Computer Supported Cooperative Work* Vol. 17, No. 5, 6 (2008) pp. 423-468
- [13] Lee, Heeseok, and Woojong Suh: A Workflow-based Methodology for Developing Hypermedia Information Systems. *Journal of Organizational Computing and Electronic Commerce*, Vol. 11, No. 2 (2001) pp. 77-106
- [14] Aversano, Lerina, Gerardo Canfora, Andrea De Lucia, and Pierpaolo Gallucci: Integrating Document and Workflow Management Systems: Proceedings of the IEEE Symposia on Human-Centric Computing Languages and Environments, Stresa, Italy, September 5-7, 2001, Los Alamitos, CA, USA: IEEE Computer Society (2001) pp. 328-329
- [15] Aversano, Lerina, Gerardo Canfora, Andrea De Lucia, and Pierpaolo Gallucci: Integrating Document and Workflow Management Tools using XML and Web Technologies: a Case Study: Proceedings of the Sixth European Conference on Software Maintenance and Reengineering, Budapest, Hungary, March 11-13, 2002, Los Alamitos, CA, USA: IEEE Computer Society (2002) pp. 24-33
- [16] Wang, Jianrui, and Akhil Kumar: A Framework for Document-driven Workflow Systems. In W. van der Aalst, B. Benatallah, F. Casati, and F. Curbera (eds): *Business Process Management - Lecture Notes in Computer Science* 3649, Berlin: Springer (2005) pp. 285-301
- [17] Velez, Ivan P., and Bienvenido Velez: Lynx: An Open Architecture for Catalyzing the Deployment of Interactive Digital Government Workflow-Based Systems: Proceedings of the International Conference on Digital Government Research, San Diego, California, USA, May 21-24, 2006, New York, NY, USA: ACM Press (2006) pp. 309-318
- [18] Mohammad Rahaman, Yves Ashiqur Roudier, and Andreas Schaad (2009) *Document-Based Dynamic Workflows: Towards Flexible and Statefull*

- Services: Proceedings of the World Conference on Services - II, Bangalore, India, September 21-25, 2009, Los Alamitos, CA, USA: IEEE Computer Society, pp. 87-94
- [19] Bing, Han, and Xia Dan-Mei: Research and Design of Document Flow Model Based on JBPM Workflow Engine: Proceedings of the International Forum on Computer Science-Technology and Applications, Chongqing, China, December 25-27, 2009, Los Alamitos, CA, USA: IEEE Computer Society (2009) pp. 336-339
- [20] Berliner, Brian: CVS II: Parallelizing Software Development. Proceedings of the Winter 1990 USENIX Conference, Washington, District of Columbia, USA, January 1990, Usenix Association (1990) pp. 341-352
- [21] Collins-Sussman, Ben, Brian W. Fitzpatrick, and C. Michael Pilato: Version Control with Subversion. Cambridge, Massachusetts, USA: O'Reilly (2004)
- [22] Lippe, Ernst and Norbert van Oosterom. Operation-Based Merging. Proceedings of the fifth ACM SIGSOFT symposium on Software development environments, Tyson's Corner, Virginia, USA, December 9-11, 1992, New York, NY, USA: ACM Press (1992) pp. 78-87
- [23] Sun, Chengzheng, Xiaohua Jia, and Yanchun Zhang, Yun Yang, and David Chen: Achieving Convergence, Causality Preservation, and Intention Preservation in Real-Time Cooperative Editing Systems. ACM Transactions on Computer-Human Interaction, Vol. 5, No. 1 (1998) pp. 63-108
- [24] Sun, Chengzheng and Clarence Ellis: Operational Transformation in Real-Time Group Editors: Issues, Algorithms, and Achievements: Proceedings of ACM CSCW'98 Conference on Computer-supported Cooperative Work (CSCW'98) Seattle, WA, USA, November 14-18, 1998, New York, NY, USA: ACM Press (1998) pp. 59-68
- [25] Suleiman, Maher, Michele Cart, and Jean Ferrie: Serialization of Concurrent Operations in a Distributed Collaborative Environment: Proceedings of the international ACM SIGGROUP conference on Supporting group work (GROUP '97) Phoenix, Arizona, USA, November 16-19, 1997, New York, NY, USA: ACM Press (1997) pp. 435-445
- [26] Li, Du and Rui Li: Preserving Operation Effects Relation in Group Editors. Proceedings of the 2004 ACM Conference on Computer Supported Cooperative Work (CSCW '04), Chicago, Illinois, USA, November 6 to November 10 2004. New York, NY, USA: ACM Press (2004) pp. 457-466
- [27] Li, Rui and Du Li: Commutativity-based Concurrency Control in Groupware. Proceedings of the IEEE Conference on Collaborative Computing: Networking, Applications and Worksharing

- (CollaborateCom'05), San Jose, California, USA, December 19-22, 2005, Los Alamitos, CA, USA: IEEE Computer Society (2005) pp. 1-10
- [28] Ignat, Claudia-Lavinia and Gerald Oster: Peer-to-peer Collaboration over XML Documents. In Y. Luo (ed): Lecture Notes in Computer Science, 5220, Cooperative Design, Visualization, and Engineering, Berlin: Springer (2008) pp. 66-73
- [29] Assmann, Uwe. Architectural Styles for Active Documents. Science of Computer Programming, Vol. 56 (2005) pp. 79-98
- [30] Duhl, Joshua, and Susan Feldman: Industry Developments and Models, Active Documents: Changing How the Enterprise Works, IDC, Framingham, MA, USA (2003)
- [31] United States Patent and Trademark Office (USTO) (2004) Office of the Chief Information Officer, Operational Information Technology Plan, FY 2005 – FY2006, USTO, Department of Commerce, Washington, DC, USA
- [32] Leng, Gillian, Nicola Bent, and Ian Saunders: Electronic Guidance Access Project (EGAP) (Interim report V1.0) National Institute for Health and Clinical Excellence, London, UK (2008)
- [33] Teohari, Mihai, and Copcea Larisa: XML Authoring Tool: Proceedings of the 4th Conference on European Computing, Bucharest, Romania, April 20-22, 2010, New York, NY, USA: ACM Press (2010) pp. 143-147
- [34] Yang, Haijun: Design and Implementation of Electronic Medical Record Template Based on XML Schema: Proceedings of the Second WRI World Congress on Software Engineering, Wuhan, Hubei, China, December 19-20, 2010, Los Alamitos, CA, USA: IEEE Computer Society (2010) pp. 225-118
- [35] Gostojić, Stevan, Goran Sladić, Branko Milosavljević, and Zora Konjović: Context-Sensitive Access Control Model for Government Services, Journal of Organizational Computing and Electronic Commerce, Vol. 22, No. 2, (2012) pp. 184-213
- [36] Sladić, Goran, Branko Milosavljević, Zora Konjović, and Milan Vidaković: Access Control Framework for XML Document Collections. Computer Science and Information System (ComSIS) Vol. 8, No. 3 (2011) pp. 591-609
- [37] Sladić, Goran, Branko Milosavljević, Dušan Surla, and Zora Konjović: Flexible Access Control Framework for MARC Records. The Electronic Library, Vol. 30, No. 5 (2012) pp. 623-652
- [38] Sladić, Goran, Branko Milosavljević, and Zora Konjović: Context-Sensitive Access Control Model for Business Processes: Computer Science and Information System (ComSIS) Vol. 10, No. 3 (2013) pp. 939-972

Reduced-Order Sliding Mode Observer-based Speed Sensorless Vector Control of Double Stator Induction Motor

Houari Khouidmi

Hassiba Benbouali University Faculty of Technology
Po.Box 151, Hay Es-Salem Chlef 02000, Algeria, h.khouidmi@univ-chlef.dz

Ahmed Massoum

Djillali Liabès University of Sidi Bel-abbès, Faculty of Technology
Sidi Bel-abbès, 22000 Algeria, amassoum@univ-sba.dz

Abstract: In this paper a reduced-order sliding mode observer-based speed sensorless vector control of a double stator induction motor (DSIM) is presented. The conventional reduced-order observer has large chattering on the speed and the torque. In order to solve this problem, the sliding mode technique with smooth function is used. The simulation tests show the effectiveness of the proposed method especially in the load disturbances and/or the change of the reference speed.

Keywords: Double stator induction motor; Indirect Field Oriented Control; Reduced-order observer; Sliding mode observer; Sensorless control

1 Introduction

Sensorless speed vector control is a currently a fundamental part of industrial reseach because it features in the strategic business plans of most manufacturers of electric actuators [1-2]. Indeed, the operation with mechanical speed sensorless vector control has become one of the main interests of researchers currently trying to fulfill its function implicitly by electrical sensors and algorithms to reconstruct the motor speed.

The field oriented control (FOC), developed for double stator induction machine (DSIM), requires the measurement of the speed to perform the coordinate transformations. Physically, this measurement is performed using a mechanical speed sensor mounted on the rotor shaft, which unfortunately increases the

complexity and cost of installation (additional wiring and maintenance) [3-5]. Moreover, the mechanical speed sensors are usually expensive, fragile and affect the reliability of the control. In this context, our study focuses mainly the speed estimation using the Luenberger reduced-order observer for a sensorless vector control of a double stator induction motor.

The observers are very attractive and give good performance in a wide range of speeds. The observation algorithms are using an analytical model of the machine to produce the speed and the rotor flux estimations from the stators' currents and voltages.

Among the observational methods we have deterministic observers (Luenberger, reduced order or full order observer), the Kalman filter, and the Model Reference Adaptive System (MRAS). These observers are used to observe the flux and speed estimation in a closed loop [4] [6-7]. Although such approaches lead to different performance in relation to the degree of algorithmic and computational complexity, they generally offer good performance in a wide range of speed but cannot estimate very low speeds in a stable manner [8-9].

The sliding mode observer represents one of the most attractive and popular solutions for sensorless control of electrical motor drives. Currently, applications of this strategy to double stator induction motors (DSIM) are largely unexplored and involve only a few research laboratories. For example reduced-order observer has been applied to IMs for speed sensorless control [10-11], for speed and flux sensorless control [12] and, later, for speed and/or flux sensorless control of DSIM [13-14]. However, some limitations on operation of conventional observers were large chattering on the speed, which very low speeds quickly highlighted.[8-9].

The chattering phenomenon is harmful to the proper functioning of the system, because it adds high frequency components to the control signal spectrum. These components can damage the system by exciting the dynamics neglected in the modelling or by damaging the actuators from frequent solicitations.

The main contribution of this paper is to overcome this inconvenience in DSIM observation. Many studies have been performed [15-16]. One of them involved replacing the "*sign*" function by a continuous approximation near the sliding surface. Among the methods which reduce the effect of the "*sign*" function, we find the "*smooth*" function of *dead zone* suitable for filtering high frequencies and eliminating the *chattering phenomenon* and generated transient electromagnetic torque in dynamic and low speed profiles.

The paper is organized as follows: the reduced-order observer structure is discussed in Section 2. In Section 3, the double stator induction motor (DSIM) model and the control strategy are presented. In Section 4 the reduced-order observer of DSIM is developed. Sections 5 and 6 provides the application of the resulting sliding mode speed observer of DSIM. Finally, a numerical simulation and its discussion are presented regarding the sensorless indirect vector control scheme of DSIM with reduced-order sliding mode speed observer shown in Fig. 1.

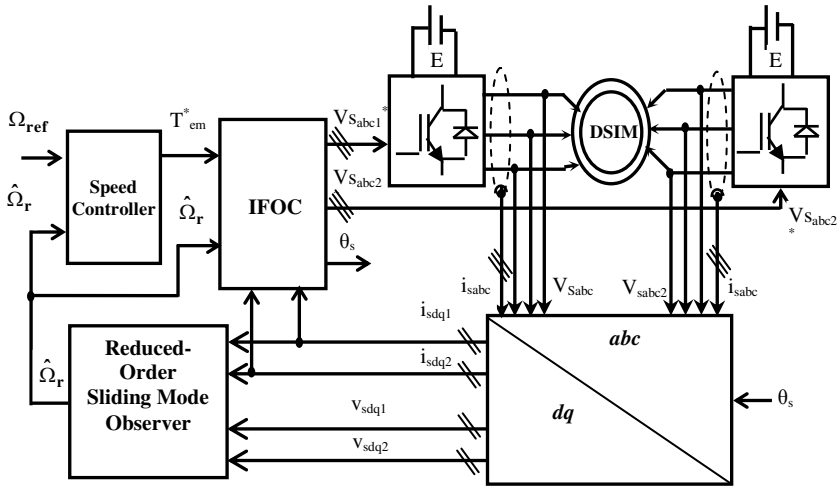


Figure 1
Sensorless indirect vector control of DSIM

2 DSIM Model and Rotor Flux Orientation Technique

2.1 DSIM Model

The double stator induction motor (DSIM) has two systems of three-phase winding (a1, b1, c1) and (a2, b2, c2) connected in a star configuration which are phase-shifted by 30° (Figure 2). The equations of this machine can be expressed in different reference field (rotating field, stator field or rotor field) according to the attributed reference (d, q).

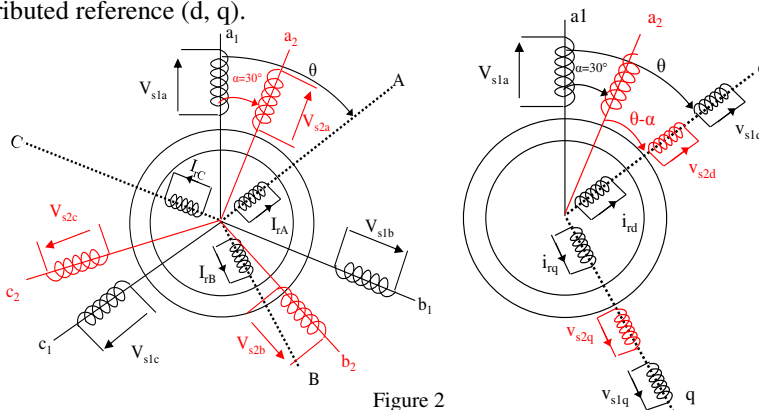


Figure 2
Six dimensional and orthogonal subspaces d-q model of DSIM

Voltages Equations

By choosing a referential related to the rotating field, we obtain the following system of equations[3]-[13]:

$$\left\{ \begin{array}{l} v_{sd1} = R_{s1}i_{sd1} + \frac{d\Phi_{sd1}}{dt} - \omega_s \Phi_{sq1} \\ v_{sq1} = R_{s1}i_{sq1} + \frac{d\Phi_{sq1}}{dt} - \omega_s \Phi_{sd1} \\ v_{sd2} = R_{s2}i_{sd2} + \frac{d\Phi_{sd2}}{dt} - \omega_s \Phi_{sq2} \\ v_{sq2} = R_{s2}i_{sq2} + \frac{d\Phi_{sq2}}{dt} - \omega_s \Phi_{sd2} \\ 0 = R_r i_{rd} + \frac{d\Phi_{rd}}{dt} - (\omega_s - \omega_r) \Phi_{rq} \\ 0 = R_r i_{rq} + \frac{d\Phi_{rq}}{dt} - (\omega_s - \omega_r) \Phi_{rd} \end{array} \right. \quad (1)$$

Where:

- $v_{s1dq} \ v_{s2dq}$:First and second stator voltages in stationary frame
- $i_{s1dq} \ i_{s2dq}$:First and second stator currents in Stationary frame
- $\Phi_{s1dq} \ \Phi_{s2dq}$:First and second stator flux in stationary frame
- Φ_{rdq} :Rotor flux in stationary frame
- $\omega_r, \ \omega_s, \ \omega_g$:Rotor and stator angular frequency
- $R_{s12} \ R_r$:First and second stator and rotor resistance

Flux Equations

The relations between flux and currents are given by:

$$\left\{ \begin{array}{l} \Phi_{sd1} = L_{s1}i_{sd1} + L_m(i_{sd1} + i_{sd2} + i_{rd}) \\ \Phi_{sq1} = L_{s1}i_{sq1} + L_m(i_{sq1} + i_{sq2} + i_{rq}) \\ \Phi_{sd2} = L_{s2}i_{sd2} + L_m(i_{sd1} + i_{sd2} + i_{rd}) \\ \Phi_{sq2} = L_{s2}i_{sq2} + L_m(i_{sq1} + i_{sq2} + i_{rq}) \\ \Phi_{rd} = L_r i_{rd} + L_m(i_{sd1} + i_{sd2} + i_{rd}) \\ \Phi_{rq} = L_r i_{rq} + L_m(i_{sq1} + i_{sq2} + i_{rq}) \end{array} \right. \quad (2)$$

Where:

- L_{s12} :First and second stator inductance
- L_r :Rotor inductance
- L_m :Mutual inductance

Replacing the system of equations (2) in (1) we obtain the mathematical DSIIM model (3).

$$\left\{ \begin{array}{l}
 v_{sd1} = R_{s1}i_{sd1} + (L_{s1} + L_m)\sigma \frac{di_{sd1}}{dt} + \frac{L_m L_r}{L_m + L_r} \frac{di_{sd2}}{dt} + \frac{L_m}{L_m + L_r} \frac{d\Phi_{rd}}{dt} \\
 \quad - \omega_s \left[(L_{s1} + L_m)\sigma i_{sq1} + \frac{L_m L_r}{L_m + L_r} i_{sq2} + \frac{L_m}{L_m + L_r} \Phi_{rq} \right] \\
 v_{sq1} = R_{s1}i_{sq1} + (L_{s1} + L_m)\sigma \frac{di_{sq1}}{dt} + \frac{L_m L_r}{L_m + L_r} \frac{di_{sq2}}{dt} + \frac{L_m}{L_m + L_r} \frac{d\Phi_{rq}}{dt} \\
 \quad + \omega_s \left[(L_{s1} + L_m)\sigma i_{sd1} + \frac{L_m L_r}{L_m + L_r} i_{sd2} + \frac{L_m}{L_m + L_r} \Phi_{rd} \right] \\
 v_{sd2} = R_{s1}i_{sd2} + (L_{s2} + L_m)\sigma \frac{di_{sd2}}{dt} + \frac{L_m L_r}{L_m + L_r} \frac{di_{sd1}}{dt} + \frac{L_m}{L_m + L_r} \frac{d\Phi_{rd}}{dt} \\
 \quad - \omega_s \left[(L_{s2} + L_m)\sigma i_{sq2} + \frac{L_m L_r}{L_m + L_r} i_{sq1} + \frac{L_m}{L_m + L_r} \Phi_{rq} \right] \\
 v_{sq2} = R_{s1}i_{sq2} + (L_{s2} + L_m)\sigma \frac{di_{sq2}}{dt} + \frac{L_m L_r}{L_m + L_r} \frac{di_{sq1}}{dt} + \frac{L_m}{L_m + L_r} \frac{d\Phi_{rq}}{dt} \\
 \quad + \omega_s \left[(L_{s2} + L_m)\sigma i_{sd2} + \frac{L_m L_r}{L_m + L_r} i_{sd1} + \frac{L_m}{L_m + L_r} \Phi_{rd} \right] \\
 0 = -\frac{L_m}{T_r} (i_{sd1} + i_{sd2}) + \frac{1}{T_r} \Phi_{rd} + \frac{d\Phi_{rd}}{dt} - (\omega_s - \omega_r)\Phi_{rq} \\
 0 = -\frac{L_m}{T_r} (i_{sq1} + i_{sq2}) + \frac{1}{T_r} \Phi_{rq} + \frac{d\Phi_{rq}}{dt} - (\omega_s - \omega_r)\Phi_{rd}
 \end{array} \right. \quad (3)$$

$$\text{With: } \sigma = 1 - \frac{L_m^2}{(L_m + L_r)(L_m + L_s)}, \quad L_{s1} = L_{s2} = L_s, \quad T_r = \frac{L_m + L_r}{R_r}$$

Where:

- σ : Total leakage factor;
- T_r : Rotor time constant.

Mechanical Equations

The equation of the electromagnetic torque is:

$$T_{em} = p \frac{L_m}{L_m + L_r} \left[(i_{sq1} + i_{sq2})\Phi_{rd} - (i_{sd1} + i_{sd2})\Phi_{rq} \right] \quad (4)$$

Where:

- T_{em} : Electromagnetic torque;
- p : Number of pole pairs

The mechanical equation is:

$$J \frac{d\Omega_r}{dt} = T_{em} - T_L - k_f \Omega_r \quad (5)$$

Where:

- J :Inertia;
- Ω_r :Mechanical rotor speed
- T_L :Load torque
- k_f :Viscous friction coefficient

3.2 Rotor Flux Orientation Technique of DSIM

The rotor flux orientation principle aligns the rotor flux on the direct axis [14]-[16]:

$$\begin{cases} \Phi_r = \Phi_{rd} \\ \Phi_{rq} = 0 \end{cases} \quad (6)$$

By imposing the condition of the rotor flux (6) to the system of equations (3) and after rearranging the mechanical equations (4) and (5), we obtain the system (7) as follows:

$$\left\{ \begin{array}{l}
 v_{sd1} = R_{s1}i_{sd1} + (L_{s1} + L_m)\sigma \frac{di_{sd1}}{dt} + \frac{L_m L_r}{L_m + L_r} \frac{di_{sd2}}{dt} + \frac{L_m}{L_m + L_r} \frac{d\Phi_r}{dt} \\
 \quad - \omega_s \left[(L_{s1} + L_m)\sigma i_{sq1} + \frac{L_m L_r}{L_m + L_r} i_{sq2} \right] \\
 v_{sq1} = R_{s1}i_{sq1} + (L_{s1} + L_m)\sigma \frac{di_{sq1}}{dt} + \frac{L_m L_r}{L_m + L_r} \frac{di_{sq2}}{dt} \\
 \quad + \omega_s \left[(L_{s1} + L_m)\sigma i_{sd1} + \frac{L_m L_r}{L_m + L_r} i_{sd2} + \frac{L_m}{L_m + L_r} \Phi_r \right] \\
 v_{sd2} = R_{s1}i_{sd2} + (L_{s2} + L_m)\sigma \frac{di_{sd2}}{dt} + \frac{L_m L_r}{L_m + L_r} \frac{di_{sd1}}{dt} + \frac{L_m}{L_m + L_r} \frac{d\Phi_r}{dt} \\
 \quad - \omega_s \left[(L_{s2} + L_m)\sigma i_{sq2} + \frac{L_m L_r}{L_m + L_r} i_{sq1} \right] \\
 v_{sq2} = R_{s1}i_{sq2} + (L_{s2} + L_m)\sigma \frac{di_{sq2}}{dt} + \frac{L_m L_r}{L_m + L_r} \frac{di_{sq1}}{dt} \\
 \quad + \omega_s \left[(L_{s2} + L_m)\sigma i_{sd2} + \frac{L_m L_r}{L_m + L_r} i_{sd1} + \frac{L_m}{L_m + L_r} \Phi_r \right] \\
 0 = -\frac{L_m}{T_r} (i_{sd1} + i_{sd2}) + \frac{1}{T_r} \Phi_r + \frac{d\Phi_r}{dt} \\
 0 = -\frac{L_m}{T_r} (i_{sq1} + i_{sq2}) - (\omega_s - \omega_r)\Phi_r \\
 T_{em} = p \frac{L_m}{L_m + L_r} \cdot \Phi_r \cdot (i_{sq1} + i_{sq2}) \\
 J \frac{d\Omega_r}{dt} = T_{em} - T_L - k_f \Omega_r
 \end{array} \right. \quad (7)$$

To ensure the torque control and to provide at all times the maximum torque, the flux is maintained at its nominal value. In contrast, the voltages equations v_{sd1} , v_{sq1} , v_{sd2} and v_{sq2} show undesired coupling, which requires the use of a decoupling circuit during the implementation of the field oriented control [11]-[16].

Taking into account that Φ_r is kept constant at its nominal value, in the established regime we have $\frac{d\Phi_r}{dt} = 0$, and system (7) becomes (8):

$$\begin{cases}
v_{sd1} = R_{s1}i_{sd1} - L_{s1} \frac{di_{sd1}}{dt} - \omega_s \cdot L_{s1} \cdot \left(\frac{L_r}{R_r} \Phi_r \cdot \omega_{gl} + L_{s1}i_{sq1} \right) \\
v_{sd2} = +R_{s2}i_{sd2} - L_{s2} \frac{di_{sd2}}{dt} - \omega_s \cdot L_{s2} \cdot \left(\frac{L_r}{R_r} \Phi_r \cdot \omega_{gl} + L_{s2}i_{sq2} \right) \\
v_{sq1} = R_{s1}i_{sq1} - L_{s1} \frac{di_{sq1}}{dt} + \omega_s L_{s1} (\Phi_r + L_{s1}i_{sd1}) \\
v_{sq2} = R_{s2}i_{sq2} - L_{s2} \frac{di_{sq2}}{dt} + \omega_s L_{s2} (\Phi_r + L_{s2}i_{sd2}) \\
\frac{1}{T_r} \cdot \Phi_r + \frac{d\Phi_r}{dt} = \frac{L_m}{T_r} (i_{sd1} + i_{sd2}) \\
\omega_{gl} = \omega_s - \omega_r = \frac{L_m}{T_r \Phi_r} (i_{sq1} + i_{sq2}) \\
T_{em} = p \frac{L_m}{L_m + L_r} \Phi_r (i_{sq1} + i_{sq2}) \\
J \frac{d\Omega_r}{dt} = T_{em} - T_L - k_f \Omega_r
\end{cases} \quad (8)$$

3 Reduced-Order Observer

An observer is an estimator operating in closed loop with an independent dynamic system [7]-[10]. It provides an estimate of the internal physical quantity of a system, based only on information about the input and output of the system with the feedback input of the measured outputs and the estimated error, using the gain matrix G to make the error dynamics converge to zero dynamics (Figure 3).

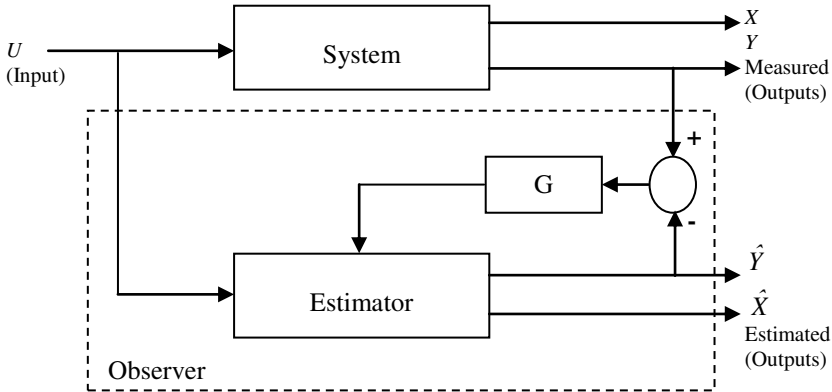


Figure 3
Overall structure of an observer

The system shown in Figure 4 is defined by the state form as follows:

$$\begin{cases} \frac{dX}{dt} = A(\Omega)X + BU \\ Y = CX \end{cases} \quad (9)$$

Where B is the input matrix of the system, C is the output matrix and $A(\Omega)$ is the non-stationary transition matrix of our system, since it depends on the rotational speed. However, it can be considered as quasi-stationary for the dynamic speed with respect to that of the electrical quantities.

By integrating equation (9), we can reconstruct the estimate state.

$$\hat{X} = \int (\hat{A}(\Omega)\hat{X} + \hat{B}U) dt \quad (10)$$

To evaluate the accuracy of the estimate, we consider the difference between the measured and estimated states:

$$\varepsilon = X - \hat{X} \quad (11)$$

Then the dynamic error is deduced from relations (9) and (10):

$$\frac{d\varepsilon}{dt} = A(\Omega)\varepsilon + \Delta A\hat{X} + \Delta BU \quad (12)$$

Where:

$$\Delta A = A(\Omega) - \hat{A}(\Omega) \text{ and } \Delta B = B - \hat{B}$$

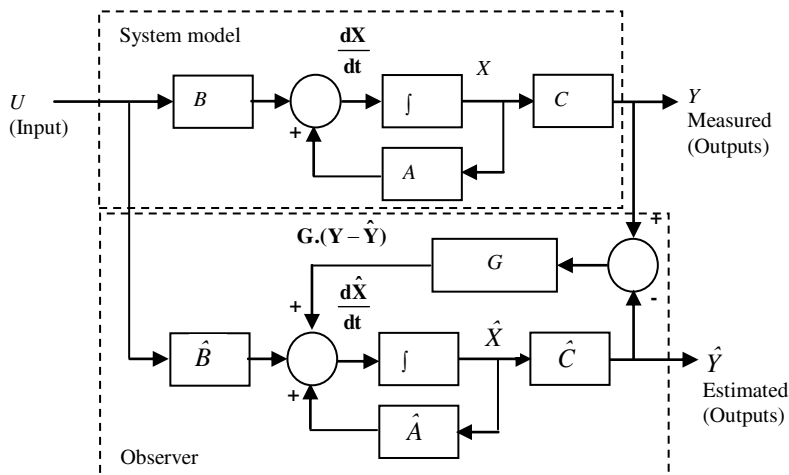


Figure 4
State space form of an observer

The principle construction of an observer is therefore to correct the dynamic of the estimate in (10) taking into account the difference between the measured output and the estimated output. This leads to the following observer [10]:

$$\frac{d\hat{X}}{dt} = A(\Omega)\hat{X} + BU + GC\varepsilon \quad (13)$$

Where: G is the gain of the observer.

We can construct a Luenberger observer by substituting equation (11) into (13) as follows:

$$\frac{d\hat{X}}{dt} = A(\hat{\Omega})\hat{X} + BU + G(Y - C\hat{X}) \quad (14)$$

The problem with this type of observer is that the selection of G depends generally on the estimated speed $\hat{\Omega}$ and involves a dynamic decay of the estimation errors.

We define as measurement error the difference between the measured and estimated variables. In the same way as the estimator, the equation describing the behavior of the estimation error is obtained using equations (9) and (13). So the equation of the estimation error becomes:

$$\frac{d\varepsilon}{dt} = (A(\Omega) - GC)\varepsilon + (\Delta A - G\Delta C)\hat{X} + \Delta BU \quad (15)$$

The main advantage of the observer to the estimator can be easily shown by equation (15). Indeed, the dynamics of convergence error is controlled by the term $(A(\Omega) - GC)$ with the correction gain matrix G .

4 Reduced-Order Speed Observer of DSIM

The use of an estimator does not allow controlling the dynamics of the error that depends on the physical system. Thus, it is preferable that the dynamics of the process estimation is much faster than the system itself, hence the interest using the observers.

The mathematical model of the DSIM shows a variable nonlinear system. To overcome this nonlinearity we use a linear observer and take Ω_r as an additional variable. In this case, we have a Luenberger observer obtained from the system of equations (15) [10]-[12].

We can rewrite the system of equations (15) in the form of two sub-systems as follows:

$$\begin{cases} \frac{di_{sd1}}{dt} = \frac{1}{L_{s1}}v_{sd1} - \frac{R_{s1}}{L_{s1}}i_{sd1} + \omega_s \left(\frac{L_r}{R_r}\Phi_r \cdot \omega_{gl} + L_{s1}i_{sq1} \right) \\ \frac{di_{sd2}}{dt} = \frac{1}{L_{s2}}v_{sd2} - \frac{R_{s2}}{L_{s2}}i_{sd2} + \omega_s \left(\frac{L_r}{R_r}\Phi_r \cdot \omega_{gl} + L_{s2}i_{sq2} \right) \\ \frac{d\Phi_r}{dt} = \frac{L_m}{T_r}(i_{sd1} + i_{sd2}) - \frac{1}{T_r}\Phi_r \end{cases} \quad (16)$$

$$\begin{cases} \frac{di_{sq1}}{dt} = \frac{1}{L_{s1}}v_{sq1} - \frac{R_{s1}}{L_{s1}}i_{sq1} - \omega_s(\Phi_r + L_{s1}i_{sd1}) \\ \frac{di_{sq2}}{dt} = \frac{1}{L_{s2}}v_{sq2} - \frac{R_{s2}}{L_{s2}}i_{sq2} - \omega_s(\Phi_r + L_{s2}i_{sd2}) \\ \frac{d\Omega_r}{dt} = \frac{p}{J} \frac{L_m}{L_m + L_r} \Phi_r (i_{sq1} + i_{sq2}) - \frac{1}{J}(k_f \Omega_r + T_L) \end{cases} \quad (17)$$

It is clear that the estimated speed described by subsystem (17) requires the estimated load torque and the rotor flux.

We can use the following model to estimate the torque load T_L [13]:

$$\frac{dT_L}{dt} \cong 0 \quad (18)$$

By adding the equation (18) to the subsystems (17), we obtain:

$$\begin{cases} \frac{di_{sq1}}{dt} = \frac{1}{L_{s1}}v_{sq1} - \frac{R_{s1}}{L_{s1}}i_{sq1} - \omega_s(\Phi_r + L_{s1}i_{sd1}) \\ \frac{di_{sq2}}{dt} = \frac{1}{L_{s2}}v_{sq2} - \frac{R_{s2}}{L_{s2}}i_{sq2} - \omega_s(\Phi_r + L_{s2}i_{sd2}) \\ \frac{d\Omega_r}{dt} = \frac{p}{J} \frac{L_m}{L_m + L_r} \Phi_r (i_{sq1} + i_{sq2}) - \frac{1}{J}(k_f \Omega_r + T_L) \\ \frac{dT_L}{dt} \cong 0 \end{cases} \quad (19)$$

From the system of equations (19) assuming Φ_r constant, we can construct our reduced-order observer as follows:

$$\begin{cases}
\frac{d\hat{i}_{sq1}}{dt} = \frac{1}{L_{s1}}v_{sq1} - \frac{R_{s1}}{L_{s1}}\hat{i}_{sq1} - \omega_s \left(\frac{1}{L_{s1}}\hat{\Phi}_r + i_{sd1} \right) + G_1\tilde{i}_{sq} \\
\frac{d\hat{i}_{sq2}}{dt} = \frac{1}{L_{s2}}v_{sq2} - \frac{R_{s2}}{L_{s2}}\hat{i}_{sq2} - \omega_s \left(\frac{1}{L_{s2}}\hat{\Phi}_r + i_{sd2} \right) + G_1\tilde{i}_{sq} \\
\frac{d\hat{\Omega}_r}{dt} = \frac{p}{J} \frac{L_m}{L_m + L_r} \hat{\Phi}_r (i_{sq1} + i_{sq2}) - \frac{1}{J} \left(k_f \hat{\Omega}_r + p \hat{T}_L \right) + G_2\tilde{i}_{sq} \\
\frac{d\hat{T}_L}{dt} = G_3\tilde{i}_{sq} \\
\frac{d\hat{\Phi}_r}{dt} = \frac{L_m}{T_r} (i_{sd1} + i_{sd2}) - \frac{1}{T_r} \hat{\Phi}_r
\end{cases} \quad (20)$$

With: $\tilde{i}_{sq} = (i_{sq1} + i_{sq2}) - (\hat{i}_{sq1} + \hat{i}_{sq2})$

G_1, G_2 and G_3 are the observer gains.

It is sufficient to ensure the system stability, with a specific choice of G_1, G_2 and G_3 dependant on the mechanical speed.

5 Sliding Mode Speed Observer of DSIIM

To achieve good performance, the sliding mode technique is known for its robustness with respect to the parametric uncertainties through the use of *High Gain* [16-18]. This technique reduces the state trajectory $\frac{d\hat{X}}{dt}$ of a given system to the sliding surface $S = Y - \hat{Y} \cong \tilde{i}_{sq}$ and choses to switch the desired operating point [19].

The vector surface $S = 0$ is attractive as it satisfies the *Lyapunov stability* criteria if $S \cdot \dot{S} < 0$ [20].

The *smooth* function figure (5), is used to eliminate the *chattering phenomenon*.

$$Smooth(S) = \frac{S}{|S| + e} \quad (21)$$

Where: e is a small positive parameter.

Finally, we define the sliding mode observer by adding the *smooth* function (21) in the system (20):

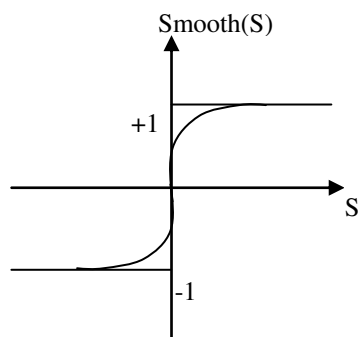


Figure 5
The Smooth function

$$\left\{ \begin{array}{l}
 \frac{d\hat{i}_{sq1}}{dt} = \frac{1}{L_{s1}} v_{sq1} - \frac{R_{s1}}{L_{s1}} \hat{i}_{sq1} - \omega_s \left(\frac{1}{L_{s1}} \hat{\Phi}_r + i_{sd1} \right) + G_1 \text{Smooth}(\tilde{i}_{sq}) \\
 \frac{d\hat{i}_{sq2}}{dt} = \frac{1}{L_{s2}} v_{sq2} - \frac{R_{s2}}{L_{s2}} \hat{i}_{sq2} - \omega_s \left(\frac{1}{L_{s2}} \hat{\Phi}_r + i_{sd2} \right) + G_1 \text{Smooth}(\tilde{i}_{sq}) \\
 \frac{d\hat{\Omega}_r}{dt} = \frac{p}{J} \frac{L_m}{L_m + L_r} \hat{\Phi}_r (i_{sq1} + i_{sq2}) - \frac{1}{J} (k_f \hat{\Omega}_r + p \hat{T}_L) + G_2 \text{Smooth}(\tilde{i}_{sq}) \\
 \frac{d\hat{T}_L}{dt} = G_3 \text{Smooth}(\tilde{i}_{sq}) \\
 \frac{d\hat{\Phi}_r}{dt} = \frac{L_m}{T_r} (i_{sd1} + i_{sd2}) - \frac{1}{T_r} \hat{\Phi}_r \\
 \tilde{i}_{sq} = (i_{sq1} + i_{sq2}) - (\hat{i}_{sq1} + \hat{i}_{sq2}) \\
 \text{Smooth}(\tilde{i}_{sq}) = \frac{\tilde{i}_{sq}}{|\tilde{i}_{sq}| + e}
 \end{array} \right. \quad (22)$$

6 Simulation Results

To test the static and the dynamic performance of the reduced-order sliding mode speed observer, the double stator induction motor (Appendix) is fed by two three-level voltage inverters controlled by rotor flux orientation.

6.1 Discussion

Figures (6-7 and 8-9) illustrate the dynamic performances of the sensorless drive at acceleration and deceleration for both high speeds ($\Omega_r = 280$ (rad/s), $\Omega_r = -280$ (rad/s)) and low speeds ($\Omega_r = 20$ (rad/s), $\Omega_r = -20$ (rad/s)) with step load change applied at $t=1.5$ sec to $t=2.5$ sec for $T_L = 14$ (N.m) to $T_L = 0$ (N.m).

The obtained simulation results (Figures 6 and 8, for both high and low speed) show that the speed tends to its reference and takes its steady state after 1sec without overshoot. Also the direct component of rotor flux is set to ≈ 1 Wb after 1 sec to start, and the quadratic component is cancelled at the same time (Figures 7 and 9). During start-up, the electromagnetic torque is set to 50 Nm and decreased to zero after 1 sec. At time 1.5 sec, a nominal load torque of 14 Nm is applied, there was a slight decrease in speed and an increase of the stator currents. This affects the electromagnetic torque increases (14 Nm), in order to compensate for (approximately 0.1 seconds) the load torque. We also note that the electromagnetic torque is proportional to the quadratic component of stator current; however, the flux remains constant.

It can be seen that the observed speed tracks the real one, the dynamic error is not important (Figures 8 and 9) and the static error is practically zero for both high and low speed. Generally, the reduced-order sliding mode speed observer works very well especially if the observer gains are smoothed out by the *smooth* function.

6.2 Robustness Test

In this section, the influences of parameter variations are investigated in order to test the sensitivity of our SM-observer. The sensitivity of stators resistances, rotor resistance and inertia variation is studied for a step change of $+50\%R_s$, $+50\%R_r$ and $+100\%J$ simultaneously for $t=1.5$ s to 2.5 s for both high and low speeds. Figures (10a) and (10b) shows that the behavior of the observer is not affected at high speeds but the speed error is highlighted at low speeds, the simulations clearly show the performance of the proposed sliding mode speed observer.

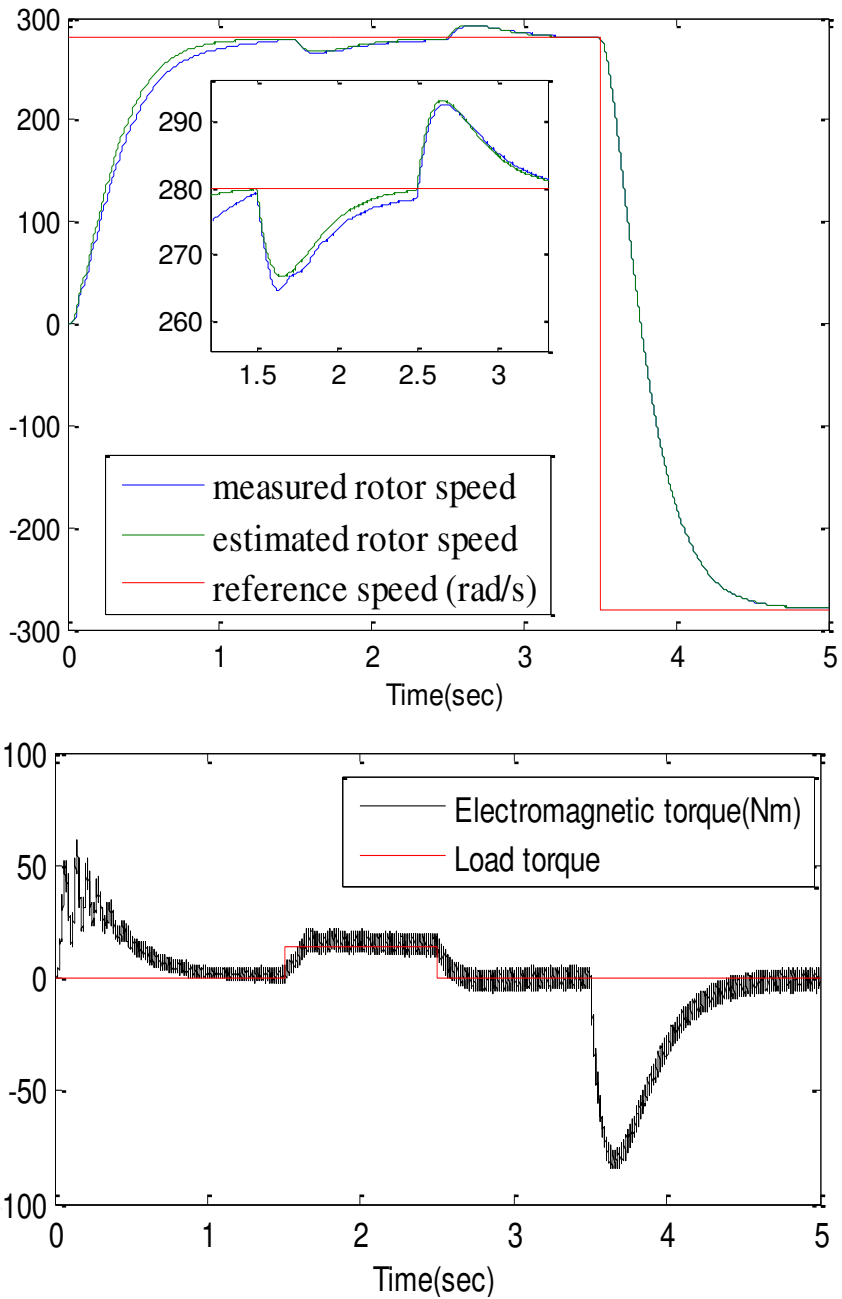


Figure 6

Measured, estimated speed and electromagnetic torque results for high speed sensorless control

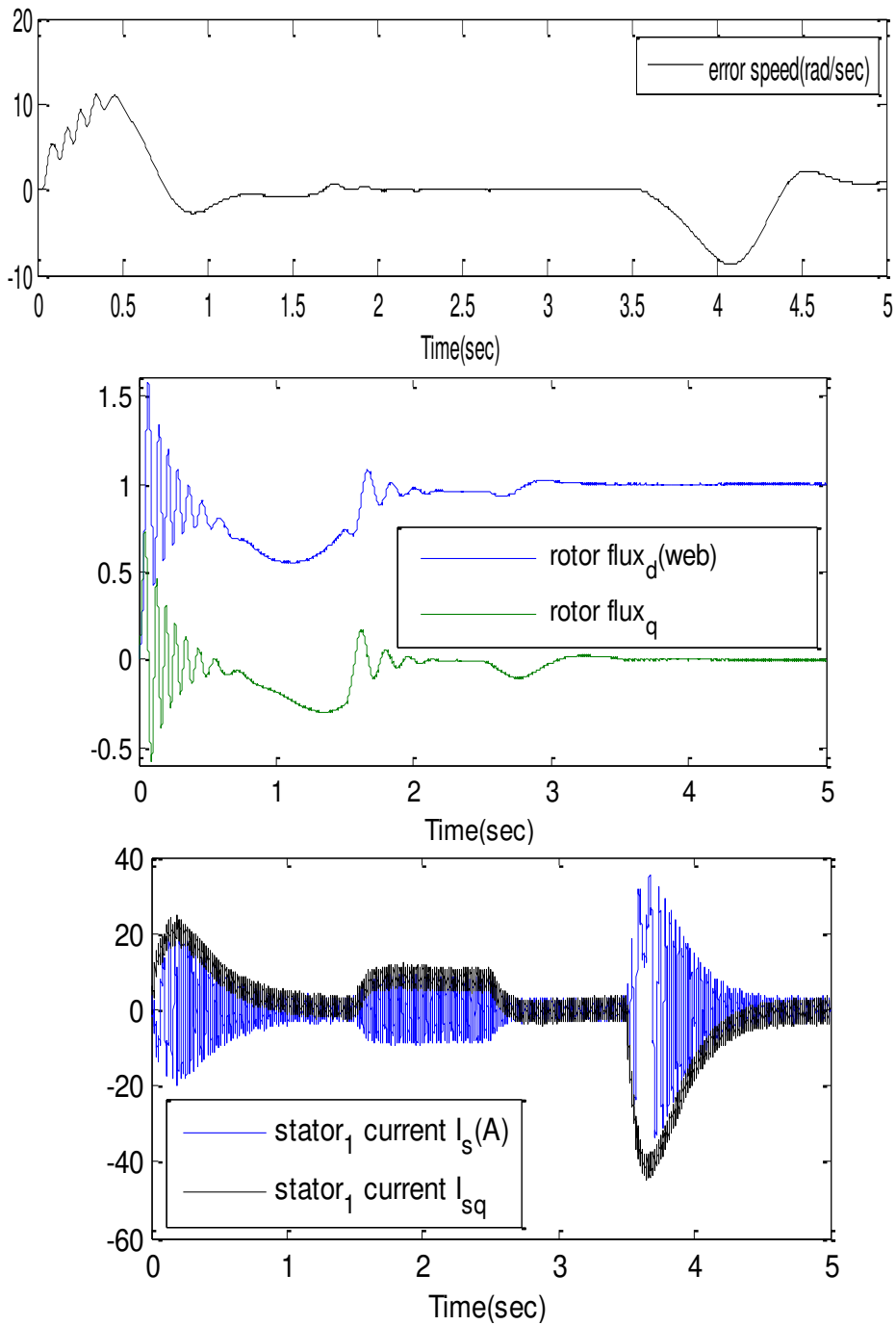


Figure 7

Error speed ,rotor flux and stator current results for high speed sensorless control

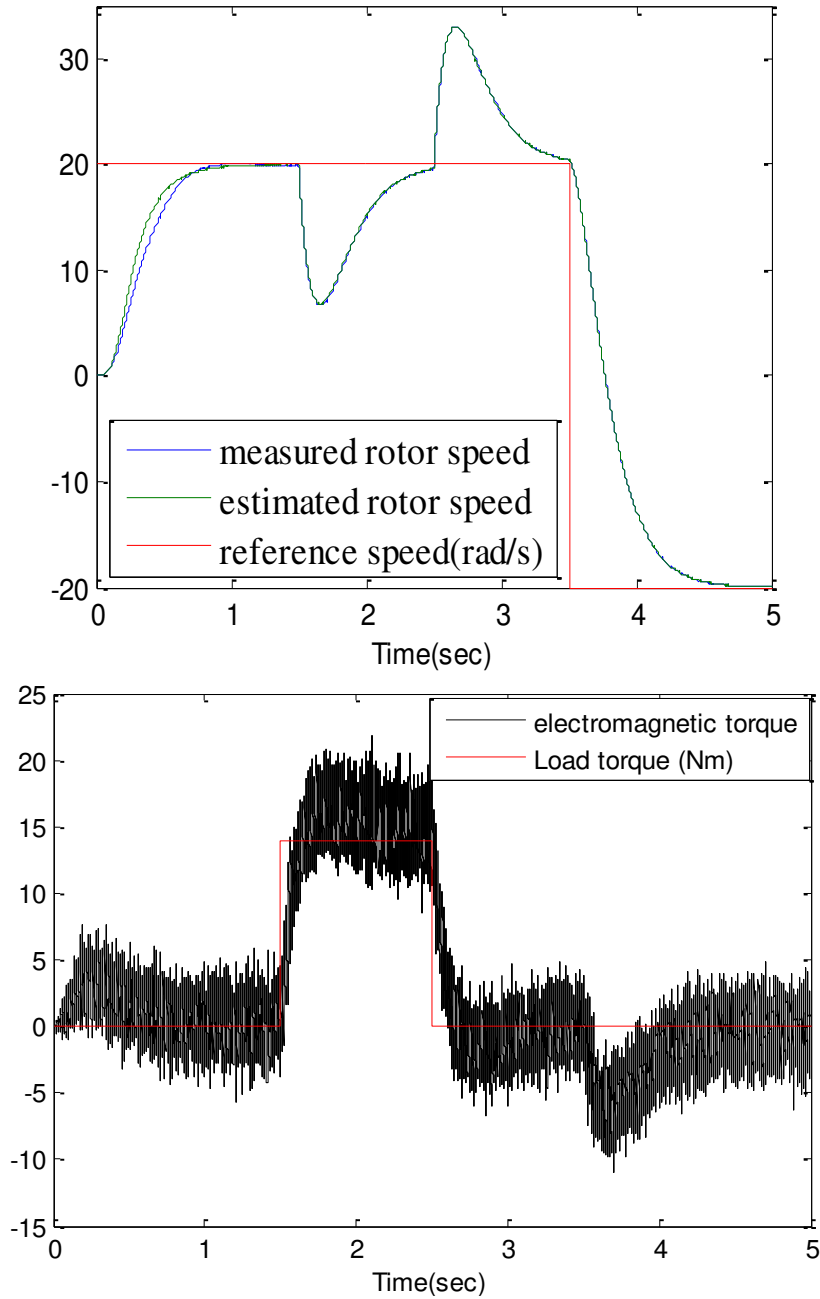


Figure 8

Measured, estimated speed and electromagnetic torque results for low speed sensorless control

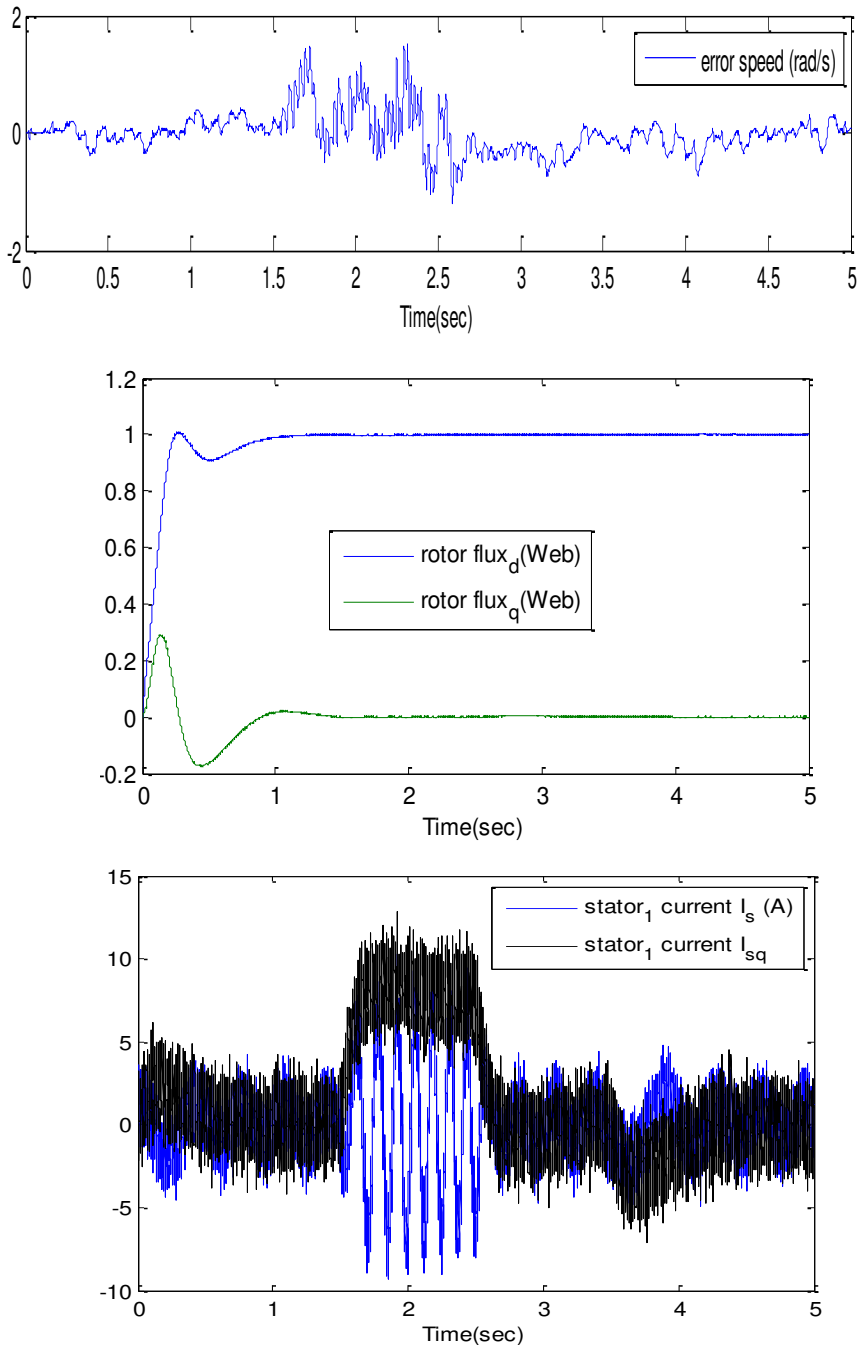


Figure 9

Error speed ,rotor flux and stator current results for low speed sensorless control

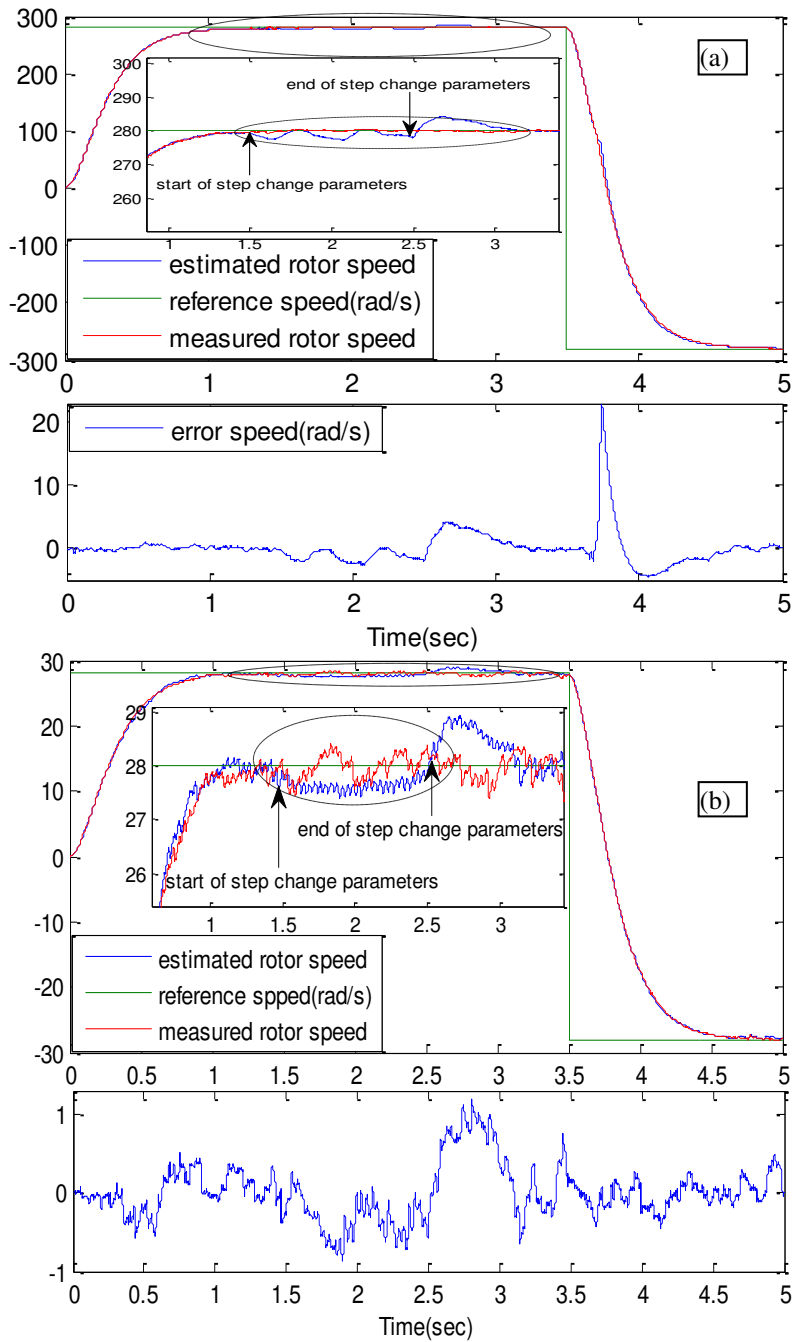


Figure 10

Robustness test; (a) for high speed (b) for low speed sensorless vector control of DSIM

Conclusions

In this paper we presented the sensorless vector control of DSIM, where the “*sign*” function used by the majority of authors is replaced with the *smooth* function. With the use of the “*sign*” function, undesired oscillations appear in the speed and torque. These oscillations can excite the neglected errors dynamics, or even damage the observer.

The sliding mode speed observer is sufficiently fast and robust with respect to parametric variation, load disturbance and the change of the reference speed. We also note that this technique is characterized by its simplicity of design and robustness; most importantly it eliminated the need for the mechanical speed sensor, which is expensive and fragile.

Appendix

Double stator induction motor parameters

$$P_n=4.5 \text{ kW}, f=50 \text{ Hz}, V_n(\Delta/Y)=220/380 \text{ V}, I_n(\Delta/Y)=6.5 \text{ A}, \Omega_n=2751 \text{ rpm}, p=1$$

$$R_{s1}=R_{s2}=3.72 \text{ } \Omega, R_r=2.12 \text{ } \Omega, L_{s1}=L_{s2}=0.022 \text{ H}, L_r=0.006 \text{ H}, L_m=0.3672 \text{ H}$$

$$J=0.0625 \text{ Kg}\cdot\text{m}^2, K_f=0.001 \text{ Nm}(\text{rad/s})^{-1}$$

References

- [1] A. Khedher, MF. Mimouni, N. Derbel, A. Masmoudi. Sensorless-Adaptive DTC of Double Star Induction Motor. *Energy Convers Manage*, 2010; 51: 2878-2892
- [2] M. Rizwan Khan, I. Atif, A. Mukhtar. MRAS-based Sensorless Control of a Vector-controlled Five-Phase Induction Motor drive. *Electric Power Systems Research*, Vol. 78, 2008, pp. 1311-1321
- [3] H. Ben Azza, M. Jemli, M. Boussak, M. Gossa. High Performance Sensorless Speed Vector Control of SPIM Drives with On-Line Stator Resistance Estimation. *Simulation Modelling Practice and Theory*, Vol. 19, 2011, pp. 271-282
- [4] P. Vas. *Sensorless Vector and Direct Torque Control*, Oxford University Press, Oxford, 1998
- [5] A. M. Trzynadlowski. *Control of Induction Motors*, Academic Press, London, 2001
- [6] O. Aydogmus, S. Sünter. Implementation of EKF-based Sensorless Drive System using Vector-controlled PMSM Fed by a Matrix Converter. *Electrical Power and Energy Systems*, Vol. 43, 2012, pp. 736-743
- [7] R. Nilsen, M. P. Kazmierkowski. Reduced-Order Observer with Parameter Adaptation for Fast Rotor Flux Estimation in Induction Machine. *IEE Proceedings*, Vol. 136, No. 1, 1989, pp. 35-43
- [8] R. Beguenane, M. A. Ouhrouche, A. M. Trzynadlowski. A New Scheme for Sensorless Induction Motor Control Drives Operating in Low Speed

- Region, Mathematics and Computers in Simulation. Vol. 71, No. 02, 2006, pp. 109-120
- [9] M. S. Zaky, M. Khater, H. Yasin, S. S. Shokralla. Very Low Speed and Zero Speed Estimations of Sensorless Induction Motor Drives. *Electric Power Systems Research*, Vol. 80 (2010) pp. 143-151
- [10] J. Song, K. B. Lee, J. H. Song, I. Choy, K. B. Kim, Sensorless Vector Control of Induction Motor using a Novel Reduced-Order Extended Luenberger Observer, *Proceeding of the IEEE Industry Applications Conference*, Vol. 3, 2000, pp. 1828-1834
- [11] M. Mena, O. Touhami, R. Ibtouen, M. Fadel. Sensorless Direct Vector Control of an Induction Motor. *Control Engineering Practice*, Vol. 16, 2008, pp. 67-77
- [12] T. S. Kwon, M. H. Shin, D. S. Hyun. Speed Sensorless Stator Flux-oriented Control of Induction Motor in the Field Weakening Region using Luenberger Observer. *IEEE Trans. on Power Electron*, Vol. 20, No. 04, 2005, pp. 864-869
- [13] MF. Mimouni, R. Dhifaoui. A Robust Air-Gap Flux Estimation for Speed Sensorless Vector Control of Double-Star Induction Machine. *Int J Adapt Control Signal Process*, Vol. 18, 2004, pp. 523-46
- [14] R. Kianinezhad, B. Nahid-Mobarakeh, F. Betin, G. A. Capolino. Sensorless Field-oriented Control for Six-Phase Induction Machines. *IEEE Trans. on Ind. Appl*, Vol. 71, 2005, pp. 999-1006
- [15] A. Mezouar, M. K. Fellah, S. Hadjeri. Adaptive Sliding-Mode-Observer for Sensorless Induction Motor Drive using Two-Time-Scale Approach. *Simulation Modelling Practice and Theory*, Vol. 16, 2008, pp. 1323-133
- [16] M. Marcello, P. Sergei, T. Andrea. A speed-Sensorless Indirect Field-oriented Control for Induction Motors Based on High Gain Speed Estimation. *Automatica*, Vol. 42, 2006, pp. 1637-1650
- [17] K. Vrdoljak, N. Perić, I. Petrović. Sliding Mode-based Load-Frequency Control in Power Systems. *Electric Power Systems Research*, Vol. 80, 2010, pp. 514-527
- [18] F. Plestan, et al. Sliding Mode Control with Gain Adaptation-Application to an Electropneumatic Actuator. *Control Engineering Practice* (2012) <http://dx.doi.org/10.1016/j.conengprac.2012.04.012>
- [19] V. Brégeault, F. Plestan, Y. Shtessel, Y. Hu. Adaptive Sliding Mode Control for an Electropneumatic Actuator. In *Proceedings of the international workshop on variable structure systems VSS10, 2010, Mexico, D.F., Mexico*
- [20] L. Jingchuan, X. Longya, Z. Zheng, An Adaptive Sliding-Mode Observer for Induction Motor Sensorless Speed Control, *IEEE Transaction on Industry Applications*, Vol. 41, No. 4, 2005, pp. 1039-1046